University of Alberta

Mechanistic and biological analysis of Cdc34/SCF function.

by

Xaralabos Varelas

A thesis submitted to the Faculty of Graduate Studies and Research in partial fulfillment of the requirements for the degree of Doctor of Philosophy

Department of Biochemistry

Edmonton, Alberta
Spring, 2005

0-494-08307-7

Library and Archives Canada

Published Heritage Branch

395 Wellington Street
Ottawa ON K1A 0N4
Canada

Bibliothèque et Archives Canada

Direction du Patrimoine de l'édition

395, rue Wellington
Ottawa ON K1A 0N4
Canada

Your file *Votre référence*
ISBN
Our file *Notre reference*
ISBN

NOTICE:
The author has granted a non-exclusive license allowing Library and Archives Canada to reproduce, publish, archive, preserve, conserve, communicate to the public by telecommunication or on the Internet, loan, distribute and sell theses worldwide, for commercial or non-commercial purposes, in microform, paper, electronic and/or any other formats.

The author retains copyright ownership and moral rights in this thesis. Neither the thesis nor substantial extracts from it may be printed or otherwise reproduced without the author's permission.

AVIS:
L'auteur a accordé une licence non exclusive permettant à la Bibliothèque et Archives Canada de reproduire, publier, archiver, sauvegarder, conserver, transmettre au public par télécommunication ou par l'Internet, prêter, distribuer et vendre des thèses partout dans le monde, à des fins commerciales ou autres, sur support microforme, papier, électronique et/ou autres formats.

L'auteur conserve la propriété du droit d'auteur et des droits moraux qui protège cette thèse. Ni la thèse ni des extraits substantiels de celle-ci ne doivent être imprimés ou autrement reproduits sans son autorisation.

In compliance with the Canadian Privacy Act some supporting forms may have been removed from this thesis.

While these forms may be included in the document page count, their removal does not represent any loss of content from the thesis.

Conformément à la loi canadienne sur la protection de la vie privée, quelques formulaires secondaires ont été enlevés de cette thèse.

Bien que ces formulaires aient inclus dans la pagination, il n'y aura aucun contenu manquant.

Canada

ABSTRACT

The covalent modification of proteins with the highly conserved ubiquitin (Ub) protein is vital in the regulation of numerous eukaryotic processes. Ubiquitination of these proteins signals for a multitude of events, typically targeting them for proteasomal degradation. Cellular proliferation depends upon the ubiquitination of several key cell cycle regulators. The Cdc34 Ub-conjugating enzyme and the SCF Ub-ligase together mediate the ubiquitination of a subset of these regulators. The work presented in this thesis is aimed at understanding the catalytic mechanism and biological roles of the Cdc34/SCF complex.

Analysis of the properties of *Saccharomyces cerevisiae* Cdc34 has revealed that its catalytic function is dependent on its ability to self-associate into a dimer, and that this interaction is dependent upon Cdc34~Ub thiolester formation. Mutational studies have identified several key residues that function in part to position Ub properly onto Cdc34, allowing for its self-association. The results presented also indicate that the self-association of Cdc34 is in turn a prerequisite for both poly-Ub chain assembly and Cdc34's essential function(s).

Using a genetic approach, evidence is also presented that the Cdc34/SCF complex mediates the integrity of the *S. cerevisiae* cell wall. The growth characteristics of Cdc34/SCF mutants suggest a role for this complex in the mediation of cell wall biosynthesis partly through the regulation of the cell integrity signal transduction pathway. A detailed examination of this function suggests that the Cdc34/SCF complex participates in directing the signals required for these events, and that misregulation of these signals results in a multitude of effects, including cell cycle defects and a weakened

cell wall. Further analysis of these mutants also revealed a role for the Cdc34/SCF complex in the down-regulation of several transcriptional programs, including those directly related to the cell integrity pathway.

Taken together, this study provides novel insight into both the mechanism of Cdc34 function, and the essential roles of the Cdc34/SCF complex in cell growth.

ACKNOWLEDGEMENTS

I would like to thank the many people that have made my time as a graduate student such a great part of my life. Thanks to my supervisor, Mike Ellison, for supporting me and allowing me to learn how to think for myself. Thanks to my supervisory committee, Dave Stuart and Luis Schang, for their helpful advice and discussions. Special thanks to Chris Ptak for the helpful discussions, and experimental support.

I would also like to thank the great friends that I have made here, whom without I don't think I would be where I am today. In particular, I would like to thank Sean McKenna, Trevor Moraes, Sheetal Raithaitha, Scott Williams, Dave Arthur, and Raj Pannu.

Finally and above all, I would like to thank my family and Richelle for all their love and encouragement.

TABLE OF CONTENTS

CHAPTER 1 – Introduction 1

1.1 Protein Ubiquitination. 1

1.1.1 The ubiquitin pathway. 2

1.1.2 Ubiquitin-like proteins. 5

1.1.3 Ubiquitin-activating enzymes. 7

1.1.4 Ubiquitin-conjugating enzymes. 9

1.1.5 Ubiquitin-ligases. 13

1.1.5a HECT-domain E3s. 15

1.1.5b RING finger E3s. 17

1.1.5c U-box domain E3s. 23

1.1.6 Poly-ubiquitin chains. 26

1.1.7 Ubiquitin binding and related motifs. 29

1.1.8 The 26S Proteasome. 30

1.1.9 De-ubiquitinating enzymes. 31

1.2 Ubiquitin and the budding yeast cell cycle. 32

1.2.1 START and the G1-S phase transition. 33

1.2.2 S phase. 46

1.2.3 G2 phase and Mitosis. 47

1.3 The cell integrity signaling pathway. 56

1.3.1 Cell wall composition. 55

1.3.2 Cell integrity surface receptors. 57

1.3.3 The Rho1 GTPase. 59

1.3.4 The Pkc1 kinase. 63

1.3.5 The MAPK phosphorylation cascade. 64

1.3.6 Cell integrity pathway phosphatases. 65

1.3.7 Transcriptional targets. 66

1.3.8 Other features. 71

1.4 Overview 73

1.5 References 75

CHAPTER 2 – Cdc34 self-association is facilitated by Ub thiolester formation and is required for its catalytic function. 103

2.1 Introduction 103

2.2 Results 105

2.2.1 Cdc34 self-associates. 105

2.2.2 The carboxyl-terminal extension and the catalytic domain insertion of Cdc34 are not required for Cdc34 self-association 107

2.2.3 Cdc34 self-association is not dependent on a functional SCF complex. 109

2.2.4 Residues within the Cdc34 catalytic domain that are required for self-association. 110

2.2.5 The relationship between Cdc34 self-association, Cdc34~Ub thiolester, and Cdc34 autoubiquitination. 114

2.2.6 Cdc34 self-association depends on thiolester-linked ubiquitin. 118

2.2.7 The stoichiometry and in vitro properties of Cdc34~Ub thiolester. 120

2.2.8 Dimerization of Cdc34 increases the rate of ubiquitin thiolester reduction. 124

2.2.9 A constant source of Cdc34~ubiquitin thiolester is required for efficient poly-ubiquitin chain assembly. 126

2.3 Discussion 128

2.4 Materials and Methods 135

2.4.1 Plasmids and yeast strains. 135

2.4.2 Cdc34 crosslinking. 138

2.4.3 Immunoprecipitation and immunoblotting. 138

2.4.4 Protein Expression and purification. 139

2.4.5 Cdc34~ubiquitin thiolester purification and stability. 140

2.4.6 In vitro Cdc34~ubiquitin thiolester assays. 141

2.4.7 Cdc34 autoubiquitination reactions. 142

2.5 References 143

CHAPTER 3 – The Cdc34/SCF complex ubiquitination complex functions to mediate cell integrity. 145

3.1 Introduction 145

3.2 Results 148

3.2.1 Cdc34/SCF mutants exhibit cell integrity phenotypes. 148

3.2.2 The *cdc53-1* mutant exhibits phenotypes atypical of other Cdc34/SCF mutants. 151

3.2.3 Cdc34/SCF mutants are defective in the induction of Slt2 phosphorylation in response to heat stress and caffeine. 154

3.2.4 *cdc34-2 slt2Δ* and *cdc53-1 slt2Δ* strains show strong lysis defects. 156

3.2.5 Effect of *LRG1*, *SAC7*, and *KNR4* deletions on phospho-Slt2 levels. 158

3.2.6 Deletion of *KNR4* enhances the cell integrity defects in *cdc53-1* and *cdc34-2* mutants. 160

3.2.7 Deletion of SAC7 enhances the defects in cdc34-2 and cdc53-1 mutants. 160

3.2.8 Deletion of *LRG1* suppresses the *cdc34-2* and *cdc53-1* growth and cell integrity defects. 163

3.3 Discussion 165

3.4 Materials and Methods 169

3.4.1 Yeast strains. 169

3.4.2 Growth media. 171

3.4.3 Plating experiments. 171

3.4.4 Sic1 turnover experiments. 172

3.4.5 Slt2 phosphorylation assays. 173

3.4.6 Microscopy. 174

3.4.7 Flow cytometry. 174

3.5 References 176

CHAPTER 4 – Characterization of the relationship between the Cdc34/SCF ubiquitination complex and transcription. 180

4.1 Introduction 180

4.2 Results 183

4.2.1 The activities of the SBF, MBF, and Rlm1 transcription factors are induced in the *cdc53-1* and *cdc34-2* mutants. 183

4.2.2 The transcriptional profile of *cdc53-1* and *cdc34-2* strains. 188

4.2.3 Variation in cell wall related transcripts in *cdc53-1* and *cdc34-2* mutants. 193

4.2.4 Deletion Gcn4 regulated transcripts are induced in *cdc53-1* and *cdc34-2* mutants. 198

4.2.5 Met4 specific transcripts are induced in *cdc53-1* and *cdc34-2* mutants. 200

4.2.6 A role for the Cdc34/SCF complex in maintaining genomic integrity. 200

4.3 Discussion 202

4.4 Materials and Methods 206

4.4.1 Plasmids and yeast strains. 206

4.4.2 β-galactosidase reporter assays. 207

4.4.3 Microarray cultures and RNA isolation. 208

4.4.4 Microarray analysis. 208

4.4.5 Promoter analysis. 209

Appendix 4.1 210

Appendix 4.2 218

Appendix 4.3 222

4.5 References 228

CHAPTER 5 – Summary and future directions 233

5.1 Thesis summary 233

5.1.1 Summary of Chapter 2 233

5.1.2 Summary of Chapter 3 234

5.1.3 Summary of Chapter 4 235

5.2 Future directions 236

5.2.1 Cdc34 self-association and the assembly of poly-Ub chains. 236

5.2.2 The role of Ser73 and Ser97 phosphorylation with respect to thiolester formation, Cdc34 self-association, and poly-Ub chain assembly. 239

5.2.3 Structural analysis of Cdc34 and Cdc34~Ub thiolester. 241

5.2.4 Identification of Cdc34/SCF target protein(s) that relate to cell integrity. 245

5.2.5 Identifying the F.box component(s) of the SCF complex that mediate cell integrity. 246

5.2.6 Investigating the cell cycle relationship between the Cdc34/SCF complex and cell integrity. 248

5.2.7 Further examination of the roles of the Cdc34/SCF complex in cell integrity pathway mediated transcription. 249

5.2.8 Cdc34/SCF regulation of Gcn4 and Met4, and their connection to cell growth. 250

5.3 Conclusions 251

5.4 Materials and Methods 251

5.4.1 Autoubiquitination of phospho-Ser97 Cdc34. 251

5.4.2 ATP independent Cdc34~Ub thiolester autoubiquitination reactions.

5.4.3 NMR spectroscopy. 252

5.4.4 Cell integrity related examination of the *cdc4-1* mutant. 253

5.5 References 254

LIST OF TABLES

Table 1.1	APC subunits	22
Table 1.2	Cell cycle ubiquitination targets	34
Table 1.3	Identified Rlm1 target genes	68
Table 2.1	Yeast strains and plasmids used in Chapter 2	136
Table 3.1	Yeast strains used in Chapter 3	170
Table 4.1	Genes repressed in *cdc53-1* and *cdc34-2* cells	192
Table 4.2	Cell integrity related genes induced in *cdc53-1* and *cdc34-2* cells	194
Table 4.3	Met4 related genes induced in *cdc53-1* and *cdc34-2* cells	201

LIST OF APPENDIXES

Appendix 4.1	Genes induced by 2 fold or greater in *cdc53-1* and *cdc34-2* mutants.	210
Appendix 4.2	Promoter analysis of the induced genes in *cdc53-1* and *cdc34-2* mutants.	218
Appendix 4.3	Comparison between the transcriptional profiles of *cdc53-1* and *cdc34-2* mutants with previously published datasets.	225

LIST OF FIGURES

Figure 1.1	Surface lysine residues on ubiquitin involved in the assembly of poly-ubiquitin chains.	3
Figure 1.2	Structural insight into the ubiquitin-activating enzyme.	8
Figure 1.3	Structure of the ubiquitin-conjugating enzyme catalytic core domain.	10
Figure 1.4	Proposed mechanism for ubiquitin conjugation.	12
Figure 1.5	NMR derived model of the Mms2•Ub-Ubc13~Ub complex.	14
Figure 1.6	The proposed mechanism of HECT domain E3s based on structural studies.	16
Figure 1.7	Structural insight into RING domain E3s.	18
Figure 1.8	The low resolution structure of the APC complex.	24
Figure 1.9	Structure of the ubiquitin-ligase U-box domain.	25
Figure 1.10	NMR derived models of Lys48 and Lys63 linked di-Ub chains.	27
Figure 1.11	The Saccharomyces cerevisiae cell cycle.	35
Figure 1.12	Waves of cell cycle transcription in *S. cerevisiase* cells.	37
Figure 1.13	Morphological effects of Sic1 stabilization in *S.cerevisiae* cells.	39
Figure 1.14	A model of Far1 function.	42
Figure 1.15	The Stages of Mitosis.	49

Figure 1.16	MAPK pathways in budding yeast.	55
Figure 1.17	Known proteins that possess RhoGAP activity.	61
Figure 2.1	Cdc34 self-associates in vivo.	106
Figure 2.2	The Cdc34 carboxyl-terminal extension and catalytic domain insertion are dispensable with respect to Cdc34 self-association.	108
Figure 2.3	Cdc34 self-association is not dependent upon a functional SCF complex.	111
Figure 2.4	Key residues that mediate Cdc34 self-association.	113
Figure 2.5	Cdc34 derivatives ability to form Ub thiolester.	116
Figure 2.6	Autoubiquitination of Cdc34 derivatives.	117
Figure 2.7	Cdc34 self-association is facilitated by Ub thiolester formation.	119
Figure 2.8	The composition of self-associated Cdc34~Ub thiolester complexes.	122
Figure 2.9	Cdc34~Ub thiolester self-associates into a dimer.	123
Figure 2.10	Dimeric Cdc34~Ub thiolester is less stable than monomeric Cdc34~Ub thiolester.	125
Figure 2.11	Poly-Ub chain assembly mediated by purified Cdc34~Ub thiolester.	127
Figure 2.12	A functional comparison between the Cdc34 derivatives.	130
Figure 2.13	Determinants of Cdc34 self-association.	132

Figure 2.14	Hypothetical scheme for Cdc34 self-association and poly-Ub chain formation.	133
Figure 3.1	LRG1 overexpression is toxic to Cdc34/SCF mutants.	149
Figure 3.2	Cell integrity defects associated with cdc53-1 and cdc34-2 cells.	150
Figure 3.3	*cdc53-1* mutants display uncharacterized defects.	152
Figure 3.4	Slt2 phosphorylation is defective in *cdc53-1* and *cdc34-2* cells in response to heat or caffeine stress.	155
Figure 3.5	Deletion of *SLT2* in *cdc53-1* and *cdc34-2* mutants enhances lysis defects.	157
Figure 3.6	Effect of *LRG1*, *SAC7* and *KNR4* deletions on phospho-Slt2 levels.	159
Figure 3.7	Deletion of *KNR4* enhances the cell integrity defects in Cdc34/SCF mutants.	161
Figure 3.8	Deletion of *SAC7* enhances the defects in Cdc34/SCF mutants.	162
Figure 3.9	Deletion of *LRG1* suppresses the growth defects associated with Cdc34/SCF mutants.	164
Figure 3.10	Proposed functions of the Cdc34/SCF complex in the regulation of cell integrity.	168
Figure 4.1	The SBF, MBF and Rlm1 transcription factors show increased activity in *cdc53-1* and *cdc34-2* mutants.	185
Figure 4.2	Cdc34/SCF mediated transcriptional effects are specific and novel.	187
Figure 4.3	A strong correlation exists between the transcriptional profiles of *cdc53-1* and *cdc34-2* mutants.	190
Figure 4.4	Overlap between the significantly induced genes in *cdc53-1* and *cdc34-2* mutants and those suggested to be Gcn4 targets.	199

Figure 4.5 A simplified model illustrating the known modes of Cdc34/SCF mediated regulation of transcription. 204

Figure 5.1 ATP independent function for E1 in Cdc34~Ub thiolester mediated autoubiquitination of Cdc34. 238

Figure 5.2 Autoubiquitination of phopho-S97 Cdc34. 240

Figure 5.3 Distinct surface regions on Ub responsible for mediating the thiolester interaction with Cdc34. 243

Figure 5.4 A non-covalent interaction between Ub and Cdc34. 244

Figure 5.5 Cell integrity defects associated with *cdc4-1* cells. 247

LIST OF ABBREVIATIONS

- Distinct amino acids found within proteins are abbreviated in the text using their three-letter code (e.g. lysine 48 found within ubiquitin is abbreviated Lys48).
- Amino acid substitutions within proteins are annotated using their single letter code. This is arranged by starting with the amino acid that is being substituted, followed by its position, and then the amino acid that it is being changed into (e.g. substitution of lysine 48 to an arginine within ubiquitin is abbreviated K48R).
- Pyrimidine and purine bases are abbreviated using their single letter codes (e.g. adenine is abbreviated A).
- Lengths, volumes, amounts and time are abbreviated using the International Systems of Units (e.g. nanometers is abbreviated as nm, microliter as µl, mole as mol, and hour as hr).

Δ	deletion of a gene
::	disruption of a gene
~	thiolester bond
3AT	3-amino-triazole
Å	Angstrom
°C	degrees Celsius
α-factor	alpha factor mating pheromone
AMP	adenosine 5'-monophosphate
APC	Anaphase promoting complex
ATP	adenosine 5'-triphosphate
ARS	autonomously replicating sequences
BTB/POZ	bric a brac, tramtrack and broad complex/Pox virus and zinc finger
CDC	Cell division cycle
Cdc34/SCF	Cdc34 functioning together with the SCF ubiquitin-ligase
$Cdc34/SCF^{F.box}$	Cdc34/SCF with the F.box protein depicted in superscript
CDK	cyclin dependent kinase
cDNA	complementary DNA

CKI	cyclin dependent kinase inhibitor
Clb	B-type cyclin (Clb1, Clb2, Clb3, Clb4, Clb5, Clb6)
Cln	G1 cyclin (Cln1, Cln2, Cln3)
CUE	similar to the domain of the yeast Cue1
CPM	counts per minute
DIC	differential interference contrast
DNA	deoxyribonucleic acid
DTT	dithiothreitol
E1	ubiquitin-activating enzyme
E2	ubiquitin-conjugating enzyme
E3	ubiquitin-ligase
ECL	enhanced chemiluminescence
E. coli	*Escherichia coli*
EDTA	ethylenediaminetetraacidic acid
FACS	fluorescence-activated cell sorting
GAP	GTPase activating protein
GDI	guanine nucleotide dissociation inhibitor
GDP	guanosine 5'-diphosphate
GEF	guanine nucleotide exchange factor
GTP	guanosine 5'triphosphate
HA	hemagglutinin
HECT	homologous to E6-AP carboxyl-terminus
HRP	horseradish peroxidase
HOG	high osmolarity glycerol
JAMM	JAB1/MPN domain metalloenzyme
kb	kilobase pair
kDa	kilodalton
LRR	leucine rich repeats
MADS	Mcm1-Agamous-Deficiens-serum response factor
MAPK	mitogen activated protein kinase
MAPKK	mitogen activated protein kinase kinase

MAPKKK	mitogen activated protein kinase kinase kinase
MAT a	mating type a
MAT α	mating type α
MBF	MCB-binding factor (made of up Mbp1 and Swi6)
MCB	MluI cell cycle box
MPF	maturation promoting factor
mRNA	messenger ribonucleic acid
NMR	nuclear magnetic resonance
OD	optical density
ORC	origin of replication
ORF	open reading frame
PAGE	polyacrylamide gel electrophoresis
PCR	polymerase chain reaction
PEST	proline, glutamine, serine, and threonine rich domain
PI	propidium iodide
Pi	inorganic phosphate
PPi	inorganic pyrophosphate
pre-RC	pre-replicative complex
RNA	ribonucleic acid
RING	really interesting new gene
SBF	SCB-binding factor (made up of Swi4 and Swi6)
SCB	Swi4/Swi6 cell cycle box
S. cerevisiae	*Saccharomyces cerevisiae*
SCF	Skp1-Cullin-Rbx1/Hrt1-F.box complex
$SCF^{F.box}$	SCF with the F.box protein depicted in superscript
SDS	sodium dodecyl sulphate
SPB	spindle pole body
SOCS	suppressors of cytokine signaling
TS	temperature sensitive
YGP	yeast extract/peptone/galactose rich medium
YPD	yeast extract/peptone/dextrose rich medium

UASs	upstream activating sequences
Ub	ubiquitin
UBA	ubiquitin-associated
Ubl	ubiquitin-like protein
UBP	ubiquitin processing protease
UCH	ubiquitin carboxyl-terminal hydrolase
UDP	ubiquitin domain protein
UEV	ubiquitin-conjugating enzyme variant
UIM	ubiquitin-interacting motif
VHL	von-Hipple-Lindau

CHAPTER 1 – Introduction

1.1 Protein Ubiquitination

The dynamic nature of the eukaryotic cell requires the efficient and faithful regulation of its biological processes. One of the most wide spread mechanisms of regulation involves the covalent modification of proteins with ubiquitin (Ub). This small 76-residue protein has the unusual property of forming an isopeptide bond between its carboxyl-terminal glycine residue and the ε-amino group of surface exposed lysine residues. Conjugation of Ub to another protein, which is known as ubiquitination, targets that protein for a multitude of effects. Ub can also serve as a target itself, as a number of its lysine residues allow for the formation of different types of poly-Ub chains. A highly complex cascade of enzymatic events, known as the Ub pathway, exists to selectively catalyze the formation of these linkages.

Ub was discovered in the early 1970s as a protein that was found in many eukaryotic cells, hence its name (130). It was later found covalently linked to chromatin through an interaction with histone H2A (129). It was not until several years later, however, that a biologically significant role for Ub was discovered in mediating non-lysosomal intracellular proteolysis (62). This role was dependant on ATP, which allowed for the fractionation, and subsequent identification, of the minimal enzymatic components of the Ub conjugation cascade from cell-free rabbit reticulocyte lysates (162, 164).

The most prevalent and best-characterized role for ubiquitination is the targeted degradation of the substrate protein by the 26S proteasome (161, 412). This method of rapid and selective degradation can be found in a variety of essential events, a few of which include cell cycle regulation (82, 215), development (159, 307), apoptosis (231, 439) and the inflammatory response (249). Alternatively, ubiquitination has many signaling properties independent of proteolysis that can be found in such diverse processes as endocytosis (167, 257), ribosome biogenesis (108, 382), and DNA damage repair (35, 267). Ub's role in determining these varying processes is mediated by the number of Ubs linked and the kind of chains that are formed.

Due to the pervasive nature of ubiquitination, misregulation of this modification can result in defects within biological systems. Many diseases have been linked to errors in this pathway, including Liddle's syndrome, Angelman syndrome, Parkinson's disease, Cystic fibrosis, many forms of neurological diseases such as Alzheimer's disease, and numerous cancers (59, 60, 63, 359). Much research has been focused on understanding the Ub pathway and on developing therapeutics to target its misregulation.

The work presented in this thesis has utilized the budding yeast, *Saccharomyces cerevisiae*, as a model eukaryotic organism. Its contents provide us with novel insight into the mechanism of poly-Ub chain formation and into a role for ubiquitination in mediating yeast cell integrity. This chapter is intended to provide a framework for this work. It begins by discussing the specifics of the Ub pathway, including its known mechanistic elements. This is followed by a summary of the *S. cerevisiae* cell cycle and the identified roles of Ub in its regulation. Lastly, a review of the signaling pathways known to mediate yeast cell integrity is provided.

1.1.1 The ubiquitin pathway

Ub is one of the most highly conserved eukaryotic proteins (only three residues differ between budding yeast Ub and human Ub). It consists of a stable hydrogen-bonded globular structure with a free carboxyl-terminal extension that ends in two glycine residues (Gly75 and Gly76), the later of which forms the covalent linkage with target lysines (Figure 1.1) (410, 419). Within the globular domain of Ub are 7 surface lysine residues that can serve as a substrate to generate differential poly-Ub chains (Lys6, Lys11, Lys27, Lys29, Lys33, Lys48 and Lys63) (14, 53, 197, 316, 383). Furthermore, distinct surface regions of Ub have been identified in mediating a variety of events, such as proteasomal recognition and endocytosis (377).

The selective covalent attachment of Ub and subsequent formation of poly-Ub chains onto protein substrates involves the action of three enzymatic steps (161, 323). Initially, Ub non-covalently interacts with an Ub-activating enzyme (E1 or UBA), which through the Mg^{2+} dependent hydrolysis of ATP "activates" Ub by mediating the formation of an AMP adenylate with the carboxyl-terminus of Ub (61, 141-143, 325).

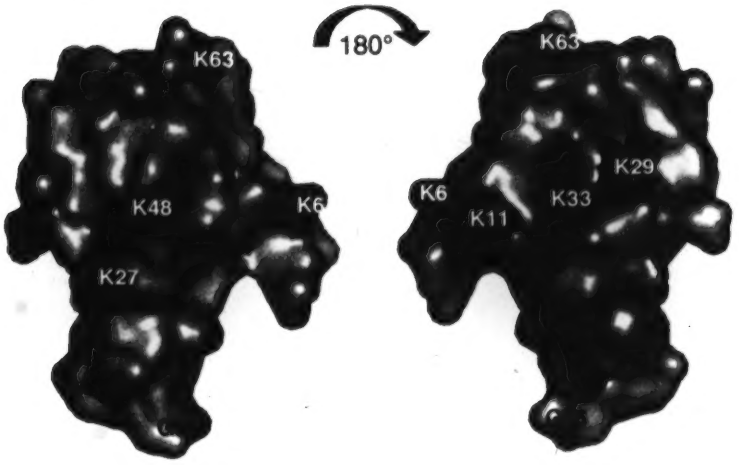

Figure 1.1 Surface lysine residues on ubiquitin involved in the assembly of poly-ubiquitin chains. Shown is a surface model based on the three-dimensional structure of ubiquitin, highlighting the carboxyl-terminal glycine residue (G76), and the lysine residues (in blue) involved in the assembly of poly-ubiquitin chains.

$$E1 + ATP + Mg^{2+} + Ub \longleftrightarrow E1{\cdot}AMP\text{-}Ub + PP_i$$

This allows for the transfer of Ub to the active site cysteine of the E1 to form a thiolester bond (represented herein by ~) between the carboxyl-terminal Gly76 of Ub and the thiol group of this active site (61, 141-143).

$$E1{\cdot}AMP\text{-}Ub \longleftrightarrow E1{\sim}Ub + AMP$$

Another ATP dependent Ub-AMP adenylate may then form, resulting in an E1 enzyme "charged" with two Ub molecules (141-143).

$$E1{\sim}Ub + ATP + Mg^{2+} + Ub \longleftrightarrow E1{\sim}Ub(\cdot AMP\text{-}Ub) + PP_i$$

This "activated" form of Ub is primed for recognition by the next enzymes in the cascade, known as the Ub-conjugating enzymes (E2 or UBC). In a transthiolesterification reaction the thiolester bond involving the carboxyl-terminal Gly76 of Ub is transferred from the E1 active site to the thiol group of active site cysteine of the E2 (164).

$$E1{\sim}Ub(\cdot AMP\text{-}Ub) + E2 \longleftrightarrow E2{\sim}Ub + E1{\cdot}AMP\text{-}Ub$$

The E1 enzyme is then free to form another E1~Ub thiolester and begin the pathway over again. The E2~Ub thiolester can then proceed to transfer Ub from its active site through another transthiolesterifaction reaction to the active site cysteine of the third enzyme in the pathway the Ub-ligase (E3), thus forming an E3~Ub thiolester intermediate (24, 356).

$$E2{\sim}Ub + E3 \longleftrightarrow E3{\sim}Ub + E2$$

Ub is finally transferred from the E3~Ub thiolester to the target substrate resulting in an isopeptide linkage between the carboxyl-terminal Gly76 of Ub and a lysine residue on a target protein.

$$E3\sim Ub + Protein \longleftrightarrow Protein\text{-}Ub + E3$$

Alternatively, the E2~Ub thiolester by itself, or often together with another kind of E3 enzyme, can catalyze the formation of the isopeptide linkage between Gly76 of Ub and a lysine residue on the final target protein (326, 365, 376).

$$E2\sim Ub + Protein \xleftrightarrow{E3} Protein\text{-}Ub + E2$$

This process can be repeated several times on the target protein to attach multiple Ubs onto multiple lysine residues on the protein, or to form poly-Ub chains by repetitively attaching multiple Ubs onto the terminal Ub originating at a single lysine residue on the target protein (163).

The hierarchical nature of the Ub pathway allows for its diverse specificity. Few E1 enzymes exist (sometimes only one) to activate and pass on Ub to numerous E2 enzymes. These E2 enzymes are capable of interacting with larger numbers of E3 enzymes. The differing combinations of E2•E3 interactions allow for the target substrate specificity, and the formation of either mono-Ub or specific types of poly-Ub chains. A general understanding of the catalytic mechanism involved in this cascade is known, however many of the details of the process remain uncharacterized.

1.1.2 Ubiquitin-like protein pathways

Other proteins that share some of the distinct features of Ub and its mechanism of conjugation exist, which are known as Ub-like proteins (Ubls). These proteins share a common structural fold with Ub, containing a globular core with a carboxyl-terminal extension ending with two glycine residues. Protein targets are similarity targeted by Ubls on surface lysine residues through an enzymatic cascade consisting of unique E1, E2 and E3 enzymes. To date 11 Ubls have been identified and have been found to regulate a number of cellular processes, some of which directly modulate the Ub pathway and its functions (170, 192, 360).

Of the Ubls, the best studied is the small Ub-related modifier protein, SUMO/Smt3/sentrin. SUMO conjugation is accomplished through an enzymatic cascade

consisting of the E1 enzyme Aos1/Uba2, the E2 enzyme Ubc9, and numerous E3 enzymes that select for a variety of targets (275, 291, 363). However, unlike Ub, a biological relevance for the formation of poly-SUMO chains has not been demonstrated. It appears that the role(s) for SUMO are mediated by mono-SUMO conjugates. Its role(s) have been implicated in a number of processes that include nuclear trafficking, transcriptional regulation, modulation of signaling pathways and chromosomal structure and dynamics. In addition, conjugation of SUMO has been shown to play a negative role in processes regulated by ubiquitination, through competition for lysine resides on target proteins (146, 173).

Another well-characterized Ubl is Nedd8/Rub1. This protein has the highest sequence identity with Ub (60% identity). Covalent attachment of Nedd8 to its targets is achieved through an enzymatic cascade consisting of an E1 enzyme dimer of Ula1/APPBP1 and Uba3, followed by the E2 enzyme Ubc12 (180, 309). The only known targets for Nedd8 are the cullins, which are core components of SCF (Skp1-Rbx1/Hrt1-Cullin-F.box) Ub-ligase enzymes. Conjugation of Nedd8 onto the cullin component of the SCF enzyme increases its ability to interact with the E2 enzyme (208, 428). The dynamic nature of the Nedd8 linkage is important for the function of the SCF complex. However, it the nature of its importance is unclear.

The examples of SUMO and Nedd8 illustrate the conservation with the Ub pathway, and suggest they have all evolved from a common ancestral conjugation pathway. One potential relative is the *Escherichia coli* molybdenum cofactor biosynthesis pathway, which is involved in the transfer of sulfur-containing moieties to metabolites. The MoaD subunit of the molybdopterin synthase enzyme is activated in a parallel manner to that of Ub by the molybdopterin synthase-activating enzyme MoeB. Despite a lack of sequence similarity between MoaD and Ub, the two are comparable in that they have a similar structural fold and carboxyl-terminal di-glycine residues. Additionally, MoaD is activated in a similar manner to that of Ub by the formation an AMP-MoaD adenylate between its carboxyl-terminus and a site within the MoeB activating enzyme. Subsequent to its activation, MoaD does not form a thiolester with MoeB, but rather it is recognized by a sulphurtransferase that converts MoaD adenylate to a thiocarbonate that acts as a sulphur donor (139, 230, 236). The similarities between MoaD and Ub

activation have prompted numerous studies into this pathway in an attempt to better understand the mechanism of Ub activation.

1.1.3 Ubiquitin-activating enzymes

The first enzyme in the Ub pathway, the Ub-activating enzyme, is a highly selective enzyme that only recognizes Ub as its substrate. In an ATP and Mg^{2+} dependent manner the E1 "activates" Ub by catalyzing the adenylation of its carboxyl-terminus. Subsequently, a highly reactive thiolester intermediate is formed between its active site cysteine and the carboxyl-terminus of Ub that is eventually passed on to the next enzyme in the pathway, the E2 (61, 141-143, 164). The catalytic events involving adenylation, thiolester formation of Ub and its transfer to the E2 are highly efficient, occurring at a maximum turnover rate of 1-2 Ubs per second, whereas the rate limiting conjugation of Ub to the substrate is 10 to 100 times slower (141, 262). Very often, as in the case of humans and *S. cerevisiae*, a single E1 enzyme (hUba1 and Uba1 respectively) is sufficient to activate all the Ub required in the cell (270, 437, 438).

Recent structural studies of Ub-like-activating enzymes have shed some light into the mechanism of E1 catalysis. The first of these studies examined the adenyation reaction of the MoeB•MoaD protein complex. As mentioned in section 1.1.2, MoeB is the activating enzyme for the Ub-like MoaD protein. MoeB activates the carboxyl-terminal di-glycines of MoaD by forming an acyl-adenylate intermediate, much like the initial activation of Ub by E1 (236). The crystal structure of the MoeB•MoaD complex provides a view of this conserved process (Figure 1.2A) (230). This structure reveals how a conserved aspartic acid residue co-ordinates a Zn^{2+} ion required for the MoaD carboxylate to attack the α-phosphate of an ATP molecule within a nucleotide-binding pocket. Additionally, this structure outlines a hydrophobic interaction interface between MoeB and MoaD. These conserved features provide insight into how Ub adenylate is formed.

The human Nedd8 activating enzyme dimer, APPB3•Uba3, has also provided a model for the mechanistic understanding of Ub activation (413, 414). This activating enzyme consists of two proteins: APPB3, (which is homologous to MoeB and the N-terminal adenylation domain of the Ub-activating enzyme), and Uba3 (which is

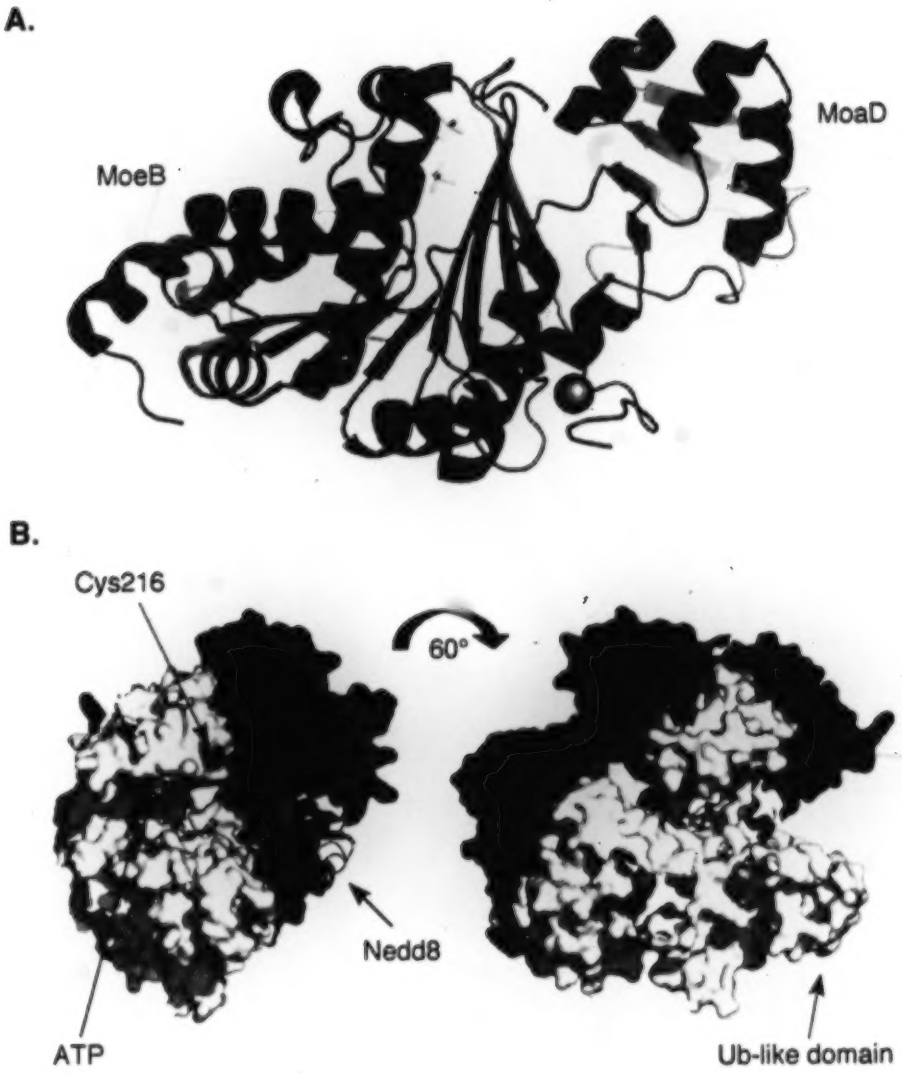

Figure 1.2 Structural insight into the ubiquitin-activating enzyme.
(A) Ribbon diagram representing the three-dimensional structure of the MoeB-MoaD complex. MoeB is shown in green with its glycine rich P-loop highlighted in blue and two of its sulfate molecules in yellow. MoaD is shown in red, and the Zn^{2+} ion that is required for the MoaD carboxylate to attack the α-phosphate of an ATP molecule is shown as a grey sphere. **(B)** Surface model of the APPB3 (shown in blue)-Uba3 (shown in yellow)-Nedd8 adenylate (shown in red)-ATP (shown in grey) complex. The catalytic cysteine residue in Uba3 is highlighted in green, and the ubiquitin-like domain within APPB3 is indicated.

homologous to the carboxyl-terminal catalytic cysteine containing domain of the Ub-activating enzyme) (131, 244). These studies describe three distinct domains within the E1 enzyme: (i) an adenylation domain resembling that of MoeB, (ii) an E1 specific domain organized around the catalytic cysteine residue, and (iii) an E2 recognition domain (Figure 1.2B). Protein and nucleotide binding are mediated by these domains within close proximities in between two grooves of the enzyme, and they are organized in a manner that drives the reaction forward. Interestingly, the E2 recognition domain within this enzyme resembles the structure of Ub, suggesting that E2 enzymes might be recruited to the E1 enzyme through an interaction with this domain. Structural studies have determined a distinct region within the Nedd8 specific E2 (Ubc12) that interacts with this domain, suggesting that it is a combination of the properties of the E2 and this domain that selects for, and positions the E2 for accepting Ub thiolester (179). It remains to be seen if Ub specific E1 enzymes function in a similar manner.

1.1.4 Ubiquitin-conjugating enzymes

While E2 enzymes are very similar in nature and function, they possess highly selective targeting properties. All E2s form a thiolester bond between their active site cysteine and the carboxyl-terminus of Ub through the efficient transfer of Ub thiolester from an activated E1 enzyme (164, 323). Some E2s catalyze the formation of mono-Ub conjugates, while others assemble an array of distinct poly-Ub chains. A catalytic domain consisting of approximately 150 amino acid residues is shared by all E2s. Within this catalytic domain lies the active site cysteine residue, at which Ub thiolester formation takes place. Structural analysis of this core E2 domain has determined that it is highly conserved, consisting of a four-stranded antiparallel β-sheet flanked by four α-helices and a short 3_{10} helix (Figure 1.3A). The most conserved residues cluster around the active site cysteine residue, which lies within a shallow groove in the E2 on a loop connecting the β4 sheet to the α2 helix (69, 70, 145, 194, 283, 286, 395, 402, 427).

The most obvious differences among the E2s are the presence or absence of amino- and/or carboxyl-terminal extensions onto the core domain of the enzyme. These extensions are thought to specify the biological activity of these enzymes by mediating a multitude of interactions, including that with substrates and E3 enzymes. Recent

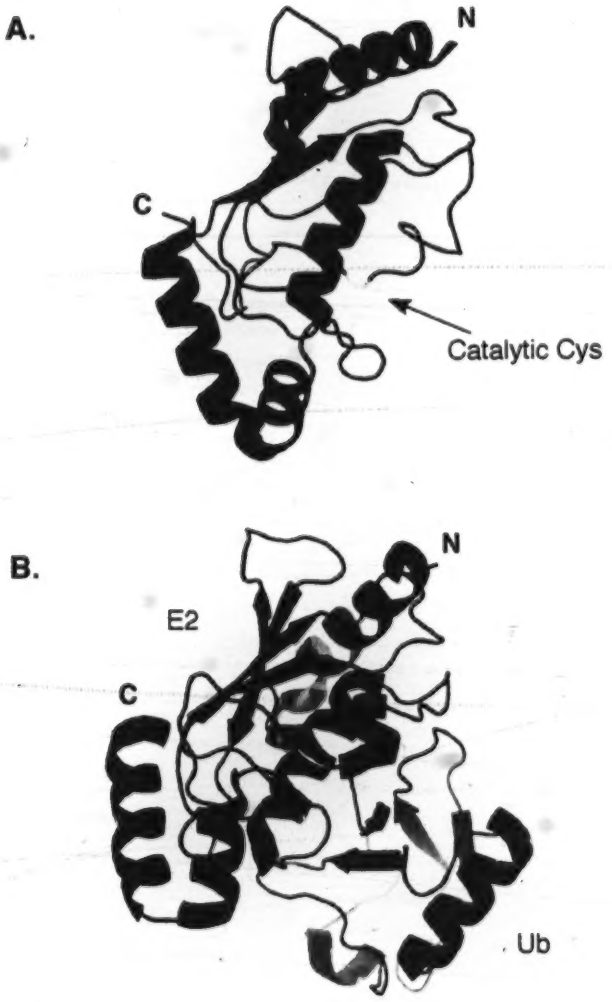

Figure 1.3 Structure of the ubiquitin-conjugating enzyme catalytic core domain .
(A) Ribbon diagram representing the three-dimensional structure of the catalytic core of *S. cerevisiae* Ubc1. **(B)** Ribbon diagram of the Ubc1~Ub thiolester interaction, based on a model derived from NMR analysis of the interaction. Ubiquitin is shown in red, and the catalytic core of Ubc1 is shown in blue, with its catalytic cysteine residue highlighted in yellow. The amino-terminus (N) and carboxyl-terminus (C) of Ubc1 are indicated.

structural analysis of the carboxyl-terminal extension of the S. cerevisiae Ubc1 E2 has shown that this region resembles a Ub-association domain (UBA domain, see 1.13). This observation suggests that this domain might be involved in binding to Ub, possibly for the formation of poly-Ub chains (279). E2 enzymes are classified into 4 different categories: type I E2s lack both the amino- and carboxyl-terminal extensions, type II E2s have only a carboxyl-terminal extension, type III E2s have only an amino-terminal extension, and type IV E2s have both amino- and carboxyl-terminal extensions (191). Additionally, some E2s contain a catalytic domain insert that lies near the active site cysteine residue, which is thought to mediate the formation and utilization of Ub thiolester (248, 278).

Although the formation of Ub thiolester by E2 enzymes is not well understood, some information into this linkage has been obtained with the use of nuclear magnetic resonance (NMR) techniques. The interactions between the E2 and Ub have been characterized for the *S. cerevisiae* Ubc1~Ub thiolester (145), for the human Ubc13~Ub thiolester (271), and for the human HsUbc2b-Ub oxyester (which was made by substituting the catalytic cysteine residue of HsUbc2b with a serine so that it can form a more stable oxyester bond with the carboxyl-terminus of Ub) (282). These NMR studies all showed a similar area surrounding the active site cysteine residue in the E2 that predominantly interact with the carboxyl-terminus of Ub. Many residues in this area are absolutely conserved amongst all the E2 enzymes, suggesting a conserved mechanism of Ub utilization. However, despite all the structural and biochemical data, the mechanistic details of Ub thiolester transfer (from the E1 to an E2, or from the E2 to an E3) and isopeptide bond formation with a lysine (on a target substrate) are not well understood.

The ability of the E2 to transfer Ub to a substrate lysine appears to be self-contained as many E2s often target themselves for autoubiquitination (observed both *in vitro* and *in vivo*) (20, 172, 235). While the significance of this autoubiquitination remains to be discovered, it suggests that the E2 possesses all the catalytic residues required for isopeptide bond formation. The chemical environment required for isopeptide bond formation to take place requires the presence of a general base to deprotonate the attacking lysine, as well as residues that can stabilize the emerging negative charge on the tetrahedral intermediate (Figure 1.4). Insight into the E2

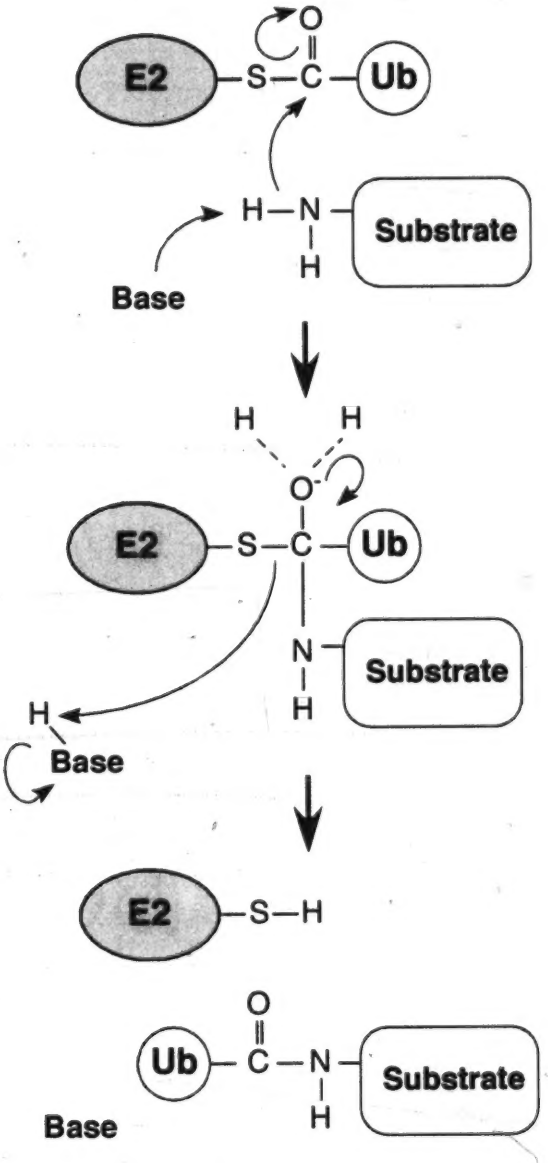

Figure 1.4 Proposed mechanism for ubiquitin conjugation.
(A) The E2~Ub thiolester is positioned (either by itself, or by an E3 enzyme) to transfer ubiquitin onto a lysine residue of a target substrate. A general base is provided by either the E2 or an E3 to deprotonate the acceptor lysine. The ε-amino nitrogen of the target lysine attacks the electrophilic carbon center of the thiolester bond between the E2 and Ub. (B) A tetrahedral intermediate is formed, within which a negative charge developes on the oxygen, which must be stabilized by residues within the E2 or an E3. (C) Finally, an isopeptide bond is formed between the carboxyl-terminus of Ub and the lysine on the target substrate.

mechanism of action has been revealed by a recent study characterizing the role of a conserved asparagine residue upstream of the catalytic cysteine (429). This study proposed that the amide side chain of this asparagine residue acts to stabilize the oxyanion intermediate. A convincing argument for this role was made by demonstrating that this residue is required for Ub transfer from the E2 to a substrate, but not in E2~Ub thiolester formation or Ub thiolester transfer to an E3, using a number of different E2/E3 systems. However, in order for this asparagine to sufficiently act as a catalytic residue, conformational changes in the E2 active site must occur during thiolester formation. Both biochemical and NMR studies performed on E2~Ub thiolester provide support for this idea.

As mentioned above, E2s function differentially in their ability to assemble poly-Ub chains. The best-characterized mechanism of poly-Ub chain assembly is that performed by Ubc13, which specifically catalyzes the formation of Lys63 linked poly-Ub chains (175). It does so by forming a hetero-dimer with an Ub-conjugating enzyme variant (UEV) protein. UEV proteins are highly similar to E2 enzymes in both sequence and structure, but lack their catalytic cysteine residue. Non-covalent interactions between UEVs and Ub have been observed, and when complexed with Ubc13~Ub, this Ub is positioned so that its Lys63 is placed in close proximity to the thiolester linked Ub on Ubc13, thus promoting the specific formation of a Lys63 linked Ub chain (Figure 1.5) (271, 272). Other E2s form hetero- and homo-dimers, and may be capable of non-covalently interacting with Ub, so it is possible that these E2s may function in a similar manner to that of the Ubc13•UEV complex (54, 125, 140, 235, 326, 336). However, very little is known about these interactions.

1.1.5 Ubiquitin-ligases

Target substrate selection of the Ub pathway is largely dependent on the Ub-ligase proteins. E2 enzymes interact with a very large number of these E3 enzymes and together participate in many biological processes. Examination of E3s has revealed at least three distinct categories of these enzymes: the HECT (homologous to E6-AP carboxyl-terminus)-domain E3s, the RING (really interesting new gene) finger E3s, and the U-box domain E3s (323). As discussed below, the differences between these

Figure 1.5 NMR derived model of the Mms2•Ub-Ubc13~Ub complex.
Ub (red ribbon, bottom) is linked to the active site cysteine residue (yellow) of Ubc13 (cyan, bottom) via a thiolester bond. Ubc13 forms a strong heteromeric complex with the UEV Mms2 (gold, top), which non-covalently interacts with another Ub (red ribbon, top). The Lys63 residue of this Ub is positioned in close proximity to the Gly76 residue of the thiolester liked Ub to facilitate the formation of a Lys63 linked Ub chain.

categories exist in the mechanism of Ub transfer to a substrate. The HECT domain E3 contributes catalytically by forming a thiolester bond between its catalytic cysteine residue and the carboxyl-terminus of Ub, and subsequently transfers the Ub to a substrate. The RING finger and the U-box domain E3s, which do not have a catalytic cysteine residue, primarily function as molecular scaffolds between the substrate and the E2 enzyme, allowing the E2 to transfer the Ub to the substrate (155, 156, 188).

1.1.5a HECT-domain E3s

The highly conserved HECT domain consists of approximately 350 amino acid residues, which include the catalytic cysteine residue at approximately 35 residues from the carboxyl-terminal end. Structural studies have revealed insight into the mechanism of HECT domain function (440). The first crystal structure solved was that of the HECT domain of the E6-associated protein (E6-AP) in complex with its interacting E2, UbcH7 (Figure 1.6A) (181). This structure revealed two distinct regions within the HECT domain: an amino-terminal and carboxyl-terminal "lobe". Together, these lobes form an L structure with the α-helical rich amino-lobe sitting at the bottom and the carboxyl-lobe standing upright. The E2, UbcH7, interacts with the far end of the amino-lobe on the opposite side of the carboxyl-lobe, and the active site cysteine residue sits near the amino- and carboxyl-lobe junction approximately 41 Å from the E2. This structure alone did not provide information into how Ub thiolester would be transferred from the E2 to the E3 active site, but did suggest that major structural rearrangements must occur for it to happen.

A second structural study of a different HECT domain E3, WWP1/AIP5, revealed information on how Ub might be transferred (405). This study showed that the structurally conserved amino- and carboxyl-lobes could exist in an upside down T shaped structure, with the carboxyl-lobe packed against the amino-lobe (Figure 1.6B). This study showed that there is flexibility in the hinge loop connecting the two lobes, and that this is required for catalytic activity. Many possible models of how the HECT domain might function can be proposed by comparing the two structures (Figure 1.6C). One model, known as the "sequential addition" model, proposes that the carboxyl-lobe shifts over far enough over to accept an Ub from the E2, and subsequently rotates over to the other side

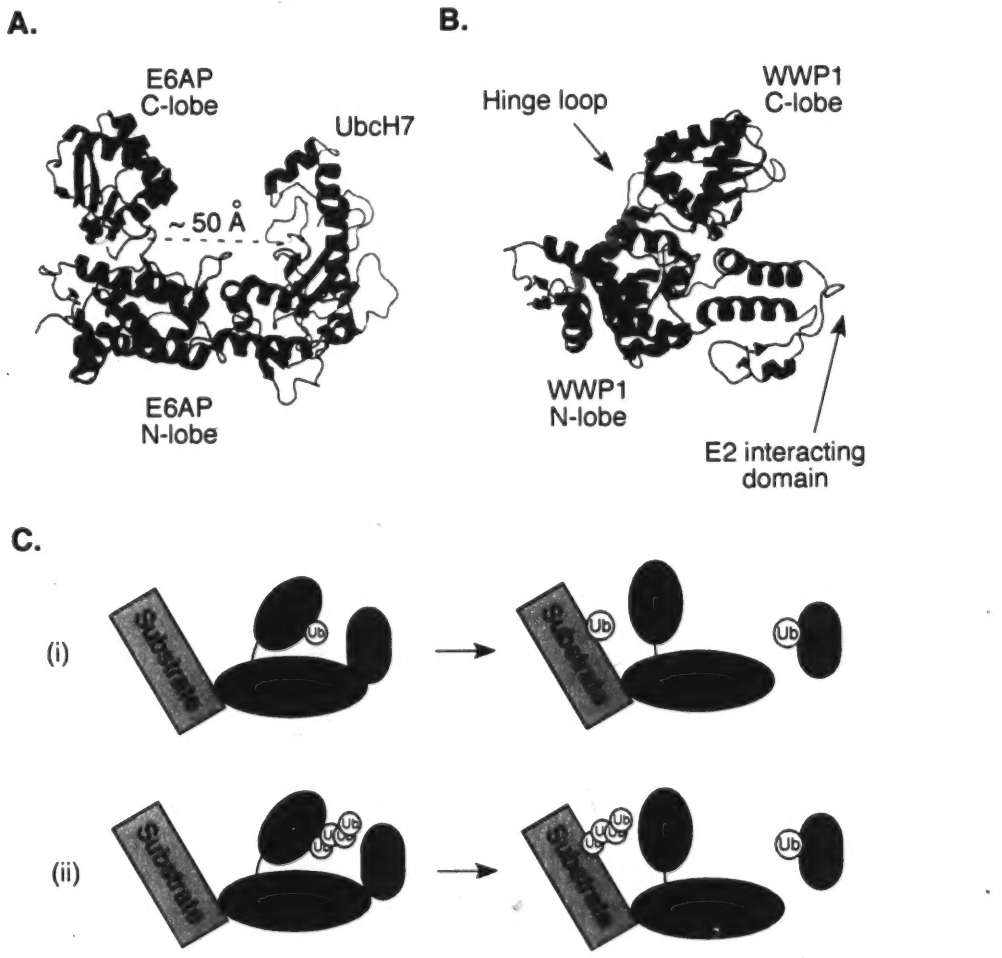

Figure 1.6 The proposed mechanism of HECT domain E3s based on structural studies.
(A) Ribbon diagram displaying the three-dimensional structure of the E6AP HECT domain E3 (shown in blue) in complex with the UbcH7 E2 (shown in red). The catalytic cysteine residue found within E6AP and UbcH7 are shown in yellow. Also indicated are the amino- and carboxyl-terminal lobes of E6AP, which are positioned in an L shape. **(B)** Ribbon diagram showing the three-dimensional structure of the HECT domain E3 WWP1/AIP5 with its catalytic cysteine residue is highlighted in yellow. The amino- and carboxyl-terminal lobes of WWP1/AIP5 are positioned in an upside down T shape. **(C)** Two proposed mechanisms of HECT domain E3 catalysis of poly-ubiquitin chains: (i) The sequential addition model proposes that the carboxyl-lobe shifts back and forth from the E2 to the substrate, sequentially adding multiple Ubs to assemble poly-Ub chains; (ii) The indexation model proposes that the carboxyl-lobe shifts over and positions the bound Ub so that the E2 can catalyze the formation of poly-Ub chains onto the E3~Ub. The carboxyl-lobe can then shift over and transfer the entire chain onto the substrate

of the amino-lobe and transfers that Ub to a bound substrate. Sequential addition of multiple Ubs can then occur in the same manner to build poly-Ub chains (405). An alternate model is the "indexation" model, which proposes that the carboxyl-lobe shifts over to allow for the transfer of Ub thiolester. In a ratchet like manner it can then position the bound Ub so that the E2 can catalyze the formation of poly-Ub chains onto the E3~Ub. The carboxyl-lobe can then shift over and transfer the entire chain onto the substrate (405). The advantage of this model is that it would be much more efficient than "sequential addition" as the carboxyl-lobe is not required to flip back and forth between the E2 and the substrate. Other models can also be proposed such as one that would involve the E2 enzyme assembling distinct poly-Ub chains that can be passed on the E3. However, since very little information on the mechanism of Ub transfer exists a favored model remains to be determined.

1.1.5b RING finger E3s

Probably the most widespread type of E3 enzymes have RING finger domains. This domain is the fifteenth most common domain in humans and the twelfth most common domain in budding yeast that is known. It is defined by approximately 50-60 amino acid residues (mostly histidines and cysteines: $CX_2CX_{(9-39)}CX_{(1-3)}HX_{(2-3)}C/HX_2CX_{(4-48)}CX_2C$) that co-ordinate two Zn^{2+} ions in a cross brace arrangement (Figure 1.7A) (196). This domain was originally thought to act catalytically by positioning the two Zn^{2+} ions in a manner that can stabilize the oxyanion tetrahedral intermediate in the isopepetide formation of Ub. However, structural studies of numerous RING finger domain E3s have suggested that this is not the case, and rather that this domain functions as a molecular scaffold that can position the E2~Ub thiolester correctly for Ub transfer to the substrate (441, 442).

The types of RING finger E3s vary in nature, and can exist as either single- or multi-subunit complexes. The crystal structure of selected examples of these E3s has been determined, and from these studies both appear to function as molecular scaffolds. The structure of the single subunit c-Cbl in complex with the E2, UbcH7, suggests that c-Cbl positions the E2 into a relative close proximity with a target (Figure 1.7B) (442).

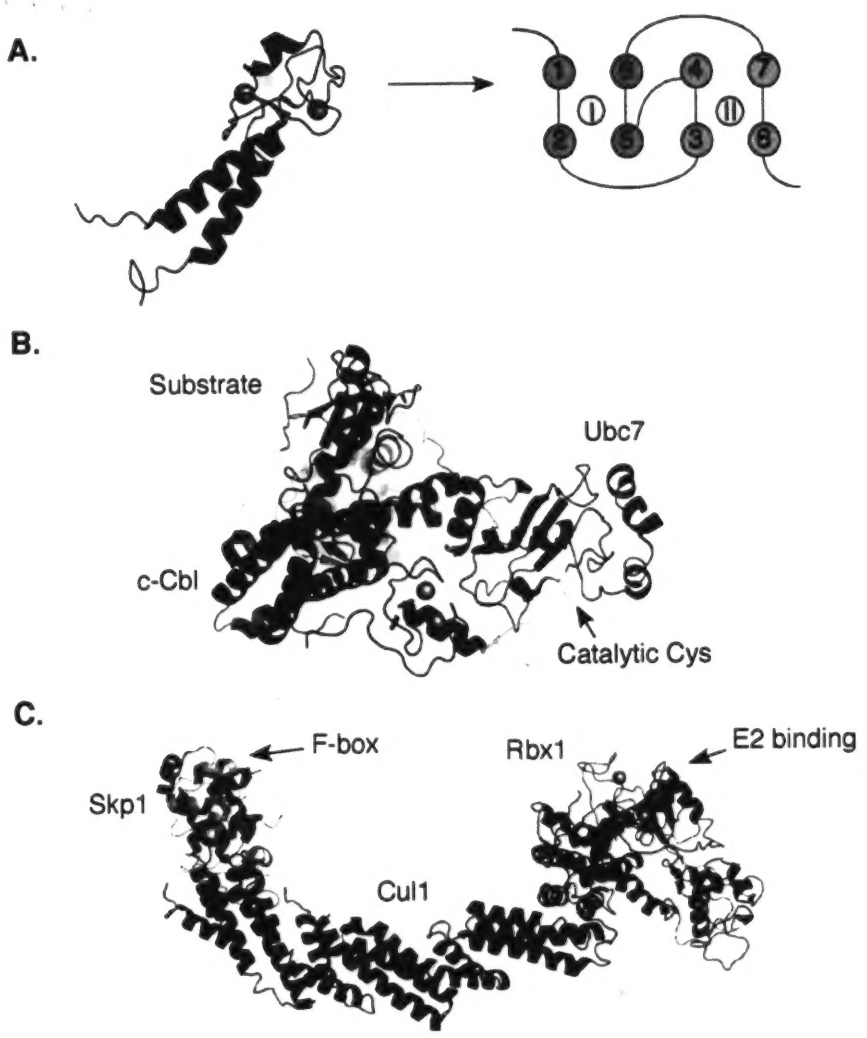

Figure 1.7 Structural insight into RING domain E3s.

(A) Ribbon diagram showing the three-dimensional structure of the RING domain of BARD1 (shown in blue). The RING domain is made up of cysteines/hystidines residues that coordinate two zinc atoms (shown as grey spheres) in a cross-brace arrangement. Displayed on the right is a representation of the cross-brace arrangement of eight cyseine/hystidine residues (1-8) coordinating two zinc atoms (I & II). **(B)** The three-dimensional structure of c-Cbl (shown in blue) in complex with UbcH7 (shown in red). The zinc atoms within the RING domain are shown as grey spheres. The position of substrate binding is shown in green, and the catalytic cysteine residue found within UbcH7 is highlighted in yellow. **(C)** The three-dimensional structure of the SCF complex. Rbx1 is shown in green, with the zinc atoms coordinated within the RING domain shown as grey spheres, Cul1 is shown in blue, Skp1 is shown in red, and an F-box domain is shown in orange.

However, the distance between the E2 and the substrate would not likely promote poly-Ub chain formation. Therefore, the mechanism of how Ub is transferred remains unclear.

The RING domain is capable of homo- or hetero-associating with other RING domains. In certain circumstances these RING domain complexes function more efficiently than the monomers. A well-characterized example of this is the tumor suppressor BRCA1-BARD1 complex, which hetero-associates through the two respective RING domains (39). The complex possesses much higher E3 activity than the individual subunits alone (154). Interestingly, it has been shown that only the RING domain of BRCA1 within this complex interacts with the E2, raising questions into the mechanism of the RING complex function (38).

There are a number of multi-subunit RING finger E3s that possess only one RING finger domain containing protein. The best studied are the anaphase-promoting complex (APC), the SCF complex and the SCF related complexes. The common feature between these multi-complex E3s is that they possess a RING domain protein that associates with a protein containing an evolutionarily conserved cullin domain. The cullin together with the RING finger protein assembles a core complex, which together with an E2 can promote the assembly of poly-Ub chains (365, 391).

The prototype member of the cullin family is the Cul1 (known as Cdc53 in budding yeast) subunit of the SCF complex (83, 216, 247, 315). Although this complex has been implicated in a variety of events, an essential function is in cell cycle regulation, particularly at the G1-S phase transition (226, 342, 385). The structure of the Cul1 containing SCF complex demonstrates that Cul1 acts as a scaffold, connecting (via its amino-terminus) Skp1 and the F.box protein to (via its carboxyl-terminus which includes the cullin domain) the RING finger protein (Figure 1.7C) (441). In this manner, Cul1 places the F.box containing protein (which is involved in substrate recognition) within close proximity to the RING finger protein (which recruits the E2 enzyme). A very large number of F.box domain proteins exist, and they function to specifically interact with, and recruit, a variety of substrates for ubiquitination (18). The F.box domain itself is involved in the interaction with the Skp1 protein that in turn interacts with the cullin (18). Sometimes the F.box containing proteins will also contain another protein interacting domain, such as WD-40 domains or leucine rich repeats (LRR) that mediate their

interaction with the substrate (76). Commonly, phosphorylated proteins (sometimes found within a proline, glutamine, serine and threonine rich domain, known as the PEST motif (354)) have been shown to interact with F.box containing proteins, indicating other layers of regulation in the ubiquitination process.

Many substrates of the SCF are multiply phosphorylated. For example, the well-characterized substrate Sic1 requires a minimal number of phosphorylated residues for its efficient interaction with the SCF and subsequent ubiquitination (293). Structural and *in vivo* observations favor a model for the interaction of Sic1 with the F.box protein Cdc4 (293, 306). This model proposes that there is one binding site on the F.box protein for the phosphorylated substrate, and that the association rate between the two proteins depends on the neighboring sequence of the phosphorylated binding site. In such a manner, different substrates would have different association rates with the SCF. In the case of poorly associating substrates, however, increasing the number of phosphorylation sites would increase the local concentration of binding sites, therefore increasing the association rate. In such a manner, phosphorylation of the substrate would provide a highly regulated manner by which it would interact with the SCF. In fact, for Sic1 it has been shown that this method of regulation is essential for timing its ubiquitination and subsequent degradation during cell cycle progression (293, 306).

Although the structures of the c-Cbl and SCF complex RING finger E3s reveal some important characteristics, the mechanism by which they mediate poly-Ub chain assembly is unclear. Modeling of the E2 position in these structures places it approximately 60Å from the substrate-binding site on the E3s. Additionally, there is a lack of E3 residues in close proximity to the reaction site. Recent biochemical studies of the budding yeast SCF^{Cdc4} (Cdc4 being the F.box protein) complex and its interacting E2, Cdc34, have shed some light on this process (80). It was observed that the association rate between Cdc34 and the SCF is unaffected by the presence or absence of Cdc34~Ub thiolester. However, the dissociation rate constant between Cdc34 and the SCF increases when Cdc34~Ub thiolester is present. A model was proposed from these observations, which suggests that Cdc34~Ub thiolester is released from the SCF prior to the conjugation of Ub to a target. Therefore, the role of the SCF would be to increase the local concentration of the E2 in the vicinity of a substrate, thereby promoting the

assembly of poly-Ub chains. This model is supported by the observation that a mutation (F72V-Cdc34) that increases Cdc34's ability to interact with the SCF, and decreases its ability to disassociate from the SCF, is defective in the assembly of poly-Ub chains onto a substrate (80). These studies suggest that mechanistically the catalysis of poly-Ub chains is dependent largely on the E2, but do not provide insight into the transfer of Ub to the substrate.

Several other multi-protein RING domain containing E3s also exist. One such complex consists of the von-Hipple-Lindau (VHL) tumor suppressor protein, the elongin C/B dimer, Cul2 and Rbx1/Roc1 (205). This complex assembles similarly to the SCF with Skp1 being replaced by the elongin C/B dimer, which interacts with the SOCS (suppressors of cytokine signaling)-box containing VHL protein rather than with an F.box protein (206). SOCS-box containing proteins can vary within this complex, as the F.box protein does in the SCF, and are emerging as an important substrate recognition domain for these types of E3s (213). Another example of a related E3 is the complex of Cul3, Rbx1/Roc1 and a member of the BTB/POZ (bric a brac, tramtrack and broad complex/Pox virus and zinc finger) protein family (329). While the BTB/POZ domain resembles the F.box protein in its ability to recognize substrates, it binds directly to the cullin, Cul3 (116, 121, 329, 430). It seems that a large number of variations can occur from the well-characterized SCF complex and it remains to be seen if they interact with E2 enzymes and catalyze poly-Ub chains in a similar manner (328, 401).

The final RING finger E3 discussed here is the APC complex. This is one of the largest E3 enzymes known, and is composed of at least eleven subunits (Table 1.1) (319). Its most prominent role is in the regulation of the cell cycle, specifically mitotic entry and exit. The core ubiquitination domain of the APC consists of the RING finger protein Apc11 and the cullin containing protein Apc2 (391). However, *in vivo* the APC is only fully active when it assembles with Cdc20, Cdh1/Hct1, or related factors implicated in substrate recognition (411). Another important subunit of the APC is Doc1/Apc10. This subunit contains a domain known as the "DOC" domain, which is also found in other E3s, and may play an important role in poly-Ub chain assembly (136, 229). APC dependent ubiquitination relies on one of at least two poorly defined motifs present in the substrate known as the destruction box (D-Box: RxxLxxxN) and the KEN box

Table 1.1* APC subunits

Saccharomyces cerevisiae	*Schizosaccharomyces pombe*	Drosophila melanogaster	*Caenorhabditis elegans*	*Homo sapien*	Description
Apc1	Cut4	CG9198	mat-2/pod-3	Apc1/tsg24	
Apc2	SPBP23A.10.04	CG3060	K06H7.6	Apc2	Cullin, Scaffold, binds Apc11/E2s
Cdc27	Nuc2	cdc27	mat-1/pod-5	Cdc27	
Apc4	Cut20/Lid1	CG4350		Apc4	
Apc5	Apc5	CG10850/ida	M163.4	Apc5	
Cdc16	Cut9	cdc16	pod-6/emb-27	Cdc16/Apc6	
Cdc26	Hcn1			Cdc26	
Cdc23	Cut23	CG2508	mat-3	Cdc23/Apc8	
Apc9					
Apc10/Doc1	Apc10	CG11419	F15H10.3	Apc10	specificity factor
Apc11	Apc11	lmg	F35G12.9	Apc11	RING finger, recognition of E2s
Cdc20	Alp1	fzy	cdc20	Cdc20	APC activator/specificity factor
Cdh1/Hct1	Ste9	fzr, rap	fzr	Cdh1	APC activator/specificity factor
Ama1	Mfr1	OG14444	B0464.2	Apc7	Meiosis specific activator

* adapted from a table in ref. (147)

(KENxxxN) (136, 229). An important question remaining with regards to the APC is how its various subunits are assembled, which may provide us with a better understanding of its mechanism of action. A low-resolution structure of the human APC complex was determined by cryo-electron microscopy (Figure 1.8) (124). This structure displayed a complex arrangement of its proteins, which adopt a cage-like shape. From this structure it was proposed that the inner chamber might act as the catalytic center into which a substrate would enter. Further studies are required to define the composition of the APC and its mechanism of substrate recognition and poly-Ub chain assembly.

1.1.5c U-box domain E3/E4s

The first identified U-box domain protein involved in ubiquitination was the budding yeast Ufd2. This protein in conjunction with an E1, an E2 and an E3 was able to mediate poly-Ub chain assembly and was therefore originally termed an E4 enzyme (222). However, further studies have shown that U-box containing proteins can promote poly-Ub chain assembly in the presence of only an E1 and an E2 and thus were reclassified as novel E3s (155). U-box domain E3s appear to function in a similar manner to RING finger E3s in that they do not possess a catalytic cysteine residue, and most likely act by providing a scaffold between the substrate and the E2 enzyme.

The U-box is an evolutionarily conserved domain of approximately 70 amino acid residues that is present in a large number of proteins (155). It has sequence similarity to the RING finger domain, but noticeably lacks the essential cysteines and histidines that chelate the Zn^{2+} ions that stabilize the RING domain. The NMR determined structure of the U-box domain is very similar to the RING finger domain (Figure 1.9) (304). However, rather than Zn^{2+} binding sites supporting the cross-brace arrangement found in the RING finger, a hydrogen bonded network exists within the U-box to mediate structural stability and activity of the protein. A comparison between the U-box and RING finger domains suggests a structurally conserved surface involved in mediating the interaction with E2 enzymes. Therefore for all the differences that exist between the U-box and RING finger domains, there appears to be a common mechanism of function.

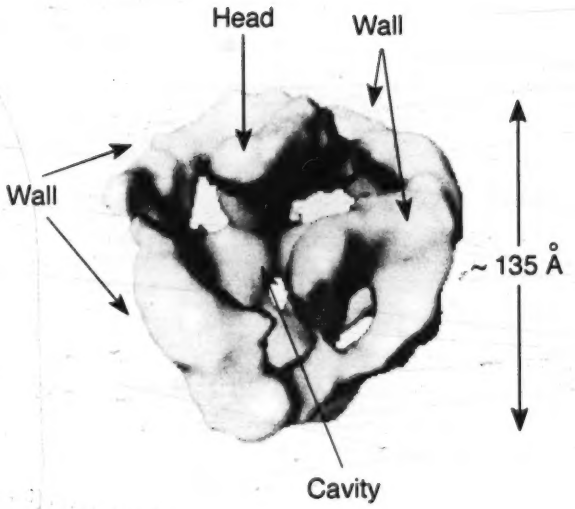

Figure 1.8 The low resolution structure of the APC complex.
A 24 Å structure of the anaphase promoting complex as determined by cryo-electron microscopy. The most prominent features and size of the complex are indicated.

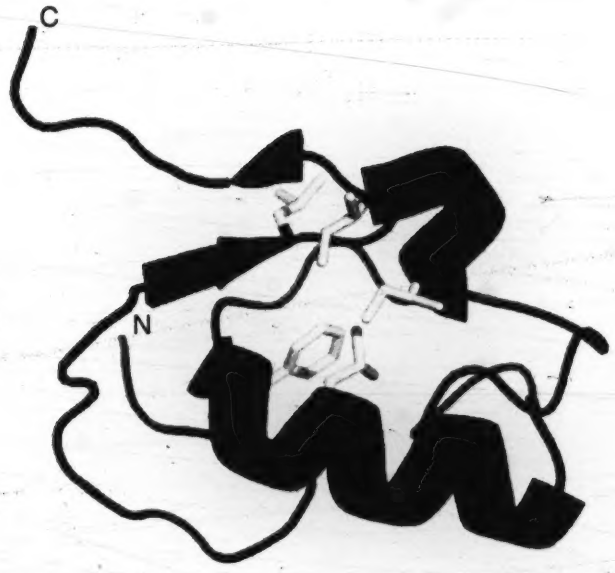

Figure 1.9 Structure of the ubiquitin-ligase U-box domain.
A ribbon diagram of a U-box domain is shown based on the NMR analysis of the *S. cerevisiae* pre-mRNA splicing factor Prp19. Core hydrophobic residues that mediate the structural stability of the U-box domain are highlighted in yellow, and the amino (N)- and carboxyl (C)-terminal ends are indicated.

1.1.6 Poly-ubiquitin chains

Seven surface lysine residues that can allow the assembly of poly-Ub chains are present on Ub (Lys6, Lys11, Lys27, Lys29, Lys33, Lys48 and Lys63). All seven types of chains have been detected *in vivo*, and the potential for differential signals by the formation of varying lengths and linkages of poly-Ub chains are exponential (316).

The best understood are Lys48 linked poly-Ub chains, which typically target the substrate protein for 26S proteasomal degradation (171). However, in addition to targeting for proteasomal degradation, these chains also have a multitude of other biological effects, such as transcriptional regulation and signal transduction (249, 292, 387). The minimal length for proteasomal targeting has been suggested to be a chain of 4 Ubs (Ub_4) (394). The structures of varying lengths of Lys48 linked chains have been determined using both crystallographic and NMR methodologies (67, 68, 322, 403, 404). However, each structure is distinct from the other, suggesting that the Lys48 linked Ub chain structure is flexible. Recent NMR analysis of di-Ub chains (Ub_2) and Ub_4 suggests that poly-Ub chain conformation depends on the solution environment (404). Under physiological conditions, Ub_2 and Ub_4 Lys48 linked chains adopt specific conformations. Ub_2 was shown to adopt a "closed" structure, with its surface exposed hydrophobic residues (Leu8, Ile44, Val70) contained within the interaction interface, while still being accessible for direct interactions with recognition factors (Figure 1.10A). This study also suggested that the distal two Ubs in Ub_4 also adopt a similar conformation. Together, these studies have led to a hypothesis that the orientation of Ub's hydrophobic residues mediate interactions with trans recognition factors.

Recent progress has been made in the understanding of the assembly of Lys63 linked poly-Ub chains. Synthesis of these chains does not appear to target substrate proteins to the 26S proteasome, but rather to have various signaling properties (387). Examples include NF-κB signal transduction (81, 415), post-replicative DNA repair (173, 383), ribosome function (382), stress response (14), mitochondrial DNA inheritance (109), and endocytosis (117, 384). Recent structural analysis of an Ub_2 linked Lys63 linked chain was performed in solution using NMR methodologies (403). Under physiological conditions, this structure displayed an extended "open" conformation with no direct contacts between the hydrophobic residues (Leu8, Ile44, and Val70) in the Ub

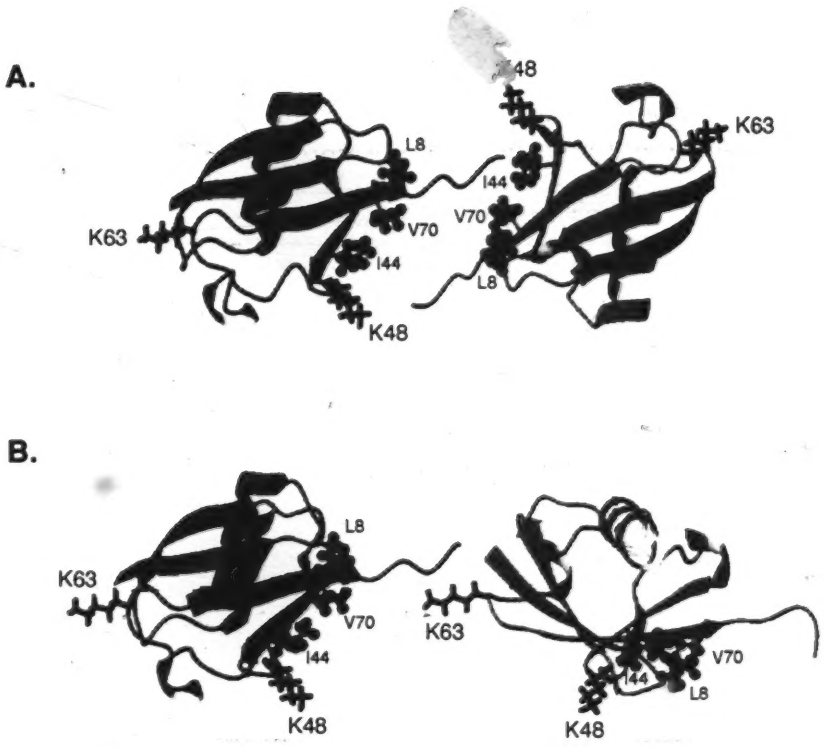

Figure 1.10 NMR derived models of Lys48 and Lys63 linked di-Ub chains.
Representations of the **(A)** "closed" conformation of Lys48 linked di-Ub , and **(B)** the "open" conformation of Lys63 linked di-Ub at neutral pH in solution. The side chains of the hydrophobic residues Leu8, Ile44, and Val70 are shown as spheres. Also shown (in red) are the side chains of Lys48 and Lys63 residues. Figure was adapted from ref. (403,404).

chains (Figure 1.10B). This differs from the interlinked "closed" domain created by the hydrophobic residues in the structure of the Lys48 linked chain (Figure 1.10A vs. B). Both Ubs in the Lys63 linked di-Ub chain were capable of interacting with an Ub-associated (UBA) domain that can be found in many Ub-interacting proteins in a similar manner to mono-Ub. However, these Ubs were shown to bind with much less affinity than Lys48 linked di-Ub, suggesting a functional relevance for the "open" and "closed" conformations of the chain. As mentioned above, Lys63 linked chains are assembled by a complex of the E2 Ubc13, and one of many ubiquitin-conjugating enzyme variants (UEV) proteins, such as Mms2. Structural analysis has shown that this complex positions two Ubs, one linked to Ubc13 by a thiolester bond, and the other non-covalently interacting with the UEV in a manner such that its Lys63 is positioned in close proximity to the carboxyl-terminal Gly76 of the thiolester bound Ub (271, 272, 286, 402). This is the first structural analysis describing poly-Ub chain assembly and it remains to be determined if other types of Ub chains are assembled in a similar manner.

Poly-Ub chains of Lys6, Lys11, Lys27, Lys29 and Lys33 have also been observed both *in vivo* and *in vitro* (14, 262, 316, 433). The E2 UbcH5A together with the HECT domain E3 KIAA10 have been observed to assemble Lys29 linked Ub chains (262, 433). Two high affinity interacting proteins of Lys29 linked Ub chains have also been observed in budding yeast lysates, further demonstrating a biological role for this linkage (352). Additionally, the BRCA1-BARD1 tumor suppressor complex assembles Lys29 as well as Lys6 linked Ub chains (298). Auto-Ub chains formed onto BRCA1 *in vivo* are composed primarily of Lys6 linked chains and these chains are recognized by the 26S proteasome, where they are deubiquitinated rather than targeting the substrate for degradation (298). As for Lys11, Lys27 and Lys33 linked Ub chains, they have only been observed *in vivo* by mass spectrometry analysis, and little is known about their formation and function (316). The importance of ubiquitination, combined with the variety of Ub chain linkages, clearly demonstrates the need for further examination of poly-Ub chain assembly.

1.1.7 Ubiquitin-binding and related motifs

The signaling properties of Ub are primarily carried out by its specific interactions with other proteins. The discovery of a variety of distinct Ub-binding domains, together

with domains structurally resembling Ub, has shed some light into these processes. Characterized Ub-binding motifs include the Ub-associated (UBA) motif, the CUE (similar to a domain of the yeast Cue1 protein) domain, and the Ub-interacting motif (UIM) (40, 246). The UBA domain is composed of approximately 45 amino acid residues that was originally identified in Ub pathway proteins (such as E2s and E3s) (174). Its function in binding to Ub has been well established, but its specificity to distinct Ub chain linkages and length is under debate. Structural analysis of many of these domains shows a conserved large hydrophobic patch within a similarly folded domain (57, 85, 289, 426). This hydrophobic patch has been predicted to interact with the hydrophobic surface of Ub (which includes Leu8, Ile44, Val70). These UBA domains have been implicated in a number of processes, including both recruitment and sequestering Lys48 linked poly-Ub chains to and from the 26S proteasome (214, 290).

Structural analysis of the approximately 40 residue CUE domain demonstrated that it has a similar overall architecture to the UBA domain. NMR analysis of this domain in complex with Ub revealed a conserved hydrophobic patch within the CUE domain that interacts with the hydrophobic patch on Ub as predicted for the UBA domain (207).

The well conserved 15 residue UIM domain has been found in a number of different proteins, including numerous proteins involved in endocytosis (29, 330), proteasomal subunits (281, 434), E3s, and deubiquitinating proteins (353). UIMs of endocytic proteins have been observed to play a role in binding to, and promoting the formation of mono-ubiquitinated targets. Proteasomal UIMs have been shown to interact with poly-Ub chains, whereas other UIMs have been shown to play a role in promoting the assembly of poly-Ub chains. Multiple UIMs are often found in proteins, and it appears that varying numbers of UIMs exhibit different binding properties to ubiquitinated targets. Structural analysis of a double UIM motif within the proteasomal S5a subunit revealed an α-helix that is stabilized by an unexpected amino-terminal hairpin turn, which contributes to its Ub binding affinity (115).

Various proteins contain domains with similarity to Ub, and are divided into either Ubls (as described in section 1.1.2) or non-conjugatable Ub domain proteins (UDPs) (150). Proteins that contain UDPs often are large poly-domain proteins. Two classes of UDPs have been described: (i) the UBQ domain, defined by a stretch of

approximately 45-80 residues with homology to Ub, is commonly involved in binding to the 26S proteasome; (ii) the UBX domain, which is approximately 80 residues and commonly found at the carboxyl-terminus of a number of proteins (41). The general function of the UBX domain remains unclear. These domains together with the Ub-binding motifs provide an attractive mode of protein-protein interactions.

1.1.8 The 26S proteasome

The 26S proteasome is a highly conserved 2.5 MDa eukaryotic complex that is composed of approximately 31 different subunits (28, 324, 412). This complex catalyzes the degradation of the majority of proteins in the cell. The subunits of the proteasome form a 20S barrel-shaped core (the 20S core) that is capped at one or both ends by a 19S regulatory complex (19S cap). The 20S core is the proteolytic center of the complex that catalyzes protein degradation, whereas the 19S caps are the substrate recognition components of the complex. The 20S core is composed of structurally similar rings: the outer α-rings, which mediate the interactions with the 19S caps, and the inner β-rings, which form a proteolytic chamber (135, 223, 421). Cleavage of peptide bonds occurs within this chamber and typically peptides of approximately seven to nine residues are generated, which are then hydrolyzed by downstream peptidases or are recycled to be presented as antigens, such as those presented by MHC class I antigens (344). Much of the enzymatic mechanism along with the structure and composition of the 20S core has been elucidated. However, the mechanism of action of the 19S caps remains more elusive.

It is the 19S caps that perform the regulatory function of the proteasome, which includes the recognition of substrates (primarily through the recognition of attached Lys48 linked poly-Ub chains), removal of poly-Ub chains from the substrate (as Ub is not degraded, but rather is recycled), as well as unfolding and translocation of the substrate into the 20S core (22, 107, 327). The 19S caps can be further sub-divided into lid and base complexes based on these functions. The base complex is composed of the proteasome ATPase subunits, which are thought to perform the unfolding and translocation function of the cap. The lid complex is made up of the Ub recognition factors and the deubiquitinating activity of the proteasome (19, 33, 126, 177, 386). A

low-resolution structure determined by electron microscopy has provided an outline of the 19S caps together with the 20S core, but the arrangement of the subunits within the 19S cap is unclear (1).

1.1.9 De-ubiquitinating enzymes

Enzymes that are capable of catalyzing the removal of a covalently linked Ub protein from either a substrate protein or a poly-Ub chain have been known for some time. However, only recently has significant insight been made on the functions of these de-ubiquitinating enzymes (6, 379). The nature of ubiquitination relies on the function of de-ubiquitinating enzymes in many respects. Ub has the distinct feature of being encoded as a fusion protein to either itself or a ribosomal subunit, and it is the function of de-ubiquitinating enzymes to process this Ub fusion protein into individual Ubs. De-ubiquitinating enzymes also play an essential role in removing poly-Ub chains from substrates prior to their proteasomal degradation. Furthermore, many processes regulated by Ub are dynamic in nature, and require a balance of Ub-conjugation and de-ubiquitination to ensure proper cellular function. A large number of genes encode de-ubiquitinating enzymes, suggesting that these functions are specific and highly regulated. Analysis of the various de-ubiquitinating enzymes has allowed for their classification into several groups, which include the Ub carboxyl-terminal hydrolases (UCH), the Ub processing proteases (UBPs) and metalloproteases (also known as the JAMM family of hydrolases) (425).

The UCHs contain four conserved motifs of approximately 200 residues. Structural analysis has revealed that the UCH active site is composed of a critical cysteine and glutamine residue from one motif, and histidine and aspartic acid residues from another motif (198, 199). Together they act catalytically to effectively attack the Ub-linked peptide bond in a similar manner to that of cysteine proteases. Specificity for Ub is achieved by a conformational change that occurs once the enzyme binds to an ubiquitinated target.

Many, and possibly all, UBPs remove Ub conjugates off specific proteins. The UBP HAUSP is a well-studied member of this group, as it functions to modulate the stability and function of the tumor suppressor protein p53 (243). Structural analysis of the

approximately 40 kDa catalytic core of HAUSP has revealed important insight into the function of UBPs (178). This catalytic core has a palm, thumb and finger-like hand structure that coordinates the targeted Ub in a manner such that its carboxyl-terminus is placed near the active site of the enzyme (between the palm and thumb). Despite their overall differences, UBPs employ a very similar catalytic mechanism to UCHs.

Metalloprotease de-ubiquitinating enzymes have very little homology to UCHs and UBPs, and as such were not discovered until recently. Two such proteins have been characterized: Jab1/Csn5 (a component of the COP9 signalosome that is involved in removing Nedd8 from cullin proteins) and Rpn11 (a non-ATPase subunit of the lid complex of the 26S proteasome involved in de-ubiquitinating proteins prior to their degradation) (71, 407). These enzymes depend on a conserved histidine, aspartic acid and glutamic acid triad (known as the JAB1/MPN domain metalloenzyme or JAMM motif) that is similar to the metal binding active site of hydrolytic enzymes. A crystal structure of a related bacterial JAMM motif revealed that the conserved histidine and aspartic acid residues coordinate a zinc, whereas the glutamic acid hydrogen bonds with water (5). From this it was suggested that the glutamic acid might act as an acid-base catalyst in the attack of the Ub peptide bond.

1.2 Ubiquitin and the budding yeast cell cycle

Eukaryotic cell division entails a highly complex series of coordinated events that are collectively known as the cell cycle. These events are highly regulated and many backup mechanisms exist to ensure their faithful execution. The eukaryotic cell cycle is commonly divided into four "phases": G1 phase, S phase (in which DNA replication takes place), G2 phase and M phase (in which chromosomal and cellular separation takes place) (301). The irreversible nature of the cell cycle ensures the faithful execution of only one stage of chromosomal replication and segregation.

The first well-characterized mode of cell cycle regulation was the discovery of a factor that could stimulate the initiation of meiotic entry of frog oocytes (264). This was called the "maturation promoting factor" or MPF, and was later found to be composed of a protein know as a "cyclin". Cyclins were originally identified as proteins that were

periodically expressed and degraded in rapidly dividing sea urchin embryos (104). The timely expression and degradation of these proteins, which were termed "cyclins", was essential for cell cycle progression. Cyclins were later shown to be crucial regulatory subunits of serine/threonine protein kinases known as cyclin-dependent kinases (CDKs) (277, 288). Together these complexes were observed to regulate many of the essential events in the cell. The instability of cyclins during cell cycle progression suggested a regulated mechanism of proteolysis, which led to the discovery of a role for the Ub pathway in cell cycle regulation (127). The Ub pathway rapidly emerged as one of the prominent cell cycle regulatory mechanisms. Many studies over the years have compiled an extensive list of cell cycle protein targets by the Ub pathway (some examples are shown in Table 1.2) (342). In most cases these ubiquitinated proteins are subsequently degraded by the 26S proteasome, thus ensuring the unidirectional progression through the four phases of the cell cycle.

Many of the processes in the cell cycle are highly conserved in all eukaryotic cells. One of the simplest and best-characterized eukaryotic organisms is the budding yeast *S. cerevisiae*. The genome of *S. cerevisiae* is one of the best studied of all eukaryotes. Description of its approximately 5700 genes, together with the ease of its genetic manipulation has facilitated its study (113, 209). This in combination with many high-throughput approaches, pioneered utilizing *S. cerevisiae* cells, has promoted a more comprehensive study of numerous biological processes (227). As with other higher eukaryotic systems, *S. cerevisiae* cells have a cell cycle composed of four phases: G1, S, G2 and M (Figure 1.11A). Many of the regulatory proteins required for cell cycle progression are functionally conserved, including cyclin-CDKs (Figure 1.11B) and Ub pathway proteins. As such, the study of *S. cerevisiae* has helped in the discovery and understanding of many of the regulatory events of the cell cycle. For these reasons this section focuses mainly on *S. cerevisiae* proteins and their contributions to cell division.

1.2.1 START and the G1-S transition

The life cycle of a yeast cell normally alternates between a homothallic (haploid) and heterothallic (diploid) state (165). Mating of two haploid cells of opposite mating types (MATa and MATα) results in the formation of a diploid yeast cell (a/α). The yeast

Table 1.2 Cell cycle ubiquitination targets

SCF targets	Organism	Targeting subunit	Function
Sic1/Rum1	S.c./S.p.	Cdc4/Pop1,2	G1/S inhibitor
Far1	S.c.	Cdc4	G1/S inhibitor
Cdc6/Cdc18	S.c., S.p.	Cdc4/Pop1,2	DNA replication
Swe1	S.c.	Met30(?)	mitosis inhibitor
Cln1	S.c.	Grr1	G1 cyclin
Cln2	S.c.	Grr1	G1 cyclin
Gic2	S.c.	Grr1	budding
Cyclin E	H.s, D.m.	Cdc4/Ago	G1/S cyclin
p27/Kip1	H.s., M.m.	Skp2	G1/S inhibitor
p21/Cip1	H.s.	Skp2	G1/S inhibitor
p130	H.s., M.m.	Skp2	G1/S inhibitor
Orc1	H.s.	Skp2	DNA replication
Emi1	M.m.	β-TrCP	APC inhibitor
Wee1	X.l.	Tome-1	mitosis inhibitor
APC targets	**Organism**	**Targeting subunit**	**Function**
Pds1/Securin	H.s., S.c., others	Cdc20	anaphase inhibitor
Clb2	S.c.	Cdc20, Cdh1	mitotic cyclin
Clb5	S.c.	Cdc20	S-phase cyclin
Cyclin A	metazoan	Cdc20, Cdh1	S-phase/mitotic cyclin
Cyclin B	metazoan	Cdc20, Cdh1	mitotic cyclin
Cdc20	S.c, H.s.	Cdh1	mitosis
Cdc5/Plk	S.c, H.s.	Cdh1	mitosis
Aurora A	H.s.	Cdh1	mitosis
Dbf4	S.c	Cdc20	S phase
Ase1	S.c.	Cdh1	mitotic-spindle dynamics
Nek2A	H.s.	Cdh1	centrosome development
Cdc6	S.c., H.s.	Cdh1	DNA replication
Geminin	metazoan	Cdh1	DNA replication
Cin8/Kip1	S.c.	Cdh1	mitotic-spindle motor
Xkid	X.l.	Cdh1	mitotic-spindle motor
Hsl1	S.c.	Cdc20, Cdh1	G2/M transition
Skp2	H.s.	Cdh1	SCF component

S.c. (*Saccharomyces cerevisiae*), S.p. (*Schzosaccharomyces pombe*), D.m. (*Drosophila melanogaster*), H.s. (*Homo Sapien*), M.m. (*Mus musculus*), X.l. (*Xenopus laevis*)

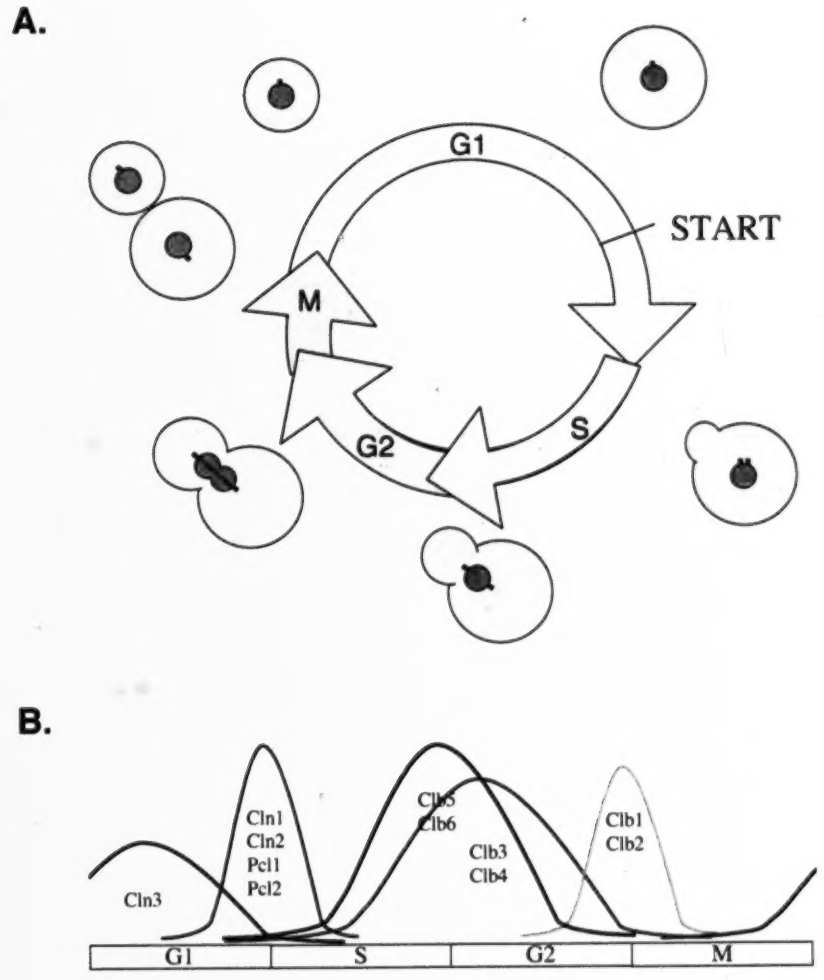

Figure 1.11 The Saccharomyces cerevisiae cell cycle.

(A) Displayed are the four phases of the cell cycle: G1, S, G2 and M phases. A critical signal within the G1 phase, known as START, irreversibly commits the cell to proceed through the cell cycle. The general morphology of the cells is shown, with the nucleus in dark grey and the SPBs in black. Also shown in black are the mitotic spindles. **(B)** The levels of cyclin activity throughout the cell cycle are shown.

cycle entails both periodic and continuous events that can be distinguished into intimately coupled pathways for budding, spindle pole body (SPB) replication and separation, DNA replication and division, and cytokinesis. The periodicity of these events is largely dependent on the timely expression and repression of genes coupled together with the activation and programmed proteolysis of their gene products. More than 800 of the approximately 6200 open reading frames are part of sequentially activated bursts of transcription, which occur periodically to form an intertwined network of transcription to drive the cell cycle (Figure 1.12) (58, 381).

The decision for a yeast cell to divide is made in the G1 phase of the cell cycle. It is during this stage that the cell senses its environment for favorable growth conditions (such as sufficient nutrients and lack of cellular stress). If conditions are not favorable, yeast cells may exit the mitotic cell cycle and enter either a stationary phase known as G0 (haploid yeast cells), or a meiotic cycle ultimately leading to the formation of spores (diploid yeast cells) (101, 134). Stationary phase cells have a thickened cell wall, accumulated carbohydrates, and acquired thermotolerance, allowing them to survive for a long time in the absence of nutrients (134). Similarly, meiotically formed spores are contained within a durable ascus, and each spore has undergone chromosomal recombination during meiosis, thus favoring adaptation to adverse environmental conditions (101, 320). Both stationary cells and spores enter the mitotic cell cycle once environmental conditions are favorable.

A cell in the G1 phase of the cell cycle continues growing until it reaches a critical cell size. The cell subsequently proceeds through a stage known as START (analogous to the "restriction point" in mammalian cells) at which it is irreversibly committed to replicate its DNA and divide into two cells (77, 151, 350). Signaling to proceed through START requires the proper coordination of a number of signal transduction networks. The interconnectivity of these networks synchronizes the execution of DNA replication, budding and SPB duplication together with changing intracellular and extracellular environmental conditions. The G1 cyclin Cln3 together with Cdc28/Cdk1 (the only essential CDK present in budding yeast) is thought to be one of the primarily mediators of START signaling (86, 88).

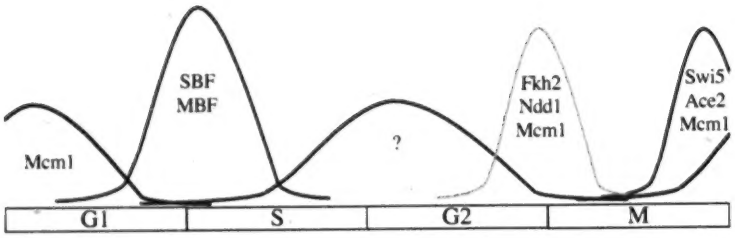

Figure 1.12 Waves of cell cycle transcription in *S. cerevisiase* cells.

The major transcription factors responsible for driving the waves of cell cycle transcription. The heights of the waves are approximately proportional to the number of genes induced at the particular stage of the cell cycle.

Coincident with START, a transcriptional burst of approximately 120 genes occurs that is mediated primarily by two transcription factors: the SBF (composed of the Swi4 and Swi6 proteins) and the MBF (composed of the Mbp1 and Swi6 proteins) (87, 176, 187, 221, 284, 285, 294). These two transcription factors induce the expression of many genes required for the G1 to S phase transition. The expression of genes include those required for DNA replication, SPB duplication, cell wall biogenesis, budding and the next wave of cell cycle transcription that occurs at the G2-M phase transition (176, 187). Genes within the G1 transcriptional burst encode the G1 cyclins Cln1 and Cln2 (that act together with Cdc28), the G1 cyclins Pcl1 and Pcl2 (that act together with another CDK known as Pho85), as well as the S-phase cyclins Clb5 and Clb6 (that act together with Cdc28) (285, 303).

Cyclin-kinase inhibitor proteins (CKIs) are important regulators of cell cycle progression, particularly at the G1-S phase transition (277, 361). One of the best-characterized CKI is Sic1, which inhibits Clb-CDK activity. *SIC1* is transcriptionally induced during mitotic exit, leading to the inhibition of the mitotic Clbs (Clb1-, Clb2-, Clb3- and Clb4-Cdc28 complexes) and driving the cells out of mitosis and into the G1 phase of the cell cycle (this will be discussed further in 1.2.3) (220, 361). Sic1 maintains the cells in G1 phase by inhibiting the activity of the S-phase Clb5- and Clb6-Cdc28 kinases, thereby preventing the onset of DNA replication. The cell proceeds into S-phase by targeting Sic1 for Ub-mediated proteolysis (361).

The signal for Sic1 ubiquitination is accomplished through its phosphorylation by the G1 cyclin-CDK complexes (primarily by the Cln1-, Cln2- and Cln3-Cdc28 kinases, and partially by the Pcl1- and Pcl2-Pho85 kinases) (86, 299, 398). The phosphorylation of Sic1 allows for its association with the F.box protein Cdc4, which is a subunit of the SCF Ub-ligase. The SCF together with the E2 enzyme Cdc34 (Cdc34/SCF) assemble poly-Ub chains onto Sic1 subsequently targeting it for proteasomal degradation (106, 361, 408). Substitution of the phosphorylation sites within Sic1 dramatically stabilizes the protein and causes a growth arrest resulting in the accumulation of 1N DNA content (406). Additionally, Sic1 stabilization causes uncoupling of DNA replication and budding, resulting in multiple rounds of budding and an elongated multi-budded morphology for these cells (Figure 1.13). It is thought that the delayed timing of the G1-S

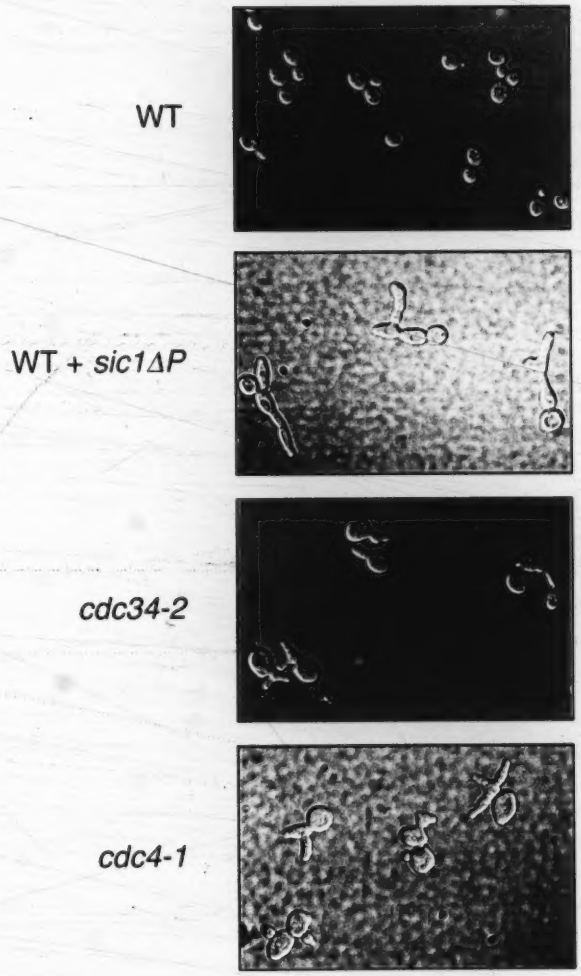

Figure 1.13 Morphological effects of Sic1 stabilization in *S.cerevisiae* cells.
The morphology of wild-type (WT) growing cells are shown at the top. Also shown are the elongated multi-budded morphologies resulting from the stabilization of Sic1 in WT cells expressing *sic1ΔP* (a derivative of Sic1 with with alanine substitutions at potential CDK phosphorylation sites) (ref. 394) , or from *cdc34-2* or *cdc4-1* temperature sensitive mutants growing at their non-permissive temperature. Images were taken with 100X DIC microscopy.

phase transition is partially accomplished through a mechanism that requires a threshold of Sic1 phosphorylation. As the cell proceeds through G1, Sic1 becomes more phosphorylated (particularly at the G1-S transition, where Cln activity is high), thereby increasing the affinity for its interaction with the Cdc4 F.box component of the Cdc34/SCF complex (293, 406).

The Cdc34/SCF complex is one of the central regulators of the G1-S phase transition. Temperature sensitive (TS) mutations of the Cdc34/SCF complex were originally identified in screens for cell cycle mutants (95, 265, 296, 365). At their restrictive temperature, these cells display a cell cycle arrest with an accumulation of 1N DNA content and replicated but undivided SPBs. Furthermore, these mutants have an elongated multi-budded morphology that is characteristic of Sic1 accumulation (Figure 1.13). Deletion of the *SIC1* gene suppresses these phenotypes. For instance, *cdc34-2 sic1Δ* cells are capable of DNA replication and do not display an elongated multi-budded morphology (361). However, despite the deletion of *SIC1*, Cdc34/SCF ts cells still display growth defects and accumulate with 2N DNA content, suggesting additional essential roles for this complex in cell cycle regulation.

Many key cell cycle targets other than Sic1 have been characterized for the Cdc34/SCF complex, most of which are involved in the regulation of the G1-S phase transition. One such target is Far1, a bifunctional protein required for G1 arrest and the mediation of cell polarity during yeast mating. Far1 is thought to possess G1 cyclin-CDK (primarily Cln1-Cdc28) inhibiting activity, although this function has not been definitively demonstrated biochemically (52, 120, 193, 318, 399). During the G1 phase of the cell cycle, Far1 is in complex with Cdc24, an activator for the cell polarity mediating protein Cdc42, sequestering Cdc24 within the nucleus and inactivating it (44, 368). Export of Cdc24 from the nucleus occurs at the G1-S transition as a result of Far1 degradation. The proteolysis of Far1 occurs in response to its phosphorylation by the G1 cyclin-CDKs and occurs within the nucleus through its interaction with the F.box protein Cdc4 (27). Poly-Ub chains are built onto Far1 by the Cdc34/SCF^{Cdc4} complex and target it for proteasomal degradation (27, 160). The absence of Far1 allows Cdc24 to localize to the site of budding, allowing for proper bud formation, actin polarization and cell cycle progression. During mating, however, Far1 is phosphorylated by another signal, which

does not lead to it degradation (26). In response to this signal, Far1 in complex with Cdc24 is exported out of the nucleus, and Far1 guides Cdc24 to the site of the mating signal, thus triggering the polarized growth of the cell to that site (forming a morphological structure known as a "schmoo"). An elegant model can be constructed for the functional control of Far1 by its differential phosphorylation signals (Figure 1.14) (97).

As mentioned above, cell cycle progression is dependent on the periodic increase and decrease in cyclin-CDK activity (280). The G1-S phase transition is largely dependent on the activity of the Cln1-, Cln2- and Cln3-CDKs. As the cell cycle proceeds, inactivation of the Cln1 and Cln2 cyclins is dependent on their Cdc34/SCF mediated proteolysis (354, 358, 376, 422). Both *in vivo* and *in vitro* observations have indicated that the Grr1 F.box protein targets the G1 cyclins for Cdc34/SCF dependent ubiquitination in a phosphorylation dependent manner (21, 217, 218, 375, 376). The G1 cyclin-CDK complexes are capable of self-phosphorylation, resulting in their instability (358). However, the rates of their instability are differential, suggesting additional modes of regulation.

Another important target of the Cdc34/SCF complex for cell cycle progression is the Cdc6 DNA replication initiation factor. Cdc6 is required for the assembly of pre-replicative complexes (pre-RCs) at origins of DNA replication (334). Pre-RCs mark the sites of replication initiation across the genome, and their proper regulation is crucial for genomic integrity. The assembly of pre-RCs occurs early in G1 phase, where there is a burst of Cdc6 transcription and Cln-CDK activity is low. The increase in Cln-CDK activity at the G1-S transition leads to the recognition of Cdc6 by the Cdc4 F.box protein component of the $Cdc34/SCF^{Cdc4}$ complex (93, 94, 99). Cdc6 is then ubiquitinated by the $Cdc34/SCF^{Cdc4}$ complex and efficiently degraded (a half life of less than 2 minutes), thus preventing the assembly of another round of pre-RCs. The large increase in Cln-CDK activity at this stage in the cell cycle suggests that Cdc6 recognition by the $Cdc34/SCF^{Cdc4}$ complex is dependent on its Cln-CDK phosphorylation. However, $Cdc34/SCF^{Cdc4}$ dependent proteolysis (albeit it at a much less efficient rate; a half life of approximately 15 minutes) of Cdc6 continues following S phase after Cln-CDK activity disappears, suggesting another mode of regulation for its ubiquitination at this stage of the cell cycle

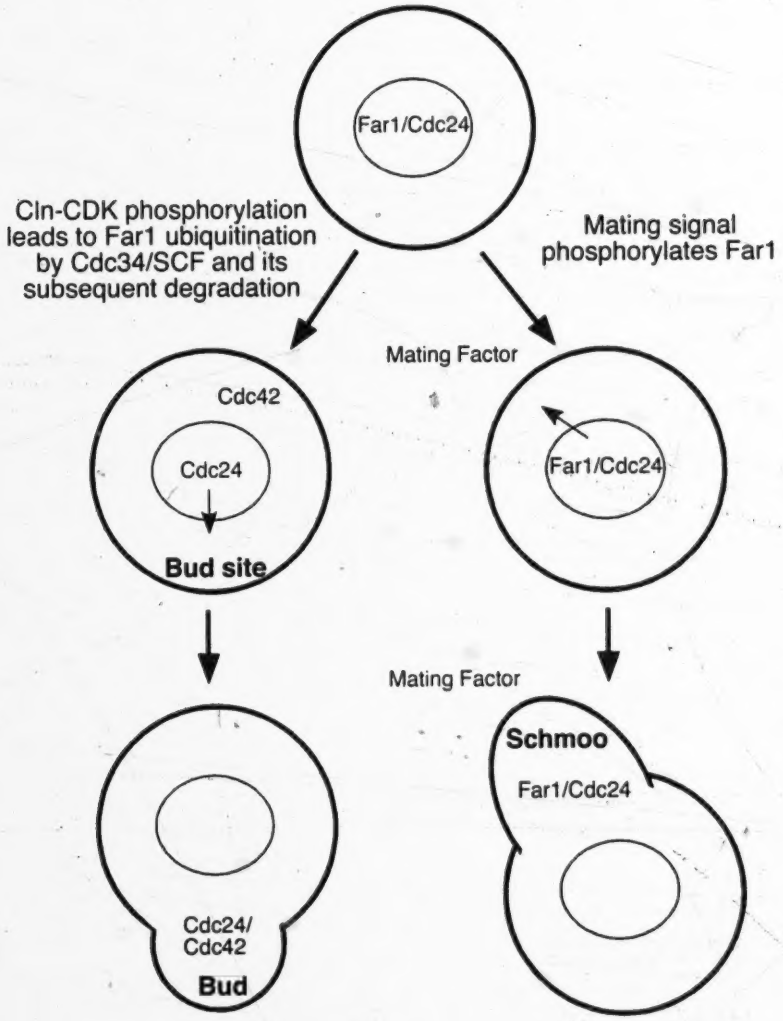

Figure 1.14 A model of Far1 function.

Far1 sequesters Cdc24 in the nucleus and prevents its access to the cell periphery. (Left) During normal cell cycle progression Far1 is phosphorylated by G1 cyclin-CDKs, targetting it for ubiquitination by the Cdc34/SCF complex and subsequent degradation. Cdc24 is exported out of the nucleus to the site of bud formation, where it interacts with and activates the Cdc42 GTPase. (Right) In response to mating pheromone, Far1 is differentially phosphorylated by the mating signaling pathway, signaling the Far1/Cdc24 complex to localize to the site of the mating signal and cause the polarization of cell growth to this site.

(94, 99, 317). This tightly regulated method of Cdc6 activity ensures DNA replication is licensed to occur only once during the cell cycle. Cdc6 is also suggested to possess CKI activity, and together with Sic1 has been shown to inhibit the activity of the mitotic cyclin-CDKs (13, 49, 100). Although this role for Cdc6 is less clear, it appears to be separate from its role in DNA replication and is important for mitotic exit. Therefore, Cdc6 proteolysis by the Cdc34/SCF^{Cdc4} complex also contributes to the activation of cyclin-CDK activity in mitosis.

Highly regulated mechanisms are integrated with cellular growth to cope with insufficiencies in required nutrients. The Cdc34/SCF^{Cdc4} complex is central to the regulation of these mechanisms through the selective ubiquitination and degradation of the transcriptional activator Gcn4 (56, 185, 274). Many genes involved in regulating the biosynthesis of amino acids and purines in the cell are under the strict control of Gcn4 (34, 295). An increase in Gcn4 activity occurs under amino acid starvation as a result of an increase in its translation coupled with an increase the protein's stability (168, 185). Gcn4 degradation is normally rapid and, as with other Cdc34/SCF targets, occurs in response to its phosphorylation. Two CDKs, Pho85 and Srb10, are the primary regulators of Gcn4 phosphorylation. Deletion of both *SRB10* and *PHO85*, or mutation of the potential phosphorylation sites within Gnc4, almost completely stabilize Gcn4 protein levels (56). The Pcl5 cyclin is thought to be the primary regulator of Pho85 CDK activity with regards to Gcn4 phosphorylation (367). It has been proposed to act as a general sensor for cellular protein biosynthesis, and together with Pho85 mediates the degradation of excess Gcn4. Pcl5 is itself a transcriptional target of Gcn4, and therefore acts in a negative regulatory feedback loop. Alternatively, Srb10 is thought to mediate the degradation of a smaller pool of Gcn4 that is bound to promoters of regulated genes.

Only two of the many F.box proteins that can associate into the SCF complex are essential for yeast cell growth. The first is Cdc4 (its functions are described in the previous paragraphs), and the second is Met30. Deletion of *MET30* results in a G1 phase cell cycle arrest with a phenotype that includes an accumulation of a large unbudded morphology and 1N DNA content (314). The essential function for Met30 is the inactivation of the bZIP family transcriptional activator Met4, as shown by the viablility of a *met30Δ met4Δ* strain (314). The essential role that Met4 plays in cell cycle control is

unclear. However, *CLN1* and *CLN2* (but not *CLN3*) transcript levels fail to accumulate in *met30Δ* cells, suggesting that Met4 is involved in the transcriptional regulation of a set of genes required for cell cycle progression (314).

The best-defined function for Met4 is in the regulation of genes (known as MET genes) responsible for the synthesis of sulfur containing amino acids (such as methionine and cysteine) when cellular methionine levels are low (393). High levels of methionine leads to an increase in intracellular S-adenosylmethionine (SAM), which signals to target Met4 for Cdc34/SCF^{Met30} mediated ubiquitination (202, 347). This subsequently results in the inactivation of Met4 function and down regulation of MET gene expression. The mechanism of Met4 inactivation by the Cdc34/SCF^{Met30} complex appears to depend on the growth medium. When SAM levels are high in minimal media (media containing only essential amino acids, vitamins, and salts, but no sulfur compounds), Met4 ubiquitination leads to its rapid degradation by the 26S proteasome (228, 347). However, in rich media (in which there is an abundant sulfur source) Met4 ubiquitination leads to its inactivation by a proteolysis independent manner (202, 228). This mechanism for Met4 inactivation is somewhat controversial. One group has observed that under these conditions polyubiquitinated Met4 specifically targets genes that increase intracellular SAM levels, but is not recruited to other MET genes (228). Another group, however, reported that stable polyubiquitinated Met4 still binds to MET gene promoters, but fails to recruit transcriptional co-factors to these sites (202). A Lys48 linked poly-Ub chain attached to only one specific lysine on Met4 (Lys163) has been observed to mediate its inactivation (112). Mutation of this lysine to an arginine activates Met4 function, but does not stabilize Met4 protein levels, lending support to a proteolysis independent mechanism of poly-Ub regulation. These are the first observations demonstrating that Lys48 linked poly-Ub chains possess non-proteasomal signaling properties.

Transcriptional regulation of the G1-S transition is highly complex and is mediated by multiple transcription factors, transcriptional regulators and signal transduction networks. As mentioned above, the SBF and MBF transcription factors are the primary regulators of G1-S transcription (87, 221, 284, 285, 294, 303). These two transcription factors are mediated in similar, but differential manners. Both transcription factors have a DNA binding factor (Swi4 for the SBF, and Mbp1 for the MBF) and a

common transcriptional activator (Swi6) (221, 284, 285). The coordinated cell cycle activity of these complexes is regulated by the common factor. Swi6 is shuttled into the nucleus at the G1-S phase transition and activates both complexes for transcription (122, 338, 372). Following SBF and MBF activation, Swi6 is exported out of the nucleus until the next round of the cell cycle. The SBF and the MBF have overlapping functions in cell cycle regulation (221). This overlap of function is partially accomplished by the redundant binding to their respective recognition motifs. Swi4 normally binds to DNA regions known as SCB elements, whereas Mbp1 binds to MCB elements (335). However, both transcriptional complexes are able to interact with the SCB and MCB elements thus providing an explanation for their redundancy (312, 392). Despite the functional similarities between the two, differences in their expression and regulation do exist.

Signaling differences have been observed between the SBF and the MBF. The "cell integrity" signaling cascade (which will be introduced in detail in section 1.3) has been shown to mediate Swi4 specific transcription (17, 133, 157, 254). Signaling from this pathway activates Swi4 transcription in a Swi6 dependent and independent manner suggesting multiple layers of regulation (17). Another regulator of SBF specific function is Whi5, which negatively regulates SBF function by specifically binding to the Swi4/Swi6 complex (72, 78). Cln3 mediated phosphorylation of Whi5 following START promotes its dissociation from the SBF resulting in its nuclear export, and SBF activation (72, 78). Deletion of the *WHI5* gene bypasses the requirement for Cln3 signaling in the cell, suggesting that it is one of the major inhibitors the G1-S phase transition (72, 78). An MBF specific regulator is Stb1. This protein acts as a positive regulator of MBF function by binding to Swi6, which is thought to require Cln3 phosphorylation (73, 169). The differences between the SBF and MBF result in somewhat distinct transcriptional effects. The MBF generally targets the S-phase cyclins genes and genes required for DNA replication, whereas the SBF primarily targets the G1-phase cyclin genes and genes required for cell wall biosynthesis.

Other than "priming" the cell for DNA replication, the two other main processes that are initiated in G1 are SPB duplication and budding. SPBs are the functional equivalent of centrosomes in mammalian cells, and are required for spindle formation and chromosomal segregation (114, 158). SPBs are a gigadalton multi-protein complexes

composed of six structural stacks, which span the yeast nuclear envelope (43, 302). Most of the major components of the SPB have been determined, however, much of the mechanism of its duplication and its dynamic regulation is unknown.

Yeast bud formation is also not very well understood, despite the characterization of many required events. Budding is observed as the polarized extension of the cell wall at a region known as the bud site (51). This occurs through a complex series of events that result in the localized weakening of the cell wall followed by the projected construction of new cell wall and plasma membrane material. Many enzymes involved in cell wall synthesis and transport work together with many signaling networks to mediate these events. A chitin ring is assembled at the junction between the mother cell and the bud, and is retained after the separation of each daughter cell (45). This chitin ring is known as the bud scar and is useful to measure the age of the cell.

Only a subset of the processes involved in the progression from G1 into S phase has been discussed above. Many processes are poorly understood and much more research into this area is required for a better understanding of these events. Ub mediated regulation, particularly by the Cdc34/SCF complex, appears to be one of the central regulators of the G1-S transition and understanding of its functionality is of great importance in the understanding of cell growth.

1.2.2 S phase

Several proteins are involved in mediating the structural and mechanistic aspects of DNA duplication and segregation. An extensive signaling network regulates these events, ensuring the fidelity of this process. In all eukaryotic cells, DNA replication is accomplished by the formation of multiple origins of replication complexes (ORCs) on each chromosome (96). In yeast, this occurs at DNA sequences known as autonomously replicating sequences (ARS) (297). There are approximately 400 ARS elements within the 16 yeast chromosomes. The coordinated initiation of replication forks from each ORC and subsequent chromosomal duplication occurs during the S-phase of the cell cycle.

ORCs are composed of a complex of proteins (Orc1-6) that remain bound to the DNA throughout the cell cycle (48, 96, 396). Cdc6 binds to ORCs, which recruit minichomosome maintenance proteins (MCMs) to these sites to form pre-RCs (48, 96,

396). The regulated changes in the assembly and disassembly of MCMs at these sites is critical for the replication of the chromosomes only once per cell cycle. After a series of events, the MCM complex is converted into an active helicase, which is followed by the action of DNA replication polymerases. Polyubiquitination of the most abundant of the MCMs, Mcm3, has been observed. It has further been suggested to target Mcm3 for proteasomal degradation in mitosis (55). Excess levels of Mcm3 results in DNA replication defects, which supports this hypothesis. This may be one of several mechanisms to modulate the periodic assembly of pre-RCs.

Replication origin firing in S phase is not a random process, but rather occurs at each ARS only once per cell cycle. These origins can be classified as either early or late origins depending on their timing. The two S-phase cyclin-CDK (Clb5- and Clb6-Cdc28) complexes are the primary regulators of this process (362, 396, 424). Sic1's role as a Clb-CDK specific inhibitor is important in this process (361). The timing of origin firing is largely dependent on the targeted degradation of Sic1 by the Cdc34/SCF^{Cdc4} complex, which subsequently activates Clb5 and Clb6 function (293, 406, 408). Deletion of *SIC1* results in an extended S-phase, fewer origins being fired and mis-segregated chromosomes in mitosis, resulting in genomic instability (237).

Cells often have to cope with DNA structural abnormalities, such as strand breaks or base modifications that may cause inaccuracies in genomic replication and segregation. Many regulatory networks that are connected to cell cycle checkpoints exist to prevent this from happening (96, 250). Checkpoints can be defined as a system that blocks the cell from undertaking the next stage in the cell cycle if the previous step is incomplete (152). Several DNA repair mechanisms exist within the cell to accommodate for improper DNA replication, and the Ub pathway has been shown to be one of the major regulators for several of these mechanisms (2, 146, 175, 355).

1.2.3 G2 and Mitosis

As with all the other processes in the cell cycle, the faithful segregation of replicated chromosomes is dependent on the coordinated action of a variety of events. Some of these events, such as SPB separation and spindle orientation, begin as early as the G1-S phase transition. Other events, such the paring of replicated chromosomes

(sister chromatids), parallel S phase. The events that follow DNA replication are primarily designed to ensure for the bipolar separation of sister chromatids.

Many features are important for sister chromatid separation. First, each sister chromatid has a centromere that mediates the formation of a protein complex known as the kinetochore (or the centrosome in higher eukaryotes), onto the DNA (268). The kinetochore allows for the bipolar attachment of chromosomes to the microtubules of the mitotic spindle and mediates their movement toward opposing poles. Second, the sister chromatids are paired through a protein complex known as cohesin (400). The pairing of sister chromatids is required for their bipolar attachment to the mitotic spindle, which ensures the correct segregation of each chromosome. Third, sister chromatids are condensed, which shortens each chromosome helping to prevent their entanglement (252).

The G2 phase of the cell cycle is primarily composed of checkpoints that ensure that these features are performed correctly. G2 checkpoints act in response to cytoskeletal disruptions, or incorrectly aligned sister chromatids. They can also act in concert with DNA damage repair mechanisms in S phase to repair any damage that may remain following DNA replication (9, 240, 343). These checkpoints have sophisticated mechanisms of halting the cell cycle until the problems have been repaired.

Mitosis is the stage in the cell cycle at which chromosomal separation and cell division takes place. Mitosis can be sub-divided into four stages (Figure 1.15). Prophase is the first stage of mitosis, and is defined by the condensation of the chromosomes and the binding of key proteins to the kinetochores to allow for spindle attachment. Once attached (the attachment of the mitotic spindle to the chromosomes is sometimes known as prometaphase), the chromosomes are aligned at the center of the opposing SPBs, which is known as metaphase. The separation of the sister chromatids is known as anaphase, and this stage continues until each chromosome is moved to the poles of their spindle and the cell starts to divide into two. The metaphase to anaphase transition is a very highly regulated stage in the cell cycle and many mitotic checkpoints ensure that this process is correctly completed. The dissolution of the spindle and the physical separation of the mother cell from the daughter cell by cytokinesis, known as telophase, is the final stage of mitosis.

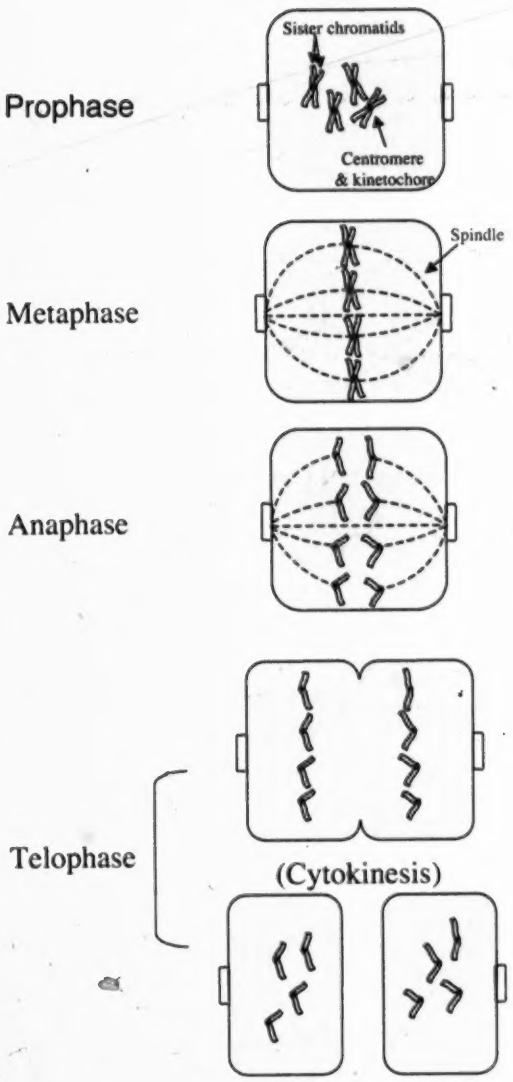

Figure 1.15 The Stages of Mitosis.

Shown in blue are the yeast nuclei during the different stages of mitosis. The SPB are shown in grey, and the chromosomes are shown in yellow.

Regulation of all these processes depends largely on the activity of the G2-M cyclin-CDK complexes (Clb1-, Clb2-, Clb3- and Clb4-Cdc28) (277, 288). Deletion of any one of these genes does not result in significant growth defects suggesting overlapping functions for these cyclins (110, 123, 388). Combinatorial deletions of these genes have suggested a key role for Clb2, as any combination of deletions including Clb2 is lethal, whereas a clb1Δclb3Δclb4Δknockout strain is viable (110). Conditional mutants of this kind arrest as large budded cells with a 2N DNA content, no mitotic spindle, and replicated but not separated SPBs.

The expression patterns for the four Clb cyclins do not parallel each other. Clb1 and Clb2 transcription is strongly periodic, peaking at the onset of mitosis (about 10 minutes before anaphase) (110, 132). Their transcription is part of a large wave of cell cycle transcription that is mediated by a transcriptional complex that includes Mcm1, Fkh2 and Ndd1 (225). Clb3 and Clb4 proteins are expressed early in S-phase and continue to be expressed until mitosis (110, 132). Clb3 and Clb4 have been implicated in the regulation of DNA replication, spindle assembly and the G2/M transition, whereas Clb1 and Clb2 are involved primarily in mediating mitosis and mitotic exit. Measurement of CDK kinase activity during mitosis showed that the large majority of the activity was from Clb2-CDK complexes, confirming a major role for Clb2 in mitosis (132). Other important roles for Clb2 include the negative regulation of bud emergence and SBF mediated transcription. Regulation of Clb2 activity is central to ensure the unidirectional movement of the cell cycle (8, 242).

The Clb cyclins are unstable proteins and are only active at defined periods during the cell cycle (7, 132, 366). Ub mediated proteolysis appears to be the central regulator of Clb function. The APC (described in section 1.1.5b), an Ub-ligase protein complex, is responsible for targeting the Clbs for proteolysis (147, 319). It both positively and negatively regulates the cell cycle by reducing the activity of Clb cyclins during the G2 and mitotic phases, and by preventing their accumulation during the G1 phase. Two regulatory components, Cdc20 and Cdh1, regulate APC function and have been implicated in these processes (411).

Cdc20 and Cdh1 are important mediators of APC substrate selection. They are thought to mediate the binding of the APC to at least two defined domains within targets:

the D-box and the KEN box. Cdc20 is thought to mediate the interaction with D-box containing proteins, although recent evidence suggests a larger role for Apc10 in this process (50, 313, 431), whereas Cdh1 is thought to target KEN box proteins (105). However, this does not hold true in all cases, suggesting that the mechanism of substrate recognition is complex. Cdc20 and Cdh1 display contrasting modes of activation, allowing them to function at different stages of the cell cycle. Cdc20 activation is primarily dependent on the phosphorylation of APC subunits by CDKs (348, 349). Therefore, APC^{Cdc20} activity increases simultaneous to CDK activity as cells progress from S-phase to G2. However, since APC^{Cdc20} targets Clb cyclins for proteolysis it functions to down-regulate its own activity. Important for the transition from S-G2 phase, and one of the essential functions for APC^{Cdc20}, is the Ub-mediated degradation of the S phase cyclin, Clb5 (369). APC^{Cdc20} is also thought to target Clb3 for proteolysis (435, 436). Clb1 and Clb2 degradation is somewhat more complicated as it occurs in two waves (23). APC^{Cdc20} mediates the first wave during the metaphase to anaphase transition. The second wave occurs via APC^{Cdh1} during mitotic exit. Unlike APC^{Cdc20}, APC^{Cdh1} activity is negatively regulated by CDK phosphorylation, and therefore several events occur to allow for efficient Cdh1 mediated proteolysis. First, Clb-CDK activity lessens due to APC^{Cdc20} mediated proteolysis. Second, the protein phosphatase activity of Cdc14 increases towards Cdh1, thereby antagonizing its inactivation (147). Third, the final transcriptional burst of the cell cycle occurs, which is dependent on the Swi5, Ace2 and Mcm1 transcription factors (373). Several important mitotic exit proteins are then expressed, including Sic1 and Cdc6, both of which inhibit Clb-CDK activity (269). The sum of these processes allows for the simultaneous inactivation of Clb-CDK activity and the activation of APC^{Cdh1} activity, thus targeting the remaining Clb proteins for proteolysis. The increase in APC^{Cdh1} activity also targets Cdc20 for Ub mediated degradation, further exacerbating the down-regulation of APC^{Cdc20} activity (147, 319). This drives the cells out of mitosis and into the G1 phase of a new cell cycle.

Cyclin-CDK regulation at the G2-M phase transition is also mediated by direct CDK phosphorylation. In budding yeast, a kinase known as Swe1 (Wee1 in higher eukaryotes) negatively regulates Clb-CDK activity by phosphorylating Cdc28 (at Tyr19) (30, 371). This process is antagonized by the Mih1 phosphatase (30). The negative role of

Swe1 on CDK activity is normally regulated by the phosphorylation of Swe1 prior to the onset of mitosis (370). This phosphorylation targets Swe1 for ubiquitination and subsequent degradation. The Cdc34/SCF^{Met30} complex was originally determined to assemble poly-Ub chains onto Swe1, but recent data suggests that this process is Met30 independent (203, 273). Observations still suggest that Swe1 degradation depends on the Cdc34/SCF complex, but the F.box protein required to target it for ubiquitination is not clearly known. Clb-CDK activity is required for efficient Swe1 degradation suggesting a possible negative feedback loop.

The regulation of Swe1 activity is under some debate. Several studies support the idea that Swe1 functions in coordinating morphogenetic effects, such as in bud formation, with chromosomal segregation (239). Stresses on the cell that may impose defects in cellular polarization or morphology, are thought to activate a checkpoint that results in the stabilization and activation of Swe1, subsequently leading to the inhibition of Clb-Cdc28. This response may be strengthened through another process that inhibits Mih1 activity, thus delaying the cell cycle until the problems can be resolved. Collectively, these processes are known as the "morphogenesis" checkpoint. The cell integrity signal transduction pathway (described in detail in section 1.3) has been observed to be a key regulator of this checkpoint (148). In contrast, Swe1 is also suggested to regulate cell size with cell cycle progression. Therefore, it thought to activate a checkpoint known as the "cell size" checkpoint in response to miregulation of cell size (153). Many conditions can impinge on cell size, including defects in morphogenetic events, thereby making it difficult to clearly rule out either hypothesis from the current studies.

Other than targeting Clb5 for degradation, another essential role for APC^{Cdc20} is to target a regulator of sister-chromatid separation for Ub-mediated degradation (65, 245). A protein complex composed minimally of Scc1, Scc3, Smc1 and Smc3 (known as cohesin) functions to hold sister chromatids together prior to their separation (400). Complete loss of cohesin from the sister chromatids occurs upon cleavage of the Scc1 subunit by the endoprotease Esp1. The activity of Esp1 (called separase in higher eukaryotes) is controlled though its interaction with an inhibitor known as Pds1 (called securing in higher eukaryotes). At the metaphase to anaphase transition this inhibition is relieved by APC^{Cdc20} mediated ubiquitination and subsequent degradation of Pds1 (64).

This releases Esp1, which then promotes the dissolution of cohesin through the cleavage of Scc1. Consequently, sister chromatid separation occurs and mitosis proceeds. Several other important targets for both APC^{Cdc20} and APC^{Cdh1} have been determined for G2 and mitotic progression (see Table 1.2).

A "spindle assembly" checkpoint inhibits APC^{Cdc20} in response to phenomena that may result in improper chromosomal segregation (420). The effect of this inhibition is a cell cycle delay to allow for correction of the error. The mechanism of how APC^{Cdc20} inactivation occurs is not entirely clear, although many proteins in this process have been identified.

A connection between the roles of APC^{Cdc20} and the $Cdc34/SCF^{Cdc4}$ has been observed at the G2-M transition. Three alleles of the *CDC4* gene (*cdc4-10*, *cdc4-11* and *cdc4-16*) were isolated as suppressors of the TS nuclear segregation defects of the *cdc20-1* strain indicating a genetic relationship between the two (128). These *cdc4* strains, as well as two other *CDC4* alleles (*cdc4-1* and *cdc4-12*) and a conditionally viable *cdc4Δ* strain displayed growth defects resulting in both G1-S and G2-M phase transition defects (128). Analysis of the *cdc4-12* strain showed that it had pre-anaphase defects, such as short mitotic spindles. Deletion of the *SIC1* gene in these cells bypasses the G1-S defect, but not the G2-M defects, as has been observed with other Cdc34/SCF TS mutants. However, deletion of the *PDS1* gene suppresses the G2-S defects, but not the G1-S defects in these cells (128). This observation, together with the genetic relationship between Cdc4 and Cdc20, suggests a link between the G2-M function for the $Cdc34/SCF^{Cdc4}$ complex and the degradation of Pds1. However, a direct or indirect relationship between the two processes has yet to be established.

Another potential connection between the Cdc34/SCF complex and mitotic progression is Skp1. TS alleles of the *SKP1* gene (*skp1-12* and *skp1-4*) that display specific defects in the progression through mitosis have been isolated (18, 66). Cells carrying these alleles have a growth arrest with a large budded morphology, 2N DNA content, and a mixture of short and elongated spindles, among other defects. To a lesser extent *skp1-12* cells also display a G1 defect reminiscent of other SCF mutants even though they do not accumulate Sic1 to any significant extent (18). The *skp1-4* TS allele additionally displays chromosomal segregation defects with no G1 defects, and

overexpression of the core kinetochore protein Ctf13 suppresses the defects associated with the *skp1-4* strain (66). Analysis of the yeast kinetochore revealed that Skp1 is one of its core components, suggesting that Skp1 mediates a Cdc34/SCF independent function in this complex (66). However, Ctf13 is an F.box protein, which raises the possibility for a role for Cdc34/SCF ubiquitination in mediating this complex (351).

It is not surprising that the Ub pathway is interconnected with the irreversible nature of the cell cycle. Although much is known about Ub mediated regulation, much remains to be uncovered. This becomes evident as more cell cycle targets are identified. This thesis describes work uncovering novel roles for the Ub pathway in relation to cell cycle progression and ultimately cell proliferation.

1.3 The cell integrity signaling pathway

Yeast possess rapidly responding, highly complex signaling networks that allow them to adapt to and coordinate cell growth with changing environmental conditions. As with higher eukaryotes, yeast utilize several mitogen activated protein kinase (MAPK) cascades to mediate these responses (102, 103). These generally involve a series of sequential phosphorylation events that activate three protein kinases: a MAP kinase kinase kinase (MAPKKK/MEKK), a MAP kinase kinase (MAPKK/MEK) and a MAP kinase (MAPK). Many of these pathways are linked to G-protein associated cell surface receptors that sense the changing environment. Signaling through the pathway is initiated by activation of the MAPKKK, which subsequently phosphorylates the MAPKK on a conserved serine and threonine residue resulting in its activation. Activated MAPKK proceeds to activate the MAPK by phosphorylating both a threonine and tyrosine residue within its kinase domain activation loop. Activated MAPK usually proceeds to regulate a number of processes, very commonly resulting in a specific program of gene expression.

S. cerevisiae possess five known MAPK pathways: (i) the mating pathway, (ii) the filamentous growth pathway, (iii) the high-osmolarity growth pathway, (iv) the cell integrity pathway, and (v) the spore wall assembly pathway (Figure 1.16) (97, 138, 157, 166, 333). These pathways are interconnected in function and are composed of multiply redundant and highly complex events. A fairly good mechanistic understanding of these

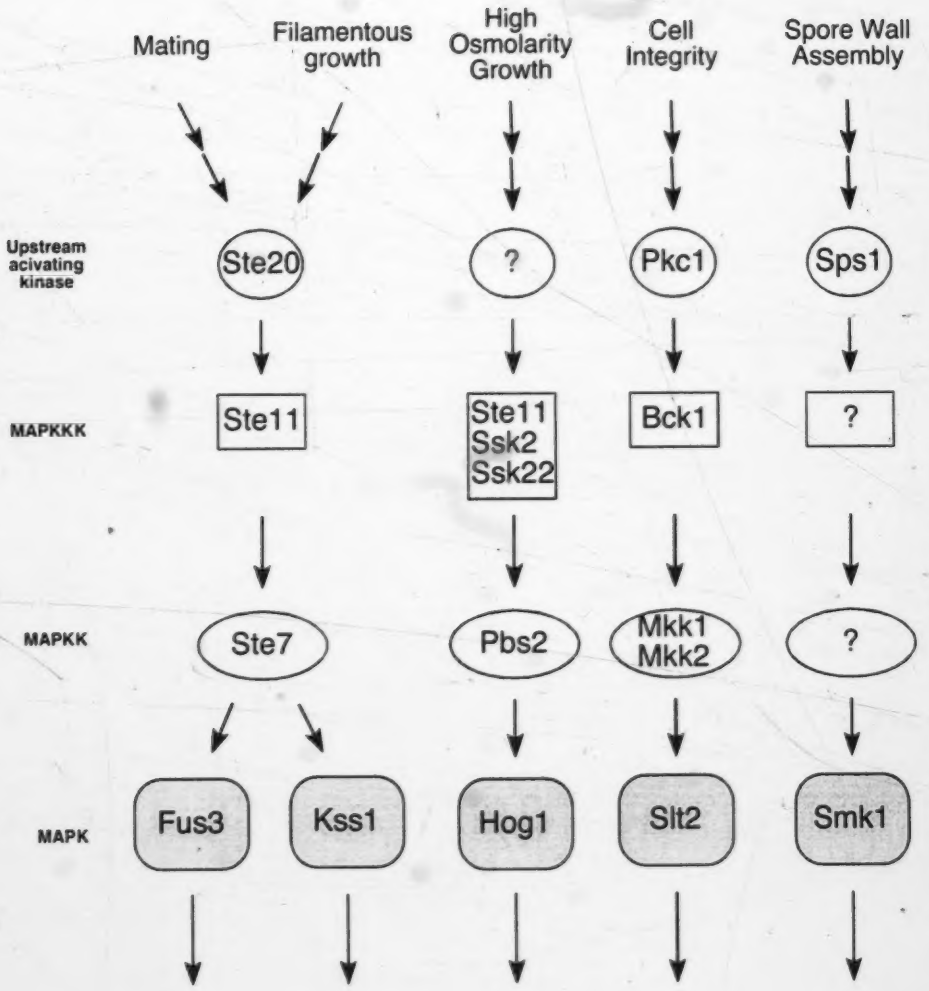

Figure 1.16 MAPK pathways in budding yeast.
There are five identified MAPK pathways in *S. cerevisiae*, each of which have an unique MAPK. The question marks indicate that a protein kinase has not yet been identified for this step in a cascade. The arrows represent known or postulated steps in signal transduction.

pathways has been accomplished from a large number of genetic and biochemical analyses.

The cell integrity pathway has been shown to be a vital regulator of yeast cell growth (157). It is induced during morphogenic events, such as that occurring during periods of polarized growth, and in response to conditions that result in compromised cell wall integrity. The MAPK cascade components of the cell integrity pathway consist of Bck1 (MAPKKK), the redundant Mkk1 and Mkk2 kinases (MAPKK) and Slt2/Mpk1 (MAPK) (Figure 1.16) (138, 157). Signaling originating at the cell wall involves a variety of effectors that result in the regulation of the MAPK cascade and subsequently distinct transcriptional complexes. This leads to the regulation of cell wall biosynthesis, morphogenic homeostasis and cell cycle progression. This thesis will introduce a relationship between the function of the Cdc34/SCF ubiquitination complex and the cell integrity pathway in mediating cell growth, and as such, a detailed introduction of this pathway is presented in this section.

1.3.1 Cell wall composition

The cell wall is a rigid, but dynamic, structure that defines cell shape (46, 219). It is primarily composed of three interconnected elements: β-glucan, chitin, and mannoproteins. Large linear 1,3-β-glucan polymers are the most abundant components, forming a structural network together with mannoproteins and branched 1,6-β-glucan. Mannoproteins are proteins tethered to mannose polysaccharides (they are composed of approximately 95% carbohydrates), and are fundamental in cell wall biosynthesis (195). Chitin is much less abundant, but is essential for cell growth (346). It is normally restricted to an area surrounding an emerging bud or previous bud sites (bud scars). Chitin is unique to fungal cell walls and specific inhibitors of chitin synthesis (such as calcofluor white) that are toxic to yeast.

Many proteins are required for to the proper formation, deconstruction, regulation, and distribution of these elements within the cell wall, many of which have a direct or indirect relationship to the cell integrity signaling pathway. Of these, proteins involved in cell wall polymer synthesis are of particular importance. These include the chitin synthase enzymes CSI, CSII and CSIII, as well as the 1,3-β-glucan synthase, which

is composed of the catalytic subunits Fks1, Fks2 and the regulatory GTPase Rho1 (Rho1 is also a signal mediator of the cell integrity pathway, and will be discussed in detail in section 1.3.4) (90, 346). Several mutants that affect the general structure of the cell wall have been discovered. They characteristically alter the composition and architecture of the cell wall to compensate for defects caused by the mutation, which can include enhanced chitin deposition and induced expression of a number of cell wall related genes (such as *FKS2*) (331). The regulating mechanisms behind proper cell wall synthesis and maintenance are not well understood, but that several pathways may play roles in mediating cell wall integrity.

One recent study has described a cell cycle checkpoint that specifically monitors the integrity of the cell wall, termed the cell integrity checkpoint. This checkpoint responds to defects that result in the alteration of the cell wall composition, such as mutations in the 1,3-β-glucan synthase subunit Fks1 (390). In response to these defects the Fkh2 G2-M phase cell cycle transcription factor is down-regulated, resulting in reduced transcription of the Clb2 mitotic cyclin and inactivation of mitotic CDK activity (390). This causes a G2-M phase cell cycle delay to allow the cell to correct the damaged cell wall. An important regulator for this checkpoint involves the dynactin complex, as deletion of *ARP1* results in the inactivation of the checkpoint (390). However, a specific signal transduction cascade that may mediate this checkpoint has not been discovered. It does not appear to involve the cell integrity pathway as deletion of *BCK1* or *SLT2* have no response on the checkpoint, but because of its role in cell wall biosynthesis it is possible that this connection has not yet been observed.

1.3.2 Cell integrity surface receptors

The rapid response of the cell integrity pathway relies on both internal and external signals relayed by several different proteins, and allow the cell to adapt to the variability of its environment. Many proteins specific for the cell integrity pathway are involved in sensing changes in the extra-cellular environment, including Wsc1/Slg1/Hcs77, Wsc2, Wsc3, Wsc4, Mid2, and Mtl1 (133, 211, 340, 409). Many similarities exist between these proteins. First, they all have a type I transmembrane proteins domain. Second, they all have an amino-terminal signal sequence. Third, they

have a serine/threonine rich extracellular domain that is heavily glycosylated and extends into the cell wall. Fourth, Wsc1, Wsc2, Wsc3 and Wsc4 all have a cysteine rich region located between their signal sequence and their serine/threonine rich domain (409). Genetic and biochemical observations suggest that these proteins act collectively and individually as cell surface receptors to direct the activation of the downstream cell integrity signal events. However, the mechanisms of how these receptors sense environmental conditions are not well understood.

Wsc1 and Mid2 are probably the best characterized of the receptors. The *WSC1* and *MID2* genes have been isolated in numerous genetic screens connecting them to the cell integrity pathway. Strains with *WSC1* or *MID2* deletions share several phenotypes with other mutants of the cell integrity pathway. These phenotypes include caffeine sensitivity, α-factor (the pheromone produced by haploid a cells) sensitivity, resistance to calcofluor white, and sensitivity to both high and low temperatures that are osmotically suppressed. Osmotic suppression is thought to occur as a result of a decrease on the turgor pressure on the cell wall as the solvent concentration in the cell decreases in response to an increase in extra-cellular solute concentration. Additionally, many of these defects can be suppressed by increasing the activity of the downstream components of the cell integrity pathway (190, 211, 305, 340, 409). Cell cycle progression defects are also observed in these mutants, specifically in the coordination of post-START events. This is evident by the fact that a *wsc1Δ* strain at its non-permissive temperature has undergone bud emergence, but not DNA replication or SPB duplication (186). Furthermore, *WSC1* is a multi-copy suppressor of defects associated with a *swi4Δ* strain, and displays a genetic interaction with the Ub-conjugating enzyme Cdc34 (186), which are also important in the regulation of post-START events.

Several observations suggest that Wsc1 and Mid2 have overlapping but differential functions. For example, activation of the downstream MAPK Slt2 by heat stress depends on *MID2*, but not on *WSC1* (260, 364). Additionally, actin depolarization in response to a variety of cell wall stresses, as well as the activity of the 1,3-β-glucan synthase, are dependent on *WSC1* but not on *MID2* (364). A genetic connection between Wsc1 and the G-protein Ras2 has also been observed, suggesting a link between the cAMP pathway and the cell integrity pathway (409). Both Wsc1 and Mid2 have been

shown to interact with Rom2, a GDP/GTP exchange factor (GEF) that stimulates the activity of the GTPase Rho1. In addition, cellular extracts from *wsc1Δ* and *mid2Δ* strains are defective for the catalysis of GTP loading onto Rho1 *in vitro* (321). This suggests that their role in sensing changes in cell wall properties is likely through the mediation of Rho1 activity.

1.3.3 The Rho1 GTPase.

Rho1 is a small GTP binding protein of the Ras superfamily that is essential for yeast cell viability. It is made up of 209 amino acid residues that share homology to several other GTP binding proteins in yeast (Rho2, Rho3, Rho4, and Cdc42). It functions primarily in processes related to cellular morphogenesis and polarity (47, 91, 92). Rho1 is typically localized at the plasma membrane at sites of growth, such as at incipient bud sites, bud tips, and the bud neck during cytokinesis (337, 432). Five direct effectors for Rho1 have been described to date: i) Pkc1, which is an upstream kinase of the cell integrity pathway (204, 300); ii) Fks1 and Fks2, the catalytic components of the 1,3-β-glucan synthase (337); iii) Bni1, which is involved in budding and mitotic spindle orientation by mediating the formation of linear actin filaments (224); iv) Skn7, which is a transcriptional activator that has been implicated in cell cycle control, oxidative and heat stress response, and cell wall metabolism) (4); v) Sec3, which is a spatial landmark that mediates polarized exocytosis (137). Therefore, Rho1 can be thought of as a multifunctional regulator that responds to varying stimuli to mediate differential effects.

Rho1 is ideally suited to function as a modulator of signaling, as it rapidly switches from a GTP-bound active form to a GDP-bound inactive form (47). Only the active form of Rho1 has been observed to transduce a signal to a downstream mediator, and therefore functions unidirectionally as it promotes the reduction of GTP. Rho1 can be locked into its GTP-bound active form by mutation of a key glutamine residue involved in the hydrolysis of GTP (G68H) (253). Continuous activation of Rho1 is lethal to cells, indicating that the proper regulation of Rho1 activity is vital (149, 253). Activation of Rho1 is regulated by several GTP-GDP exchange factors (GEFs) that lead to an increase in its GTP-bound state. The intrinsic GTPase activity of Rho1, and thus it inactivation, can be promoted by distinct GTPase activating proteins (GAPs). Furthermore, proteins

that inhibit the dissociation of GDP from Rho1 (GDI) have also been observed to inhibit Rho1 activity (263).

Rom1 and Rom2 are the only GEFs characterized for Rho1 (25, 308). They were isolated as multi-copy suppressors of a TS dominant negative mutant allele of Rho1 (308). Rom2 appears be the major GEF for Rho1 as deletion of the *ROM2* gene results in TS growth that can be suppressed by the overexpression of Rho1. In contrast, deletion of *ROM1* has no obvious phenotype (308). However, overlap in their function is indicated by the lethality of a *rom1Δ rom2Δ* strain (308). The phenotype associated with *rom1Δ rom2Δ* strains is very similar to that of a *rho1Δ* strain, which includes a growth arrest with a small bud morphology and high levels of cell lysis (308). The TS *rom2Δ* strain exhibits similar phenotypes at its non-permissive temperature, and an elongated bud morphology at its permissive temperature (255). As mentioned above, Rom2 interacts with the cell surface receptors Wsc1 and Mid2, through which signaling from the cell wall to Rho1 is thought to originate (133, 189, 211). Rom2 activity has also been shown to depend on signaling from other factors, such as the phosphatidylinositol (PI) kinase homologue Tor2 (25), the 1-PI-4-kinase Stt4, and the 1-PI-4-phosphate 5-kinase Mss4 (16).

Several potential GAPs for Rho1 have been identified based on their homology to a conserved, approximately 200 residue domain (GAP domain) that is responsible for the stimulation of Rho-type GTPase. These potential GAPs include Sac7, Bem2, Bem3, Bag7, Lrg1, Rga1, Rga2 and Rgd1 (Figure 1.17), but their roles in the regulation of Rho1 are not well understood. Sac7 and Bem2 are probably the best characterized of the GAPs. Both Sac7 and Bem2 have GAP activity for Rho1 *in vitro*, and have been implicated in actin cytoskeleton reorganization and maintenance of the cell wall (260). Deletion of *SAC7* or *BEM2* results in the misregulation of signaling through the cell wall integrity pathway, but not the 1,3-β-glucan synthesis pathway, suggesting that both GAPs specifically regulate the Pkc1 activity of Rho1 (260, 416). Additionally, overexpression of either *SAC7* or *BEM2* down-regulates the cell integrity pathway (357). Despite the similarities between the two, however, some differences are apparent. For example, deletion of *SAC7*, but not *BEM2*, rescues the defects associated with *rom2Δ* cells, suggesting that the function of Sac7 on Rho1 is in direct opposition to that of Rom2

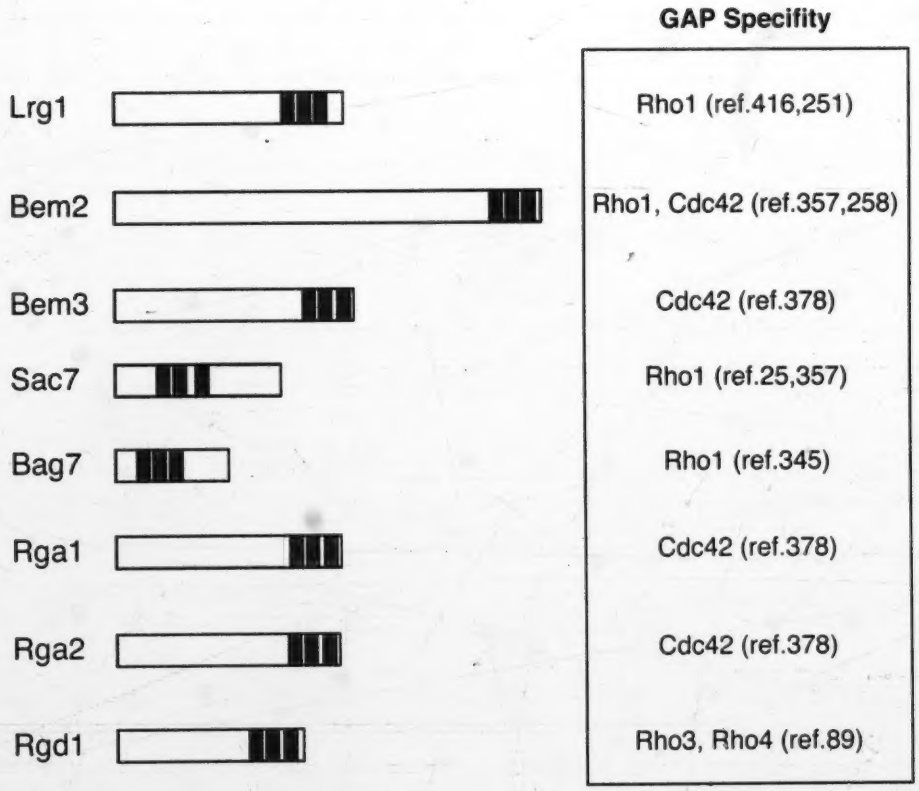

Figure 1.17 Known proteins that possess Rho-GAP activity.
Illustrated are eight known proteins that possess Rho-GAP activity. The approximate length of each protein is shown, with the approximate position of the highly conserved Rho-GAP domains shown (as dark grey boxes).

(357). In contrast, Bem2 has a distinct function in the morphogenesis checkpoint, and possesses GAP activity towards the Cdc42 GTPase (258).

Lrg1 has recently been suggested to have GAP activity towards Rho1, although such a role is not as well characterized. Yeast two-hybrid interactions between Lrg1 and Rho1, and *in vitro* GAP activity specific for Rho1 have been observed (416). It has been suggested that Lrg1 functions in mediating both the Pkc1-cell integrity and the 1,3-β glucan synthase activities of Rho1 (251, 416). The analysis of *lrg1Δ* cells has provided much of this insight. Deletion of *LRG1* can suppress the defects associated with mutants of the upstream regulators of Rho1, which include *wsc1Δ* and *rom2Δ* cells, but not the defects associated with downstream components, such as in *bck1Δ* or *slt2Δ cells* (251). However, misregulation of the downstream activity of the cell integrity pathway has been observed in *lrg1Δ* cells, such that Slt2 is hyperphosphorylated, as in *sac7Δ* cells (251). Additionally, it was observed that the downstream transcriptional activity of the cell integrity pathway was increased (251). Interestingly, a *lrg1Δsac7Δ* strain is lethal, suggesting that there is some essential overlapping function between the two (251). These results have been disputed by other observations, suggesting that deletion of *LRG1* does not affect the downstream activity of the cell integrity pathway, but rather specifically affects 1,3-β-glucan synthase activity (416). This last study showed that deletion of *LRG1* suppresses the defects associated with a *rho1-2* TS mutant strain, and a *fks1-1154 fks2Δ* strain. This study also observed that out of all the potential RhoGAPs, Lrg1 was the only one that regulates 1,3-β-glucan synthesis.

Bag7 is the only other GAP that has been studied. It has been confirmed both *in vivo* and *in vitro* to have GAP activity towards Rho1 (357). Bag7 is highly homologous to Sac7, and when over-expressed can partially complement the defects of *sac7Δ* cells. However, unlike Sac7, its over-expression does not downregulate the cell integrity pathway (357). These observations suggest that Sac7 and Bag7 have overlapping but distinct functions. The functions of the other potential GAPs remains to be determined, but from what has been observed from the studied GAPs it appears that each regulate Rho1 activity differentially, directing its function to the appropriate place and time during cell growth.

1.3.4 The Pkc1 kinase

The central regulator of the cell integrity pathway is the only yeast protein kinase C (PKC) homologue, Pkc1. It is thought to be pivotal in cell cycle progression and in responses to environmental conditions through its role as an upstream activator of the MAPK phosphorylation cascade. Analysis of *pkc1Δ* cells demonstrates its significance in mediating cell wall formation, as these cells display a modified cell wall structure (310). Deletion of the *PKC1* gene also results in a growth arrest with a small bud morphology and replicated DNA, which can be partially rescued by osmotic stabilization like many other mutants of the cell integrity pathway (238). Unlike the downstream components of the cell integrity pathway, however, *pkc1Δ* cells display severe growth defects even in the presence of osmotic stabilization, suggesting that Pkc1 plays other roles in cell viability.

Analysis of the amino acid sequence of yeast Pkc1 reveals many similar functional domains to its mammalian homologues. The most obvious are a kinase domain, two cysteine rich zinc-finger domains implicated in diacylglycerol (DAG) binding, a calcium-dependent phospholipid binding domain, a carboxyl-terminal region thought to control intracellular localization, a pseudosubstrate site, and two amino-terminal HR1 domains that are involved in binding to GTP binding-proteins (276). The activity of PKC in mammalian cells is dependent on Ca^{2+} and DAG binding, but such regulation has not been described for yeast Pkc1 (12). The DAG binding site within Pkc1 is important for its activity, but the reason for this is unclear.

The activity of Pkc1 in the regulation of the cell integrity pathway depends on its activation by the GTPase Rho1. GTP-bound active Rho1 can interact with Pkc1 leading to the activation of Pkc1 kinase function (204, 300), as well as its proper localization (10). Dominant mutations within the pseudosubstrate domain of Pkc1 can suppress phenotypic defects within TS *rho1* strains further supporting the function of Rho1 in Pkc1 activation (300). Activation of Pkc1 can also occur in response to signals from cyclin-Cdc28 (256). It has been suggested that as cells pass through START in the cell cycle, cyclin-CDKs (most likely Cln3-Cdc28) activate Pkc1 and the cell integrity pathway, contributing to an increase in cell cycle regulating transcription (see section 1.3.7). Activation of Pkc1 results in an increase in its kinase activity, and genetic analysis

of the cell integrity MAPK pathway has suggested that Pkc1 specifically targets the MAPKKK Bck1. In doing so, Pkc1 controls the activation of the MAPK phosphorylation cascade (184).

1.3.5 The MAPK phosphorylation cascade

The central components of the cell integrity MAPK pathway were primarily discovered by the genetic analysis of the downstream regulation events of Pkc1 (184). The MAPKKK Bck1 was first identified by analysis of a hyperactive mutant allele, which suppressed the defects of a *pkc1Δ* strain (234). The redundant MAPKKs Mkk1 and Mkk2 were identified as multi-copy suppressors of the *pkc1Δ* strain (184). The MAPK Slt2 was identified as a multi-copy suppressor of the defects associated with both *pkc1Δ* and *bck1Δ* strains (233). Two-hybrid analysis identified interactions between Bck1 and Mkk1, between Mkk1 and Mkk2, and between Mkk2 and Slt2, thus supporting their relationships in the cell integrity pathway (311, 380).

Deletion of *BKC1* (234), *SLT2* (184, 233, 259), or both *MKK1* and MKK2 (but not individual *MKK1* or *MKK2* deletions) (184) results in TS lysis defects that can be suppressed by osmotic stabilization, similar but less severe to that of a *pkc1Δ* strain. Haploid *bck1Δ* cells also display morphological defects, which include inconsistencies in cell size and defects in schmoo formation in response to mating factor. In contrast, diploid *bck1Δ* cells display poor viability and sporulation defects under limited nutrient conditions, suggesting a role for Bck1 in meiotic entry (74, 75). Deletion of *SLT2* results in an accumulation of round cells that have a small bud, sensitivity to lysis, sensitivity to caffeine, and delocalization of actin and chitin (233, 259, 397).

The best-studied protein of the cascade is Slt2. Its function depends on a lysine residue (Lys58) that lies within its ATP binding, active site (259). Activation of Slt2 is thought to depend on phosphorylation of one of its threonine (Thr190), and to a lesser extent a tyrosine (Tyr192) residue, both of which are conserved in most MAPKs (233). Generally, the phosphorylation status of Slt2 correlates with its downstream activity. However, several observations indicate that this is not an absolute, indicating that other modes of regulation exist (42, 261). Nonetheless, the activation of Slt2 is commonly

measured by the level of its phosphorylation, which can be detected by an antibody specific for the dually phosphorylated form of the protein (79).

1.3.6 Cell integrity pathway phosphatases

Since signaling through the cell integrity cascade is mediated by protein kinases, it is not surprising that many phosphatases are also linked to the proper function of the pathway. The most upstream acting phosphatase is Sit4. The *SIT4* gene encodes a serine/threonine protein phosphatase of the PP2A-like family (15). It down-regulates Pkc1 activity and thus cell integrity pathway signaling (11). Deletion of *SIT4* results in G1-S phase cell cycle defects (389). Consistent with this, Sit4 is implicated in the regulation of the SBF transcription factor (84). A genetic relationship between *SIT4* and the Ub pathway has also been observed. Combinations of *sit4* mutants together with proteasomal mutants or mutants in the Ub-conjugating enzymes Cdc34 or Rad6 results in synthetic lethality on minimal medium (374). These synthetic lethal combinations result in growth arrest with a large unbudded morphology and 1N DNA content. Similar to mutants in the cell integrity pathway, synthetic lethal combinations of mutants that include *SIT4* are redeemed by osmotic stabilization. Furthermore, it has been shown that Sit4 is not a target of the Ub pathway, but rather the two work functionally in parallel (374).

The redundant type I related protein phosphatases Ppz1 and Ppz2 have also been implicated in the regulation of the cell integrity pathway. Deletion of both *PPZ1* and *PPZ2* results in TS cell lysis defects and caffeine sensitivity that can be osmotically suppressed, similar to the defects in cell integrity mutants (232, 332). Additionally, overexpression of either Ppz1 or Ppz2 suppresses the defects associated with *slt2Δ* or *pkc1Δ* cells (232). Although the target(s) for Ppz1 and Ppz2 in the cell integrity pathway have not been identified, they appear to positively regulate the pathway.

Several phosphatases have been shown to negatively regulate the cell integrity pathway by targeting active Slt2. These include the protein-tyrosine phosphatases Ptp2 and Ptp3, and the dual specificity phosphatases Msg5 and Sdp1. The Ptp2 and Ptp3 tyrosine phosphatases have a somewhat redundant function in targeting a number of MAPKs, one of which is Slt2 (266). A connection between the cell integrity pathway and

these phosphatases was initially deduced by the ability of Ptp2 to act as a multi-copy suppressor of the defects caused by the expression of hyperactive mutants of *bck1* or *mkk1* (266). Further characterization led to the observation that Ptp2 and Ptp3 could bind to, and dephosphorylate, active Slt2. The predominantly nuclear localization of Ptp2 suggests that active Slt2 might be primarily localized in the nucleus of the cell (266).

Dual-specificity phosphatases, such as Msg5 and Sdp1, have the ability to dephosphorylate both the active site threonine and tyrosine residues of MAPKs. Msg5 and Sdp1 are essential at maintaining low levels of signaling through the cell integrity pathway under normal growth conditions (111, 144). Deletion of *SDP1* has been observed to exacerbate the growth defects associated with a hyperactive mutant of *mkk1*, whereas over-expression of *SDP1* suppresses these defects (144). Consistent with a role in mediating the cell integrity pathway the deletion of *MSG5* increases cell sensitivity to cell wall interfering compounds (111). Under normal Slt2 activating conditions, Slt2 has been shown to phosphorylate Msg5, which results in a decreased association between the two, thus providing a mechanism by which Slt2 regulates its own activity (111, 260).

1.3.7 Transcriptional targets

Several downstream effectors of the cell integrity pathway have been observed, most of which are involved in mediating transcriptional responses. Although many transcription factors may be regulated at some level by the cell integrity pathway (for example the MBF, Skn7, Msn2, Msn4 and Crz1 transcription factors) only two of them (Rlm1 and SBF) have been observed to be direct targets of the MAPK cascade.

The function of the Rlm1 transcription factor was originally identified through a genetic relationship with various components of the cell integrity pathway (417). Deletion of the *RLM1* gene suppresses the defects associated with the uncontrolled up-regulation of the cell integrity pathway as a result of the expression of a hyperactive Mkk1 mutant (417). Deletion of *RLM1* also causes caffeine sensitivity, which is similar to other cell integrity pathway defects. The expression of a fusion protein that has the transcriptional activation domain of Gal4 replacing that of Rlm1, constitutively activated a Rlm1 specific transcriptional program, and was observed to suppress the defects associated with *bck1Δ* and *slt2Δ* cells (417).

Analysis of the 676 amino acid sequence of Rlm1 reveals that it possesses an amino-terminal MADS (Mcm1-Agamous-Deficiens-serum response factor)-like DNA binding domain and a carboxyl-terminal transcriptional activation domain, which are connected together by a Slt2 phosphorylation domain (418). A direct interaction between Slt2 and Rlm1 has been observed using a yeast two-hybrid assay (417). Furthermore, the transcriptional activity of Rlm1 is dependent on the presence of Slt2, as revealed by transcriptional reporter assays and DNA-array filter studies (200, 201). Rlm1 has been observed to regulate at least 25 genes (Table 1.3), most of which are involved in the regulation of cell wall metabolism. The transcription of these genes has also been shown to increase when the cell integrity pathway is stimulated, such as in response to heat shock and by over-expressing Rho1, Pkc1, or a hyperactive Mkk1 mutant (200, 345). Global microarray studies on cells that have undergone cell wall damage have also revealed several other genes that are potentially regulated by Rlm1 and the cell integrity pathway (31, 118). Analysis of the promoters of these genes has revealed a putative Rlm1 binding site, $CTA(A/T)_4TAG$. Mutation of this sequence in the promoters of these genes alters their expression levels confirming its importance for Rlm1 induced transcription (201).

The importance of the cell integrity pathway in mediating cell cycle progression has been observed on many occasions. As mentioned above, Pkc1 activation is partially dependent on the cell cycle activity of cyclin-CDKs. Genetic studies have connected this activation to a role in mediating cell cycle progression by regulating the SBF transcription factor (composed of Swi4 and Swi6; described in section 1.2.1). Analysis of *swi4Δ* cells provided the initial relationship, as these mutants display TS cell lysis defects and sensitivity to compounds that weaken the strength of the cell wall (254). Further connections are suggested by the synthetic lethality of *pkc1Δ swi4Δ* and *slt2Δ swi4Δ* cells, and by the observation that overexpression of *PKC1* that suppresses the defects associated with *swi4Δ* cells (133, 182, 183, 254). Additionally, defects associated with *slt2Δ* cells are suppressed by overexpression of *SWI4*, or the SBF targets *PCL1* or *PCL2* (254).

Co-immunoprecipitation analysis, together with *in vivo* and *in vitro* phosphorylation assays have indicated that Slt2 can interact with the SBF, and lead to the

Table 1.3 Identified Rlm1 target genes

Gene	Potential Rlm1 binding site		
CHS3	-208 (ATAAAAATAG)		
PST1	-134 (ATATAAATAG)	-305 (CTAAAAATAG)	-639 (CCATAAATAG)
SED1	-207 (TTATTTTTAG)	-294 (CTAAAAATAG)	-480 (CTAAAATTAG)
CRH1	-216 (ATATAATTAG)	-359 (GTAAAAATAG)	-711 (CTATTTTAAG)
BGL2	-219 (CTATTTTTAG)		
MPK1	-233 (TTAAAAATAG)		
SEC28	-500 (TTATAAATAC)		
YIL117C	-224 (CTAAAAATAA)		
CIS3	-766 (GTATAAATAG)	-992 (CTAATTATGG)	
PIR2	-223 (CTAAATTTAG)	-587 (CTATAATTAG)	
CWP1	-386 (CTAAAAATAG)	-438 (CTAAAAAAAG)	
MLP1	-359 (TTAAAAATAG)	-510 (ATAAAAATAG)	
PIR3	-251 (CTAAAAATGG)	-280 (CTAATTATAG)	
PIR1	-222 (CAAATATTAG)	-356 (CTAAAAAAAG)	-374 (CCAATTATAG)
YLR194C	-149 (TTATTTTTAG)	-194 (CTATAATTAG)	-217 (CCAAAAATAG)
FKS1	-424 (CTAAAAAAAG)		
SSR1	-219 (CTGTATATAG)	-282 (CTATTTATAG)	
DFG5	-134 (ATATAAATAG)	-305 (CTAAAAATAG)	-639 (CCATAAATAG)
YMR295C	-130 (TTATTAATAG)	-328 (ATAAAAATAG)	
YNL058C	-123 (TTATATTTAG)	-151 (GTATAATTAG)	
PGK1	-609 (CTATTATCAG)	-851 (GTATTTTTAG)	-927 (ATAATAATAG)
CTT1	-705 (GTAATAATAG)		
SPS100	-600 (TCATTTTTAG)		
YGP1	-428 (CGAAAATTAG)		
YOR382W	-124 (GTATAATTAG)		

Genes induced by Rlm1 are shown above dotted line, genes down-regulated by Rlm1 are shown below the dotted line.

phosphorylation of both Swi4 and Swi6 (17). Chromatin immunoprecipitation experiments have indicated that Slt2 is recruited to the promoters of distinct SBF genes following the activation of the cell integrity pathway (17). Interestingly, global microarray analysis has revealed that certain genes are uniquely regulated by Slt2-dependent Swi4 activation, independent of Swi6 (17). The majority of these genes are crucial for cell wall metabolism suggesting multiple modes of SBF cell cycle regulation. Therefore, it appears that cell integrity signaling is directly integrated with cell cycle progression, particularly at the G1-S transition.

It has been suggested that differing signals through the cell integrity pathway are involved in mediating distinct transcriptional responses. There is considerable overlap between many of the genes regulated by the Rlm1 and SBF transcription factors, lending support to this hypothesis. Knr4, a protein known to be involved in mediating cell wall integrity has been implicated in regulating the transcriptional signal through the cell integrity pathway. Deletion of *KNR4* results in a decrease in Rlm1 dependent transcription, and also results in an increase in SBF dependent transcription (261). A direct interaction between Knr4 and Slt2 has been observed, suggesting that Knr4 might regulate transcription by directing the activity of Slt2 (261). This uncoupling of Rlm1 and SBF transcription further supports the idea of different signals mediating different transcriptional responses. However, very few other studies have addressed this issue.

As mentioned above, the cell integrity pathway is indirectly involved in the regulation of several other transcription factors. The best relationship is probably with the transcriptional regulator Skn7. An obvious link is that Skn7 directly interacts with Rho1 (4). This interaction is of considerable interest as Skn7 is thought to reside in the nucleus, and Rho1 at the cell surface. Nevertheless, a role for Skn7 in regulating cellular integrity appears to be important as a *skn7Δ pkc1Δ* strain is lethal (36). Furthermore, *SKN7* can act as a multi-copy suppressor of *pkc1Δ* defects, suggesting that Skn7 and Pkc1 have some parallel functions (36). Skn7 is an interesting protein, as it possesses both signaling and transcriptional properties. It has been implicated in the regulation of the cell cycle, cell wall metabolism, and in heat shock response, and is thought to be involved in coordinating signals from a variety of pathways, including the HOG and the cell integrity pathways (32, 37, 287, 339).

Transcriptional control by Skn7 is very diverse, as it acts on several transcription factors. A role for mediating the cell cycle is apparent from genetic interactions with the SBF and MBF transcription factors. The synthetic lethality of *swi4Δ swi6Δ* cells can be overcome by overexpression of *SKN7*, which restores the expression of the *CLN1* and *CLN2* genes (287). Overexpression of *SKN7* on its own is toxic to cells, and this can be suppressed by deletion of *MBP1*, suggesting a relationship between the two (32). A direct interaction between Skn7 and Mbp1 has been observed both *in vitro* and by two-hybrid analysis (32). In addition, *SKN7* is required in order for a $swi4^{TS}$ *swi6Δ* strain to be suppressed by over-expression of *MBP1* (32). Skn7 is not a component of the SBF or the MBF, but together these observations suggest that Skn7 plays a role in their regulation.

The Ca^{2+} regulated transcription factor Crz1 also appears to be regulated by Skn7. Skn7 genetically interacts with calcineurin, a Ca^{2+} and calmodulin dependent phosphatase (423). Deletion of *SKN7*, in combination with inactivation of calcineurin (by deletion of one of its essential components), results in sensitivity to a variety of stress factors. Interestingly, inactivation of calcineurin together with the inactivation of the cell integrity pathway (*pck1Δ* or *slt2Δ*) results in lethality (423). Deletion of *SKN7* also results in a decrease in Crz1 regulated transcription (423). Several genes regulated by Crz1 are involved in cell wall metabolism (such as *FKS2*), implicating it in mediating cellular integrity. It appears that Skn7 regulates Crz1 by stabilizing its protein levels. When *SKN7* is absent, Crz1 is efficiently degraded, likely by the Ub pathway (423).

Another role for the cell integrity pathway in transcription involves the regulation of the transcriptional silencing protein Sir3. Silencing in yeast is dependent on four Sir proteins that alter chromatin structure to silence transcription at various chromosomal locations, including the telomeres, the silent-mating-type cassettes and ribosomal RNA genes (119). Slt2 has been shown to phosphorylate Sir3, which alters the distribution of silencing and leads to a decrease in the life span of the cells (341). It has previously been shown that Sir3 phosphorylation results in reduced telomeric silencing, increased telomeric cell wall gene expression and increased cellular stress resistance (3); this could be a mechanism by which the cell responds to varying environmental conditions.

1.3.8 Other features

It appears that the primary role of the cell integrity pathway is mediating cell wall integrity. However, this pathway has also been implicated in the regulation of other cellular tasks, such as in SPB duplication, morphogenesis checkpoint and, possibly, Ub recognition by the 26S proteasome. It is unclear if these roles are independent of the other functions of the pathway, and will therefore be discussed in this section.

The initial events in SPB duplication require the function of its integral components Kar1, Cdc31 and Spc110 (158). Several genetic interactions between these proteins and the cell integrity pathway have been observed, thus implicating this pathway in their regulation. Overexpression of *WSC1*, *MID2* or *PKC1* rescued the temperature sensitivity of *kar1*, *cdc31* and *spc110* mutants (212). With the exception of *cdc31* TS mutants, all the SPB mutants that have been tested are synthetically lethal with *slt2*Δ and a *pkc1* TS mutant (212). It was proposed that this genetic relationship was unrelated to the cell wall related function of the cell integrity pathway, as most of these TS mutants did not display cell lysis defects. However, *cdc31* and *kar1* TS mutants also show synthetic lethality with *swi4Δ* suggesting a possible connection (212). In fact, SBF is a central transcriptional regulator of many SPB genes, further strengthening the connection (176). An argument against this has been made by the fact that transcript and protein levels of Cdc31, Kar1 and Spc110 are unchanged in cell integrity pathway mutants, suggesting a direct mode of regulation of these proteins by the pathway (200).

A relationship with Rad23 and Dsk2, both of which are Ub-like domain-containing proteins, has been suggested by studies of the SPB (212). Rad23 and Dsk2 were originally identified as being important in mediating SPB duplication, but were later found to have more diverse functions such as recruiting poly-Ub chain linked proteins to the 26S proteasome (98, 214). Deletion of *RAD23* and *DSK2* results in a TS block in SPB duplication and overexpression of *WSC1* and *PKC1* was found to suppress these defects similarly to those of other SPB mutants (212). This suggests a function for the cell integrity pathway in mediating the activity of these proteins either at the SPB or elsewhere.

Another important function for the cell integrity pathway is in the regulation of the morphogenesis checkpoint of the cell cycle. As mentioned above (in section 1.2.3),

the morphogenesis checkpoint responds to morphogenic defects that can occur due to environmental stresses that result in the depolarization of the actin cytoskeleton (239, 241). In response to these defects, progression from the G2-M phase of the cell cycle is inhibited so that the cell can adapt to the environmental conditions. This checkpoint relies on the inactivation of Cdc28 through its Swe1-dependent phosphorylation. Normally, Swe1 protein levels are reduced at the G2-M transition by Ub-mediated proteolysis, and are counteracted by the function of the phosphatase Mih1 (210). However, in response to the morphogenesis checkpoint Swe1 is stabilized and Mih1 is inactivated, therefore promoting Cdc28 phosphorylation and cell cycle inhibition (239).

The function of the checkpoint has been observed to be dependent on the cell integrity pathway, but interestingly only the pathway from Rho1 to Slt2 is required (148). Deletion of the upstream components (*MID2*, *WSC1* and *ROM2*) or the downstream transcription factors (*SWI4* and *RLM1*) had no effect on the checkpoint, whereas disruption of the function of any one the other signaling components severely disrupted the cell's ability to respond to defects that would induce the checkpoint. An increase in signaling through the pathway normally occurs in response to checkpoint inducing conditions, leading to an increase in Slt2 phosphorylation (148). Swe1 protein levels in these cells do not change significantly, therefore suggesting that the cell integrity pathway might directly down-regulate Mih1 function to contribute to the cell cycle delay mechanism. This hypothesis is supported by a *slt2Δ mih1Δ* strain, which displays no defects in the checkpoint (148).

An additional connection between the morphogenesis checkpoint and the cell integrity pathway was observed from the analysis of the RhoGAP Bem2. Deletion of *BEM2* results in reduced levels of Cdc28 phosphorylation and, consequently, a defective checkpoint. However, Slt2 phosphorylation is unchanged, and Swe1 protein levels are normal in these cells (258). Furthermore, the role for Bem2 in the checkpoint does not require its GAP domain, but instead requires its amino-terminal domain. Together, these observations suggest that Bem2 might participate in an independent regulatory pathway for the activation of the checkpoint.

1.4 Overview of the thesis

This thesis focuses primarily on the study of the Ub-conjugating enzyme Cdc34 and its functional partner the SCF Ub-ligase. The specific objectives were to provide insight into the mechanism by which Cdc34 catalyzes the assembly of poly-Ub chain assembly, and to expand on our knowledge of the known physiological roles of this enzyme and of the SCF complex.

The work in Chapter 2 reveals important mechanistic insight into the function of Cdc34. This chapter describes that Cdc34 self-association is a crucial event in the assembly of poly-Ub chains. Critical residues within Cdc34's catalytic domain, which are responsible for mediating this interaction, were determined, including the catalytic cysteine residue involved in forming the thiolester bond with Ub. The Ub thiolester linkage is described as the key mediator of Cdc34 self-association, a conclusion supported by the analysis of the interaction under thiolester reducing conditions, and by the dimerization of Cdc34~Ub thiolester *in vitro*. My results together with other studies, indicate that the formation of Cdc34~Ub thiolester determines its distinct mode of action, and may provide a general model by which E2 enzymes assemble poly-Ub chains.

Chapter 3 describes a novel essential function for the Cdc34/SCF complex in mediating the integrity of the *S. cerevisiae* cell wall. Temperature sensitive mutants of *CDC34* and the SCF component *CDC53* are shown to display defects consistent with a role in mediating the cell integrity signal transduction pathway. Several genetic and biochemical observations also suggest that misregulation of signaling through this pathway occurs in these mutants, which contributes significantly to the cell growth defects associated with these cells.

The work in Chaper 4 describes the roles of the Cdc34/SCF complex in mediating transcription. This chapter addresses the effect caused by the misregulation of the cell integrity pathway on transcription. Temperature sensitive mutants of *CDC34* and the SCF component *CDC53*, which are defective in cell integrity signaling, display an induction of downstream gene expression of this pathway, linking Cdc34/SCF function to these transcription responses. Furthermore, this chapter describes the global role of the Cdc34/SCF complex in mediating transcription by examining gene expression in the

cdc53-1 and *cdc34-2* temperature sensitive mutants by DNA microarray analysis. A variety of transcriptional effects were observed in these cells.

Finally, Chapter 5 summarizes and discusses the data in this thesis, and introduces some related results that may help direct future work.

1.5 References

1. Adams, J. 2003. The proteasome: structure, function, and role in the cell. Cancer Treat Rev 29 Suppl 1:3-9.
2. Agarwal, R., Z. Tang, H. Yu, and O. Cohen-Fix. 2003. Two distinct pathways for inhibiting pds1 ubiquitination in response to DNA damage. J Biol Chem 278:45027-33.
3. Ai, W., P. G. Bertram, C. K. Tsang, T. F. Chan, and X. F. Zheng. 2002. Regulation of subtelomeric silencing during stress response. Mol Cell 10:1295-305.
4. Alberts, A. S., N. Bouquin, L. H. Johnston, and R. Treisman. 1998. Analysis of RhoA-binding proteins reveals an interaction domain conserved in heterotrimeric G protein beta subunits and the yeast response regulator protein Skn7. J Biol Chem 273:8616-22.
5. Ambroggio, X. I., D. C. Rees, and R. J. Deshaies. 2004. JAMM: A Metalloprotease-Like Zinc Site in the Proteasome and Signalosome. PLoS Biol 2:E2.
6. Amerik, A. Y., S. J. Li, and M. Hochstrasser. 2000. Analysis of the deubiquitinating enzymes of the yeast Saccharomyces cerevisiae. Biol Chem 381:981-92.
7. Amon, A., S. Irniger, and K. Nasmyth. 1994. Closing the cell cycle circle in yeast: G2 cyclin proteolysis initiated at mitosis persists until the activation of G1 cyclins in the next cycle. Cell 77:1037-50.
8. Amon, A., M. Tyers, B. Futcher, and K. Nasmyth. 1993. Mechanisms that help the yeast cell cycle clock tick: G2 cyclins transcriptionally activate G2 cyclins and repress G1 cyclins. Cell 74:993-1007.
9. Andreassen, P. R., O. D. Lohez, and R. L. Margolis. 2003. G2 and spindle assembly checkpoint adaptation, and tetraploidy arrest: implications for intrinsic and chemically induced genomic instability. Mutat Res 532:245-53.
10. Andrews, P. D., and M. J. Stark. 2000. Dynamic, Rho1p-dependent localization of Pkc1p to sites of polarized growth. J Cell Sci 113 (Pt 15):2685-93.
11. Angeles de la Torre-Ruiz, M., J. Torres, J. Arino, and E. Herrero. 2002. Sit4 is required for proper modulation of the biological functions mediated by Pkc1 and the cell integrity pathway in Saccharomyces cerevisiae. J Biol Chem 277:33468-76.
12. Antonsson, B., S. Montessuit, L. Friedli, M. A. Payton, and G. Paravicini. 1994. Protein kinase C in yeast. Characteristics of the Saccharomyces cerevisiae PKC1 gene product. J Biol Chem 269:16821-8.
13. Archambault, V., C. X. Li, A. J. Tackett, R. Wasch, B. T. Chait, M. P. Rout, and F. R. Cross. 2003. Genetic and biochemical evaluation of the importance of Cdc6 in regulating mitotic exit. Mol Biol Cell 14:4592-604.
14. Arnason, T., and M. J. Ellison. 1994. Stress resistance in Saccharomyces cerevisiae is strongly correlated with assembly of a novel type of multiubiquitin chain. Mol Cell Biol 14:7876-83.

15. Arndt, K. T., C. A. Styles, and G. R. Fink. 1989. A suppressor of a HIS4 transcriptional defect encodes a protein with homology to the catalytic subunit of protein phosphatases. Cell 56:527-37.
16. Audhya, A., and S. D. Emr. 2002. Stt4 PI 4-kinase localizes to the plasma membrane and functions in the Pkc1-mediated MAP kinase cascade. Dev Cell 2:593-605.
17. Baetz, K., J. Moffat, J. Haynes, M. Chang, and B. Andrews. 2001. Transcriptional coregulation by the cell integrity mitogen-activated protein kinase Slt2 and the cell cycle regulator Swi4. Mol Cell Biol 21:6515-28.
18. Bai, C., P. Sen, K. Hofmann, L. Ma, M. Goebl, J. W. Harper, and S. J. Elledge. 1996. SKP1 connects cell cycle regulators to the ubiquitin proteolysis machinery through a novel motif, the F-box. Cell 86:263-74.
19. Bajorek, M., and M. H. Glickman. 2004. Keepers at the final gates: regulatory complexes and gating of the proteasome channel. Cell Mol Life Sci 61:1579-88.
20. Banerjee, A., L. Gregori, Y. Xu, and V. Chau. 1993. The bacterially expressed yeast CDC34 gene product can undergo autoubiquitination to form a multiubiquitin chain-linked protein. J Biol Chem 268:5668-75.
21. Barral, Y., S. Jentsch, and C. Mann. 1995. G1 cyclin turnover and nutrient uptake are controlled by a common pathway in yeast. Genes Dev 9:399-409.
22. Baumeister, W., J. Walz, F. Zuhl, and E. Seemuller. 1998. The proteasome: paradigm of a self-compartmentalizing protease. Cell 92:367-80.
23. Baumer, M., G. H. Braus, and S. Irniger. 2000. Two different modes of cyclin clb2 proteolysis during mitosis in Saccharomyces cerevisiae. FEBS Lett 468:142-8.
24. Berleth, E. S., J. Li, J. A. Braunscheidel, and C. M. Pickart. 1992. A reactive nucleophile proximal to vicinal thiols is an evolutionarily conserved feature in the mechanism of Arg aminoacyl-tRNA protein transferase. Arch Biochem Biophys 298:498-504.
25. Bickle, M., P. A. Delley, A. Schmidt, and M. N. Hall. 1998. Cell wall integrity modulates RHO1 activity via the exchange factor ROM2. Embo J 17:2235-45.
26. Blondel, M., P. M. Alepuz, L. S. Huang, S. Shaham, G. Ammerer, and M. Peter. 1999. Nuclear export of Far1p in response to pheromones requires the export receptor Msn5p/Ste21p. Genes Dev 13:2284-300.
27. Blondel, M., J. M. Galan, Y. Chi, C. Lafourcade, C. Longaretti, R. J. Deshaies, and M. Peter. 2000. Nuclear-specific degradation of Far1 is controlled by the localization of the F-box protein Cdc4. Embo J 19:6085-97.
28. Bochtler, M., L. Ditzel, M. Groll, C. Hartmann, and R. Huber. 1999. The proteasome. Annu Rev Biophys Biomol Struct 28:295-317.
29. Bonifacino, J. S., and L. M. Traub. 2003. Signals for sorting of transmembrane proteins to endosomes and lysosomes. Annu Rev Biochem 72:395-447.
30. Booher, R. N., R. J. Deshaies, and M. W. Kirschner. 1993. Properties of Saccharomyces cerevisiae wee1 and its differential regulation of p34CDC28 in response to G1 and G2 cyclins. Embo J 12:3417-26.
31. Boorsma, A., H. de Nobel, B. ter Riet, B. Bargmann, S. Brul, K. J. Hellingwerf, and F. M. Klis. 2004. Characterization of the transcriptional response to cell wall stress in Saccharomyces cerevisiae. Yeast 21:413-27.

32. Bouquin, N., A. L. Johnson, B. A. Morgan, and L. H. Johnston. 1999. Association of the cell cycle transcription factor Mbp1 with the Skn7 response regulator in budding yeast. Mol Biol Cell 10:3389-400.
33. Braun, B. C., M. Glickman, R. Kraft, B. Dahlmann, P. M. Kloetzel, D. Finley, and M. Schmidt. 1999. The base of the proteasome regulatory particle exhibits chaperone-like activity. Nat Cell Biol 1:221-6.
34. Braus, G. H. 1991. Aromatic amino acid biosynthesis in the yeast Saccharomyces cerevisiae: a model system for the regulation of a eukaryotic biosynthetic pathway. Microbiol Rev 55:349-70.
35. Broomfield, S., T. Hryciw, and W. Xiao. 2001. DNA postreplication repair and mutagenesis in Saccharomyces cerevisiae. Mutat Res 486:167-84.
36. Brown, J. L., H. Bussey, and R. C. Stewart. 1994. Yeast Skn7p functions in a eukaryotic two-component regulatory pathway. Embo J 13:5186-94.
37. Brown, J. L., S. North, and H. Bussey. 1993. SKN7, a yeast multicopy suppressor of a mutation affecting cell wall beta-glucan assembly, encodes a product with domains homologous to prokaryotic two-component regulators and to heat shock transcription factors. J Bacteriol 175:6908-15.
38. Brzovic, P. S., J. R. Keeffe, H. Nishikawa, K. Miyamoto, D. Fox, 3rd, M. Fukuda, T. Ohta, and R. Klevit. 2003. Binding and recognition in the assembly of an active BRCA1/BARD1 ubiquitin-ligase complex. Proc Natl Acad Sci U S A 100:5646-51.
39. Brzovic, P. S., P. Rajagopal, D. W. Hoyt, M. C. King, and R. E. Klevit. 2001. Structure of a BRCA1-BARD1 heterodimeric RING-RING complex. Nat Struct Biol 8:833-7.
40. Buchberger, A. 2002. From UBA to UBX: new words in the ubiquitin vocabulary. Trends Cell Biol 12:216-21.
41. Buchberger, A., M. J. Howard, M. Proctor, and M. Bycroft. 2001. The UBX domain: a widespread ubiquitin-like module. J Mol Biol 307:17-24.
42. Buehrer, B. M., and B. Errede. 1997. Coordination of the mating and cell integrity mitogen-activated protein kinase pathways in Saccharomyces cerevisiae. Mol Cell Biol 17:6517-25.
43. Bullitt, E., M. P. Rout, J. V. Kilmartin, and C. W. Akey. 1997. The yeast spindle pole body is assembled around a central crystal of Spc42p. Cell 89:1077-86.
44. Butty, A. C., P. M. Pryciak, L. S. Huang, I. Herskowitz, and M. Peter. 1998. The role of Far1p in linking the heterotrimeric G protein to polarity establishment proteins during yeast mating. Science 282:1511-6.
45. Cabib, E. 2004. The septation apparatus, a chitin-requiring machine in budding yeast. Arch Biochem Biophys 426:201-7.
46. Cabib, E., T. Drgon, J. Drgonova, R. A. Ford, and R. Kollar. 1997. The yeast cell wall, a dynamic structure engaged in growth and morphogenesis. Biochem Soc Trans 25:200-4.
47. Cabib, E., J. Drgonova, and T. Drgon. 1998. Role of small G proteins in yeast cell polarization and wall biosynthesis. Annu Rev Biochem 67:307-33.
48. Calzada, A., and A. Bueno. 2002. Genes involved in the initiation of DNA replication in yeast. Int Rev Cytol 212:133-207.

49. Calzada, A., M. Sacristan, E. Sanchez, and A. Bueno. 2001. Cdc6 cooperates with Sic1 and Hct1 to inactivate mitotic cyclin-dependent kinases. Nature 412:355-8.
50. Carroll, C. W., and D. O. Morgan. 2002. The Doc1 subunit is a processivity factor for the anaphase-promoting complex. Nat Cell Biol 4:880-7.
51. Casamayor, A., and M. Snyder. 2002. Bud-site selection and cell polarity in budding yeast. Curr Opin Microbiol 5:179-86.
52. Chang, F., and I. Herskowitz. 1990. Identification of a gene necessary for cell cycle arrest by a negative growth factor of yeast: FAR1 is an inhibitor of a G1 cyclin, CLN2. Cell 63:999-1011.
53. Chau, V., J. W. Tobias, A. Bachmair, D. Marriott, D. J. Ecker, D. K. Gonda, and A. Varshavsky. 1989. A multiubiquitin chain is confined to specific lysine in a targeted short-lived protein. Science 243:1576-83.
54. Chen, P., P. Johnson, T. Sommer, S. Jentsch, and M. Hochstrasser. 1993. Multiple ubiquitin-conjugating enzymes participate in the in vivo degradation of the yeast MAT alpha 2 repressor. Cell 74:357-69.
55. Cheng, I. H., L. A. Roberts, and B. K. Tye. 2002. Mcm3 is polyubiquitinated during mitosis before establishment of the pre-replication complex. J Biol Chem 277:41706-14.
56. Chi, Y., M. J. Huddleston, X. Zhang, R. A. Young, R. S. Annan, S. A. Carr, and R. J. Deshaies. 2001. Negative regulation of Gcn4 and Msn2 transcription factors by Srb10 cyclin-dependent kinase. Genes Dev 15:1078-92.
57. Chim, N., W. E. Gall, J. Xiao, M. P. Harris, T. R. Graham, and A. M. Krezel. 2004. Solution structure of the ubiquitin-binding domain in Swa2p from Saccharomyces cerevisiae. Proteins 54:784-93.
58. Cho, R. J., M. J. Campbell, E. A. Winzeler, L. Steinmetz, A. Conway, L. Wodicka, T. G. Wolfsberg, A. E. Gabrielian, D. Landsman, D. J. Lockhart, and R. W. Davis. 1998. A genome-wide transcriptional analysis of the mitotic cell cycle. Mol Cell 2:65-73.
59. Ciechanover, A. 2003. The ubiquitin proteolytic system and pathogenesis of human diseases: a novel platform for mechanism-based drug targeting. Biochem Soc Trans 31:474-81.
60. Ciechanover, A., and P. Brundin. 2003. The ubiquitin proteasome system in neurodegenerative diseases: sometimes the chicken, sometimes the egg. Neuron 40:427-46.
61. Ciechanover, A., S. Elias, H. Heller, and A. Hershko. 1982. "Covalent affinity" purification of ubiquitin-activating enzyme. J Biol Chem 257:2537-42.
62. Ciechanover, A., H. Heller, S. Elias, A. L. Haas, and A. Hershko. 1980. ATP-dependent conjugation of reticulocyte proteins with the polypeptide required for protein degradation. Proc Natl Acad Sci U S A 77:1365-8.
63. Ciechanover, A., and A. L. Schwartz. 2002. Ubiquitin-mediated degradation of cellular proteins in health and disease. Hepatology 35:3-6.
64. Ciosk, R., W. Zachariae, C. Michaelis, A. Shevchenko, M. Mann, and K. Nasmyth. 1998. An ESP1/PDS1 complex regulates loss of sister chromatid cohesion at the metaphase to anaphase transition in yeast. Cell 93:1067-76.

65. Cohen-Fix, O., J. M. Peters, M. W. Kirschner, and D. Koshland. 1996. Anaphase initiation in Saccharomyces cerevisiae is controlled by the APC-dependent degradation of the anaphase inhibitor Pds1p. Genes Dev 10:3081-93.
66. Connelly, C., and P. Hieter. 1996. Budding yeast SKP1 encodes an evolutionarily conserved kinetochore protein required for cell cycle progression. Cell 86:275-85.
67. Cook, W. J., L. C. Jeffrey, M. Carson, Z. Chen, and C. M. Pickart. 1992. Structure of a diubiquitin conjugate and a model for interaction with ubiquitin conjugating enzyme (E2). J Biol Chem 267:16467-71.
68. Cook, W. J., L. C. Jeffrey, E. Kasperek, and C. M. Pickart. 1994. Structure of tetraubiquitin shows how multiubiquitin chains can be formed. J Mol Biol 236:601-9.
69. Cook, W. J., L. C. Jeffrey, Y. Xu, and V. Chau. 1993. Tertiary structures of class I ubiquitin-conjugating enzymes are highly conserved: crystal structure of yeast Ubc4. Biochemistry 32:13809-17.
70. Cook, W. J., P. D. Martin, B. F. Edwards, R. K. Yamazaki, and V. Chau. 1997. Crystal structure of a class I ubiquitin conjugating enzyme (Ubc7) from Saccharomyces cerevisiae at 2.9 angstroms resolution. Biochemistry 36:1621-7.
71. Cope, G. A., G. S. Suh, L. Aravind, S. E. Schwarz, S. L. Zipursky, E. V. Koonin, and R. J. Deshaies. 2002. Role of predicted metalloprotease motif of Jab1/Csn5 in cleavage of Nedd8 from Cul1. Science 298:608-11.
72. Costanzo, M., J. L. Nishikawa, X. Tang, J. S. Millman, O. Schub, K. Breitkreuz, D. Dewar, I. Rupes, B. Andrews, and M. Tyers. 2004. CDK activity antagonizes Whi5, an inhibitor of G1/S transcription in yeast. Cell 117:899-913.
73. Costanzo, M., O. Schub, and B. Andrews. 2003. G1 transcription factors are differentially regulated in Saccharomyces cerevisiae by the Swi6-binding protein Stb1. Mol Cell Biol 23:5064-77.
74. Costigan, C., S. Gehrung, and M. Snyder. 1992. A synthetic lethal screen identifies SLK1, a novel protein kinase homolog implicated in yeast cell morphogenesis and cell growth. Mol Cell Biol 12:1162-78.
75. Costigan, C., and M. Snyder. 1994. SLK1, a yeast homolog of MAP kinase activators, has a RAS/cAMP-independent role in nutrient sensing. Mol Gen Genet 243:286-96.
76. Craig, K. L., and M. Tyers. 1999. The F-box: a new motif for ubiquitin dependent proteolysis in cell cycle regulation and signal transduction. Prog Biophys Mol Biol 72:299-328.
77. Cross, F., and J. McKinney. 1992. Is START a switch? Ciba Found Symp 170:20-5; discussion 25-9.
78. de Bruin, R. A., W. H. McDonald, T. I. Kalashnikova, J. Yates, 3rd, and C. Wittenberg. 2004. Cln3 activates G1-specific transcription via phosphorylation of the SBF bound repressor Whi5. Cell 117:887-98.
79. de Nobel, H., C. Ruiz, H. Martin, W. Morris, S. Brul, M. Molina, and F. M. Klis. 2000. Cell wall perturbation in yeast results in dual phosphorylation of the Slt2/Mpk1 MAP kinase and in an Slt2-mediated increase in FKS2-lacZ expression, glucanase resistance and thermotolerance. Microbiology 146 (Pt 9):2121-32.

80. Deffenbaugh, A. E., K. M. Scaglione, L. Zhang, J. M. Moore, T. Buranda, L. A. Sklar, and D. Skowyra. 2003. Release of ubiquitin-charged Cdc34-S - Ub from the RING domain is essential for ubiquitination of the SCF(Cdc4)-bound substrate Sic1. Cell 114:611-22.

81. Deng, L., C. Wang, E. Spencer, L. Yang, A. Braun, J. You, C. Slaughter, C. Pickart, and Z. J. Chen. 2000. Activation of the IkappaB kinase complex by TRAF6 requires a dimeric ubiquitin-conjugating enzyme complex and a unique polyubiquitin chain. Cell 103:351-61.

82. DeSalle, L. M., and M. Pagano. 2001. Regulation of the G1 to S transition by the ubiquitin pathway. FEBS Lett 490:179-89.

83. Deshaies, R. J. 1999. SCF and Cullin/Ring H2-based ubiquitin ligases. Annu Rev Cell Dev Biol 15:435-67.

84. Di Como, C. J., H. Chang, and K. T. Arndt. 1995. Activation of CLN1 and CLN2 G1 cyclin gene expression by BCK2. Mol Cell Biol 15:1835-46.

85. Dieckmann, T., E. S. Withers-Ward, M. A. Jarosinski, C. F. Liu, I. S. Chen, and J. Feigon. 1998. Structure of a human DNA repair protein UBA domain that interacts with HIV-1 Vpr. Nat Struct Biol 5:1042-7.

86. Dirick, L., T. Bohm, and K. Nasmyth. 1995. Roles and regulation of Cln-Cdc28 kinases at the start of the cell cycle of Saccharomyces cerevisiae. Embo J 14:4803-13.

87. Dirick, L., T. Moll, H. Auer, and K. Nasmyth. 1992. A central role for SWI6 in modulating cell cycle Start-specific transcription in yeast. Nature 357:508-13.

88. Dirick, L., and K. Nasmyth. 1991. Positive feedback in the activation of G1 cyclins in yeast. Nature 351:754-7.

89. Doignon, F., C. Weinachter, O. Roumanie, and M. Crouzet. 1999. The yeast Rgd1p is a GTPase activating protein of the Rho3 and rho4 proteins. FEBS Lett 459:458-62.

90. Douglas, C. M. 2001. Fungal beta(1,3)-D-glucan synthesis. Med Mycol 39 Suppl 1:55-66.

91. Drgonova, J., T. Drgon, D. H. Roh, and E. Cabib. 1999. The GTP-binding protein Rho1p is required for cell cycle progression and polarization of the yeast cell. J Cell Biol 146:373-87.

92. Drgonova, J., T. Drgon, K. Tanaka, R. Kollar, G. C. Chen, R. A. Ford, C. S. Chan, Y. Takai, and E. Cabib. 1996. Rho1p, a yeast protein at the interface between cell polarization and morphogenesis. Science 272:277-9.

93. Drury, L. S., G. Perkins, and J. F. Diffley. 1997. The Cdc4/34/53 pathway targets Cdc6p for proteolysis in budding yeast. Embo J 16:5966-76.

94. Drury, L. S., G. Perkins, and J. F. Diffley. 2000. The cyclin-dependent kinase Cdc28p regulates distinct modes of Cdc6p proteolysis during the budding yeast cell cycle. Curr Biol 10:231-40.

95. Dutcher, S. K., and L. H. Hartwell. 1982. The role of S. cerevisiae cell division cycle genes in nuclear fusion. Genetics 100:175-84.

96. Early, A., L. S. Drury, and J. F. Diffley. 2004. Mechanisms involved in regulating DNA replication origins during the cell cycle and in response to DNA damage. Philos Trans R Soc Lond B Biol Sci 359:31-8.

97. Elion, E. A. 2000. Pheromone response, mating and cell biology. Curr Opin Microbiol 3:573-81.
98. Elsasser, S., D. Chandler-Militello, B. Muller, J. Hanna, and D. Finley. 2004. Rad23 and Rpn10 serve as alternative ubiquitin receptors for the proteasome. J Biol Chem 279:26817-22.
99. Elsasser, S., Y. Chi, P. Yang, and J. L. Campbell. 1999. Phosphorylation controls timing of Cdc6p destruction: A biochemical analysis. Mol Biol Cell 10:3263-77.
100. Elsasser, S., F. Lou, B. Wang, J. L. Campbell, and A. Jong. 1996. Interaction between yeast Cdc6 protein and B-type cyclin/Cdc28 kinases. Mol Biol Cell 7:1723-35.
101. Engebrecht, J. 2003. Cell signaling in yeast sporulation. Biochem Biophys Res Commun 306:325-8.
102. Errede, B., R. M. Cade, B. M. Yashar, Y. Kamada, D. E. Levin, K. Irie, and K. Matsumoto. 1995. Dynamics and organization of MAP kinase signal pathways. Mol Reprod Dev 42:477-85.
103. Errede, B., A. Gartner, Z. Zhou, K. Nasmyth, and G. Ammerer. 1993. MAP kinase-related FUS3 from S. cerevisiae is activated by STE7 in vitro. Nature 362:261-4.
104. Evans, T., E. T. Rosenthal, J. Youngblom, D. Distel, and T. Hunt. 1983. Cyclin: a protein specified by maternal mRNA in sea urchin eggs that is destroyed at each cleavage division. Cell 33:389-96.
105. Fang, G., H. Yu, and M. W. Kirschner. 1999. Control of mitotic transitions by the anaphase-promoting complex. Philos Trans R Soc Lond B Biol Sci 354:1583-90.
106. Feldman, R. M., C. C. Correll, K. B. Kaplan, and R. J. Deshaies. 1997. A complex of Cdc4p, Skp1p, and Cdc53p/cullin catalyzes ubiquitination of the phosphorylated CDK inhibitor Sic1p. Cell 91:221-30.
107. Ferrell, K., C. R. Wilkinson, W. Dubiel, and C. Gordon. 2000. Regulatory subunit interactions of the 26S proteasome, a complex problem. Trends Biochem Sci 25:83-8.
108. Finley, D., B. Bartel, and A. Varshavsky. 1989. The tails of ubiquitin precursors are ribosomal proteins whose fusion to ubiquitin facilitates ribosome biogenesis. Nature 338:394-401.
109. Fisk, H. A., and M. P. Yaffe. 1999. A role for ubiquitination in mitochondrial inheritance in Saccharomyces cerevisiae. J Cell Biol 145:1199-208.
110. Fitch, I., C. Dahmann, U. Surana, A. Amon, K. Nasmyth, L. Goetsch, B. Byers, and B. Futcher. 1992. Characterization of four B-type cyclin genes of the budding yeast Saccharomyces cerevisiae. Mol Biol Cell 3:805-18.
111. Flandez, M., I. C. Cosano, C. Nombela, H. Martin, and M. Molina. 2004. Reciprocal regulation between Slt2 MAPK and isoforms of Msg5 dual-specificity protein phosphatase modulates the yeast cell integrity pathway. J Biol Chem 279:11027-34.
112. Flick, K., I. Ouni, J. A. Wohlschlegel, C. Capati, W. H. McDonald, J. R. Yates, and P. Kaiser. 2004. Proteolysis-independent regulation of the transcription factor Met4 by a single Lys 48-linked ubiquitin chain. Nat Cell Biol 6:634-41.
113. Forsburg, S. L. 2001. The art and design of genetic screens: yeast. Nat Rev Genet 2:659-68.

114. Francis, S. E., and T. N. Davis. 2000. The spindle pole body of Saccharomyces cerevisiae: architecture and assembly of the core components. Curr Top Dev Biol 49:105-32.
115. Fujiwara, K., T. Tenno, K. Sugasawa, J. G. Jee, I. Ohki, C. Kojima, H. Tochio, H. Hiroaki, F. Hanaoka, and M. Shirakawa. 2004. Structure of the ubiquitin-interacting motif of S5a bound to the ubiquitin-like domain of HR23B. J Biol Chem 279:4760-7.
116. Furukawa, M., Y. J. He, C. Borchers, and Y. Xiong. 2003. Targeting of protein ubiquitination by BTB-Cullin 3-Roc1 ubiquitin ligases. Nat Cell Biol 5:1001-7.
117. Galan, J. M., and R. Haguenauer-Tsapis. 1997. Ubiquitin lys63 is involved in ubiquitination of a yeast plasma membrane protein. Embo J 16:5847-54.
118. Garcia, R., C. Bermejo, C. Grau, R. Perez, J. M. Rodriguez-Pena, J. Francois, C. Nombela, and J. Arroyo. 2004. The global transcriptional response to transient cell wall damage in Saccharomyces cerevisiae and its regulation by the cell integrity signaling pathway. J Biol Chem 279:15183-95.
119. Gartenberg, M. R. 2000. The Sir proteins of Saccharomyces cerevisiae: mediators of transcriptional silencing and much more. Curr Opin Microbiol 3:132-7.
120. Gartner, A., A. Jovanovic, D. I. Jeoung, S. Bourlat, F. R. Cross, and G. Ammerer. 1998. Pheromone-dependent G1 cell cycle arrest requires Far1 phosphorylation, but may not involve inhibition of Cdc28-Cln2 kinase, in vivo. Mol Cell Biol 18:3681-91.
121. Geyer, R., S. Wee, S. Anderson, J. Yates, and D. A. Wolf. 2003. BTB/POZ domain proteins are putative substrate adaptors for cullin 3 ubiquitin ligases. Mol Cell 12:783-90.
122. Geymonat, M., A. Spanos, G. P. Wells, S. J. Smerdon, and S. G. Sedgwick. 2004. Clb6/Cdc28 and Cdc14 regulate phosphorylation status and cellular localization of Swi6. Mol Cell Biol 24:2277-85.
123. Ghiara, J. B., H. E. Richardson, K. Sugimoto, M. Henze, D. J. Lew, C. Wittenberg, and S. I. Reed. 1991. A cyclin B homolog in S. cerevisiae: chronic activation of the Cdc28 protein kinase by cyclin prevents exit from mitosis. Cell 65:163-74.
124. Gieffers, C., P. Dube, J. R. Harris, H. Stark, and J. M. Peters. 2001. Three-dimensional structure of the anaphase-promoting complex. Mol Cell 7:907-13.
125. Girod, P. A., and R. D. Vierstra. 1993. A major ubiquitin conjugation system in wheat germ extracts involves a 15-kDa ubiquitin-conjugating enzyme (E2) homologous to the yeast UBC4/UBC5 gene products. J Biol Chem 268:955-60.
126. Glickman, M. H., D. M. Rubin, V. A. Fried, and D. Finley. 1998. The regulatory particle of the Saccharomyces cerevisiae proteasome. Mol Cell Biol 18:3149-62.
127. Glotzer, M., A. W. Murray, and M. W. Kirschner. 1991. Cyclin is degraded by the ubiquitin pathway. Nature 349:132-8.
128. Goh, P. Y., and U. Surana. 1999. Cdc4, a protein required for the onset of S phase, serves an essential function during G(2)/M transition in Saccharomyces cerevisiae. Mol Cell Biol 19:5512-22.
129. Goldknopf, I. L., and H. Busch. 1977. Isopeptide linkage between nonhistone and histone 2A polypeptides of chromosomal conjugate-protein A24. Proc Natl Acad Sci U S A 74:864-8.

130. Goldstein, G., M. Scheid, U. Hammerling, D. H. Schlesinger, H. D. Niall, and E. A. Boyse. 1975. Isolation of a polypeptide that has lymphocyte-differentiating properties and is probably represented universally in living cells. Proc Natl Acad Sci U S A 72:11-5.

131. Gong, L., and E. T. Yeh. 1999. Identification of the activating and conjugating enzymes of the NEDD8 conjugation pathway. J Biol Chem 274:12036-42.

132. Grandin, N., and S. I. Reed. 1993. Differential function and expression of Saccharomyces cerevisiae B-type cyclins in mitosis and meiosis. Mol Cell Biol 13:2113-25.

133. Gray, J. V., J. P. Ogas, Y. Kamada, M. Stone, D. E. Levin, and I. Herskowitz. 1997. A role for the Pkc1 MAP kinase pathway of Saccharomyces cerevisiae in bud emergence and identification of a putative upstream regulator. Embo J 16:4924-37.

134. Gray, J. V., G. A. Petsko, G. C. Johnston, D. Ringe, R. A. Singer, and M. Werner-Washburne. 2004. "Sleeping beauty": quiescence in Saccharomyces cerevisiae. Microbiol Mol Biol Rev 68:187-206.

135. Groll, M., M. Bajorek, A. Kohler, L. Moroder, D. M. Rubin, R. Huber, M. H. Glickman, and D. Finley. 2000. A gated channel into the proteasome core particle. Nat Struct Biol 7:1062-7.

136. Grossberger, R., C. Gieffers, W. Zachariae, A. V. Podtelejnikov, A. Schleiffer, K. Nasmyth, M. Mann, and J. M. Peters. 1999. Characterization of the DOC1/APC10 subunit of the yeast and the human anaphase-promoting complex. J Biol Chem 274:14500-7.

137. Guo, W., F. Tamanoi, and P. Novick. 2001. Spatial regulation of the exocyst complex by Rho1 GTPase. Nat Cell Biol 3:353-60.

138. Gustin, M. C., J. Albertyn, M. Alexander, and K. Davenport. 1998. MAP kinase pathways in the yeast Saccharomyces cerevisiae. Microbiol Mol Biol Rev 62:1264-300.

139. Gutzke, G., B. Fischer, R. R. Mendel, and G. Schwarz. 2001. Thiocarboxylation of molybdopterin synthase provides evidence for the mechanism of dithiolene formation in metal-binding pterins. J Biol Chem 276:36268-74.

140. Gwozd, C. S., T. G. Arnason, W. J. Cook, V. Chau, and M. J. Ellison. 1995. The yeast UBC4 ubiquitin conjugating enzyme monoubiquitinates itself in vivo: evidence for an E2-E2 homointeraction. Biochemistry 34:6296-302.

141. Haas, A. L., and I. A. Rose. 1982. The mechanism of ubiquitin activating enzyme. A kinetic and equilibrium analysis. J Biol Chem 257:10329-37.

142. Haas, A. L., J. V. Warms, A. Hershko, and I. A. Rose. 1982. Ubiquitin-activating enzyme. Mechanism and role in protein-ubiquitin conjugation. J Biol Chem 257:2543-8.

143. Haas, A. L., J. V. Warms, and I. A. Rose. 1983. Ubiquitin adenylate: structure and role in ubiquitin activation. Biochemistry 22:4388-94.

144. Hahn, J. S., and D. J. Thiele. 2002. Regulation of the Saccharomyces cerevisiae Slt2 kinase pathway by the stress-inducible Sdp1 dual specificity phosphatase. J Biol Chem 277:21278-84.

145. Hamilton, K. S., M. J. Ellison, K. R. Barber, R. S. Williams, J. T. Huzil, S. McKenna, C. Ptak, M. Glover, and G. S. Shaw. 2001. Structure of a conjugating

enzyme-ubiquitin thiolester intermediate reveals a novel role for the ubiquitin tail. Structure (Camb) 9:897-904.

146. Haracska, L., C. A. Torres-Ramos, R. E. Johnson, S. Prakash, and L. Prakash. 2004. Opposing effects of ubiquitin conjugation and SUMO modification of PCNA on replicational bypass of DNA lesions in Saccharomyces cerevisiae. Mol Cell Biol 24:4267-74.
147. Harper, J. W., J. L. Burton, and M. J. Solomon. 2002. The anaphase-promoting complex: it's not just for mitosis any more. Genes Dev 16:2179-206.
148. Harrison, J. C., E. S. Bardes, Y. Ohya, and D. J. Lew. 2001. A role for the Pkc1p/Mpk1p kinase cascade in the morphogenesis checkpoint. Nat Cell Biol 3:417-20.
149. Harrison, J. C., T. R. Zyla, E. S. Bardes, and D. J. Lew. 2004. Stress-specific activation mechanisms for the "cell integrity" MAPK pathway. J Biol Chem 279:2616-22.
150. Hartmann-Petersen, R., and C. Gordon. 2004. Integral UBL domain proteins: a family of proteasome interacting proteins. Semin Cell Dev Biol 15:247-59.
151. Hartwell, L. H., J. Culotti, J. R. Pringle, and B. J. Reid. 1974. Genetic control of the cell division cycle in yeast. Science 183:46-51.
152. Hartwell, L. H., and T. A. Weinert. 1989. Checkpoints: controls that ensure the order of cell cycle events. Science 246:629-34.
153. Harvey, S. L., and D. R. Kellogg. 2003. Conservation of mechanisms controlling entry into mitosis: budding yeast wee1 delays entry into mitosis and is required for cell size control. Curr Biol 13:264-75.
154. Hashizume, R., M. Fukuda, I. Maeda, H. Nishikawa, D. Oyake, Y. Yabuki, H. Ogata, and T. Ohta. 2001. The RING heterodimer BRCA1-BARD1 is a ubiquitin ligase inactivated by a breast cancer-derived mutation. J Biol Chem 276:14537-40.
155. Hatakeyama, S., and K. I. Nakayama. 2003. U-box proteins as a new family of ubiquitin ligases. Biochem Biophys Res Commun 302:635-45.
156. Hatakeyama, S., M. Yada, M. Matsumoto, N. Ishida, and K. I. Nakayama. 2001. U box proteins as a new family of ubiquitin-protein ligases. J Biol Chem 276:33111-20.
157. Heinisch, J. J., A. Lorberg, H. P. Schmitz, and J. J. Jacoby. 1999. The protein kinase C-mediated MAP kinase pathway involved in the maintenance of cellular integrity in Saccharomyces cerevisiae. Mol Microbiol 32:671-80.
158. Helfant, A. H. 2002. Composition of the spindle pole body of Saccharomyces cerevisiae and the proteins involved in its duplication. Curr Genet 40:291-310.
159. Hellmann, H., and M. Estelle. 2002. Plant development: regulation by protein degradation. Science 297:793-7.
160. Henchoz, S., Y. Chi, B. Catarin, I. Herskowitz, R. J. Deshaies, and M. Peter. 1997. Phosphorylation- and ubiquitin-dependent degradation of the cyclin-dependent kinase inhibitor Far1p in budding yeast. Genes Dev 11:3046-60.
161. Hershko, A., and A. Ciechanover. 1998. The ubiquitin system. Annu Rev Biochem 67:425-79.

162. Hershko, A., A. Ciechanover, and I. A. Rose. 1979. Resolution of the ATP-dependent proteolytic system from reticulocytes: a component that interacts with ATP. Proc Natl Acad Sci U S A 76:3107-10.
163. Hershko, A., and H. Heller. 1985. Occurrence of a polyubiquitin structure in ubiquitin-protein conjugates. Biochem Biophys Res Commun 128:1079-86.
164. Hershko, A., H. Heller, S. Elias, and A. Ciechanover. 1983. Components of ubiquitin-protein ligase system. Resolution, affinity purification, and role in protein breakdown. J Biol Chem 258:8206-14.
165. Herskowitz, I. 1988. Life cycle of the budding yeast Saccharomyces cerevisiae. Microbiol Rev 52:536-53.
166. Herskowitz, I. 1995. MAP kinase pathways in yeast: for mating and more. Cell 80:187-97.
167. Hicke, L., and R. Dunn. 2003. Regulation of membrane protein transport by ubiquitin and ubiquitin-binding proteins. Annu Rev Cell Dev Biol 19:141-72.
168. Hinnebusch, A. G. 1997. Translational regulation of yeast GCN4. A window on factors that control initiator-trna binding to the ribosome. J Biol Chem 272:21661-4.
169. Ho, Y., M. Costanzo, L. Moore, R. Kobayashi, and B. J. Andrews. 1999. Regulation of transcription at the Saccharomyces cerevisiae start transition by Stb1, a Swi6-binding protein. Mol Cell Biol 19:5267-78.
170. Hochstrasser, M. 2000. Evolution and function of ubiquitin-like protein-conjugation systems. Nat Cell Biol 2:E153-7.
171. Hochstrasser, M. 1996. Ubiquitin-dependent protein degradation. Annu Rev Genet 30:405-39.
172. Hodgins, R., C. Gwozd, T. Arnason, M. Cummings, and M. J. Ellison. 1996. The tail of a ubiquitin-conjugating enzyme redirects multi-ubiquitin chain synthesis from the lysine 48-linked configuration to a novel nonlysine-linked form. J Biol Chem 271:28766-71.
173. Hoege, C., B. Pfander, G. L. Moldovan, G. Pyrowolakis, and S. Jentsch. 2002. RAD6-dependent DNA repair is linked to modification of PCNA by ubiquitin and SUMO. Nature 419:135-41.
174. Hofmann, K., and P. Bucher. 1996. The UBA domain: a sequence motif present in multiple enzyme classes of the ubiquitination pathway. Trends Biochem Sci 21:172-3.
175. Hofmann, R. M., and C. M. Pickart. 1999. Noncanonical MMS2-encoded ubiquitin-conjugating enzyme functions in assembly of novel polyubiquitin chains for DNA repair. Cell 96:645-53.
176. Horak, C. E., N. M. Luscombe, J. Qian, P. Bertone, S. Piccirrillo, M. Gerstein, and M. Snyder. 2002. Complex transcriptional circuitry at the G1/S transition in Saccharomyces cerevisiae. Genes Dev 16:3017-33.
177. Horwich, A. L., E. U. Weber-Ban, and D. Finley. 1999. Chaperone rings in protein folding and degradation. Proc Natl Acad Sci U S A 96:11033-40.
178. Hu, M., P. Li, M. Li, W. Li, T. Yao, J. W. Wu, W. Gu, R. E. Cohen, and Y. Shi. 2002. Crystal structure of a UBP-family deubiquitinating enzyme in isolation and in complex with ubiquitin aldehyde. Cell 111:1041-54.

179. Huang, D. T., D. W. Miller, R. Mathew, R. Cassell, J. M. Holton, M. F. Roussel, and B. A. Schulman. 2004. A unique E1-E2 interaction required for optimal conjugation of the ubiquitin-like protein NEDD8. Nat Struct Mol Biol.
180. Huang, D. T., H. Walden, D. Duda, and B. A. Schulman. 2004. Ubiquitin-like protein activation. Oncogene 23:1958-71.
181. Huang, L., E. Kinnucan, G. Wang, S. Beaudenon, P. M. Howley, J. M. Huibregtse, and N. P. Pavletich. 1999. Structure of an E6AP-UbcH7 complex: insights into ubiquitination by the E2-E3 enzyme cascade. Science 286:1321-6.
182. Igual, J. C., A. L. Johnson, and L. H. Johnston. 1996. Coordinated regulation of gene expression by the cell cycle transcription factor Swi4 and the protein kinase C MAP kinase pathway for yeast cell integrity. Embo J 15:5001-13.
183. Igual, J. C., W. M. Toone, and L. H. Johnston. 1997. A genetic screen reveals a role for the late G1-specific transcription factor Swi4p in diverse cellular functions including cytokinesis. J Cell Sci 110 (Pt 14):1647-54.
184. Irie, K., M. Takase, K. S. Lee, D. E. Levin, H. Araki, K. Matsumoto, and Y. Oshima. 1993. MKK1 and MKK2, which encode Saccharomyces cerevisiae mitogen-activated protein kinase-kinase homologs, function in the pathway mediated by protein kinase C. Mol Cell Biol 13:3076-83.
185. Irniger, S., and G. H. Braus. 2003. Controlling transcription by destruction: the regulation of yeast Gcn4p stability. Curr Genet 44:8-18.
186. Ivanovska, I., and M. D. Rose. 2000. SLG1 plays a role during G1 in the decision to enter or exit the cell cycle. Mol Gen Genet 262:1147-56.
187. Iyer, V. R., C. E. Horak, C. S. Scafe, D. Botstein, M. Snyder, and P. O. Brown. 2001. Genomic binding sites of the yeast cell-cycle transcription factors SBF and MBF. Nature 409:533-8.
188. Jackson, P. K., A. G. Eldridge, E. Freed, L. Furstenthal, J. Y. Hsu, B. K. Kaiser, and J. D. Reimann. 2000. The lore of the RINGs: substrate recognition and catalysis by ubiquitin ligases. Trends Cell Biol 10:429-39.
189. Jacoby, J. J., S. M. Nilius, and J. J. Heinisch. 1998. A screen for upstream components of the yeast protein kinase C signal transduction pathway identifies the product of the SLG1 gene. Mol Gen Genet 258:148-55.
190. Jacoby, J. J., H. P. Schmitz, and J. J. Heinisch. 1997. Mutants affected in the putative diacylglycerol binding site of yeast protein kinase C. FEBS Lett 417:219-22.
191. Jentsch, S. 1992. The ubiquitin-conjugation system. Annu Rev Genet 26:179-207.
192. Jentsch, S., and G. Pyrowolakis. 2000. Ubiquitin and its kin: how close are the family ties? Trends Cell Biol 10:335-42.
193. Jeoung, D. I., L. J. Oehlen, and F. R. Cross. 1998. Cln3-associated kinase activity in Saccharomyces cerevisiae is regulated by the mating factor pathway. Mol Cell Biol 18:433-41.
194. Jiang, F., and R. Basavappa. 1999. Crystal structure of the cyclin-specific ubiquitin-conjugating enzyme from clam, E2-C, at 2.0 A resolution. Biochemistry 38:6471-8.
195. Jigami, Y., and T. Odani. 1999. Mannosylphosphate transfer to yeast mannan. Biochim Biophys Acta 1426:335-45.

196. Joazeiro, C. A., and A. M. Weissman. 2000. RING finger proteins: mediators of ubiquitin ligase activity. Cell 102:549-52.
197. Johnson, E. S., P. C. Ma, I. M. Ota, and A. Varshavsky. 1995. A proteolytic pathway that recognizes ubiquitin as a degradation signal. J Biol Chem 270:17442-56.
198. Johnston, S. C., C. N. Larsen, W. J. Cook, K. D. Wilkinson, and C. P. Hill. 1997. Crystal structure of a deubiquitinating enzyme (human UCH-L3) at 1.8 A resolution. Embo J 16:3787-96.
199. Johnston, S. C., S. M. Riddle, R. E. Cohen, and C. P. Hill. 1999. Structural basis for the specificity of ubiquitin C-terminal hydrolases. Embo J 18:3877-87.
200. Jung, U. S., and D. E. Levin. 1999. Genome-wide analysis of gene expression regulated by the yeast cell wall integrity signalling pathway. Mol Microbiol 34:1049-57.
201. Jung, U. S., A. K. Sobering, M. J. Romeo, and D. E. Levin. 2002. Regulation of the yeast Rlm1 transcription factor by the Mpk1 cell wall integrity MAP kinase. Mol Microbiol 46:781-9.
202. Kaiser, P., K. Flick, C. Wittenberg, and S. I. Reed. 2000. Regulation of transcription by ubiquitination without proteolysis: Cdc34/SCF(Met30)-mediated inactivation of the transcription factor Met4. Cell 102:303-14.
203. Kaiser, P., R. A. Sia, E. G. Bardes, D. J. Lew, and S. I. Reed. 1998. Cdc34 and the F-box protein Met30 are required for degradation of the Cdk-inhibitory kinase Swe1. Genes Dev 12:2587-97.
204. Kamada, Y., H. Qadota, C. P. Python, Y. Anraku, Y. Ohya, and D. E. Levin. 1996. Activation of yeast protein kinase C by Rho1 GTPase. J Biol Chem 271:9193-6.
205. Kamura, T., D. M. Koepp, M. N. Conrad, D. Skowyra, R. J. Moreland, O. Iliopoulos, W. S. Lane, W. G. Kaelin, Jr., S. J. Elledge, R. C. Conaway, J. W. Harper, and J. W. Conaway. 1999. Rbx1, a component of the VHL tumor suppressor complex and SCF ubiquitin ligase. Science 284:657-61.
206. Kamura, T., S. Sato, D. Haque, L. Liu, W. G. Kaelin, Jr., R. C. Conaway, and J. W. Conaway. 1998. The Elongin BC complex interacts with the conserved SOCS-box motif present in members of the SOCS, ras, WD-40 repeat, and ankyrin repeat families. Genes Dev 12:3872-81.
207. Kang, R. S., C. M. Daniels, S. A. Francis, S. C. Shih, W. J. Salerno, L. Hicke, and I. Radhakrishnan. 2003. Solution structure of a CUE-ubiquitin complex reveals a conserved mode of ubiquitin binding. Cell 113:621-30.
208. Kawakami, T., T. Chiba, T. Suzuki, K. Iwai, K. Yamanaka, N. Minato, H. Suzuki, N. Shimbara, Y. Hidaka, F. Osaka, M. Omata, and K. Tanaka. 2001. NEDD8 recruits E2-ubiquitin to SCF E3 ligase. Embo J 20:4003-12.
209. Kellis, M., N. Patterson, M. Endrizzi, B. Birren, and E. S. Lander. 2003. Sequencing and comparison of yeast species to identify genes and regulatory elements. Nature 423:241-54.
210. Kellogg, D. R. 2003. Wee1-dependent mechanisms required for coordination of cell growth and cell division. J Cell Sci 116:4883-90.

211. Ketela, T., R. Green, and H. Bussey. 1999. Saccharomyces cerevisiae mid2p is a potential cell wall stress sensor and upstream activator of the PKC1-MPK1 cell integrity pathway. J Bacteriol 181:3330-40.
212. Khalfan, W., I. Ivanovska, and M. D. Rose. 2000. Functional interaction between the PKC1 pathway and CDC31 network of SPB duplication genes. Genetics 155:1543-59.
213. Kile, B. T., B. A. Schulman, W. S. Alexander, N. A. Nicola, H. M. Martin, and D. J. Hilton. 2002. The SOCS box: a tale of destruction and degradation. Trends Biochem Sci 27:235-41.
214. Kim, I., K. Mi, and H. Rao. 2004. Multiple interactions of rad23 suggest a mechanism for ubiquitylated substrate delivery important in proteolysis. Mol Biol Cell 15:3357-65.
215. King, R. W., R. J. Deshaies, J. M. Peters, and M. W. Kirschner. 1996. How proteolysis drives the cell cycle. Science 274:1652-9.
216. Kipreos, E. T., L. E. Lander, J. P. Wing, W. W. He, and E. M. Hedgecock. 1996. cul-1 is required for cell cycle exit in C. elegans and identifies a novel gene family. Cell 85:829-39.
217. Kishi, T., T. Seno, and F. Yamao. 1998. Grr1 functions in the ubiquitin pathway in Saccharomyces cerevisiae through association with Skp1. Mol Gen Genet 257:143-8.
218. Kishi, T., and F. Yamao. 1998. An essential function of Grr1 for the degradation of Cln2 is to act as a binding core that links Cln2 to Skp1. J Cell Sci 111 (Pt 24):3655-61.
219. Klis, F. M., P. Mol, K. Hellingwerf, and S. Brul. 2002. Dynamics of cell wall structure in Saccharomyces cerevisiae. FEMS Microbiol Rev 26:239-56.
220. Knapp, D., L. Bhoite, D. J. Stillman, and K. Nasmyth. 1996. The transcription factor Swi5 regulates expression of the cyclin kinase inhibitor p40SIC1. Mol Cell Biol 16:5701-7.
221. Koch, C., T. Moll, M. Neuberg, H. Ahorn, and K. Nasmyth. 1993. A role for the transcription factors Mbp1 and Swi4 in progression from G1 to S phase. Science 261:1551-7.
222. Koegl, M., T. Hoppe, S. Schlenker, H. D. Ulrich, T. U. Mayer, and S. Jentsch. 1999. A novel ubiquitination factor, E4, is involved in multiubiquitin chain assembly. Cell 96:635-44.
223. Kohler, A., M. Bajorek, M. Groll, L. Moroder, D. M. Rubin, R. Huber, M. H. Glickman, and D. Finley. 2001. The substrate translocation channel of the proteasome. Biochimie 83:325-32.
224. Kohno, H., K. Tanaka, A. Mino, M. Umikawa, H. Imamura, T. Fujiwara, Y. Fujita, K. Hotta, H. Qadota, T. Watanabe, Y. Ohya, and Y. Takai. 1996. Bni1p implicated in cytoskeletal control is a putative target of Rho1p small GTP binding protein in Saccharomyces cerevisiae. Embo J 15:6060-8.
225. Koranda, M., A. Schleiffer, L. Endler, and G. Ammerer. 2000. Forkhead-like transcription factors recruit Ndd1 to the chromatin of G2/M-specific promoters. Nature 406:94-8.
226. Krek, W. 1998. Proteolysis and the G1-S transition: the SCF connection. Curr Opin Genet Dev 8:36-42.

227. Kumar, A., and M. Snyder. 2001. Emerging technologies in yeast genomics. Nat Rev Genet 2:302-12.
228. Kuras, L., A. Rouillon, T. Lee, R. Barbey, M. Tyers, and D. Thomas. 2002. Dual regulation of the met4 transcription factor by ubiquitin-dependent degradation and inhibition of promoter recruitment. Mol Cell 10:69-80.
229. Kurasawa, Y., and K. Todokoro. 1999. Identification of human APC10/Doc1 as a subunit of anaphase promoting complex. Oncogene 18:5131-7.
230. Lake, M. W., M. M. Wuebbens, K. V. Rajagopalan, and H. Schindelin. 2001. Mechanism of ubiquitin activation revealed by the structure of a bacterial MoeB-MoaD complex. Nature 414:325-9.
231. Lee, J. C., and M. E. Peter. 2003. Regulation of apoptosis by ubiquitination. Immunol Rev 193:39-47.
232. Lee, K. S., L. K. Hines, and D. E. Levin. 1993. A pair of functionally redundant yeast genes (PPZ1 and PPZ2) encoding type 1-related protein phosphatases function within the PKC1-mediated pathway. Mol Cell Biol 13:5843-53.
233. Lee, K. S., K. Irie, Y. Gotoh, Y. Watanabe, H. Araki, E. Nishida, K. Matsumoto, and D. E. Levin. 1993. A yeast mitogen-activated protein kinase homolog (Mpk1p) mediates signalling by protein kinase C. Mol Cell Biol 13:3067-75.
234. Lee, K. S., and D. E. Levin. 1992. Dominant mutations in a gene encoding a putative protein kinase (BCK1) bypass the requirement for a Saccharomyces cerevisiae protein kinase C homolog. Mol Cell Biol 12:172-82.
235. Leggett, D. S., and P. M. Candido. 1997. Biochemical characterization of Caenorhabditis elegans UBC-1: self-association and auto-ubiquitination of a RAD6-like ubiquitin-conjugating enzyme in vitro. Biochem J 327 (Pt 2):357-61.
236. Leimkuhler, S., M. M. Wuebbens, and K. V. Rajagopalan. 2001. Characterization of Escherichia coli MoeB and its involvement in the activation of molybdopterin synthase for the biosynthesis of the molybdenum cofactor. J Biol Chem 276:34695-701.
237. Lengronne, A., and E. Schwob. 2002. The yeast CDK inhibitor Sic1 prevents genomic instability by promoting replication origin licensing in late G(1). Mol Cell 9:1067-78.
238. Levin, D. E., and E. Bartlett-Heubusch. 1992. Mutants in the S. cerevisiae PKC1 gene display a cell cycle-specific osmotic stability defect. J Cell Biol 116:1221-9.
239. Lew, D. J. 2003. The morphogenesis checkpoint: how yeast cells watch their figures. Curr Opin Cell Biol 15:648-53.
240. Lew, D. J., and D. J. Burke. 2003. The spindle assembly and spindle position checkpoints. Annu Rev Genet 37:251-82.
241. Lew, D. J., and S. I. Reed. 1995. A cell cycle checkpoint monitors cell morphogenesis in budding yeast. J Cell Biol 129:739-49.
242. Lew, D. J., and S. I. Reed. 1993. Morphogenesis in the yeast cell cycle: regulation by Cdc28 and cyclins. J Cell Biol 120:1305-20.
243. Li, M., D. Chen, A. Shiloh, J. Luo, A. Y. Nikolaev, J. Qin, and W. Gu. 2002. Deubiquitination of p53 by HAUSP is an important pathway for p53 stabilization. Nature 416:648-53.
244. Liakopoulos, D., G. Doenges, K. Matuschewski, and S. Jentsch. 1998. A novel protein modification pathway related to the ubiquitin system. Embo J 17:2208-14.

245. Lim, H. H., P. Y. Goh, and U. Surana. 1998. Cdc20 is essential for the cyclosome-mediated proteolysis of both Pds1 and Clb2 during M phase in budding yeast. Curr Biol 8:231-4.
246. Lima, C. D. 2003. CUE'd up for Monoubiquitin. Cell 113:554-6.
247. Lisztwan, J., A. Marti, H. Sutterluty, M. Gstaiger, C. Wirbelauer, and W. Krek. 1998. Association of human CUL-1 and ubiquitin-conjugating enzyme CDC34 with the F-box protein p45(SKP2): evidence for evolutionary conservation in the subunit composition of the CDC34-SCF pathway. Embo J 17:368-83.
248. Liu, Y., N. Mathias, C. N. Steussy, and M. G. Goebl. 1995. Intragenic suppression among CDC34 (UBC3) mutations defines a class of ubiquitin-conjugating catalytic domains. Mol Cell Biol 15:5635-44.
249. Liu, Y. C. 2004. Ubiquitin ligases and the immune response. Annu Rev Immunol 22:81-127.
250. Longhese, M. P., M. Clerici, and G. Lucchini. 2003. The S-phase checkpoint and its regulation in Saccharomyces cerevisiae. Mutat Res 532:41-58.
251. Lorberg, A., H. P. Schmitz, J. J. Jacoby, and J. J. Heinisch. 2001. Lrg1p functions as a putative GTPase-activating protein in the Pkc1p-mediated cell integrity pathway in Saccharomyces cerevisiae. Mol Genet Genomics 266:514-26.
252. Losada, A., and T. Hirano. 2001. Shaping the metaphase chromosome: coordination of cohesion and condensation. Bioessays 23:924-35.
253. Madaule, P., R. Axel, and A. M. Myers. 1987. Characterization of two members of the rho gene family from the yeast Saccharomyces cerevisiae. Proc Natl Acad Sci U S A 84:779-83.
254. Madden, K., Y. J. Sheu, K. Baetz, B. Andrews, and M. Snyder. 1997. SBF cell cycle regulator as a target of the yeast PKC-MAP kinase pathway. Science 275:1781-4.
255. Manning, B. D., R. Padmanabha, and M. Snyder. 1997. The Rho-GEF Rom2p localizes to sites of polarized cell growth and participates in cytoskeletal functions in Saccharomyces cerevisiae. Mol Biol Cell 8:1829-44.
256. Marini, N. J., E. Meldrum, B. Buehrer, A. V. Hubberstey, D. E. Stone, A. Traynor-Kaplan, and S. I. Reed. 1996. A pathway in the yeast cell division cycle linking protein kinase C (Pkc1) to activation of Cdc28 at START. Embo J 15:3040-52.
257. Marmor, M. D., and Y. Yarden. 2004. Role of protein ubiquitylation in regulating endocytosis of receptor tyrosine kinases. Oncogene 23:2057-70.
258. Marquitz, A. R., J. C. Harrison, I. Bose, T. R. Zyla, J. N. McMillan, and D. J. Lew. 2002. The Rho-GAP Bem2p plays a GAP-independent role in the morphogenesis checkpoint. Embo J 21:4012-25.
259. Martin, H., J. Arroyo, M. Sanchez, M. Molina, and C. Nombela. 1993. Activity of the yeast MAP kinase homologue Slt2 is critically required for cell integrity at 37 degrees C. Mol Gen Genet 241:177-84.
260. Martin, H., J. M. Rodriguez-Pachon, C. Ruiz, C. Nombela, and M. Molina. 2000. Regulatory mechanisms for modulation of signaling through the cell integrity Slt2-mediated pathway in Saccharomyces cerevisiae. J Biol Chem 275:1511-9.
261. Martin-Yken, H., A. Dagkessamanskaia, F. Basmaji, A. Lagorce, and J. Francois. 2003. The interaction of Slt2 MAP kinase with Knr4 is necessary for signalling

through the cell wall integrity pathway in Saccharomyces cerevisiae. Mol Microbiol 49:23-35.

262. Mastrandrea, L. D., J. You, E. G. Niles, and C. M. Pickart. 1999. E2/E3-mediated assembly of lysine 29-linked polyubiquitin chains. J Biol Chem 274:27299-306.
263. Masuda, T., K. Tanaka, H. Nonaka, W. Yamochi, A. Maeda, and Y. Takai. 1994. Molecular cloning and characterization of yeast rho GDP dissociation inhibitor. J Biol Chem 269:19713-8.
264. Masui, Y., and C. L. Markert. 1971. Cytoplasmic control of nuclear behavior during meiotic maturation of frog oocytes. J Exp Zool 177:129-45.
265. Mathias, N., S. L. Johnson, M. Winey, A. E. Adams, L. Goetsch, J. R. Pringle, B. Byers, and M. G. Goebl. 1996. Cdc53p acts in concert with Cdc4p and Cdc34p to control the G1-to-S-phase transition and identifies a conserved family of proteins. Mol Cell Biol 16:6634-43.
266. Mattison, C. P., S. S. Spencer, K. A. Kresge, J. Lee, and I. M. Ota. 1999. Differential regulation of the cell wall integrity mitogen-activated protein kinase pathway in budding yeast by the protein tyrosine phosphatases Ptp2 and Ptp3. Mol Cell Biol 19:7651-60.
267. Matunis, M. J. 2002. On the road to repair: PCNA encounters SUMO and ubiquitin modifications. Mol Cell 10:441-2.
268. McAinsh, A. D., J. D. Tytell, and P. K. Sorger. 2003. Structure, function, and regulation of budding yeast kinetochores. Annu Rev Cell Dev Biol 19:519-39.
269. McBride, H. J., Y. Yu, and D. J. Stillman. 1999. Distinct regions of the Swi5 and Ace2 transcription factors are required for specific gene activation. J Biol Chem 274:21029-36.
270. McGrath, J. P., S. Jentsch, and A. Varshavsky. 1991. UBA 1: an essential yeast gene encoding ubiquitin-activating enzyme. Embo J 10:227-36.
271. McKenna, S., T. Moraes, L. Pastushok, C. Ptak, W. Xiao, L. Spyracopoulos, and M. J. Ellison. 2003. An NMR-based model of the ubiquitin-bound human ubiquitin conjugation complex Mms2.Ubc13. The structural basis for lysine 63 chain catalysis. J Biol Chem 278:13151-8.
272. McKenna, S., L. Spyracopoulos, T. Moraes, L. Pastushok, C. Ptak, W. Xiao, and M. J. Ellison. 2001. Noncovalent interaction between ubiquitin and the human DNA repair protein Mms2 is required for Ubc13-mediated polyubiquitination. J Biol Chem 276:40120-6.
273. McMillan, J. N., C. L. Theesfeld, J. C. Harrison, E. S. Bardes, and D. J. Lew. 2002. Determinants of Swe1p degradation in Saccharomyces cerevisiae. Mol Biol Cell 13:3560-75.
274. Meimoun, A., T. Holtzman, Z. Weissman, H. J. McBride, D. J. Stillman, G. R. Fink, and D. Kornitzer. 2000. Degradation of the transcription factor Gcn4 requires the kinase Pho85 and the SCF(CDC4) ubiquitin-ligase complex. Mol Biol Cell 11:915-27.
275. Melchior, F., M. Schergaut, and A. Pichler. 2003. SUMO: ligases, isopeptidases and nuclear pores. Trends Biochem Sci 28:612-8.
276. Mellor, H., and P. J. Parker. 1998. The extended protein kinase C superfamily. Biochem J 332 (Pt 2):281-92.

277. Mendenhall, M. D., and A. E. Hodge. 1998. Regulation of Cdc28 cyclin-dependent protein kinase activity during the cell cycle of the yeast Saccharomyces cerevisiae. Microbiol Mol Biol Rev 62:1191-243.
278. Merkley, N., and G. S. Shaw. 2003. Interaction of the tail with the catalytic region of a class II E2 conjugating enzyme. J Biomol NMR 26:147-55.
279. Merkley, N., and G. S. Shaw. 2004. Solution structure of the flexible class II ubiquitin-conjugating enzyme Ubc1 provides insights for polyubiquitin chain assembly. J Biol Chem.
280. Miller, M. E., and F. R. Cross. 2001. Cyclin specificity: how many wheels do you need on a unicycle? J Cell Sci 114:1811-20.
281. Miller, S. L., E. Malotky, and J. P. O'Bryan. 2004. Analysis of the role of ubiquitin-interacting motifs in ubiquitin binding and ubiquitylation. J Biol Chem 279:33528-37.
282. Miura, T., W. Klaus, B. Gsell, C. Miyamoto, and H. Senn. 1999. Characterization of the binding interface between ubiquitin and class I human ubiquitin-conjugating enzyme 2b by multidimensional heteronuclear NMR spectroscopy in solution. J Mol Biol 290:213-28.
283. Miura, T., W. Klaus, A. Ross, P. Guntert, and H. Senn. 2002. The NMR structure of the class I human ubiquitin-conjugating enzyme 2b. J Biomol NMR 22:89-92.
284. Moll, T., L. Dirick, H. Auer, J. Bonkovsky, and K. Nasmyth. 1992. SWI6 is a regulatory subunit of two different cell cycle START-dependent transcription factors in Saccharomyces cerevisiae. J Cell Sci Suppl 16:87-96.
285. Moll, T., E. Schwob, C. Koch, A. Moore, H. Auer, and K. Nasmyth. 1993. Transcription factors important for starting the cell cycle in yeast. Philos Trans R Soc Lond B Biol Sci 340:351-60.
286. Moraes, T. F., R. A. Edwards, S. McKenna, L. Pastushok, W. Xiao, J. N. Glover, and M. J. Ellison. 2001. Crystal structure of the human ubiquitin conjugating enzyme complex, hMms2-hUbc13. Nat Struct Biol 8:669-73.
287. Morgan, B. A., N. Bouquin, G. F. Merrill, and L. H. Johnston. 1995. A yeast transcription factor bypassing the requirement for SBF and DSC1/MBF in budding yeast has homology to bacterial signal transduction proteins. Embo J 14:5679-89.
288. Morgan, D. O. 1997. Cyclin-dependent kinases: engines, clocks, and microprocessors. Annu Rev Cell Dev Biol 13:261-91.
289. Mueller, T. D., and J. Feigon. 2002. Solution structures of UBA domains reveal a conserved hydrophobic surface for protein-protein interactions. J Mol Biol 319:1243-55.
290. Mueller, T. D., and J. Feigon. 2003. Structural determinants for the binding of ubiquitin-like domains to the proteasome. Embo J 22:4634-45.
291. Muller, S., A. Ledl, and D. Schmidt. 2004. SUMO: a regulator of gene expression and genome integrity. Oncogene 23:1998-2008.
292. Muratani, M., and W. P. Tansey. 2003. How the ubiquitin-proteasome system controls transcription. Nat Rev Mol Cell Biol 4:192-201.
293. Nash, P., X. Tang, S. Orlicky, Q. Chen, F. B. Gertler, M. D. Mendenhall, F. Sicheri, T. Pawson, and M. Tyers. 2001. Multisite phosphorylation of a CDK inhibitor sets a threshold for the onset of DNA replication. Nature 414:514-21.

294. Nasmyth, K., and L. Dirick. 1991. The role of SWI4 and SWI6 in the activity of G1 cyclins in yeast. Cell 66:995-1013.

295. Natarajan, K., M. R. Meyer, B. M. Jackson, D. Slade, C. Roberts, A. G. Hinnebusch, and M. J. Marton. 2001. Transcriptional profiling shows that Gcn4p is a master regulator of gene expression during amino acid starvation in yeast. Mol Cell Biol 21:4347-68.

296. Newlon, C. S., and W. L. Fangman. 1975. Mitochondrial DNA synthesis in cell cycle mutants of Saccharomyces cerevisiae. Cell 5:423-8.

297. Newlon, C. S., and J. F. Theis. 1993. The structure and function of yeast ARS elements. Curr Opin Genet Dev 3:752-8.

298. Nishikawa, H., S. Ooka, K. Sato, K. Arima, J. Okamoto, R. E. Klevit, M. Fukuda, and T. Ohta. 2004. Mass spectrometric and mutational analyses reveal Lys-6-linked polyubiquitin chains catalyzed by BRCA1-BARD1 ubiquitin ligase. J Biol Chem 279:3916-24.

299. Nishizawa, M., M. Kawasumi, M. Fujino, and A. Toh-e. 1998. Phosphorylation of sic1, a cyclin-dependent kinase (Cdk) inhibitor, by Cdk including Pho85 kinase is required for its prompt degradation. Mol Biol Cell 9:2393-405.

300. Nonaka, H., K. Tanaka, H. Hirano, T. Fujiwara, H. Kohno, M. Umikawa, A. Mino, and Y. Takai. 1995. A downstream target of RHO1 small GTP-binding protein is PKC1, a homolog of protein kinase C, which leads to activation of the MAP kinase cascade in Saccharomyces cerevisiae. Embo J 14:5931-8.

301. Nurse, P. 2000. A long twentieth century of the cell cycle and beyond. Cell 100:71-8.

302. O'Toole, E. T., M. Winey, and J. R. McIntosh. 1999. High-voltage electron tomography of spindle pole bodies and early mitotic spindles in the yeast Saccharomyces cerevisiae. Mol Biol Cell 10:2017-31.

303. Ogas, J., B. J. Andrews, and I. Herskowitz. 1991. Transcriptional activation of CLN1, CLN2, and a putative new G1 cyclin (HCS26) by SWI4, a positive regulator of G1-specific transcription. Cell 66:1015-26.

304. Ohi, M. D., C. W. Vander Kooi, J. A. Rosenberg, W. J. Chazin, and K. L. Gould. 2003. Structural insights into the U-box, a domain associated with multi-ubiquitination. Nat Struct Biol 10:250-5.

305. Ono, T., T. Suzuki, Y. Anraku, and H. Iida. 1994. The MID2 gene encodes a putative integral membrane protein with a Ca(2+)-binding domain and shows mating pheromone-stimulated expression in Saccharomyces cerevisiae. Gene 151:203-8.

306. Orlicky, S., X. Tang, A. Willems, M. Tyers, and F. Sicheri. 2003. Structural basis for phosphodependent substrate selection and orientation by the SCFCdc4 ubiquitin ligase. Cell 112:243-56.

307. Ou, C. Y., H. Pi, and C. T. Chien. 2003. Control of protein degradation by E3 ubiquitin ligases in Drosophila eye development. Trends Genet 19:382-9.

308. Ozaki, K., K. Tanaka, H. Imamura, T. Hihara, T. Kameyama, H. Nonaka, H. Hirano, Y. Matsuura, and Y. Takai. 1996. Rom1p and Rom2p are GDP/GTP exchange proteins (GEPs) for the Rho1p small GTP binding protein in Saccharomyces cerevisiae. Embo J 15:2196-207.

309. Pan, Z. Q., A. Kentsis, D. C. Dias, K. Yamoah, and K. Wu. 2004. Nedd8 on cullin: building an expressway to protein destruction. Oncogene 23:1985-97.
310. Paravicini, G., M. Cooper, L. Friedli, D. J. Smith, J. L. Carpentier, L. S. Klig, and M. A. Payton. 1992. The osmotic integrity of the yeast cell requires a functional PKC1 gene product. Mol Cell Biol 12:4896-905.
311. Paravicini, G., and L. Friedli. 1996. Protein-protein interactions in the yeast PKC1 pathway: Pkc1p interacts with a component of the MAP kinase cascade. Mol Gen Genet 251:682-91.
312. Partridge, J. F., G. E. Mikesell, and L. L. Breeden. 1997. Cell cycle-dependent transcription of CLN1 involves swi4 binding to MCB-like elements. J Biol Chem 272:9071-7.
313. Passmore, L. A., E. A. McCormack, S. W. Au, A. Paul, K. R. Willison, J. W. Harper, and D. Barford. 2003. Doc1 mediates the activity of the anaphase-promoting complex by contributing to substrate recognition. Embo J 22:786-96.
314. Patton, E. E., C. Peyraud, A. Rouillon, Y. Surdin-Kerjan, M. Tyers, and D. Thomas. 2000. SCF(Met30)-mediated control of the transcriptional activator Met4 is required for the G(1)-S transition. Embo J 19:1613-24.
315. Patton, E. E., A. R. Willems, D. Sa, L. Kuras, D. Thomas, K. L. Craig, and M. Tyers. 1998. Cdc53 is a scaffold protein for multiple Cdc34/Skp1/F-box proteincomplexes that regulate cell division and methionine biosynthesis in yeast. Genes Dev 12:692-705.
316. Peng, J., D. Schwartz, J. E. Elias, C. C. Thoreen, D. Cheng, G. Marsischky, J. Roelofs, D. Finley, and S. P. Gygi. 2003. A proteomics approach to understanding protein ubiquitination. Nat Biotechnol 21:921-6.
317. Perkins, G., L. S. Drury, and J. F. Diffley. 2001. Separate SCF(CDC4) recognition elements target Cdc6 for proteolysis in S phase and mitosis. Embo J 20:4836-45.
318. Peter, M., and I. Herskowitz. 1994. Direct inhibition of the yeast cyclin-dependent kinase Cdc28-Cln by Far1. Science 265:1228-31.
319. Peters, J. M. 2002. The anaphase-promoting complex: proteolysis in mitosis and beyond. Mol Cell 9:931-43.
320. Petronczki, M., M. F. Siomos, and K. Nasmyth. 2003. Un menage a quatre: the molecular biology of chromosome segregation in meiosis. Cell 112:423-40.
321. Philip, B., and D. E. Levin. 2001. Wsc1 and Mid2 are cell surface sensors for cell wall integrity signaling that act through Rom2, a guanine nucleotide exchange factor for Rho1. Mol Cell Biol 21:271-80.
322. Phillips, C. L., J. Thrower, C. M. Pickart, and C. P. Hill. 2001. Structure of a new crystal form of tetraubiquitin. Acta Crystallogr D Biol Crystallogr 57:341-4.
323. Pickart, C. M. 2001. Mechanisms underlying ubiquitination. Annu Rev Biochem 70:503-33.
324. Pickart, C. M., and R. E. Cohen. 2004. Proteasomes and their kin: proteases in the machine age. Nat Rev Mol Cell Biol 5:177-87.
325. Pickart, C. M., E. M. Kasperek, R. Beal, and A. Kim. 1994. Substrate properties of site-specific mutant ubiquitin protein (G76A) reveal unexpected mechanistic features of ubiquitin-activating enzyme (E1). J Biol Chem 269:7115-23.

326. Pickart, C. M., and I. A. Rose. 1985. Functional heterogeneity of ubiquitin carrier proteins. J Biol Chem 260:1573-81.
327. Pickart, C. M., and A. P. VanDemark. 2000. Opening doors into the proteasome. Nat Struct Biol 7:999-1001.
328. Pintard, L., A. Willems, and M. Peter. 2004. Cullin-based ubiquitin ligases: Cul3-BTB complexes join the family. Embo J 23:1681-7.
329. Pintard, L., J. H. Willis, A. Willems, J. L. Johnson, M. Srayko, T. Kurz, S. Glaser, P. E. Mains, M. Tyers, B. Bowerman, and M. Peter. 2003. The BTB protein MEL-26 is a substrate-specific adaptor of the CUL-3 ubiquitin-ligase. Nature 425:311-6.
330. Polo, S., S. Sigismund, M. Faretta, M. Guidi, M. R. Capua, G. Bossi, H. Chen, P. De Camilli, and P. P. Di Fiore. 2002. A single motif responsible for ubiquitin recognition and monoubiquitination in endocytic proteins. Nature 416:451-5.
331. Popolo, L., T. Gualtieri, and E. Ragni. 2001. The yeast cell-wall salvage pathway. Med Mycol 39 Suppl 1:111-21.
332. Posas, F., A. Casamayor, and J. Arino. 1993. The PPZ protein phosphatases are involved in the maintenance of osmotic stability of yeast cells. FEBS Lett 318:282-6.
333. Posas, F., M. Takekawa, and H. Saito. 1998. Signal transduction by MAP kinase cascades in budding yeast. Curr Opin Microbiol 1:175-82.
334. Prasanth, S. G., J. Mendez, K. V. Prasanth, and B. Stillman. 2004. Dynamics of pre-replication complex proteins during the cell division cycle. Philos Trans R Soc Lond B Biol Sci 359:7-16.
335. Primig, M., S. Sockanathan, H. Auer, and K. Nasmyth. 1992. Anatomy of a transcription factor important for the start of the cell cycle in Saccharomyces cerevisiae. Nature 358:593-7.
336. Ptak, C., J. A. Prendergast, R. Hodgins, C. M. Kay, V. Chau, and M. J. Ellison. 1994. Functional and physical characterization of the cell cycle ubiquitin-conjugating enzyme CDC34 (UBC3). Identification of a functional determinant within the tail that facilitates CDC34 self-association. J Biol Chem 269:26539-45.
337. Qadota, H., C. P. Python, S. B. Inoue, M. Arisawa, Y. Anraku, Y. Zheng, T. Watanabe, D. E. Levin, and Y. Ohya. 1996. Identification of yeast Rho1p GTPase as a regulatory subunit of 1,3-beta-glucan synthase. Science 272:279-81.
338. Queralt, E., and J. C. Igual. 2003. Cell cycle activation of the Swi6p transcription factor is linked to nucleocytoplasmic shuttling. Mol Cell Biol 23:3126-40.
339. Raitt, D. C., A. L. Johnson, A. M. Erkine, K. Makino, B. Morgan, D. S. Gross, and L. H. Johnston. 2000. The Skn7 response regulator of Saccharomyces cerevisiae interacts with Hsf1 in vivo and is required for the induction of heat shock genes by oxidative stress. Mol Biol Cell 11:2335-47.
340. Rajavel, M., B. Philip, B. M. Buehrer, B. Errede, and D. E. Levin. 1999. Mid2 is a putative sensor for cell integrity signaling in Saccharomyces cerevisiae. Mol Cell Biol 19:3969-76.
341. Ray, A., R. E. Hector, N. Roy, J. H. Song, K. L. Berkner, and K. W. Runge. 2003. Sir3p phosphorylation by the Slt2p pathway effects redistribution of silencing function and shortened lifespan. Nat Genet 33:522-6.

342. Reed, S. I. 2003. Ratchets and clocks: the cell cycle, ubiquitylation and protein turnover. Nat Rev Mol Cell Biol 4:855-64.
343. Rhind, N., and P. Russell. 1998. Mitotic DNA damage and replication checkpoints in yeast. Curr Opin Cell Biol 10:749-58.
344. Rivett, A. J., and A. R. Hearn. 2004. Proteasome function in antigen presentation: immunoproteasome complexes, Peptide production, and interactions with viral proteins. Curr Protein Pept Sci 5:153-61.
345. Roberts, C. J., B. Nelson, M. J. Marton, R. Stoughton, M. R. Meyer, H. A. Bennett, Y. D. He, H. Dai, W. L. Walker, T. R. Hughes, M. Tyers, C. Boone, and S. H. Friend. 2000. Signaling and circuitry of multiple MAPK pathways revealed by a matrix of global gene expression profiles. Science 287:873-80.
346. Roncero, C. 2002. The genetic complexity of chitin synthesis in fungi. Curr Genet 41:367-78.
347. Rouillon, A., R. Barbey, E. E. Patton, M. Tyers, and D. Thomas. 2000. Feedback-regulated degradation of the transcriptional activator Met4 is triggered by the SCF(Met30)complex. Embo J 19:282-94.
348. Rudner, A. D., K. G. Hardwick, and A. W. Murray. 2000. Cdc28 activates exit from mitosis in budding yeast. J Cell Biol 149:1361-76.
349. Rudner, A. D., and A. W. Murray. 2000. Phosphorylation by Cdc28 activates the Cdc20-dependent activity of the anaphase-promoting complex. J Cell Biol 149:1377-90.
350. Rupes, I. 2002. Checking cell size in yeast. Trends Genet 18:479-85.
351. Russell, I. D., A. S. Grancell, and P. K. Sorger. 1999. The unstable F-box protein p58-Ctf13 forms the structural core of the CBF3 kinetochore complex. J Cell Biol 145:933-50.
352. Russell, N. S., and K. D. Wilkinson. 2004. Identification of a novel 29-linked polyubiquitin binding protein, Ufd3, using polyubiquitin chain analogues. Biochemistry 43:4844-54.
353. Sakata, E., Y. Yamaguchi, E. Kurimoto, J. Kikuchi, S. Yokoyama, S. Yamada, H. Kawahara, H. Yokosawa, N. Hattori, Y. Mizuno, K. Tanaka, and K. Kato. 2003. Parkin binds the Rpn10 subunit of 26S proteasomes through its ubiquitin-like domain. EMBO Rep 4:301-6.
354. Salama, S. R., K. B. Hendricks, and J. Thorner. 1994. G1 cyclin degradation: the PEST motif of yeast Cln2 is necessary, but not sufficient, for rapid protein turnover. Mol Cell Biol 14:7953-66.
355. Schauber, C., L. Chen, P. Tongaonkar, I. Vega, D. Lambertson, W. Potts, and K. Madura. 1998. Rad23 links DNA repair to the ubiquitin/proteasome pathway. Nature 391:715-8.
356. Scheffner, M., U. Nuber, and J. M. Huibregtse. 1995. Protein ubiquitination involving an E1-E2-E3 enzyme ubiquitin thioester cascade. Nature 373:81-3.
357. Schmidt, A., T. Schmelzle, and M. N. Hall. 2002. The RHO1-GAPs SAC7, BEM2 and BAG7 control distinct RHO1 functions in Saccharomyces cerevisiae. Mol Microbiol 45:1433-41.
358. Schneider, B. L., E. E. Patton, S. Lanker, M. D. Mendenhall, C. Wittenberg, B. Futcher, and M. Tyers. 1998. Yeast G1 cyclins are unstable in G1 phase. Nature 395:86-9.

359. Schwartz, A. L., and A. Ciechanover. 1999. The ubiquitin-proteasome pathway and pathogenesis of human diseases. Annu Rev Med 50:57-74.
360. Schwartz, D. C., and M. Hochstrasser. 2003. A superfamily of protein tags: ubiquitin, SUMO and related modifiers. Trends Biochem Sci 28:321-8.
361. Schwob, E., T. Bohm, M. D. Mendenhall, and K. Nasmyth. 1994. The B-type cyclin kinase inhibitor p40SIC1 controls the G1 to S transition in S. cerevisiae. Cell 79:233-44.
362. Schwob, E., and K. Nasmyth. 1993. CLB5 and CLB6, a new pair of B cyclins involved in DNA replication in Saccharomyces cerevisiae. Genes Dev 7:1160-75.
363. Seeler, J. S., and A. Dejean. 2003. Nuclear and unclear functions of SUMO. Nat Rev Mol Cell Biol 4:690-9.
364. Sekiya-Kawasaki, M., M. Abe, A. Saka, D. Watanabe, K. Kono, M. Minemura-Asakawa, S. Ishihara, T. Watanabe, and Y. Ohya. 2002. Dissection of upstream regulatory components of the Rho1p effector, 1,3-beta-glucan synthase, in Saccharomyces cerevisiae. Genetics 162:663-76.
365. Seol, J. H., R. M. Feldman, W. Zachariae, A. Shevchenko, C. C. Correll, S. Lyapina, Y. Chi, M. Galova, J. Claypool, S. Sandmeyer, K. Nasmyth, and R. J. Deshaies. 1999. Cdc53/cullin and the essential Hrt1 RING-H2 subunit of SCF define a ubiquitin ligase module that activates the E2 enzyme Cdc34. Genes Dev 13:1614-26.
366. Seufert, W., B. Futcher, and S. Jentsch. 1995. Role of a ubiquitin-conjugating enzyme in degradation of S- and M-phase cyclins. Nature 373:78-81.
367. Shemer, R., A. Meimoun, T. Holtzman, and D. Kornitzer. 2002. Regulation of the transcription factor Gcn4 by Pho85 cyclin PCL5. Mol Cell Biol 22:5395-404.
368. Shimada, Y., M. P. Gulli, and M. Peter. 2000. Nuclear sequestration of the exchange factor Cdc24 by Far1 regulates cell polarity during yeast mating. Nat Cell Biol 2:117-24.
369. Shirayama, M., A. Toth, M. Galova, and K. Nasmyth. 1999. APC(Cdc20) promotes exit from mitosis by destroying the anaphase inhibitor Pds1 and cyclin Clb5. Nature 402:203-7.
370. Sia, R. A., E. S. Bardes, and D. J. Lew. 1998. Control of Swe1p degradation by the morphogenesis checkpoint. Embo J 17:6678-88.
371. Sia, R. A., H. A. Herald, and D. J. Lew. 1996. Cdc28 tyrosine phosphorylation and the morphogenesis checkpoint in budding yeast. Mol Biol Cell 7:1657-66.
372. Sidorova, J. M., G. E. Mikesell, and L. L. Breeden. 1995. Cell cycle-regulated phosphorylation of Swi6 controls its nuclear localization. Mol Biol Cell 6:1641-58.
373. Simon, I., J. Barnett, N. Hannett, C. T. Harbison, N. J. Rinaldi, T. L. Volkert, J. J. Wyrick, J. Zeitlinger, D. K. Gifford, T. S. Jaakkola, and R. A. Young. 2001. Serial regulation of transcriptional regulators in the yeast cell cycle. Cell 106:697-708.
374. Singer, T., S. Haefner, M. Hoffmann, M. Fischer, J. Ilyina, and W. Hilt. 2003. Sit4 phosphatase is functionally linked to the ubiquitin-proteasome system. Genetics 164:1305-21.

375. Skowyra, D., K. L. Craig, M. Tyers, S. J. Elledge, and J. W. Harper. 1997. F-box proteins are receptors that recruit phosphorylated substrates to the SCF ubiquitin-ligase complex. Cell 91:209-19.

376. Skowyra, D., D. M. Koepp, T. Kamura, M. N. Conrad, R. C. Conaway, J. W. Conaway, S. J. Elledge, and J. W. Harper. 1999. Reconstitution of G1 cyclin ubiquitination with complexes containing SCFGrr1 and Rbx1. Science 284:662-5.

377. Sloper-Mould, K. E., J. C. Jemc, C. M. Pickart, and L. Hicke. 2001. Distinct functional surface regions on ubiquitin. J Biol Chem 276:30483-9.

378. Smith, G. R., S. A. Givan, P. Cullen, and G. F. Sprague, Jr. 2002. GTPase-activating proteins for Cdc42. Eukaryot Cell 1:469-80.

379. Soboleva, T. A., and R. T. Baker. 2004. Deubiquitinating enzymes: their functions and substrate specificity. Curr Protein Pept Sci 5:191-200.

380. Soler, M., A. Plovins, H. Martin, M. Molina, and C. Nombela. 1995. Characterization of domains in the yeast MAP kinase Slt2 (Mpk1) required for functional activity and in vivo interaction with protein kinases Mkk1 and Mkk2. Mol Microbiol 17:833-42.

381. Spellman, P. T., G. Sherlock, M. Q. Zhang, V. R. Iyer, K. Anders, M. B. Eisen, P. O. Brown, D. Botstein, and B. Futcher. 1998. Comprehensive identification of cell cycle-regulated genes of the yeast Saccharomyces cerevisiae by microarray hybridization. Mol Biol Cell 9:3273-97.

382. Spence, J., R. R. Gali, G. Dittmar, F. Sherman, M. Karin, and D. Finley. 2000. Cell cycle-regulated modification of the ribosome by a variant multiubiquitin chain. Cell 102:67-76.

383. Spence, J., S. Sadis, A. L. Haas, and D. Finley. 1995. A ubiquitin mutant with specific defects in DNA repair and multiubiquitination. Mol Cell Biol 15:1265-73.

384. Springael, J. Y., J. M. Galan, R. Haguenauer-Tsapis, and B. Andre. 1999. NH4+-induced down-regulation of the Saccharomyces cerevisiae Gap1p permease involves its ubiquitination with lysine-63-linked chains. J Cell Sci 112 (Pt 9):1375-83.

385. Spruck, C. H., and H. M. Strohmaier. 2002. Seek and destroy: SCF ubiquitin ligases in mammalian cell cycle control. Cell Cycle 1:250-4.

386. Strickland, E., K. Hakala, P. J. Thomas, and G. N. DeMartino. 2000. Recognition of misfolding proteins by PA700, the regulatory subcomplex of the 26 S proteasome. J Biol Chem 275:5565-72.

387. Sun, L., and Z. J. Chen. 2004. The novel functions of ubiquitination in signaling. Curr Opin Cell Biol 16:119-26.

388. Surana, U., H. Robitsch, C. Price, T. Schuster, I. Fitch, A. B. Futcher, and K. Nasmyth. 1991. The role of CDC28 and cyclins during mitosis in the budding yeast S. cerevisiae. Cell 65:145-61.

389. Sutton, A., D. Immanuel, and K. T. Arndt. 1991. The SIT4 protein phosphatase functions in late G1 for progression into S phase. Mol Cell Biol 11:2133-48.

390. Suzuki, M., R. Igarashi, M. Sekiya, T. Utsugi, S. Morishita, M. Yukawa, and Y. Ohya. 2004. Dynactin is involved in a checkpoint to monitor cell wall synthesis in Saccharomyces cerevisiae. Nat Cell Biol 6:861-71.

391. Tang, Z., B. Li, R. Bharadwaj, H. Zhu, E. Ozkan, K. Hakala, J. Deisenhofer, and H. Yu. 2001. APC2 Cullin protein and APC11 RING protein comprise the minimal ubiquitin ligase module of the anaphase-promoting complex. Mol Biol Cell 12:3839-51.

392. Taylor, I. A., P. B. McIntosh, P. Pala, M. K. Treiber, S. Howell, A. N. Lane, and S. J. Smerdon. 2000. Characterization of the DNA-binding domains from the yeast cell-cycle transcription factors Mbp1 and Swi4. Biochemistry 39:3943-54.

393. Thomas, D., and Y. Surdin-Kerjan. 1997. Metabolism of sulfur amino acids in Saccharomyces cerevisiae. Microbiol Mol Biol Rev 61:503-32.

394. Thrower, J. S., L. Hoffman, M. Rechsteiner, and C. M. Pickart. 2000. Recognition of the polyubiquitin proteolytic signal. Embo J 19:94-102.

395. Tong, H., G. Hateboer, A. Perrakis, R. Bernards, and T. K. Sixma. 1997. Crystal structure of murine/human Ubc9 provides insight into the variability of the ubiquitin-conjugating system. J Biol Chem 272:21381-7.

396. Toone, W. M., B. L. Aerne, B. A. Morgan, and L. H. Johnston. 1997. Getting started: regulating the initiation of DNA replication in yeast. Annu Rev Microbiol 51:125-49.

397. Torres, L., H. Martin, M. I. Garcia-Saez, J. Arroyo, M. Molina, M. Sanchez, and C. Nombela. 1991. A protein kinase gene complements the lytic phenotype of Saccharomyces cerevisiae lyt2 mutants. Mol Microbiol 5:2845-54.

398. Tyers, M. 1996. The cyclin-dependent kinase inhibitor p40SIC1 imposes the requirement for Cln G1 cyclin function at Start. Proc Natl Acad Sci U S A 93:7772-6.

399. Tyers, M., and B. Futcher. 1993. Far1 and Fus3 link the mating pheromone signal transduction pathway to three G1-phase Cdc28 kinase complexes. Mol Cell Biol 13:5659-69.

400. Uhlmann, F. 2004. The mechanism of sister chromatid cohesion. Exp Cell Res 296:80-5.

401. van den Heuvel, S. 2004. Protein degradation: CUL-3 and BTB--partners in proteolysis. Curr Biol 14:R59-61.

402. VanDemark, A. P., R. M. Hofmann, C. Tsui, C. M. Pickart, and C. Wolberger. 2001. Molecular insights into polyubiquitin chain assembly: crystal structure of the Mms2/Ubc13 heterodimer. Cell 105:711-20.

403. Varadan, R., M. Assfalg, A. Haririnia, S. Raasi, C. Pickart, and D. Fushman. 2004. Solution conformation of Lys63-linked di-ubiquitin chain provides clues to functional diversity of polyubiquitin signaling. J Biol Chem 279:7055-63.

404. Varadan, R., O. Walker, C. Pickart, and D. Fushman. 2002. Structural properties of polyubiquitin chains in solution. J Mol Biol 324:637-47.

405. Verdecia, M. A., C. A. Joazeiro, N. J. Wells, J. L. Ferrer, M. E. Bowman, T. Hunter, and J. P. Noel. 2003. Conformational flexibility underlies ubiquitin ligation mediated by the WWP1 HECT domain E3 ligase. Mol Cell 11:249-59.

406. Verma, R., R. S. Annan, M. J. Huddleston, S. A. Carr, G. Reynard, and R. J. Deshaies. 1997. Phosphorylation of Sic1p by G1 Cdk required for its degradation and entry into S phase. Science 278:455-60.

407. Verma, R., L. Aravind, R. Oania, W. H. McDonald, J. R. Yates, 3rd, E. V. Koonin, and R. J. Deshaies. 2002. Role of Rpn11 metalloprotease in deubiquitination and degradation by the 26S proteasome. Science 298:611-5.

408. Verma, R., R. M. Feldman, and R. J. Deshaies. 1997. SIC1 is ubiquitinated in vitro by a pathway that requires CDC4, CDC34, and cyclin/CDK activities. Mol Biol Cell 8:1427-37.

409. Verna, J., A. Lodder, K. Lee, A. Vagts, and R. Ballester. 1997. A family of genes required for maintenance of cell wall integrity and for the stress response in Saccharomyces cerevisiae. Proc Natl Acad Sci U S A 94:13804-9.

410. Vijay-Kumar, S., C. E. Bugg, K. D. Wilkinson, R. D. Vierstra, P. M. Hatfield, and W. J. Cook. 1987. Comparison of the three-dimensional structures of human, yeast, and oat ubiquitin. J Biol Chem 262:6396-9.

411. Visintin, R., S. Prinz, and A. Amon. 1997. CDC20 and CDH1: a family of substrate-specific activators of APC-dependent proteolysis. Science 278:460-3.

412. Voges, D., P. Zwickl, and W. Baumeister. 1999. The 26S proteasome: a molecular machine designed for controlled proteolysis. Annu Rev Biochem 68:1015-68.

413. Walden, H., M. S. Podgorski, D. T. Huang, D. W. Miller, R. J. Howard, D. L. Minor, Jr., J. M. Holton, and B. A. Schulman. 2003. The structure of the APPBP1-UBA3-NEDD8-ATP complex reveals the basis for selective ubiquitin-like protein activation by an E1. Mol Cell 12:1427-37.

414. Walden, H., M. S. Podgorski, and B. A. Schulman. 2003. Insights into the ubiquitin transfer cascade from the structure of the activating enzyme for NEDD8. Nature 422:330-4.

415. Wang, C., L. Deng, M. Hong, G. R. Akkaraju, J. Inoue, and Z. J. Chen. 2001. TAK1 is a ubiquitin-dependent kinase of MKK and IKK. Nature 412:346-51.

416. Watanabe, D., M. Abe, and Y. Ohya. 2001. Yeast Lrg1p acts as a specialized RhoGAP regulating 1,3-beta-glucan synthesis. Yeast 18:943-51.

417. Watanabe, Y., K. Irie, and K. Matsumoto. 1995. Yeast RLM1 encodes a serum response factor-like protein that may function downstream of the Mpk1 (Slt2) mitogen-activated protein kinase pathway. Mol Cell Biol 15:5740-9.

418. Watanabe, Y., G. Takaesu, M. Hagiwara, K. Irie, and K. Matsumoto. 1997. Characterization of a serum response factor-like protein in Saccharomyces cerevisiae, Rlm1, which has transcriptional activity regulated by the Mpk1 (Slt2) mitogen-activated protein kinase pathway. Mol Cell Biol 17:2615-23.

419. Weber, P. L., S. C. Brown, and L. Mueller. 1987. Sequential 1H NMR assignments and secondary structure identification of human ubiquitin. Biochemistry 26:7282-90.

420. Wells, W. A. 1996. The spindle-assembly checkpoint: aiming for a perfect mitosis, every time. Trends Cell Biol 6:228-34.

421. Whitby, F. G., E. I. Masters, L. Kramer, J. R. Knowlton, Y. Yao, C. C. Wang, and C. P. Hill. 2000. Structural basis for the activation of 20S proteasomes by 11S regulators. Nature 408:115-20.

422. Willems, A. R., S. Lanker, E. E. Patton, K. L. Craig, T. F. Nason, N. Mathias, R. Kobayashi, C. Wittenberg, and M. Tyers. 1996. Cdc53 targets phosphorylated G1 cyclins for degradation by the ubiquitin proteolytic pathway. Cell 86:453-63.

423. Williams, K. E., and M. S. Cyert. 2001. The eukaryotic response regulator Skn7p regulates calcineurin signaling through stabilization of Crz1p. Embo J 20:3473-83.
424. Wilmes, G. M., V. Archambault, R. J. Austin, M. D. Jacobson, S. P. Bell, and F. R. Cross. 2004. Interaction of the S-phase cyclin Clb5 with an "RXL" docking sequence in the initiator protein Orc6 provides an origin-localized replication control switch. Genes Dev 18:981-91.
425. Wing, S. S. 2003. Deubiquitinating enzymes--the importance of driving in reverse along the ubiquitin-proteasome pathway. Int J Biochem Cell Biol 35:590-605.
426. Withers-Ward, E. S., T. D. Mueller, I. S. Chen, and J. Feigon. 2000. Biochemical and structural analysis of the interaction between the UBA(2) domain of the DNA repair protein HHR23A and HIV-1 Vpr. Biochemistry 39:14103-12.
427. Worthylake, D. K., S. Prakash, L. Prakash, and C. P. Hill. 1998. Crystal structure of the Saccharomyces cerevisiae ubiquitin-conjugating enzyme Rad6 at 2.6 A resolution. J Biol Chem 273:6271-6.
428. Wu, K., A. Chen, P. Tan, and Z. Q. Pan. 2002. The Nedd8-conjugated ROC1-CUL1 core ubiquitin ligase utilizes Nedd8 charged surface residues for efficient polyubiquitin chain assembly catalyzed by Cdc34. J Biol Chem 277:516-27.
429. Wu, P. Y., M. Hanlon, M. Eddins, C. Tsui, R. S. Rogers, J. P. Jensen, M. J. Matunis, A. M. Weissman, C. P. Wolberger, and C. M. Pickart. 2003. A conserved catalytic residue in the ubiquitin-conjugating enzyme family. Embo J 22:5241-50.
430. Xu, L., Y. Wei, J. Reboul, P. Vaglio, T. H. Shin, M. Vidal, S. J. Elledge, and J. W. Harper. 2003. BTB proteins are substrate-specific adaptors in an SCF-like modular ubiquitin ligase containing CUL-3. Nature 425:316-21.
431. Yamano, H., J. Gannon, H. Mahbubani, and T. Hunt. 2004. Cell cycle-regulated recognition of the destruction box of cyclin B by the APC/C in Xenopus egg extracts. Mol Cell 13:137-47.
432. Yamochi, W., K. Tanaka, H. Nonaka, A. Maeda, T. Musha, and Y. Takai. 1994. Growth site localization of Rho1 small GTP-binding protein and its involvement in bud formation in Saccharomyces cerevisiae. J Cell Biol 125:1077-93.
433. You, J., and C. M. Pickart. 2001. A HECT domain E3 enzyme assembles novel polyubiquitin chains. J Biol Chem 276:19871-8.
434. Young, P., Q. Deveraux, R. E. Beal, C. M. Pickart, and M. Rechsteiner. 1998. Characterization of two polyubiquitin binding sites in the 26 S protease subunit 5a. J Biol Chem 273:5461-7.
435. Zachariae, W., and K. Nasmyth. 1996. TPR proteins required for anaphase progression mediate ubiquitination of mitotic B-type cyclins in yeast. Mol Biol Cell 7:791-801.
436. Zachariae, W., T. H. Shin, M. Galova, B. Obermaier, and K. Nasmyth. 1996. Identification of subunits of the anaphase-promoting complex of Saccharomyces cerevisiae. Science 274:1201-4.
437. Zacksenhaus, E., and R. Sheinin. 1989. Molecular cloning of human A1S9 locus: an X-linked gene essential for progression through S phase of the cell cycle. Somat Cell Mol Genet 15:545-53.

438. Zacksenhaus, E., and R. Sheinin. 1990. Molecular cloning, primary structure and expression of the human X linked A1S9 gene cDNA which complements the ts A1S9 mouse L cell defect in DNA replication. Embo J 9:2923-9.
439. Zhang, H. G., J. Wang, X. Yang, H. C. Hsu, and J. D. Mountz. 2004. Regulation of apoptosis proteins in cancer cells by ubiquitin. Oncogene 23:2009-15.
440. Zheng, N. 2003. A closer look of the HECTic ubiquitin ligases. Structure (Camb) 11:5-6.
441. Zheng, N., B. A. Schulman, L. Song, J. J. Miller, P. D. Jeffrey, P. Wang, C. Chu, D. M. Koepp, S. J. Elledge, M. Pagano, R. C. Conaway, J. W. Conaway, J. W. Harper, and N. P. Pavletich. 2002. Structure of the Cul1-Rbx1-Skp1-F boxSkp2 SCF ubiquitin ligase complex. Nature 416:703-9.
442. Zheng, N., P. Wang, P. D. Jeffrey, and N. P. Pavletich. 2000. Structure of a c-Cbl-UbcH7 complex: RING domain function in ubiquitin-protein ligases. Cell 102:533-9.

CHAPTER 2 – Cdc34 self-association is facilitated by Ub thiolester and is required for its catalytic function*

* Portions of this chapter have been adapted from (25)[1] and (24).

[1] *Copyright © 2004, the American Society for Microbiology. All rights reserved.*

2.1 Introduction

Many important processes in eukaryotic cells are regulated by the covalent modification of protein targets by the highly conserved protein ubiquitin (Ub). This modification consists of a cascade of events involving three enzymes/enzyme complexes that activate and transfer Ub to appropriately selected targets (11). In an ATP-dependent first step, the Ub-activating enzyme (E1) activates Ub by forming a high-energy thiolester bond between its active site cysteine and the carboxyl-terminus of Ub. Subsequently, Ub is transferred to the active site cysteine of an Ub-conjugating enzyme (E2) via a transthiolation reaction. E2s in conjunction with an Ub-ligase enzyme (E3) bind a protein target and transfer Ub to a lysine residue of the target. E3s comprise a diverse group of proteins frequently consisting of multi-subunit complexes that function to provide the target recognition component of E2▪E3 complexes. Once the initial Ub has been linked to the target, a lysine residue of that Ub may function as the site for further ubiquitination. Repetition of this process is thought to lead to the formation of poly-Ub chains linked to a target. These Ub chains can initiate a variety of actions, most often targeting the modified protein for degradation by the 26S proteasome (26).

The specific mechanism by which poly-Ub chains are assembled is poorly understood. Proper coordination of the E2~Ub thiolester, the E3 and the target protein are required for target recognition, target ubiquitination and subsequent poly-Ub chain assembly onto the target. One model has proposed that E2s form multimeric complexes with themselves to facilitate poly-Ub chain assembly (23). Evidence supporting self-association and hetero-association of E2s has been reported. Several groups have observed that purified E2s can self-associate into dimers or higher order complexes *in vitro* (7, 20). Furthermore, purified *Caenorhabditis elegans* Ubc1 (13), as well as *S.*

cerevisiae Ubc4 (9) and Cdc34 (21) proteins can be crosslinked to themselves *in vitro* to form higher order complexes. *In vivo* evidence for such interactions also exists with the *S. cerevisiae* Ubc7 protein, which interacts with itself based on two-hybrid analysis (4). The *in vivo* observations made by Chen et al. (4) that the turnover of the *S. cerevisiae* MATα2 transcriptional regulator strongly correlates with this interaction suggests that it may be relevant.

The relationship between E2-E2 interactions and E2 function is not entirely clear. Silver *et al.* have presented a model based on genetic evidence suggesting that the function of the *S. cerevisiae* Cdc34 protein may be dependent on its interaction with itself (23). Cdc34 has generated much interest in recent years due to its essential function in cell cycle regulation. Together with the SCF (made up of Skp-Cul1-Rbx1/Hrt1-F.box) Ub-ligase, Cdc34 targets a number of key cell cycle proteins for ubiquitination, allowing for proper cell cycle progression (5, 6, 22, 27). Cdc34 consists of a typical E2 catalytic domain, but also possesses a number of distinct features that differ from other E2s, which mediate its unique function. These features include an 8-residue amino-terminal and a 126-residue carboxyl-terminal extension from its core catalytic domain. In particular, the first 38 residues of the carboxyl-terminal extension have been implicated in Cdc34's interaction with the SCF Ub-ligase. Several other distinct features also exist within Cdc34's catalytic domain, including two distinct serine residues (Ser73 and Ser97), as well as a 12-residue insert.

In this Chapter, I report evidence that Cdc34 self-associates *in vivo* and *in vitro*. Key residues involved for this interaction are also identified that are important for Cdc34's function *in vivo*, as well as for its ability to build poly-Ub chains *in vitro*. Moreover, these residues overlap with residues that are important in Ub thiolester formation. I also show that self-association is disrupted under reducing conditions that disrupt Cdc34~Ub thiolester. Analysis of Cdc34~Ub thiolester *in vitro* indicates that Ub thiolester facilitates Cdc34 dimerization, thereby promoting the assembly of poly-Ub chains. The results in the chapter emphasize the importance of Ub thiolester formation in defining Cdc34's catalytic function.

2.2 Results

2.2.1 Cdc34 self-associates

Our lab has previously shown using crosslinking studies that purified Cdc34 is capable of self-association *in vitro* (21). Our genetic observations have also suggested that Cdc34 may self-associate *in vivo* (21, 23). To investigate these observations further, I carried out crosslinking reactions using prepared whole cell lysates from cells expressing Cdc34 amino-terminally tagged with the Flag epitope, Flag-Cdc34. Flag-Cdc34 was expressed in a wild-type yeast strain from a high-copy plasmid under control of a galactose inducible promoter. Cells were grown in galactose media, harvested and lysed. The lysate was subsequently treated with or without the crosslinker disuccinimidyl suberate (DSS) and then subjected to sodium dodecyl salt (SDS)-polyacrylamide gel electrophoresis (PAGE). Flag-Cdc34 present within the lysates was visualized by immunoblotting using an anti-Flag antibody (Figure 2.1A). In both the DSS treated and untreated samples, multiple bands containing Flag-Cdc34 were detected. Bands having a molecular mass lower than that of Cdc34 likely correspond to partial degradation products. Bands having a molecular mass greater than that of Cdc34 and are shared between the DSS treated and untreated samples likely correspond to either ubiquitinated and/or phosphorylated Cdc34 as previously described (8). Interestingly, the DSS treated sample also exhibited a band that is absent in the untreated sample. This species corresponds to a specific crosslinked product containing Flag-Cdc34. The molecular mass of the crosslinked product was approximately double that of Cdc34, suggesting that it is a crosslinked dimer of Cdc34.

Although this crosslinked product may have resulted from Cdc34 self-association it remained a possibility that the unique band within the DSS treated sample represented Flag-Cdc34 crosslinked to some other protein. To eliminate this ambiguity I attempted to detect Cdc34 self-association by co-immunoprecipitation. Amino-terminally Flag and Myc tagged derivatives of Cdc34 were employed for co-immunoprecipitation. Each tagged version of Cdc34 was expressed in a wild-type yeast strain from a double expression yeast plasmid from which both derivatives were under the control of galactose inducible promoters; Gal10 for Flag-Cdc34, and Gal1 for Myc-Cdc34. The cells were

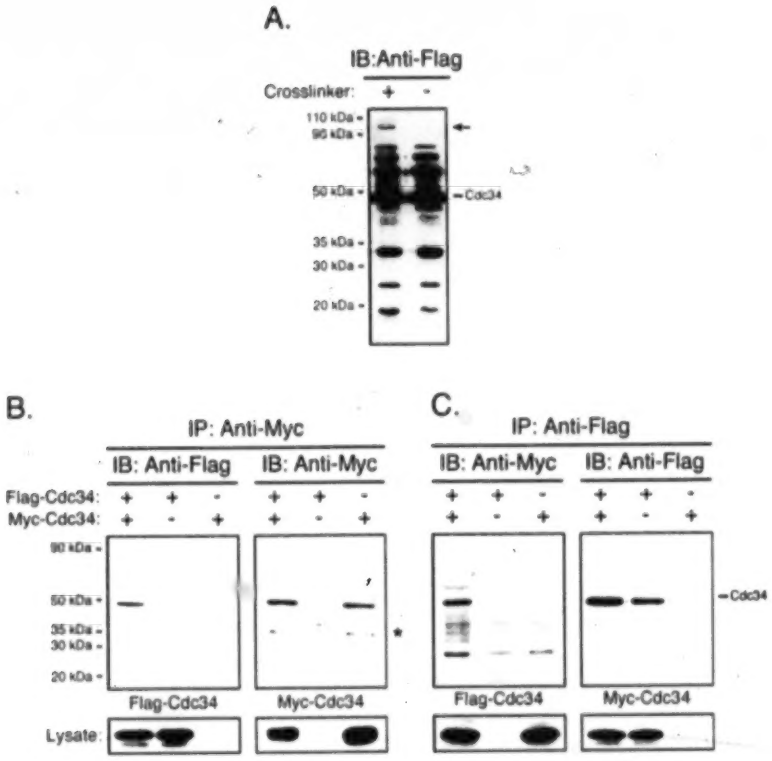

Figure 2.1 Cdc34 self-associates in vivo.

(A) Crosslinking. Cell lysates from YPH499 yeast cells expressing Flag-Cdc34 were treated with or without the chemical crosslinker DSS. Cell lysates were subsequently analyzed by immunoblotting (IB) with an anti-Flag antibody. The position of Flag-Cdc34 is indicated, as is the position of a unique crosslinked product containing Flag-Cdc34 (arrow). **(B and C)** Co-immunoprecipitation. Total cell extracts of YPH499 cells expressing Flag-Cdc34, Myc-Cdc34 or both Flag-Cdc34 and Myc-Cdc34 were prepared. **(B)** Myc-Cdc34 was immunoprecipitated (IP) with an anti-Myc antibody followed by immunoblotting (IB) with an anti-Myc antibody (right panel) to detect the amount of Myc-Cdc34 that has immunoprecipitated, and with an anti-Flag antibody (left panel) to detect the amount of Flag-Cdc34 that has co-immunoprecipitated. **(C)** The reciprocal co-immunoprecipitation experiment to that in B was performed. Flag-Cdc34 was immunoprecipitated (IP) with an anti-Flag antibody followed by immunoblotting (IB) with an anti-Flag antibody (right panel) and with an anti-Myc antibody (left panel). The position of Cdc34 is indicated, as is the position of a proteolytic product of Cdc34 (*). Protein expression levels within the lysates used for immunoprecipitations are shown for B and C under their respective panels.

induced by growth in galactose containing media and were subsequently lysed and subjected to immunoprecipitation using an anti-Myc antibody to isolate Myc-Cdc34 from the lysates. Immunoprecipitates were then analyzed by immunoblotting with an anti-Flag antibody to determine whether Flag-Cdc34 co-immunoprecipitated with Myc-Cdc34. As a control, cells expressing either Myc-Cdc34 or Flag-Cdc34 alone were also used. Flag-Cdc34 was only detected by immunoblotting when co-expressed with Myc-Cdc34 thereby demonstrating an interaction between the two (Figure 2.1B). Similar results were also generated from the reciprocal experiment, in which an anti-Flag antibody was used for immunoprecipitation followed by immunoblotting with an anti-Myc antibody (Figure 2.1C). Taken together these observations infer that Cdc34 self-associates *in vivo*.

2.2.2 The carboxyl-terminal extension and the catalytic domain insertion of Cdc34 are not required for Cdc34 self-association.

I wished to determine the elements within Cdc34 that were required for its ability to self-associate in cell lysates. The most obvious features of Cdc34 that distinguishes it from other E2s include a carboxyl-terminal extension as well as a catalytic domain insertion (see Figure 2.12). Previous work showed that deletion of the catalytic domain twelve amino-acid insert (Δ12) does not eliminate the ability of Cdc34 to carry out its cell cycle function (14), whereas the carboxyl-terminal extension, specifically residues 171-209, was required for its cell cycle function. These residues also appeared to stabilize the crosslinking of Cdc34 with itself *in vitro*, although residues 186-209 were dispensable at high concentration (21).

A Cdc34 derivative lacking the catalytic domain insert, as well as several carboxyl-terminal truncation derivatives were employed to assess whether these residues were required for Cdc34 self-association (Figure 2.2). Flag and Myc tagged versions of each derivative were constructed and each expressed from the double expression yeast plasmid from either the Gal10 (Flag-derivatives) or the Gal1 (Myc-derivatives) promoter as described above for full length Cdc34.

If either the catalytic domain insert or carboxyl-terminal extension (in particular residues 171-209) were required for Cdc34 self-association, then significant reduction or loss of signal corresponding to Flag-Cdc34 would be expected upon co-

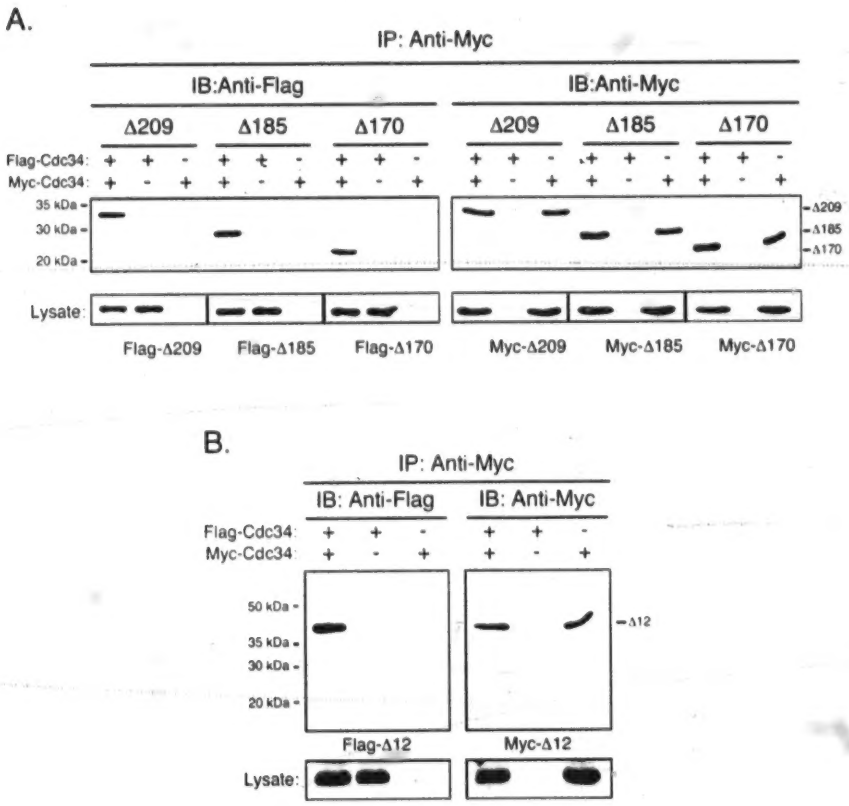

Figure 2.2 The Cdc34 carboxyl-terminal extension and catalytic domain insertion are dispensable with respect to Cdc34 self-association. The same co-immunoprecipitation strategy as employed for Cdc34 (Figure 2.1B) was employed for the carboxyl-terminal truncation derivatives Δ209 (residues 1-209), Δ185 (residues 1-185) and Δ170 (residues 1-170) **(A)** as well as the catalytic domain deletion derivative Δ12 (residues 103-114) **(B)**. Flag and Myc tagged versions of these truncation derivatives were expressed in YPH499 cells. Cell lysates were extracted and subjected to immunoprecipitation (IP) with an anti-Myc antibody followed by immunoblotting (IB) with an anti-Myc antibody (right panels) and an anti-Flag antibody (left panels). Protein expression levels within the lysates used for immunoprecipitations are shown for A and B under their respective panels.

immunoprecipitation when these derivatives were employed. Deletion of neither the catalytic domain insertion (Figure 2.2B) or portions of the carboxyl-terminal extension (Figure 2.2A) had a significant affect on the ability of Cdc34 to self-associate. In fact, truncation of the entire carboxyl-terminal extension (Δ170) had no observable affect on the interaction (Figure 2.2A, and Figure 2.4). As such, under the conditions employed here, both the catalytic domain insert and the carboxyl-terminal extension of Cdc34 are dispensable with respect to Cdc34 self-association.

2.2.3 Cdc34 self-association is not dependent upon a functional SCF.

From previous work, Cdc34 self-association had only been demonstrated *in vitro* by crosslinking experiments. Other physical means however, such as gel filtration or analytical ultracentrifugation, indicated that under the conditions used Cdc34 exhibited the hydrodynamic properties of an asymmetric monomer (22). Therefore, it appeared that Cdc34 self-association comprised a highly transient interaction and I postulated that auxiliary factor(s) are required to stabilize Cdc34's interaction with itself. The multi-subunit SCF complex, an E3 enzyme required for Cdc34's cell cycle function, interacts with Cdc34 (17) and thus provided a potential candidate for such a factor. However, the interaction of Cdc34 with the SCF is dependent upon residues 170-209 of Cdc34's carboxyl-terminal extension. As shown in Figure 2.2A, under these conditions this region is dispensable with respect to Cdc34 self-association, suggesting that a Cdc34-SCF interaction is not required for self-association.

I tested the dependence of Cdc34 self-association on the SCF complex by performing the co-immunoprecipitation experiment described above in a yeast strain carrying a temperature sensitive mutation in Cdc53, a core component of the SCF complex that directly interacts with Cdc34 (16). I used the *cdc53-1* mutant strain that has a single point mutation (R488C) in a region at the carboxyl-terminus of Cdc53 shown to be essential for Cdc34 binding (20). Expression of Myc-Cdc34 and Flag-Cdc34 was induced within the wild-type and *cdc53-1* strains by growing each in galactose media. Cells grown at either their permissive (25°C) or non-permissive (37°C) temperature were subsequently lysed and subjected to immunoprecipitation followed by immunoblotting as described above. At the non-permissive temperature, the *cdc53-1* mutation disrupts

critical SCF functions. If Cdc34 self-association required an interaction with a functional SCF complex it was expected that growth at the non-permissive temperature would result in a significant reduction or loss of signal corresponding to Flag-Cdc34. Furthermore, this signal would also be reduced relative to that observed for the wild-type strain. As seen in Figure 2.3 this comparison indicated that there is no significant loss in the ability of Cdc34 to self-associate within a strain defective in SCF function. This result, coupled with the observation that the carboxyl-terminal extension is not required for self-association, suggests that a Cdc34-SCF interaction does not mediate the ability of Cdc34 to interact with itself.

2.2.4 Residues within the Cdc34 catalytic domain that are required for self-association.

The inability to disrupt Cdc34 self-association by deleting either the carboxyl-terminal extension or the catalytic domain insertion meant that other residues within the catalytic domain had to play a role in stabilizing the interaction. Furthermore, if Cdc34 self-association is necessary for its cell cycle function, then it was possible that residues previously identified as important to Cdc34 function could also be important in self-association. Of particular relevance to this study were several Cdc34 derivatives described by Liu et al. Their genetic observations revealed an essential relationship between S73, S97 and the catalytic domain insertion (residues 103-114) (15). They reasoned that because these residues differ from their counterparts in other E2s that they contribute to Cdc34's unique functionality. In particular, they found that substitution of S97 to an aspartic acid, the residue found in the analogous position of other E2s, resulted in loss of function. Changing S73 to a lysine, the corresponding residue in other E2s, in combination with S97D slightly improved Cdc34 function, but again could not fully complement the defect. However, when the S73K/S97D substitutions were made in combination with the deletion of the catalytic insertion (Δ12) full Cdc34 function was restored.

The functional importance of these residues was not clear, but they are distinct from the residues found at analogous positions in most other E2s, suggesting that they are

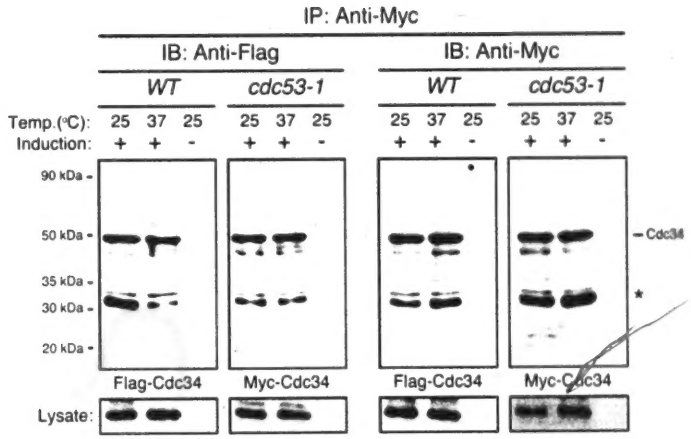

Figure 2.3 Cdc34 self-association is not dependent upon a functional SCF complex.
Flag-Cdc34 and Myc-Cdc34 were expressed in 15DaubΔ (wild-type, WT), or DSY1105 (*cdc53-1*) cells at either their permissive (25°C) or non-permissive (37°C) temperature. Cell extracts were prepared and Myc-Cdc34 was immunoprecipitated (IP) with an anti-Myc antibody followed by immunoblotting (IB) with either an anti-Myc antibody (right panel) or an anti-Flag antibody (left panel). The asterix (*) denotes a proteolytic product of Cdc34. Protein expression levels within the lysates used for immunoprecipitations are shown under their respective panels.

required for the functional specificity of Cdc34 (14). The uniqueness of these residues to Cdc34 suggested that they might play a role in the interaction between Cdc34 and the E3 SCF complex. The effect of these changes on the ability of Cdc34 to interact with the SCF was tested by co-immunoprecipitation of Cdc34 with Cdc53, its interacting partner within the SCF. Cdc53 triply tagged with the HA epitope at its carboxyl-terminus (Cdc53-3xHA) was co-expressed with each catalytic domain derivative of Cdc34 amino-terminally tagged with the Flag epitope. Cell lysates were immunoprecipitated using an anti-HA antibody to pull down Cdc53. Immunoblots were subsequently carried out to determine whether the Cdc34 derivatives and Cdc53 were present in the immunoprecipitates. As expected, the interaction between Cdc34 and Cdc53 was shown to be lost when a carboxyl-terminal truncation of Cdc34 is employed (Figure 2.4A, Δ170). On the other hand, the catalytic domain derivatives tested (Figure 2.4A, in particular S97D and SS) co-immunoprecipitated with Cdc53 to levels similar to that observed for wild-type Cdc34 (WT). These observations indicate that the *in vivo* defect associated with changes to residues 73 and 97 of the catalytic domain of Cdc34 do not affect its ability to interact with a core component of the SCF.

Based on this result, I tested the alternative possibility that these residues are required for the ability of Cdc34 to interact with itself. I therefore tested these derivatives for their ability to self-associate by co-immunoprecipitation as described above using amino-terminally tagged versions of each. Both Cdc34 and the carboxyl-terminal truncation derivative Δ170 were employed as positive controls.

The modification of these catalytic domain residues proved to have a significant affect on the ability of Cdc34 to self-associate (Figure 2.4B). In particular, the amino acid substitution S97D results in little, if any, detectable Flag-S97D in the immunoprecipitates, whereas Myc-S97D was detected at similar levels to both Cdc34 and Δ170. The complete loss of function for these derivatives *in vivo* provides further evidence that Cdc34 self-association is an important mechanistic feature of its function. Consistent with *in vivo* function, the affect of the S97D substitution was abrogated in part or fully by the introduction of additional changes to the catalytic domain. When the double substitution S73K/S97D is made, partial self-association is restored as evidenced by the weak Flag-S73K/S97D signal in the immunoprecipitate (Figure 2.4B, SS). When

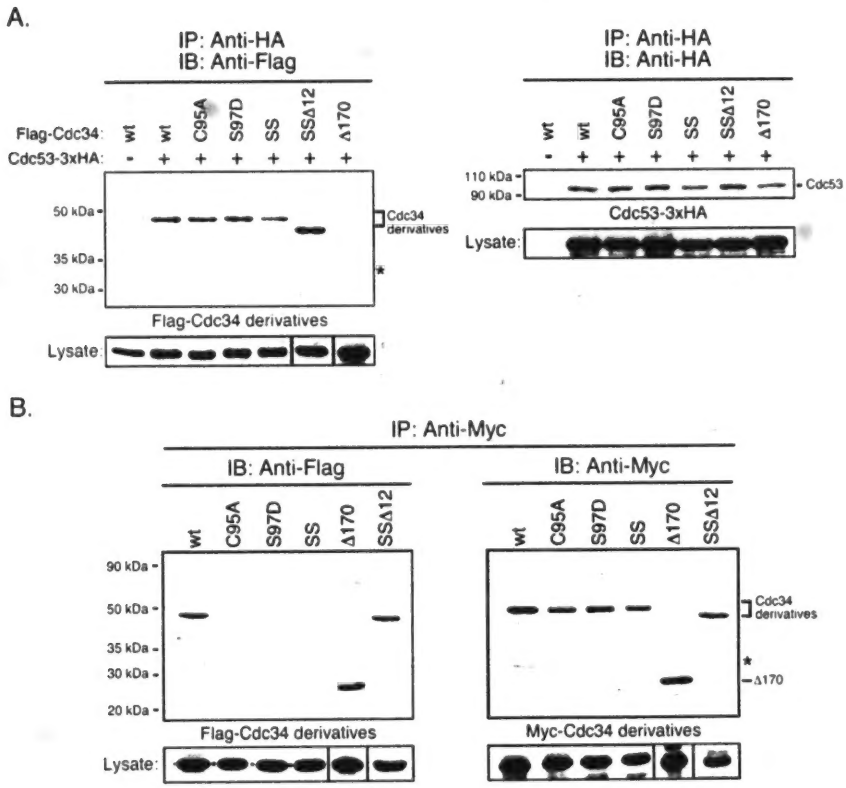

Figure 2.4 Key residues that mediate Cdc34 self-association.

(A) Catalytic domain derivatives of Cdc34 interact with Cdc53 of the SCF complex. Total cell extracts were prepared from YPH499 cells co-expressing Cdc53-3xHA and Flag-Cdc34 or one of the Flag-tagged Cdc34 derivatives: C95A, S97D, S73K/S97D (SS), S73K/S97D/Δ12 (SSΔ12) or Δ170. Cdc53-3xHA was immunoprecipitated (IP) with an anti-HA antibody and was detected by immunoblotting (IB) with an anti-HA antibody (right panel). The amount of Flag-Cdc34 or Flag-Cdc34 derivative that co-immunoprecipitated was detected by immunoblotting with an anti-Flag antibody (left panel). The position of Cdc53, Cdc34 and the Cdc34 derivatives are indicated. The asterix (*) denotes a proteolytic product of Cdc34. Protein expression levels within the lysates used for immunoprecipitations are shown under their respective panels. **(B)** Residues within the Cdc34 catalytic domain critical for self-association. The same co-immunoprecipitation strategy as employed for Cdc34 (Figure 2.1B) was employed for the catalytic domain derivatives C95A, S97D, S73K/S97D (SS), and S73K/S97D/Δ12 (SSΔ12). Flag and Myc tagged versions of these derivatives were expressed in YPH499 cells. Cell lysates were extracted and subjected to immunoprecipitation (IP) with anti-Myc antibody followed by immunoblotting (IB) with anti-Myc antibody (right panel) and anti-Flag antibody (left panel). The asterix (*) denotes a proteolytic product of Cdc34. Protein expression levels within the lysates used for immunoprecipitations are shown under their respective panels.

this latter derivative was further modified such that the catalytic domain insertion was deleted in combination with the S73K/S97D substitutions, this derivative fully restored the ability of Cdc34 to self-associate (Figure 2.4B, SSΔ12), thereby overcoming the self-association defect observed for the S97D derivative. Together these data indicate a supportive and inter-dependent role for these residues in both Cdc34 self-association and the cell cycle function of Cdc34. Furthermore, the ability of position 97 to mediate Cdc34 self-association is context dependent.

In vitro studies have previously suggested that additional factor(s) are required to stabilize Cdc34 self-association (21). It had previously been proposed that Cdc34~Ub thiolester formation could be a prerequisite for self-association, in which the covalently linked Ub of one Cdc34 monomer makes favorable contact with the other (21, 23). This model together with the close proximity of residues defective in self-association to the catalytic cysteine residue (see Figure 2.13) incited me to examine the importance of the active site in self-association. If this model were correct, it would be expected that a cysteine to alanine amino acid substitution at the active site would abrogate Cdc34's ability to self-associate, as a consequence of its inability to accept Ub. Significantly, the active site derivative C95A exhibited considerable loss of its ability to self-associate. Moreover, this loss could not be attributed to an inability to immunoprecipitate Myc-C95A (Figure 2.4B, C95A). This result therefore is consistent with the idea that Cdc34 self-association is facilitated by the Cdc34~Ub thiolester.

2.2.5 The relationship between Cdc34 self-association, Cdc34~ubiquitin thiolester, and Cdc34 autoubiquitination.

The apparent dependence of Cdc34 self-association on thiolester formation prompted me to address the converse question; does thiolester formation depend on self-association? I tested each of the Cdc34 derivatives described above with an *in vitro* thiolester formation assay that used purified E1, E2 and radio-labeled Ub as a probe (described in section 2.5.6). Restricting reactions to five minutes eliminated the complication of Cdc34 auto-ubiquitination that results from much longer incubations. With two exceptions, the level of each Cdc34 thiolester derivative was measured by exploiting the observation that they elute from an anion exchange column at a different

NaCl concentration than Ub and Uba1~Ub (Figure 2.5A). The thiolester forms of the tail deletion derivatives Δ209 and Δ185 were observed to elute at lower NaCl concentrations as a consequence of the reduced anionic character that results from tail deletion. Consequently, these species were separated from the other reaction components by gel filtration. Each of the Cdc34 thiolester derivatives exhibited sensitivity to DTT, a characteristic feature of the thiolester covalent bond.

From Figure 2.5B it is evident that only the C95A and S73K/S97D derivatives exhibit a severe defect in thiolester formation, the former for obvious reasons and the latter for reasons that are unapparent (discussion, section 2.4). Notably, the S97D self-association defect is more severe than S73K/S97D, yet exhibits a minimal defect in thiolester formation. Therefore, from these results alone there is no clear dependence of thiolester formation on self-association. Greater insight into this issue, however, was gained from the experiment described below.

I subsequently examined the ability of each Cdc34 derivative to synthesize poly-Ub chains by extending the incubation time of the thiolester assay already described, followed by separation using SDS-PAGE (Figure 2.6). The radio-labeled products that are detected in a reaction containing Cdc34 include unincorporated Ub, free di-Ub (Ub_2), and Ub chains that covalently linked to Cdc34 as a consequence of auto-ubiquitination (Cdc34-Ub_n).

The derivatives tested synthesized products that can be predicted either from previous observations or their altered peptide sequence. Not surprisingly, the active site derivative C95A was completely inactive (2). The carboxyl-terminal truncation derivatives Δ209 and Δ185 are capable of synthesizing free Ub_2, but are incapable of catalyzing the formation of poly-Ub chains linked to Cdc34. The lack of Cdc34 conjugates in these derivatives can be explained by the absence of the key target lysines that have been previously shown to reside in the carboxyl-terminal portion of the tail (3). Finally, the Δ12 derivative exhibited the capacity to auto-ubiquitinate itself (Figure 2.6).

Analysis of the remaining derivatives provided some interesting observations. In addition to the self-association defect, S97D exhibited little, if any, auto-ubiquitination in spite of its ability to synthesize thiolester with Ub. The weakly associating S73/S97D derivative however, exhibited relatively significant auto-ubiquitination even though it is

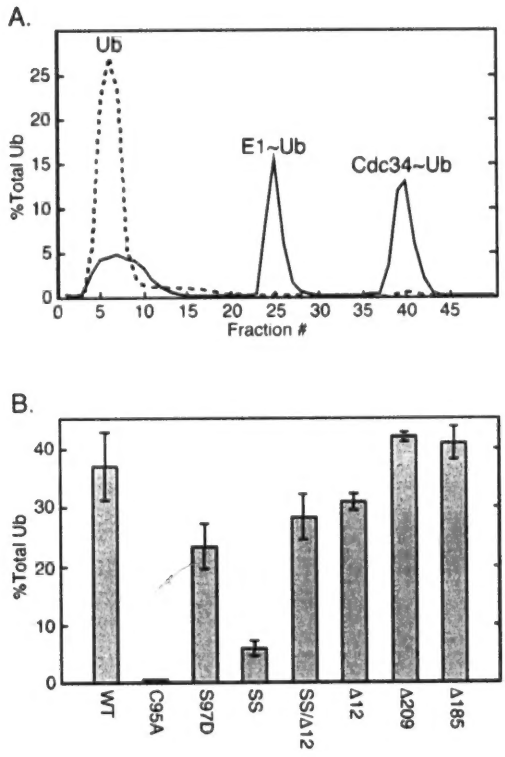

Figure 2.5 Cdc34 derivatives ability to form Ub thiolester.

In vitro Ub thiolester formation was compared for a number of Cdc34 derivatives. Reactions containing Cdc34 or one of its derivatives (100 nM), Uba1 (10 nM), ^{35}S-Ub (200 nM) and an ATP cocktail were incubated for 5 minutes at 30°C. Reactions were stopped by the addition of 50 mM EDTA then immediately loaded onto an anion exchange column to separate reaction products. The derivatives Δ209 and Δ185 were separated using a Superdex 75 HR10/30 size exclusion column (see materials and methods). **(A)** An example of the elution profile generated for a reaction containing Cdc34 is shown (solid line). Peaks containing ^{35}S-Ub correspond to free Ub, Ub incorporated into Uba1 (E1~Ub) and Cdc34 (Cdc34~Ub) thiolester. In a separate reaction 10mM DTT was added to disrupt thiolester (dotted line). **(B)** Incorporation of ^{35}S-Ub into thiolester for each Cdc34 derivative was determined as a percentage of total ^{35}S-Ub added to each reaction. The mean of thiolester observed for three separate reactions for each derivative is shown. SS represents the S73K/S97D derivative, SSΔ12 represents the S73K/S97D/Δ12 derivative, Δ12 represents the catalytic domain insert deletion (residues 103-114), Δ209 and Δ185 represent the carboxyl-terminal truncation derivatives (residues 1-209 and 1-185 respectively).

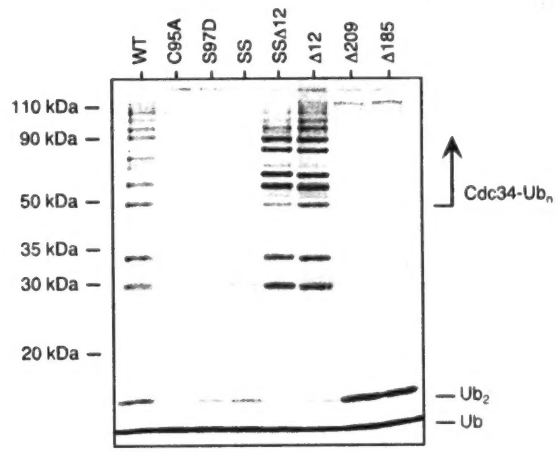

Figure 2.6 Autoubiquitination of Cdc34 derivatives.

Cdc34 autoubiquitination was assayed for Cdc34 and its various derivatives using an *in vitro* ubiquitination reaction. Reactions contained Cdc34 or one of its derivatives (100 nM), Uba1 (10 nM), ^{35}S-Ub (200 nM), and an ATP cocktail were incubated for 8 hours at 30°C representing an end point assay for autoubiquitination. 100 mM DTT was added to stop the reactions and the reaction products were analyzed using 12% SDS-PAGE followed by autoradiography. The positions of free Ub (Ub), di-Ub (Ub$_2$), and multi-Ub chains covalently linked to Cdc34 (Cdc34-Ub$_n$) are indicated. SS represents the S73K/S97D derivative, SSΔ12 represents the S73K/S97D/Δ12 derivative, Δ12 represents the catalytic domain insert deletion (residues 103-114), and Δ209 and Δ185 represent the carboxyl-terminal truncation derivatives (residues 1-209 and 1-185 respectively). A downward shift in molecular mass in the Ub chains on the Δ12 derivatives is observed consistent with the catalytic domain insert deletion. Bands not indicated are degradation products of Cdc34-Ub.

severely compromised in its ability to synthesize thiolester. Furthermore, deletion of the catalytic insert in combination with the S73K and S97D substitutions (S73/S97D/Δ12) was found to alleviate the defects associated with auto-ubiquitination and self-association, as well allows for full complementation of Cdc34 function in *cdc34* mutant strains.

2.2.6 Cdc34 self-association depends on thiolester-linked ubiquitin.

The Cdc34 active site derivative C95A cannot form Ub thiolester and is defective in its ability to self-associate. These observations suggest that that the Ub thiolester form of Cdc34 facilitates self-association. However, Cdc34~Ub thiolester is labile and there is no guarantee that Cdc34 present in either the cell lysates or Cdc34 isolated via co-immunoprecipitation would be in the Cdc34~Ub thiolester state. To confirm that Cdc34~Ub thiolester was present during the co-immunoprecipitations used in this study, amino-terminally Flag and Myc tagged derivatives of Cdc34 were co-expressed with an amino-terminally HA tagged derivative of Ub. Cell lysates were immunoprecipitated, followed by incubation in the presence of DTT to release and detect free Ub. Figure 2.7A verifies Cdc34 self-association as Flag-Cdc34 (Figure 2.7A, middle panel) co-immunoprecipitates with Myc-Cdc34 (Figure 2.7A, right panel). Furthermore, free Ub released after DTT treatment corresponds to the presence of Cdc34~(HA-Ub) thiolester in the immunoprecipitate (Figure 2.7A, left panel). To ensure that the free Ub observed is specific to Cdc34 two negative controls were included. First, immunoprecipitation using an anti-Myc antibody was carried out in the absence of expressed Myc-Cdc34 to ensure that free HA-Ub was not binding to the beads. Second, the C95A active site derivative (incapable of forming the Cdc34~Ub thiolester), which was defective in self-association (Figure 2.7A, middle panel), showed no free Ub in the immunoprecipitate (Figure 2.7A, left panel). These observations demonstrate the presence of Cdc34~Ub thiolester in the immunoprecipitates.

To demonstrate the dependence of Cdc34 self-association on the thiolester, the co-immunoprecipitation experiment described above for Figure 2.7A was repeated with three important modifications: 1) Each lysate was pretreated with or without DTT prior to immunoprecipitation resulting in samples with and without thiolester; 2) DTT treated and

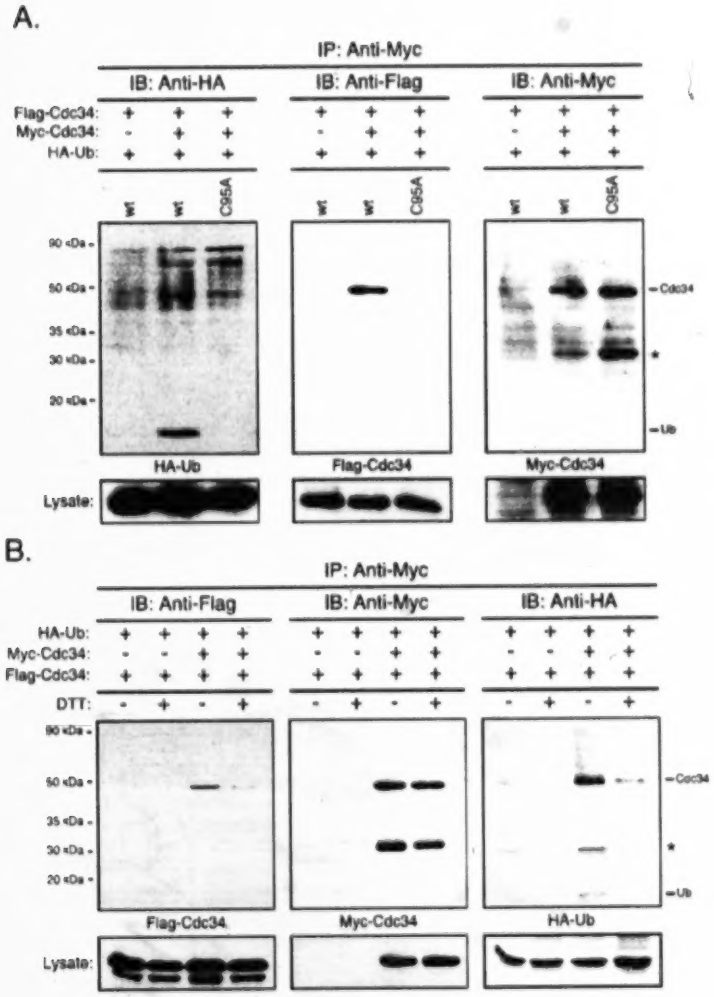

Figure 2.7 Cdc34 self-association is facilitated by Ub thiolester formation.
(A) The presence of Ub in Cdc34 immuno-coprecipitates: Myc and Flag tagged Cdc34 were co-expressed together with HA tagged Ub in YPH499 cells. Myc-Cdc34 was immunoprecipitated (IP) from cell extracts using an anti-Myc antibody. The Myc-Cdc34, Flag-Cdc34 and HA-Ub contained in the immunoprecipitate were separated by SDS-PAGE and detected by immunoblotting (IB) with an anti-Myc (left panel), anti-Flag (middle panel), and an anti-HA antibody (left panel). The substitution of Cdc34 with cdc34 C95A served as the negative control. The asterix (*) denotes a proteolytic product of Cdc34. Protein expression levels within the lysates used for immunoprecipitations are shown under their respective panels. **(B)** The dependence of Cdc34 self-association on thiolester formation: Same as above except that extracts were treated with, or without DTT followed by dialysis to remove DTT prior to immunoprecipitation.

untreated lysates were dialyzed to remove the DTT (previously found to be detrimental to antibody integrity) and then immunoprecipitated using the anti-Myc antibody; 3) At the final stage, all immunoprecipitates were treated with DTT to convert thiolester-linked Ub into the free form. Negative controls were included using cell lysates that lacked Myc-Cdc34. Cdc34 self-association in the absence of DTT is demonstrated by the co-immunoprecipitation of Flag-Cdc34 with Myc-Cdc34 (Figure 2.7B, left panel). Furthermore, the presence of HA-Ub in the same sample infers the presence of the Cdc34~Ub thiolester (Figure 2.7B, right panel). In contrast, the same lysate pretreated with DTT prior to immunoprecipitation revealed little Flag-Cdc34 in the co-immunoprecipitation, and therefore little of the self-associated form of CDC34 (Figure 2.7B, left panel). The absence of free Ub also indicates that the Cdc34~Ub thiolester is also absent (Figure 2.7B, right panel). Together, these two observations indicate that Cdc34~Ub is present under conditions where self-association is favored, and conversely, that the reduction of the thiolester disfavors Cdc34's ability to self-associate.

2.2.7 Cdc34~Ub thiolester self-associates into a dimer.

The above observations have indicated that *S. cerevisiae* Cdc34 self-association is mediated by Ub thiolester formation. However, no specific information regarding the stoichiometry of the complex was obtained from these experiments. For instance, it was not clear whether Cdc34~Ub thiolester self-associated into a dimer or into a higher order complex, or if Ub thiolester is required to be linked to one or all of the Cdc34s in the complex. I chose to initially address the question of Ub thiolester composition by using a co-immunoprecipitation approach from yeast whole-cell lysates, as described above. Cdc34 amino-terminally tagged with the Myc epitope (Myc-Cdc34) was co-expressed from the same plasmid as a Cdc34 catalytic site substitution derivative amino-terminally tagged with the Flag epitope (Flag-C95A). Substitution of the catalytic cysteine residue of Cdc34 renders it unable to form a thiolester linkage with Ub, therefore allowing me to examine the capability of Cdc34 not linked to Ub thiolester to self-associate with Cdc34 that can form Ub thiolester. Both Cdc34 derivatives were placed under the control of galactose inducible promoters, and were induced for expression by growth of the cells in galactose. This was followed by cell lysis and subsequent immunoprecipitation with an

anti-Myc antibody to isolate Myc-Cdc34 from the lysates. Immunoblot analysis of the immunoprecipitates was then carried out to determine if Flag-C95A co-immunoprecipitated with Myc-Cdc34. Since I have shown that wild-type Cdc34 can self-associate efficiently (see Figure 2.1), Myc-Cdc34 was co-expressed with Cdc34 amino-terminally tagged with the Flag epitope tag (Flag-Cdc34) as a positive control. I have also shown that the C95A derivative of Cdc34 was defective in self-association (see Figure 2.4), so I therefore co-expressed an amino-terminally Myc tagged cysteine substitution derivative of Cdc34 (Myc-C95A) with Flag-C95A as a negative control. In addition, Flag-Cdc34 was expressed alone as another negative control, as it should not be pulled down in the immunoprecipitation. Based on this analysis, I found that wild-type Cdc34 was able to associate with the C95A derivative (Figure 2.8) indicating that only one Cdc34 requires thiolester linked Ub in order for self-association to occur. However, wild-type Cdc34 self-associated more efficiently than the wild-type/C95A combination, indicating a higher affinity for self-association between two Ub thiolester linked Cdc34s (Figure 2.8).

Previous studies on Cdc34 self-association indicated that *in vitro* Cdc34 exhibits the properties of an asymmetric monomer (21). Since my data has indicated that Cdc34 self-association is facilitated by Ub thiolester, I wished to assess if Ub thiolester is sufficient to mediate Cdc34 self-association, and if so, the stoichiometry of the complex. To examine this I exploited the ability to purify Cdc34~Ub thiolester using anion exchange column chromatography (described in section 2.4.5). Purified Cdc34~^{35}S-Ub thiolester was passed over a size exclusion column, and the CPM were measured to follow ^{35}S-Ub bound moieties. Three different species were detected, running with apparent molecular weights corresponding to ^{35}S-Ub (approximately 8 KDa), Cdc34~^{35}S-Ub (approximately 120 KDa) and a complex twice that of Cdc34~^{35}S-Ub (approximately 240 KDa) (Figure 2.9, blue line). It is well characterized that Cdc34 has an increased stoke's radius that results from its carboxyl-terminal extension (21). This leads to an increase in Cdc34's apparent molecular mass from that of its predicted molecular mass of 34 KDa to approximately 120 KDa protein under the conditions used here (Figure 2.9, grey line), similar to that of Cdc34~Ub thiolester. Therefore, the 240 KDa species observed is consistent with a dimeric form of the Cdc34~Ub thiolester.

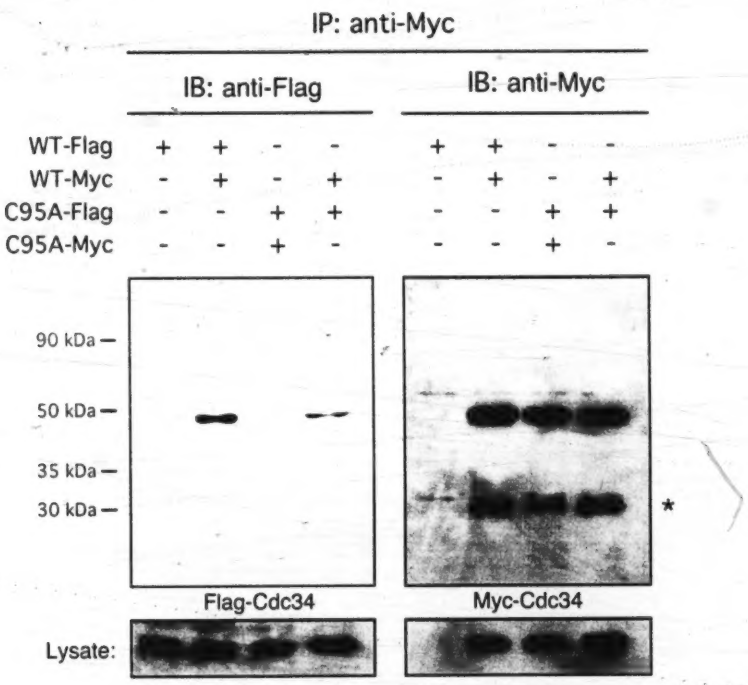

Figure 2.8 The composition of self-associated Cdc34~Ub thiolester complexes.
Total cell extracts of YPH499 cells expressing Flag-Cdc34 or both Flag-Cdc34 and Myc-Cdc34, Flag-C95A and Myc-Cdc34, or Flag-C95A and Myc-C95A were prepared. Myc-Cdc34 was immunoprecipitated (IP) with an anti-Myc antibody, followed by immunoblotting with an anti-Myc antibody (right panel) to detect the amount of Myc-Cdc34 that had immunoprecipitated and with an anti-Flag antibody (left panel) to detect the amount of Flag-Cdc34 that had co-immunoprecipitated. The position of Cdc34 is indicated, as is the position of a proteolytic product of Cdc34 (*). Protein expression levels within the lysates used for immunoprecipitations are shown at the bottoms of the panels.

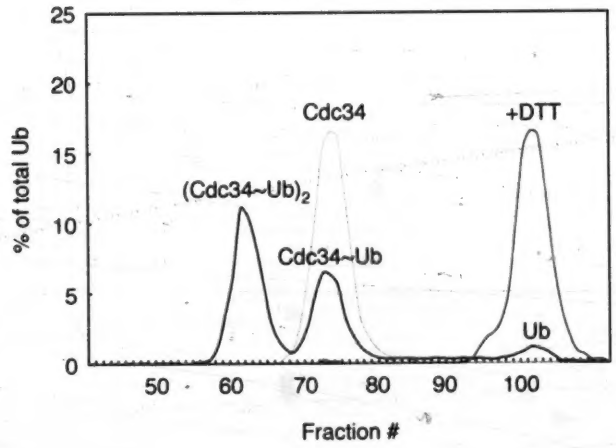

Figure 2.9 Cdc34~Ub thiolester self-associates into a dimer.

Purified Cdc34~^{35}S-Ub (as described section 2.4.5) was run over a Superdex 200 gel filtration column, and an elution profile was generated by following ^{35}S-Ub counts (blue line). Peaks containing ^{35}S-Ub were eluted that corresponded with Cdc34~Ub thiolester monomer (Cdc34~Ub), Cdc34~Ub thiolester dimer $(Cdc34\sim Ub)_2$, or free Ub (Ub). In a separate reaction, purified Cdc34~^{35}S-Ub was treated with 10 mM DTT to disrupt the thiolester linkage, and subsequently dealt with in a similar manner to determine the extent of Ub conjugate formation (red line). A peak representing monomeric Cdc34 is also depicted (grey line) that was generated by following the protein absorbance(OD_{280}) of purified Cdc34 that was run over a Superdex 200 gel filtration column.

As the major species, the dimeric peak was shown to be composed of only Cdc34 and Ub protein based on SDS-PAGE analysis. The dependence of monomeric Cdc34~Ub and dimeric Cdc34~Ub on thiolester linked Ub was confirmed by treating the Cdc34~Ub thiolester with DTT prior to separation by gel filtration. In this case, all the higher molecular weight complexes were chemically reduced to yield free Ub (Figure 2.9, red line). These results indicate that purified Cdc34~Ub self-associates under these conditions as a dimer.

2.2.8 Dimerization of Cdc34 increases the reduction of Ub thiolester.

A relationship between Cdc34 self-association and poly-Ub chain formation has been suggested by the above results. Based on this relationship the dimeric form of Cdc34~Ub thiolester *in vitro* would be positioned so that it would reduce the Ub thiolester linkage more efficiently than the monomeric form to enable the efficient transfer of Ub onto a substrate or onto another Ub. To investigate this possibility I examined the stability of the two forms of Cdc34~Ub thiolester. Purified Cdc34~^{35}S-Ub thiolester was incubated at 30°C for various amounts of time (0 to 22 hours), and then run over a size exclusion column to measure the amounts of the separate species. In addition, equivalent samples of purified Cdc34~^{35}S-Ub thiolester from each time point were treated with DTT to reduce any remaining Ub thiolester so that the amount of Cdc34-Ub conjugate that may form from autoubiquitination could be determined. The peaks corresponding with both forms of Cdc34~Ub thiolester were fairly unstable, but the rates at which the monomeric and dimeric forms reduced the thiolester linkage were quite different. The dimeric form of Cdc34 had reduced the majority of the thiolester linkage after 2 hours, and almost all of it after 4 hours (Figure 2.10A, black line). In contrast, the Ub thiolester linkage associated with the monomeric form of Cdc34 had been reduced by less than half after 4 hours, and was not completely reduced until about 8 hours (Figure 2.10A, blue line). Interestingly, there was very little Cdc34-Ub conjugate that was produced even after 22 hours (Figure 2.10A, red line), and from what was produced was of low molecular mass, suggesting limited poly-Ub chain formation (see below).

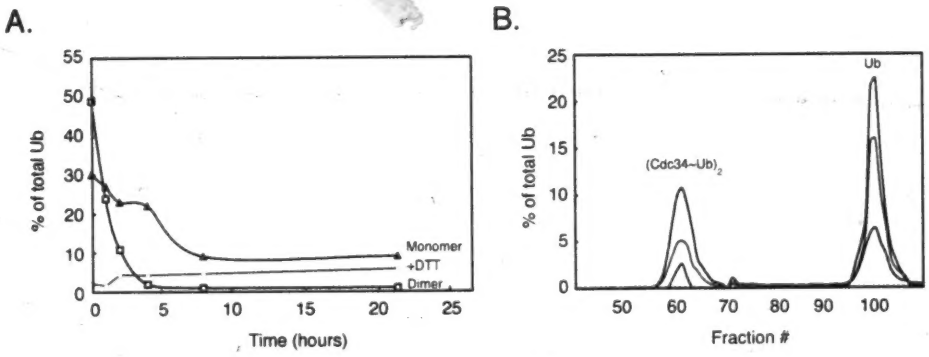

Figure 2.10 Dimeric Cdc34~Ub thiolester is less stable than monomeric Cdc34~Ub thiolester.
(A) Cdc34~Ub thiolester stability. Cdc34~^{35}S-Ub thiolester was purified (as described in section 2.4.5) and incubated at 30°C. Samples were taken at varying time points and split into two. One half was immediately run over a Superdex 200 gel filtration column, and an elution profile was generated by following ^{35}S-Ub counts. The CPM that eluted in the peaks corresponding to Cdc34~Ub thiolester monomer (blue line) and Cdc34~Ub thiolester dimer (black line) were measured and are represented as a percentage of the total CPM in the sample over time. The other half of the sample was treated with 10 mM DTT to disrupt the thiolester linkage, and subsequently treated in a similar manner to determine the amount of Ub conjugate (red line). **(B)** The stability of Cdc34~Ub thiolester dimer. The peak fractions corresponding to Cdc34~Ub thiolester dimer from the 0 hour time point in (A) were pooled and incubated at 30°C for 0 hours (blue line), 2 hours (red line) and 4 hours (green line). These samples were subsequently run over the Superdex 200 column and the profiles generated by following the ^{35}S-Ub counts are shown.

A possible explanation for the observed differences in Ub thiolester reduction is that the dimeric form of Cdc34~Ub thiolester may be disassociating into the monomeric form, thereby making it appear that the Ub thiolester linkage associated with the monomeric form is more stable. If the dimeric form of Cdc34~Ub thiolester is indeed reducing the Ub linkage more efficiently, then purifying it away from the monomeric form should result in the reduction of the Ub thiolester linkage into free Ub, or alternatively result in the conjugation of Ub onto a lysine residue on Cdc34. To address this, I pooled the peak fractions corresponding to the dimeric species of Cdc34~Ub thiolester following its separation using the size exclusion column, and incubated this sample for 1, 2 and 4 hours at 30°C. Samples from each time point were subsequently rerun over the size exclusion column to determine the fate of the Ub thiolester. Dimeric Cdc34~Ub thiolester did not disassemble into monomeric Cdc34~Ub thiolester, but rather efficiently reduced the Ub thiolester linkage resulting in free Ub (Figure 2.10B). Interestingly, only free Ub and a small peak corresponding to Cdc34 mono- or di-Ub conjugate was observed, suggesting that while the rapid reduction of Ub thiolester likely increases the rate of poly-Ub chain assembly, the rapid reduction of the thiolester linkage in the absence of a replenishing source of Ub thiolester limits the formation of poly-Ub chain assembly.

2.2.9 A constant source of Cdc34~Ub thiolester is required for efficient poly-Ub chain assembly.

To directly address the idea that the rapid reduction of Ub thiolester by dimeric Cdc34 limits its ability to assemble poly-Ub chains in the absence of a replenishing source of Ub thiolester, I incubated purified Cdc34~Ub thiolester with or without E1 and ATP cocktail at 30°C. The samples were subsequently treated with DTT and analyzed by SDS-PAGE to determine the extent of poly-Ub chain assembly. The presence of E1 and ATP should provide a *de novo* source of Ub thiolester, as Cdc34 would be recharged by E1 from the free Ub that results from the reduced Cdc34~Ub thiolester. As was observed in the thiolester stability experiment (in Figure 2.10), very little Ub from the Cdc34~Ub thiolester was incorporated into Cdc34-Ub conjugate over the time frame of the experiment when E1 was absent, and from what was incorporated, only mono-, di- and

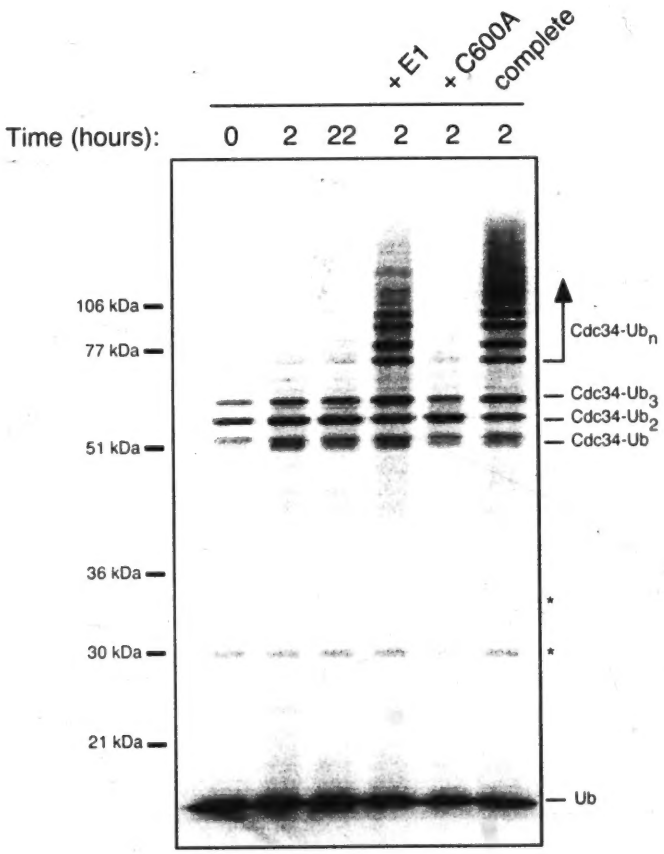

Figure 2.11 Poly-Ub chain assembly mediated by purified Cdc34~Ub thiolester.

Purified Cdc34~^{35}S-Ub thiolester was incubated at 30°C and aliquots were taken at 0, 2 and 22 hour time points. Cdc34~^{35}S-Ub thiolester was also incubated with S. cerevisiae Uba1 (E1) or the catalytic site Uba1 substitution derivative (C600A) in the presence of ATP cocktail at 30°C for 2 hours. In addition, a complete reaction containing ^{35}S-Ub, Cdc34, and E1 in the presence of ATP cocktail was incubated at 30°C for 2 hours. DTT was added to all the samples to terminate the reactions, and products from each reaction were subsequently separated by 12% SDS-PAGE and visualized by autoradiography. The position of Cdc34-Ub$_n$ conjugates is indicated by the arrow, as is the positions of free Ub. The asterisk (*) indicates a contamination band that purifies with ^{35}S-Ub.

tri-Ub conjugates were produced (Figure 2.11). This differed greatly from a reaction containing Cdc34, Ub, E1 and ATP cocktail, which efficiently catalyzes the assembly of poly-Ub chains (Figure 2.11, complete reaction). In contrast, poly-Ub chains were efficiently produced when E1 was supplemented back to the purified Cdc34~Ub thiolester (Figure 2.11). To test the requirement for a catalytically active E1, I also added a catalytic site substitution derivative of E1 (C600A) to the Cdc34~Ub reaction. We found that this derivative was not capable of catalyzing poly-Ub chains onto Cdc34, indicating that a charged form of E1 is required for mediating this reaction (Figure 2.11). These results indicate that Cdc34~Ub thiolester is rapidly reduced, thus limiting its ability to assemble poly-Ub chains, and that a replenishing source of Ub thiolester is required to mediate efficient poly-Ub chain assembly. The observation that short poly-Ub chains were assembled also suggests that they result from the close association of the dimeric Cdc34~Ub thiolester species, and were restricted to this short length by the absence of a constant source of Cdc34~Ub thiolester.

Taken together, all of the results reported in this chapter can be mechanistically rationalized in terms of the previously reported model (24) with key modifications.

2.3 Discussion

Using a combination of co-immunoprecipitation studies from cell lysates and a variety of *in vitro* assays, I have shown directly that Cdc34 self-associates. I have also identified structural determinants within the catalytic domain that are not only important in self-association but also important for growth and either of two stages related to poly-Ub chain assembly: thiolester formation, and the covalent transfer of Ub to Ub. These results are entirely consistent with, and provide further insight into, a previously proposed mechanism for poly-Ub chain assembly (22, 24). In this model, two Cdc34~Ub thiolester moieties interact in a manner that positions their Ub molecules for linkage. These and past findings make a credible circumstantial argument that: 1) The interaction of one Cdc34 molecule with another is required for poly-Ub chain synthesis; 2) The interaction is dependent on the formation of Cdc34~Ub thiolester; 3) Poly-Ub chain assembly is an obligatory step in Cdc34's function.

The interaction of Cdc34 with itself does not appear to be mediated by the E3. This conclusion is drawn from observations showing that Cdc34 self-associates in the absence of a functional SCF complex (Figure 2.3), and that the carboxyl-terminal extension of Cdc34 that is required for its interaction with the SCF (17), is dispensable for Cdc34 self-association (Figure 2.2A). Rather, it is the thiolester linkage with Ub that stabilizes the interaction between Cdc34 molecules, given that conditions that reduce the thiolester bond also disrupt Cdc34 self-association (Figure 2.7B). Similarly, residues in the catalytic domain of Cdc34 that play a role in Cdc34~Ub thiolester formation also play a role in self-association further strengthening the link between thiolester formation and self-association (see below). These observations indicate that Cdc34~Ub self-association likely precedes its interaction with the SCF resulting in a complex that is poised to build poly-Ub chains onto a target.

The dispensable nature of the carboxyl-terminal extension in Cdc34 self-association observed here presents an apparent contradiction with previously described *in vitro* crosslinking reactions (22). These *in vitro* reactions employed purified truncation derivatives of Cdc34 and crosslinking was carried out in the absence of thiolester linked Ub. Unlike the crosslinking experiments, I find that in cell lysates Cdc34 immunoprecipitates as Cdc34~Ub thiolester and that thiolester linked Ub stabilizes Cdc34 self-association (Figure 2.7). The presence of thiolester linked Ub provides sufficient stability to self-association (see Figure 2.9) that additional stabilization provided by the tail is superfluous and the carboxyl-terminal extension may be dispensed with in regard to this interaction. Rather, this study suggests that the principal role of the carboxyl-terminal extension is to provide a site of interaction with the SCF through Cdc53 as previously described (17).

A causal relationship linking the essential function(s) of Cdc34 to its self-association is suggested by the growth behavior of the association defective derivatives C95A, S97D and S73K/S97D (2, 15). These growth defects do not appear to be a result of their inability to interact with the SCF, as each retains the ability to interact with the core SCF component Cdc53 (Figure 2.4A). Rather, in each case the degree of the self-association defect directly corresponds to the degree of the growth defect (Figure 2.12). Furthermore, there is an important mechanistic relationship between these residues and

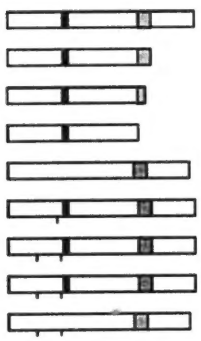

	Self-association	Thiolester formation	Auto-ubiquitination	*cdc34Δ* complementation	*cdc34-2* (37°C) complementation
WT	+++	+++	+++	+++	+++
Δ209	+++	+++	-	+++	+++
Δ185	+++	+++	-	-	++
Δ170	+++	N/A	N/A	-	-
Δ12	+++	++	+++	++	+++
C95A	-	-	-	-	-
S97D	-	++	-	-	-
SS	+	+	+	+	+
SSΔ12	+++	+++	+++	+++	+++

Figure 2.12 A functional comparison between the Cdc34 derivatives.

The primary structure of various Cdc34 derivatives is shown, with the catalytic domain shown in light gray and the 12 amino acid insert that is present within the catalytic domain shown in black (amino acids 103-114). The carboxyl-terminal extension is shown in white and residues of this domain previously shown to be necessary and sufficient for Cdc34 function are shown in dark gray (amino acids 170-209) (ref. 17). A line at the appropriate position along the block diagram indicates the position of point substitution(s) present in each derivative. The various derivatives are scored based on their abilities to self-associate, form Cdc34~Ub thiolester, build multi-Ub chains in an autoubiquitination reaction, and complement either a cdc34 disruption strain (*cdc34Δ*) or a cdc34 temperature sensitive strain (*cdc34-2*) (ref. 15, 2, 22). Each derivative was scored relative to wild type Cdc34 (+++) such that partial function was scored (++) or (+) and the absence of function was scored as (–).

the catalytic insert, which is evident by a reversal in both the self-association defect and the growth defect in a S73K/S97D/Δ12 derivative (Figure 2.12).

Based on these and the following observations, I believe that these residues play an important role in positioning the Ub thiolester correctly on the Cdc34 surface, and, that this requirement for orientation is necessary for the ability of Cdc34 to interact with itself and poly-Ub chain assembly. First, these residues are found to cluster around the active site cysteine when mapped onto the crystal structure of Ubc7 (5), another E2 that contains a catalytic domain insert that is similar to that of Cdc34 (Figure 2.13). Second, these residues coincide with analogous amino acid positions in other E2s that define key positions in the E2~Ub thiolester interaction (11, 18). Third, substitution of these positions affects their ability to form Ub thiolester and synthesize poly-Ub chains.

With respect to the third point, the derivatives C95A, S73K/S97D, S73K/S97D/Δ12 exhibit a direct correlation between their ability to synthesize Ub thiolester and their ability to synthesize poly-Ub chains (Figure 2.12). For example, the S73K/S97D derivative shows a strong defect in Ub thiolester formation that results in weak poly-Ub chain assembly. On the other hand, deletion of the catalytic domain insertion (S73K/S97D/Δ12) restores both Ub thiolester formation and poly-Ub chain assembly to wild-type levels. Furthermore, these activities parallel the ability of these derivatives to both self-associate and to carry out Cdc34's *in vivo* function as mentioned above (Figure 2.12). These analyses indicate that the *in vivo* function of Cdc34 is dependent upon three sequentially important events: 1) the formation of the Cdc34~Ub thiolester, 2) self-association, and 3) assembly of poly-Ub chains, and, that each of these mechanistic steps are dependent on the correct positioning of Ub on the Cdc34 surface (Figure 2.14).

Of the substitutions discussed thus far, S97D would appear to be the one exception. Although S97D is capable of thiolester formation to near wild-type levels, it also exhibits a loss in both self-association and poly-Ub chain assembly (Figure 2.12), a result that is not immediately accommodated into the conclusions drawn above. The behavior of S97D can be understood in light of the following argument. First, the observation that S97D forms thiolester indicates that its defect occurs downstream of Ub thiolester formation. Second, this downstream defect includes the complete loss of both

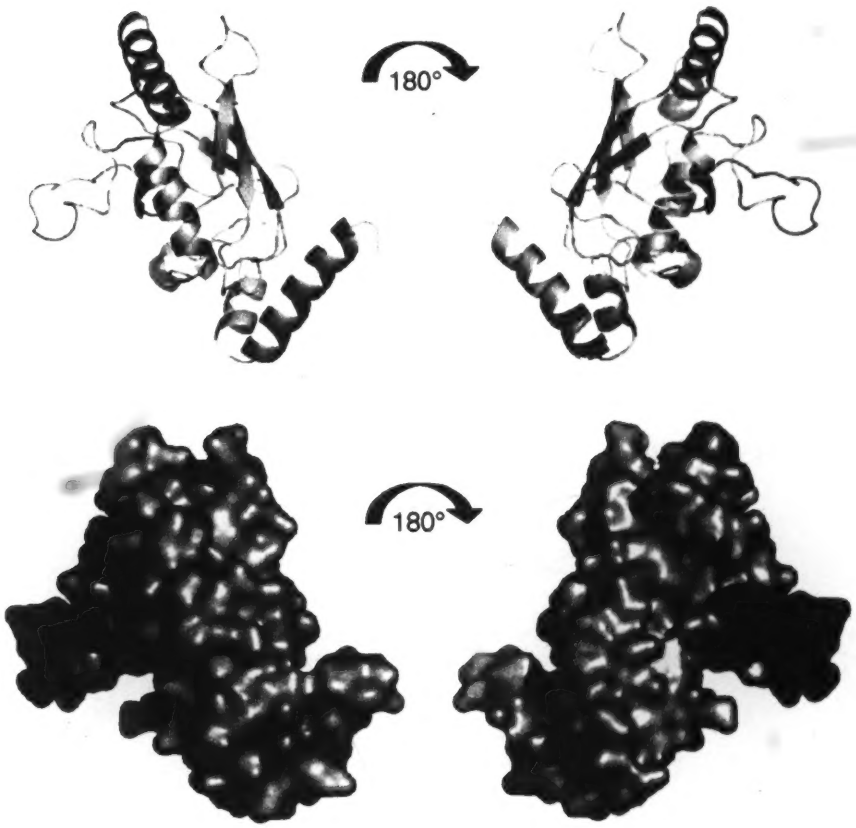

Figure 2.13 Determinants of Cdc34 self-association.

The crystal structure of the *S.cerevisiae* Ubc7 catalytic domain (ref. 5) is used here as a template for highlighting key residues within Cdc34 and is represented as both a cartoon diagram (top) and a surface model (bottom). The amino-terminus is found at the top of the structures and the carboxyl-terminus is found at the bottom. The residue that corresponds to residue 170, where the carboxyl-terminal extension of Cdc34 would start is highlighted (orange). Amino acid residues that play a role in Cdc34 self-association are also highlighted and include: the active site residue C95 (yellow), S73 (green), S97 (blue), and the catalytic domain insert (amino acids 103-114, red).

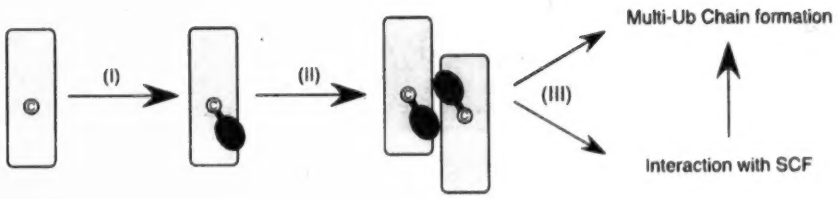

Figure 2.14 Hypothetical scheme for Cdc34 self-association and poly-Ub chain formation.
Cdc34 is represented in gray, the catalytic cysteine residue in white, and Ub in black. **(I)** Ub is transferred to Cdc34 from an activated Uba1~Ub thiolester to form Cdc34~Ub thiolester. **(II)** Cdc34~Ub thiolester formation mediates the self-association of two or more Cdc34s. **(III)** Self-associated Cdc34~Ub thiolester is charged and positioned in such a way as to interact with a target either alone or through an Ub-ligase, such as the SCF complex, and will proceed to build poly-Ub chains.

poly-Ub chain assembly and self-association. Thus, the defect is not in the synthesis of the Cdc34~Ub thiolester but within the thiolester complex itself. As mentioned above, it appears likely that amino acid positions 73, 97 along with the catalytic domain insertion play a role in positioning Ub correctly on the Cdc34 surface following thiolester formation. Based on these results, I propose that the S97D substitution perturbs the orientation of the thiolester Ub in a manner that is unfavorable to self-association and poly-Ub chain assembly.

A common mechanistic relationship between Ub binding with positions 73, 97 and the catalytic domain insertion is also supported by the following observations. The behavior of S97D changes with respect to its utilization of Ub when S73K is introduced (SS, Figure 2.12). S73K/S97D is less effective at thiolester formation relative to S97D, but more effective than S97D at chain assembly. Therefore S73K nullifies the poly-Ub chain assembly defect of S97D but results in reduced thiolester formation. Furthermore, the thiolester defect of the S73K/S97D derivative is dependent on the catalytic domain insertion, as its deletion restores both Ub thiolester formation and poly-Ub chain assembly to wild-type levels (SSΔ12, Figure 2.12). Thus, all of the derivatives examined here are at least consistent with the idea that the position Ub occupies on the Cdc34 surface is critical to Cdc34 activity.

To address the composition and stoichiometry of the self-associated Cdc34 complex more directly, I coupled the co-immunoprecipitation studies with the examination of purified Cdc34~Ub thiolester's properties *in vitro*. My results demonstrate that Cdc34~Ub thiolester self-associates into a dimeric complex (Figure 2.9), and that a Cdc34~Ub moiety is able to interact with unbound Cdc34 (Figure 2.8), suggesting that a single Ub is sufficient to mediate the self-association of Cdc34, albeit less efficiently. These results confirm that Cdc34 self-association is mediated by Ub thiolester, as only Ub and Cdc34 were present in the *in vitro* analysis. Furthermore, my results emphasize that while a mixed complex of Cdc34~Ub•Cdc34 may form; efficient self-association requires that both interacting Cdc34s be charged with Ub (Figure 2.8).

The majority of the purified Cdc34~Ub thiolester that I examined *in vitro* existed as a dimeric complex (approximately 50% as a dimer, and 30% as a monomer), indicating that this interaction is favored. However, dimeric Cdc34~Ub thiolester was

much more unstable than the monomeric form, suggesting that self-associated Cdc34 is in a more active form. This may be reflective of an increased catalytic ability for the dimeric Cdc34 to reduce the Ub thiolester linkage, a prerequisite for poly-Ub chain formation. The increased rate of Ub thiolester reduction did not lead to the efficient formation of poly-Ub chains, suggesting that the reaction was very rapid and that without a constant supply of Ub thiolester the formation of poly-Ub chains is limited. Support for this idea was gained from the analysis of Cdc34 autoubiquitination. Purified Cdc34~Ub thiolester did not exhibit the same capability in assembling poly-Ub chains as did a complete reaction consisting of Ub, E1 and ATP cocktail. Very few high order poly-Ub chains were assembled by purified Cdc34~Ub thiolester. Alternatively, this species assembled mono-, di-, and tri-Ub conjugates onto Cdc34 (Figure 2.11). This varied from the complete reaction, which was competent in the assembly of high order poly-Ub chains. Only when an active form of E1 was supplemented back to the purified Cdc34~Ub thiolester was it capable of assembling higher order poly-Ub chains.

The sequence of events that describe Cdc34 function in light of my present findings have been summarized schematically in Figure 2.14. 1) A monomer of Cdc34 is first activated with Ub by E1; 2) Thiolester formation triggers the formation of a Cdc34~Ub thiolester complex that results from favorable interactions that each Ub molecule makes across the boundary of the complex; 3) The complex then either alone or in combination with the SCF directs the assembly of a poly-Ub chain on the targeted substrate. The catalytic heart of this pathway is a multimer of the Cdc34~Ub thiolester that owes both its existence and activity to the spatial relationship between Cdc34 and Ub.

2.4 Materials and Methods

2.4.1 Plasmids and yeast strains

Plasmids and yeast strains used in this study are listed in Table 2.1. The pJD325 plasmid, containing the *S. cerevisiae UBA1-His6* gene, was provided to us by Daniel Finley (Harvard Medical School). Versions of the *S97D*, *S73K/S97D* (SS), *S73K/S97D/Δ12* (SS/Δ12) and *Δ12* derivatives (15) were provided to us by Mark Goebl

TABLE 2.1

Yeast strains used in Chapter 2

Yeast Strains	Genotype	Source
MHY501	*MATα his3-Δ200 leu2-3,112 trp1-1 ura3-52 lys2-801 gal2*	Hochstrasser M.
YPH499	*MATa ade2-101 his3-Δ200 leu2-Δ1 trp1-Δ63 ura3-52 lys2-801*	Stratagene
15DaubΔ	*MATa bar1Δ ade1 his2 leu2-3,112 trp1-1ª ura3Δns*	Stuart D.
DSY1105	*MATa bar1Δ ade1 his2 leu2-3,112 trp1-1ª ura3Δns cdc53-1*	Stuart D.

Plasmids used in Chapter 2

Plasmids	Description	Source
Wild type and control plasmids:		
pJD325	2μM P*CUP1-UBA1-6xHis* [*LEU2*]	Findley D.
pES5	2μM P*CUP1-HA-Ub* [*URA3*]	This study
pESC200	2μM P*GAL1-CDC53-3xHA* [*URA3*]	This study
pESC(Trp)	2μM P*GAL1-Myc*, P*GAL10-Flag* [*TRP1*]	Stratagene
pESC(Ura)	2μM P*GAL1-Myc*, P*GAL10-Flag* [*URA3*]	Stratagene
pESC1	2μM P*GAL10-Flag-CDC34* [*TRP1*]	This study
pESC2	2μM P*GAL1-Myc-CDC34* [*TRP1*]	This study
pESCA	2μM P*GAL1-Myc-CDC34*, P*GAL10-Flag-CDC34* [*TRP1*]	This study
Cdc34 catalytic domain derivative plasmids:		
pESC15	2μM P*GAL10-Flag-cdc34 C95A* [*TRP1*]	This study
pESC16	2μM P*GAL1-Myc-cdc34 C95A* [*TRP1*]	This study
pESCH	2μM P*GAL1-Myc-cdc34 C95A*, P*GAL10-Flag-cdc34 C95A* [*TRP1*]	This study
pESC19	2μM P*GAL10-Flag-cdc34 S97D* [*TRP1*]	This study
pESC20	2μM P*GAL1-Myc-cdc34 S97D* [*TRP1*]	This study
pESCJ	2μM P*GAL1-Myc-cdc34 S97D*, P*GAL10-Flag-cdc34 S97D* [*TRP1*]	This study
pESC3	2μM P*GAL10-Flag-cdc34 S73K/S97D* [*TRP1*]	This study
pESC4	2μM P*GAL1-Myc-cdc34 S73K/S97D* [*TRP1*]	This study
pESCB	2μM P*GAL1-Myc-cdc34 S73K/S97D*, P*GAL10-Flag-cdc34 S73K/S97D* [*TRP1*]	This study
pESC5	2μM P*GAL10-Flag-cdc34 Δ12* [*TRP1*]	This study
pESC6	2μM P*GAL1-Myc-cdc34 Δ12* [*TRP1*]	This study
pESCC	2μM P*GAL1-Myc-cdc34 Δ12*, P*GAL10-Flag-cdc34 Δ12* [*TRP1*]	This study
pESC7	2μM P*GAL10-Flag-cdc34 S73K/S97D/Δ12* [*TRP1*]	This study
pESC8	2μM P*GAL1-Myc-cdc34 S73K/S97D/Δ12* [*TRP1*]	This study
pESCD	2μM P*GAL1-Myc-cdc34 S73K/S97D/Δ12*, P*GAL10-Flag-cdc34 S73K/S97D/Δ12* [*TRP1*]	This study
pESCK	2μM P*GAL1-Myc-CDC34*, P*GAL10-Flag-cdc34 C95A* [*TRP1*]	This Study
Cdc34 carboxyl-terminal truncation plasmids:		
pESC9	2μM P*GAL10-Flag-cdc34 Δ170* [*TRP1*]	This Study
pESC10	2μM P*GAL1-Myc-cdc34 Δ170* [*TRP1*]	This Study
pESCE	2μM P*GAL1-Myc-cdc34 Δ170*, P*GAL10-Flag-cdc34 Δ170* [*TRP1*]	This Study
pESC11	2μM P*GAL10-Flag-cdc34 Δ185* [*TRP1*]	This Study
pESC12	2μM P*GAL1-Myc-cdc34 Δ185* [*TRP1*]	This Study
pESCF	2μM P*GAL1-Myc-cdc34 Δ185*, P*GAL10-Flag-cdc34 Δ185* [*TRP1*]	This Study
pESC13	2μM P*GAL10-Flag-cdc34 Δ209* [*TRP1*]	This Study
pESC14	2μM P*GAL1-Myc-cdc34 Δ209* [*TRP1*]	This Study
pESCG	2μM P*GAL1-Myc-cdc34 Δ209*, P*GAL10-Flag-cdc34 Δ209* [*TRP1*]	This Study
Bacterial expression plasmids:		
pREGB1	pET-3a derivative + *Ub*	Hodgins et al. 1996
pREGB6	pET-3a derivative + *CDC34*	Ptak et al. 1994
pCdc34Δ185	pET-3a derivative + *cdc34 Δ185*	Ptak et al. 1994
pCdc34Δ209	pET-3a derivative + *cdc34 Δ209*	Ptak et al. 1994
pBV4	pET-3a derivative + *cdc34 C95A*	This study
pBV8	pET-3a derivative + *cdc34 S97D*	This study
pBV9	pET-3a derivative + *cdc34 S73K/S97D*	This study

(Indiana University). Cdc34 C-terminal truncations were generated as previously described (22). For Myc-Cdc34 the DNA sequences of *CDC34* or *cdc34* derivatives were amplified using the polymerase chain reaction (PCR) and inserted 3' of the Myc epitope tag in the pESC-Trp galactose-inducible expression plasmid (Stratagene) using the BglII/PacI restriction enzyme sites. For Flag-Cdc34 the DNA sequences of *CDC34* or *cdc34* derivatives were amplified using PCR and inserted 3' of the Flag epitope tag in the pESC-Trp plasmid using the XhoI/KpnI restriction enzyme sites. For Cdc53-3xHA the DNA sequence of *CDC53* was amplified using PCR and inserted into the pESC-URA galactose inducible expression plasmid (Stratagene) using the BamH1/Xho1 restriction enzyme sites. Three HA epitope tags were cloned into a Not1 restriction enzyme site that was engineered at the 3' end of *CDC53* before the stop codon. The yeast HA-Ub expression plasmid was generated by inserting a DNA segment encoding the HA epitope into the high-copy-number YEP352 Ub plasmid described previously (1) using the EcoRI/BglII restriction enzyme sites.

A modified derivative of the pET3a plasmid was used to construct the *Escherichia coli* over expression plasmids as previously described (22). The DNA sequences of *CDC34* or the *cdc34* derivatives were amplified using PCR and then inserted this into the pET3a derivative plasmid using the SacI/KpnI sites.

All oligonucleotides used were synthesized by the Department of Biochemistry DNA Core Facility at the University of Alberta (Edmonton, Canada). Restriction enzymes were purchased from Promega and New England Biolabs. The *E. Coli* strain MC1061 was used as the host for all plasmid expression and was grown in Luria Broth (LB) medium in the presence of required antibiotics. All plasmids were sequenced using a Beckman Coulter CEQ 2000 XL DNA analysis system.

Yeast strains 15DaubΔ and DSY1105 were provided by David Stuart (University of Alberta). The yeast strain MHY501 (19) used for Uba1 expression was provided by Mark Hochstrasser (Yale University). All yeast strains were cultured in either a rich medium (YPD: 1% yeast extract, 2% bacto-peptone and 2% glucose) or a SD medium (0.67% yeast nitrogen base without amino acids, 2% glucose, and the appropriate amino acids) as previously described.

2.4.2 Chemical crosslinking

Yeast cells expressing Flag-Cdc34 were grown at 30°C to an OD_{600} of 0.8. The cells were then harvested, washed with water, and lysed in ice-cold crosslinking buffer [50mM HEPES (pH 7.0), 100mM NaCl, 1 mM EDTA, 0.1% NP-40, protease inhibitor cocktail (Sigma)] with the use of glass beads. The lysate was then centrifuged at 10 000 g for 15 minutes at 4°C to remove debris. The crosslinker disuccinimidyl suberate (DSS) (Pierce) was then added to the lysate (5 mM final) and was incubated for 30 minutes at 30°C. Free reactive groups of DSS were quenched by the addition of 50mM Tris-Cl (pH 7.5) to the sample for 30 minutes at 30°C.

2.4.3 Immunoprecipitation and immunoblotting

Co-immunoprecipitation experiments were carried out using the yeast strains YPH499, 15DaubΔ, and DSY1105 as stated in the results. For the galactose inducible expression of proteins in yeast, the manufacturers recommended protocol (Stratagene) was followed using SSG medium (0.67% yeast nitrogen base without amino acids, 2% galactose, and the appropriate amino acids). Yeast cells expressing Myc-Cdc34, Flag-Cdc34 or Myc- and Flag-Cdc34 were grown to an OD_{600} of 0.8. Cells were harvested, washed with water and lysed in ice-cold lysis buffer [50mM HEPES (pH 7.5), 100mM NaCl, 1 mM EDTA, 0.1% NP-40, protease inhibitor cocktail (Sigma)] using glass beads. Lysates were then centrifuged at 10 000 g for 15 minutes at 4°C to remove debris. The supernatants were precleared with 25 µl of protein G-agarose (Roche) for 1 hour with gentle rotation at 4°C. This was followed by incubation of the lysates with 5 µl of anti-Myc antibody [0.4 mg/ml] (9E10, Roche) or 5 µl of anti-Flag antibody [0.4 mg/ml] (M2, Sigma) for 2 hours at 4°C, and then by incubation with 20 µl of protein G-agarose for 2 hours with gentle rotation at 4°C. The immunoprecipitate-bead complexes were washed 4 times with ice-cold lysis buffer. The complexes were then boiled for 5 minutes in SDS load buffer + 10mM DTT. The samples were subjected to 12% SDS-PAGE, transferred to polyvinylidene fluoride membrane, and analyzed by immunoblotting with anti-Flag Horseradish Peroxidase (HRP) conjugated antibody (M2, Sigma) or anti-Myc HRP conjugated anti-body (9E10, Roche).

The identical procedure as above was used for the experiment expressing Cdc53-3xHA in combination with Flag-Cdc34 or one of the Flag-cdc34 derivatives, except that 5 µl of anti-HA antibody [0.4 mg/ml] (12CA5, Roche) was used for the immunoprecipitation, and anti-HA HRP conjugated antibody (3F10, Roche) was used for immunoblotting.

For the experiments involving HA-Ub, the cells were induced at an OD_{600} of 0.2 for HA-Ub expression by adding $CuSO_4$ to the media (0.1 mM final). Immunoprecipitation was done as described above, as was the immunoblotting for Flag and Myc Cdc34. HA-Ub was analyzed by immunoblotting with an anti-HA HRP conjugated antibody (3F10, Roche). For dithiothreitol (DTT) treatment of samples prior to the immunoprecipitation, total cell extracts expressing HA-Ub, Flag-Cdc34 and Myc-Cdc34 were treated with or without DTT (100 mM final) for 2 hours at 30°C. The lysates were subsequently dialysed into dialysis buffer [50 mM HEPES pH 7.5, 100 mM NaCl] for 2 hours at 4°C. Immunoprecipitations and immunoblots on the treated lysates were carried out as described above.

2.4.4 Protein Expression and Purification

Cdc34 and its derivatives were expressed from a modified derivative of pET3a (22). Cell harvesting, and lysis were performed as previously described for Cdc34 (22). ^{35}S-Ub was produced using labeling procedures previously described (22). Purification of ^{35}S-Ub was carried out using a variation of a previously described technique (13). Briefly, *E. coli* extracts containing ^{35}S-Ub were dialysed at 4°C for 4 hours against buffer A [50 mM Tris (pH 7.5), 1 mM DTT, 1 mM EDTA]. Dialysates were then loaded onto a 1 ml HiTrap Q-Sepharose HP anion exchange column (Pharmacia) equilibrated with buffer A and eluted using the same buffer at a flow rate of 1 ml/min. Flow-through fractions containing ^{35}S-Ub were then passed over a 1 ml HiTrap Q-Sepharose HP cation exchange column (Pharmacia) equilibrated with buffer B [50 mM HEPES (pH 7.5), 1 mM DTT, 1 mM EDTA] and chromatographed using the same buffer at a flow rate of 1 ml/min. Flow-through fractions containing ^{35}S-Ub were then concentrated to 200 µl and passed over a HR 10/30 Superdex 75 gel filtration column (Pharmacia) equilibrated with buffer

C [50 mM HEPES (pH 7.5), 150 mM NaCl, 1 mM EDTA, 0.1 mM DTT). ^{35}S-Ub that was eluted off the column was concentrated and stored frozen in 10% glycerol at -80°C.

For the purification of *S. cerevisiae* Uba1, MHY501 yeast cells carrying the pJD325 plasmid were grown in Leucine minus SD media to an OD_{600} of 0.2 at 30°C. $CuSO_4$ was then added to the media (0.1mM final) and the cells were grown to an OD_{600} of 1.0 at 30°C. Cells were then harvested, washed with water and lysed in buffer D [50 mM Tris (pH 7.5), 1mM EDTA, 1mM beta-mercaptoethanol (BME)] with a protease inhibitor cocktail (Sigma). The lysate was then passed over a 5 ml HiTrap Q-Sepharose HP anion exchange column (Pharmacia) equilibrated with buffer D and the protein was eluted with a NaCl gradient of 0 to 1 M using buffer E [50 mM Tris (pH 7.5), 1 mM EDTA, 2M NaCl, 1mM BME]. Uba1-6His eluted at approximately 250 mM NaCl. The anion exchange column fractions were then passed over a 5 ml HiTrap chelating column (Pharmacia) charged with $CuSO_4$. The column was washed with 4 times its volume of 10 mM imidazole, and Uba1-6His was eluted with 500 mM imidazole. The eluted Uba1-6His was then concentrated and run over a High Load 16/60 Superdex 200 gel filtration column (Pharmacia) equilibrated with buffer C. Peak fractions of Uba1-6His were collected, pooled and concentrated. Glycerol was added to a concentration of 10% and the protein was frozen at –80°C. Uba1 concentrations were based on ubiquitin-activating activity. A reaction containing a sample of Uba1 and a known amount of ^{35}S-Ub in 0.5 ml of ATP cocktail [30 mM HEPES (pH 7.5), 5mM $MgCl_2$, 5 mM ATP, 0.6 units/ml inorganic phosphatase] was incubated at 30°C for one hour. The sample was then run over a HR 10/30 Superdex 200 gel filtration column (Pharmacia) equilibrated with buffer C lacking DTT. The cpm of the ^{35}S-Ub were followed and the incorporation of ^{35}S-Ub into the Uba1 peak to form Uba1~$(Ub)_2$ was used to determine the concentration of Uba1.

2.4.5 Cdc34~ubiquitin thiolester purification and stability.

Cdc34~Ub thiolester was produced by incubating 1 mM Cdc34, 1 mM ^{35}S-Ub (with a specific activity of 1.5 x 10^5 cpm/μg), and 100 nM Uba1-6xHis together for 30°C for 5 minutes in 2.5 ml ATP/Mg^{2+} cocktail. The five-minute reaction time ensures that minor amounts of Cdc34-Ub conjugates form as a result of Cdc34 autoubiquitination.

Reactions were stopped by the addition of 50 mM EDTA to chelate any unused Mg^{2+} thereby inactivating Uba1. Following incubation, the reaction mixture was immediately passed over a 1 ml HiTrap Q-Sepharose HP anion exchange column (Pharmacia) equilibrated with buffer F [50 mM Tris (pH 7.5), 1 mM EDTA]. Proteins were eluted with a NaCl gradient of 0 mM to 800 mM NaCl gradient using buffer G [50 mM Tris (pH 7.5), 1 mM EDTA, 2 M NaCl] and 0.5 ml fractions were collected. Counts per minute (CPM) fell into three well-resolved peaks corresponding to either ^{35}S-Ub or ^{35}S-Ub that had been incorporated into Cdc34~Ub thiolester or Uba1~Ub thiolester. The Cdc34~^{35}S-Ub peak was pooled and the protein concentration was based on the CPM from the sample. To test thiolester stability, the Cdc34~Ub thiolester was initially synthesized and purified as described above. The sample was subsequently run over a Superdex 200 16/30 gel exclusion column, an elution profile generated as described above and the profile compared to the gel filtration run used in the initial Cdc34~Ub thiolester purification

2.4.6 *In vitro* Cdc34~ubiquitin thiolester assays.

For the *in vitro* thiolester reactions, Cdc34~Ub thiolester was produced by incubating 100 nM Cdc34 or Cdc34 derivates, 200 nM ^{35}S-Ub, and 10 nM Uba1-6xHis in 2.5 ml ATP cocktail at 30°C for 5 minutes. 50 mM EDTA was added to chelate any unused Mg^{2+} thereby inactivating Uba1 and stopping the reactions. Purification of Cdc34~Ub thiolester was performed as described in section 2.5.5. All Cdc34 derivatives were analyzed for Ub thiolester formation using the above method except Cdc34 Δ209 and Δ185 which could not be resolved in this way due to their reduced anionic character. For these two derivatives, reactions were carried out the same as above, but instead were loaded onto a High Load Superdex 75 16/60 gel filtration column (Pharmacia) equilibrated with buffer C lacking DTT. Proteins were eluted in 0.5 ml fractions and again cpm fell into three well-resolved peaks. Thiolester yields for all reactions were calculated by determining the specific radioactivity of the incorporated ^{35}S-Ub and were expressed as percentages of the total Ub in the reaction.

2.4.7 Cdc34 autoubiquitination reactions

Autoubiquitination reactions were performed by incubating 100 nM Cdc34~^{35}S-Ub thiolester in the presence of ATP cocktail at 30°C for 0, 2 or 22 hours. Additional reactions were performed by incubating 100 nM Cdc34~^{35}S-Ub and 10 nM yeast Uba1 (E1) in the presence of ATP/Mg^{2+} cocktail at 30°C for 2 hours. Complete reactions for Cdc34 or Cdc34 derivatives were similarily performed by incubating 200 nM ^{35}S-Ub, 100 nM Cdc34 and 10 nM E1 in the presence of ATP/Mg^{2+} cocktail at 30°C for 2 hours. All reactions were terminated by the addition of 10 mM DTT, immediately followed by precipitation with 10 % trichloroacetic acid. Samples were then resuspended and boiled for 5 minutes in SDS load buffer, followed by separation by 12% SDS-PAGE and analysis by autoradiography as described previously (13).

2.5 References

1. Arnason, T., and M. J. Ellison. 1994. Stress resistance in Saccharomyces cerevisiae is strongly correlated with assembly of a novel type of multiubiquitin chain. Mol Cell Biol 14:7876-83.
2. Banerjee, A., R. J. Deshaies, and V. Chau. 1995. Characterization of a dominant negative mutant of the cell cycle ubiquitin-conjugating enzyme Cdc34. J Biol Chem 270:26209-15.
3. Banerjee, A., L. Gregori, Y. Xu, and V. Chau. 1993. The bacterially expressed yeast CDC34 gene product can undergo autoubiquitination to form a multiubiquitin chain-linked protein. J Biol Chem 268:5668-75.
4. Chen, P., P. Johnson, T. Sommer, S. Jentsch, and M. Hochstrasser. 1993. Multiple ubiquitin-conjugating enzymes participate in the in vivo degradation of the yeast MAT alpha 2 repressor. Cell 74:357-69.
5. Cook, W. J., P. D. Martin, B. F. Edwards, R. K. Yamazaki, and V. Chau. 1997. Crystal structure of a class I ubiquitin conjugating enzyme (Ubc7) from Saccharomyces cerevisiae at 2.9 angstroms resolution. Biochemistry 36:1621-7.
6. Deshaies, R. J., V. Chau, and M. Kirschner. 1995. Ubiquitination of the G1 cyclin Cln2p by a Cdc34p-dependent pathway. Embo J 14:303-12.
7. Drury, L. S., G. Perkins, and J. F. Diffley. 1997. The Cdc4/34/53 pathway targets Cdc6p for proteolysis in budding yeast. Embo J 16:5966-76.
8. Girod, P. A., and R. D. Vierstra. 1993. A major ubiquitin conjugation system in wheat germ extracts involves a 15-kDa ubiquitin-conjugating enzyme (E2) homologous to the yeast UBC4/UBC5 gene products. J Biol Chem 268:955-60.
9. Goebl, M. G., L. Goetsch, and B. Byers. 1994. The Ubc3 (Cdc34) ubiquitin-conjugating enzyme is ubiquitinated and phosphorylated in vivo. Mol Cell Biol 14:3022-9.
10. Gwozd, C. S., T. G. Arnason, W. J. Cook, V. Chau, and M. J. Ellison. 1995. The yeast UBC4 ubiquitin conjugating enzyme monoubiquitinates itself in vivo: evidence for an E2-E2 homointeraction. Biochemistry 34:6296-302.
11. Hamilton, K. S., M. J. Ellison, K. R. Barber, R. S. Williams, J. T. Huzil, S. McKenna, C. Ptak, M. Glover, and G. S. Shaw. 2001. Structure of a conjugating enzyme-ubiquitin thiolester intermediate reveals a novel role for the ubiquitin tail. Structure (Camb) 9:897-904.
12. Hershko, A., and A. Ciechanover. 1998. The ubiquitin system. Annu Rev Biochem 67:425-79.
13. Hodgins, R., C. Gwozd, T. Arnason, M. Cummings, and M. J. Ellison. 1996. The tail of a ubiquitin-conjugating enzyme redirects multi-ubiquitin chain synthesis from the lysine 48-linked configuration to a novel nonlysine-linked form. J Biol Chem 271:28766-71.
14. Leggett, D. S., and P. M. Candido. 1997. Biochemical characterization of Caenorhabditis elegans UBC-1: self-association and auto-ubiquitination of a RAD6-like ubiquitin-conjugating enzyme in vitro. Biochem J 327 (Pt 2):357-61.
15. Liu, Y., N. Mathias, C. N. Steussy, and M. G. Goebl. 1995. Intragenic suppression among CDC34 (UBC3) mutations defines a class of ubiquitin-conjugating catalytic domains. Mol Cell Biol 15:5635-44.

16. Mathias, N., S. L. Johnson, M. Winey, A. E. Adams, L. Goetsch, J. R. Pringle, B. Byers, and M. G. Goebl. 1996. Cdc53p acts in concert with Cdc4p and Cdc34p to control the G1-to-S-phase transition and identifies a conserved family of proteins. Mol Cell Biol 16:6634-43.
17. Mathias, N., C. N. Steussy, and M. G. Goebl. 1998. An essential domain within Cdc34p is required for binding to a complex containing Cdc4p and Cdc53p in Saccharomyces cerevisiae. J Biol Chem 273:4040-5.
18. Miura, T., W. Klaus, B. Gsell, C. Miyamoto, and H. Senn. 1999. Characterization of the binding interface between ubiquitin and class I human ubiquitin-conjugating enzyme 2b by multidimensional heteronuclear NMR spectroscopy in solution. J Mol Biol 290:213-28.
19. Papa, F. R., and M. Hochstrasser. 1993. The yeast DOA4 gene encodes a deubiquitinating enzyme related to a product of the human tre-2 oncogene. Nature 366:313-9.
20. Patton, E. E., A. R. Willems, D. Sa, L. Kuras, D. Thomas, K. L. Craig, and M. Tyers. 1998. Cdc53 is a scaffold protein for multiple Cdc34/Skp1/F-box proteincomplexes that regulate cell division and methionine biosynthesis in yeast. Genes Dev 12:692-705.
21. Pickart, C. M., and I. A. Rose. 1985. Functional heterogeneity of ubiquitin carrier proteins. J Biol Chem 260:1573-81.
22. Ptak, C., J. A. Prendergast, R. Hodgins, C. M. Kay, V. Chau, and M. J. Ellison. 1994. Functional and physical characterization of the cell cycle ubiquitin-conjugating enzyme CDC34 (UBC3). Identification of a functional determinant within the tail that facilitates CDC34 self-association. J Biol Chem 269:26539-45.
23. Schwob, E., T. Bohm, M. D. Mendenhall, and K. Nasmyth. 1994. The B-type cyclin kinase inhibitor p40SIC1 controls the G1 to S transition in S. cerevisiae. Cell 79:233-44.
24. Silver, E. T., T. J. Gwozd, C. Ptak, M. Goebl, and M. J. Ellison. 1992. A chimeric ubiquitin conjugating enzyme that combines the cell cycle properties of CDC34 (UBC3) and the DNA repair properties of RAD6 (UBC2): implications for the structure, function and evolution of the E2s. Embo J 11:3091-8.
25. Varelas, X., S. Mckenna, C. Ptak, L. Spyracopoulos, and M. J. Ellison. 2004. Examination of the interactions between Cdc34 and Ubiquitin reveal insight into Cdc34 function. (Submitted).
26. Varelas, X., C. Ptak, and M. J. Ellison. 2003. Cdc34 self-association is facilitated by ubiquitin thiolester formation and is required for its catalytic activity. Mol Cell Biol 23:5388-400.
27. Voges, D., P. Zwickl, and W. Baumeister. 1999. The 26S proteasome: a molecular machine designed for controlled proteolysis. Annu Rev Biochem 68:1015-68.
28. Yaglom, J., M. H. Linskens, S. Sadis, D. M. Rubin, B. Futcher, and D. Finley. 1995. p34Cdc28-mediated control of Cln3 cyclin degradation. Mol Cell Biol 15:731-41.

CHAPTER 3 – The Cdc34/SCF ubiquitination complex functions to mediate cell integrity *

* Portions of this chapter were done in collaboration with Dr. Christopher Ptak, and have been adapted from (40).

3.1 Introduction

The Ub-conjugating enzyme Cdc34 and its functional partner, the SCF (Skp1-Cdc53-Rbx1/Hrt1-F.box) Ub-ligase, associate to assemble poly-Ub chains onto a number of key cell cycle regulators, which primarily directs them to the 26S proteasome for degradation (5). Included in this group are cell cycle regulators that play critical roles in the progression from the G1 to the S phase of the cell cycle, such as the cyclin dependent kinase inhibitors Sic1 (9, 36, 42) and Far1 (1, 13), the pre-replicative complex component Cdc6 (6, 31), and the G1 cyclins Cln1 and Cln2 (18, 35, 38, 39, 47) among others (2).

In the budding yeast *Saccharomyces cerevisiae*, G1/S progression is characterized by at least three separate processes that include spindle pole body (SPB) duplication, bud emergence/polarized cell growth, and DNA replication. Temperature sensitive (TS) mutants of the Cdc34/SCF complex exhibit defects in all of these processes, displaying inhibition of DNA replication, duplicated, but un-separated SPBs, and elongated multibudded morphologies (28, 36, 37). These phenotypes have been primarily attributed to the stabilization of Sic1 within these mutant backgrounds. Support for this conclusion is also derived from the expression of a non-degradable derivative of Sic1 in wild type cells that leads to similar phenotypes to those associated with Cdc34/SCF mutants (41). Deletion of *SIC1* in Cdc34/SCF mutant backgrounds suppresses these phenotypic defects given that DNA is replicated, SPBs separate, and the elongated multibudded morphology is lost (36). However, deletion of *SIC1* in Cdc34/SCF mutant backgrounds uncovers a other associated defects characterized by a cell cycle arrest with replicated DNA and a round unbudded morphology (36). This highlights that the critical role of the Cdc34/SCF complex is not solely dependent upon its ability to regulate the levels of a single protein, but instead on its ability to regulate the levels of a variety of cell cycle regulators.

The work presented in this chapter identifies a novel function for the Cdc34/SCF complex in the regulation of yeast cell integrity. Proper maintenance of yeast cell integrity requires an integrated network of signaling pathways. These pathways function in the regulation of cell wall metabolism and actin reorganization during the cell cycle and in response to stress, and primarily converge on, or diverge from, the GTPase Rho1 (10, 12). One of the essential functions for Rho1 in the mediation of yeast cell integrity is to act as a regulatory component of the 1,3-β-glucan synthase. This enzyme catalyzes the synthesis of 1,3-β-glucan, the major structural component of the yeast cell wall. Another essential function for Rho1 is to initiate a signal through a mitogen activated protein kinase (MAPK) cascade by associating with the protein kinase Pkc1. This interaction stimulates the sequential phosphorylation of the MAPK kinase kinase (MAPKKK) Bck1, the redundant MAPK kinases (MAPKK) Mkk1 and Mkk2, and finally the MAPK Slt2/Mpk1. Stimulation of Slt2 phosphorylation has been found to occur under a number of distinct cellular conditions, including: 1) Cell cycle progression, peaking at the G1/S transition during bud emergence and polarized growth (49); 2) The morphogenesis checkpoint, in response to actin depolarization (11); 3) Stress response, such as under conditions of elevated temperature (3, 26); 4) The presence of reagents in the growth media that perturb cell wall biosynthesis, such as detergents and caffeine (3, 26).

Activation and regulation of this MAPK pathway is mediated by several distinct effectors. The role of Slt2 in the G1/S phase transition appears to be partially dependent upon the Cdc28 kinase, which may function to upregulate Pkc1 in this context (24, 49). In response to stress conditions, a variety of plasma membrane sensors are thought to monitor the cell wall, and signal to the cell integrity pathway under conditions of cell wall stress. One such group of sensors includes Wsc1/Slg1 that, in response to cell wall stress, stimulates the GTPase exchange factor Rom2, which in turn activates Rho1, leading to stimulation of Slt2 phosphorylation (32, 43). This pathway is also negatively regulated by a number of Rho1 GTPase activating proteins (Rho1-GAPs), including Sac7 and Lrg1. Deletion of these Rho1-GAPs has been shown to cause constitutive phosphorylation of Slt2 (21, 34). Lrg1 has also uniquely been observed to act as a negative regulator of Rho1's role in 1,3-β-glucan synthesis (44). Other effectors directly regulate this MAPK pathway. For example, Knr4/Smi1 directly interacts with Slt2,

altering its downstream signaling properties (27).

Several downstream effects have been attributed to the role of Slt2 in its maintenance of cell integrity. The best characterized of these is its role in the activation of specific transcriptional activators, including the SBF complex and Rlm1. The SBF complex, which is composed of the DNA binding protein Swi4 and the transcriptional activator Swi6, stimulates the expression of cell cycle genes involved in bud emergence, polarized cell growth and cell wall synthesis during the G1/S transition (14, 23). Rlm1 also regulates the expression of genes required for cell wall synthesis, but primarily acts in response to stress (16, 45). The formation of a complex between Knr4 and Slt2 is thought to direct the upregulation of cell integrity genes over cell cycle genes in response to stress (27). Although transcription factors appear to be primary targets of Slt2, other types of targets have been reported. These include the Mih1 phosphatase, which dephosphorylates Cdc28, a requirement for the passage of the cell cycle into M phase (11). Defects in bud emergence or actin polymerization activates Slt2 activity, which in turn leads to the phosphorylation of Mih1, which inhibits Mih1 phosphatase activity. This prevents Cdc28 dephosphorylation resulting in a delay in the cell cycle constituting part of the morphogenesis checkpoint.

Mutations within the cell integrity pathway are characterized by a number of phenotypes, including temperature sensitive lysis defects, suppression of this lysis defect by increasing the osmolarity of the external environment, increased temperature sensitivity in the presence of low concentrations of detergent, and caffeine sensitivity, among others (19, 20, 25, 30). In this study, we show that mutations in the Cdc34/SCF complex exhibit phenotypes associated with defects in maintaining cellular integrity. Furthermore, we find that Slt2 phosphorylation is misregulated in these strains, and we identify a number of genetic interactions between effectors of the cell integrity pathway and the Cdc34/SCF ubiquitination complex. Together, these results show that the Cdc34/SCF complex plays a key role in the regulation of the cell integrity pathway in response to stress and possibly during the cell cycle.

3.2 Results

3.2.1 Cdc34/SCF mutants exhibit cell integrity phenotypes.

In a search for genes that cause growth repression when expressed at high levels in either a *cdc34-2* or *cdc53-1* strain, we identified the Rho1-GAP Lrg1. Figure 3.1 shows this effect wherein the induction of *LRG1* expression by growth on galactose medium was shown to be synthetically lethal in the *cdc34-2* and *cdc53-1* strains at 30°C. In its role as a Rho1-GAP, Lrg1 has been implicated in negatively regulating Rho1's function as an activator of the cell integrity MAPK pathway and Rho1's function as an activator of the 1,3-β-glucan synthase enzyme (21, 44). The cell integrity function of Lrg1 and its genetic interaction with both *cdc34-2* and *cdc53-1* indicated that the Cdc34/SCF complex might also function as a regulator of yeast cell integrity.

Several phenotypes are associated with cell integrity mutants, including 1) temperature sensitive cell lysis that may be suppressed by high concentrations of extracellular solutes such as sorbitol or NaCl, 2) sensitivity to low levels of the anionic detergent SDS, and 3) sensitivity to reagents that affect cell integrity signaling such as caffeine (19, 20, 25, 30). We therefore tested the *cdc34-2* and *cdc53-1* strains to determine if these strains exhibited phenotypes associated with cell integrity defects (Figure 3.2A). Growth of either strain in the presence of high concentrations of sorbitol or NaCl was shown to significantly elevate the temperature restrictive for proliferation. When grown on medium containing 0.005% SDS the *cdc53-1* strain showed increased sensitivity, in that its non-permissive temperature was reduced from 37°C to 35°C and growth at 33°C only occurred at higher cell densities. The *cdc34-2* strain also showed SDS sensitivity, but only at the higher concentration of 0.0075%. Somewhat similar results were obtained when these strains were grown on medium containing 2 mM caffeine. The *cdc53-1* strain showed a reduced non-permissive temperature, whereas the *cdc34-2* strain showed no caffeine sensitivity. Based on these observations, the *cdc53-1* strain, and to a lesser extent the *cdc34-2* strain, exhibit cell integrity phenotypes suggestive of a role for the Cdc34/SCF complex in the maintenance of yeast cell integrity.

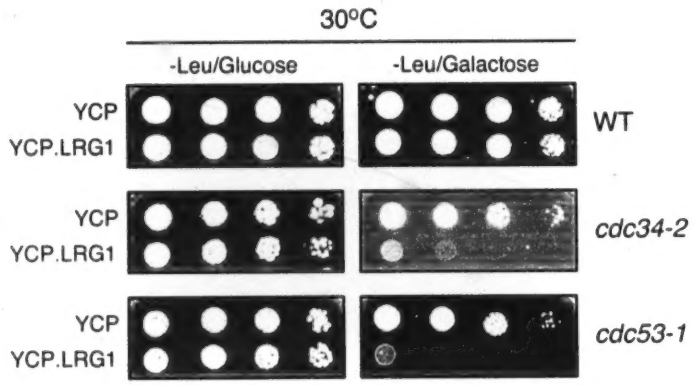

Figure 3.1 *LRG1* overexpression is toxic to Cdc34/SCF mutants.
Wild-type (*WT*), *cdc34-2* and *cdc53-1* cells were transformed with an empty control plasmid (YCP) or a plasmid expressing *LRG1* from a *GAL1* promoter (YCP.LRG1). Cell were grown in -Leu SD medium containing raffinose to mid-log phase at 30°C. The cells were then serially diluted, and 10^5, 10^4, 10^3 and 10^2 cells were plated on -Leu SD medium containing galactose or glucose. The cells were grown at 30°C for 3 days.

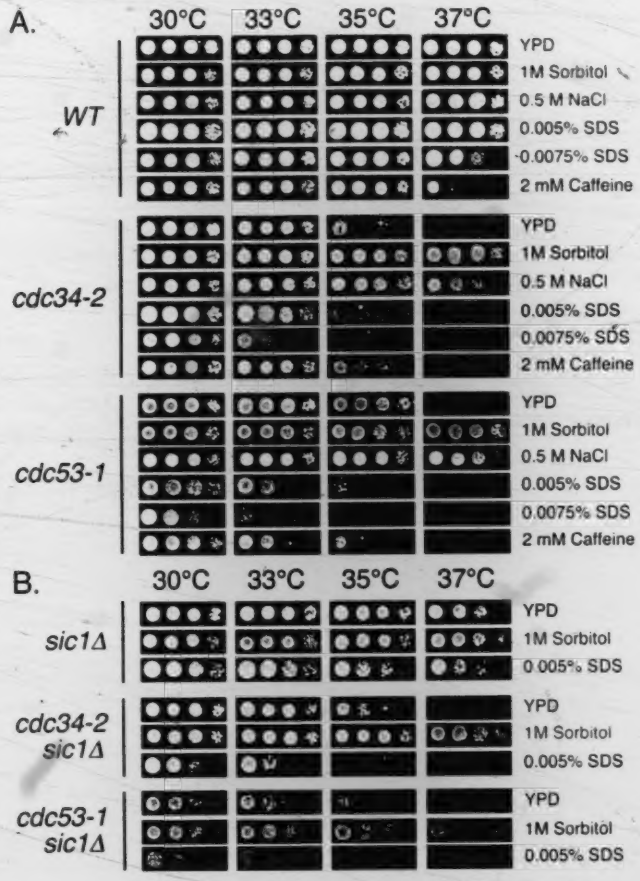

Figure 3.2 Cell integrity defects associated with *cdc53-1* and *cdc34-2* cells.
(A) Wild-type (*WT*), *cdc34-2* and *cdc53-1* cells were grown to mid-log phase in liquid YPD medium at 30°C. Serial dilutions of the cells were prepared, and 10^5, 10^4, 10^3 and 10^2 cells were spotted onto YPD, YPD containing 1 M sorbitol, YPD containing 0.0050% or 0.0075% SDS, YPD containing 0.5 M NaCl, and YPD containing 2 mM caffeine media. The cells were then grown at 30°C, 33°C, 35°C and 37°C for 3 days. **(B)** *sic1Δ*, *cdc34-2 sic1Δ* and *cdc53-1 sic1Δ* cells were prepared as described above, and 10^5, 10^4, 10^3 and 10^2 cells were spotted onto plates with YPD, YPD containing 1 M sorbitol and YPD containing 0.0050% SDS. The cells were then grown at 30°C, 33°C, 35°C and 37°C for 3 days.

A possible cause for the *cdc34-2* and *cdc53-1* cell integrity phenotypes might stem from Sic1 stabilization. Failure to degrade Sic1 in these strains causes hyperpolarized growth leading to an elongated, multibudded phenotype. It was possible that this aberrant morphology affected the yeast cell wall sufficiently to cause the observed cell integrity phenotypes. If true, it would be expected that deletion of *SIC1* in the *cdc34-2* and *cdc53-1* backgrounds would suppress the cell lysis defect associated with these strains. To test this possibility, we carried out plating experiments using the *sic1Δ*, *cdc34-2 sic1Δ*, and *cdc53-1 sic1Δ* strains (Figure 3B). Deletion of *SIC1* in *WT* cells caused minimal defects, given that the *sic1Δ* strain only showed weak SDS sensitivity at 37°C. Deletion of *SIC1* in the *cdc34-2* mutant also had little effect under normal growth conditions. In fact, the *cdc34-2 sic1Δ* strain showed greater sensitivity to 0.005% SDS then did *cdc34-2* alone. By comparison, the *cdc53-1 sic1Δ* strain showed a strong synthetic defect under all conditions tested. Thus, rather then alleviating defects associated with the *cdc34-2* and *cdc53-1* mutants, deletion of *SIC1* caused synthetic defects. Thus, the cell integrity defects associated with these strains do not result from hyperpolarized growth caused by the accumulation of Sic1, rather they appear to be mitigated by its presence.

3.2.2 The *cdc53-1* mutant exhibits phenotypes atypical of other Cdc34/SCF mutants.

The plating experiments shown in Figure 3.2 illustrate differential sensitivities to cell wall stress and *SIC1* deletion for the *cdc34-2* and *cdc53-1* mutants. To determine whether these differences were reflected in their behavior under normal growth conditions we expanded our comparison of the *cdc34-2* and *cdc53-1* strains.

Strains harboring Cdc34/SCF temperature sensitive mutations typically arrest at the non-permissive temperature with a 1N DNA content and single or multiple elongated buds (28, 36). For example, the *cdc34-2* strain used in this study arrests at 37°C with a 1N DNA content and a predominantly elongated, multi-budded cell morphology (Figure 3.3A). Unlike the *cdc34-2* strain, *cdc53-1* exhibited characteristics not typically associated with Cdc34/SCF mutants. In particular, the *cdc53-1* cells arrested at 37°C as a mixed population with either a 1N or 2N DNA content (Figure 3.3A). Furthermore, the

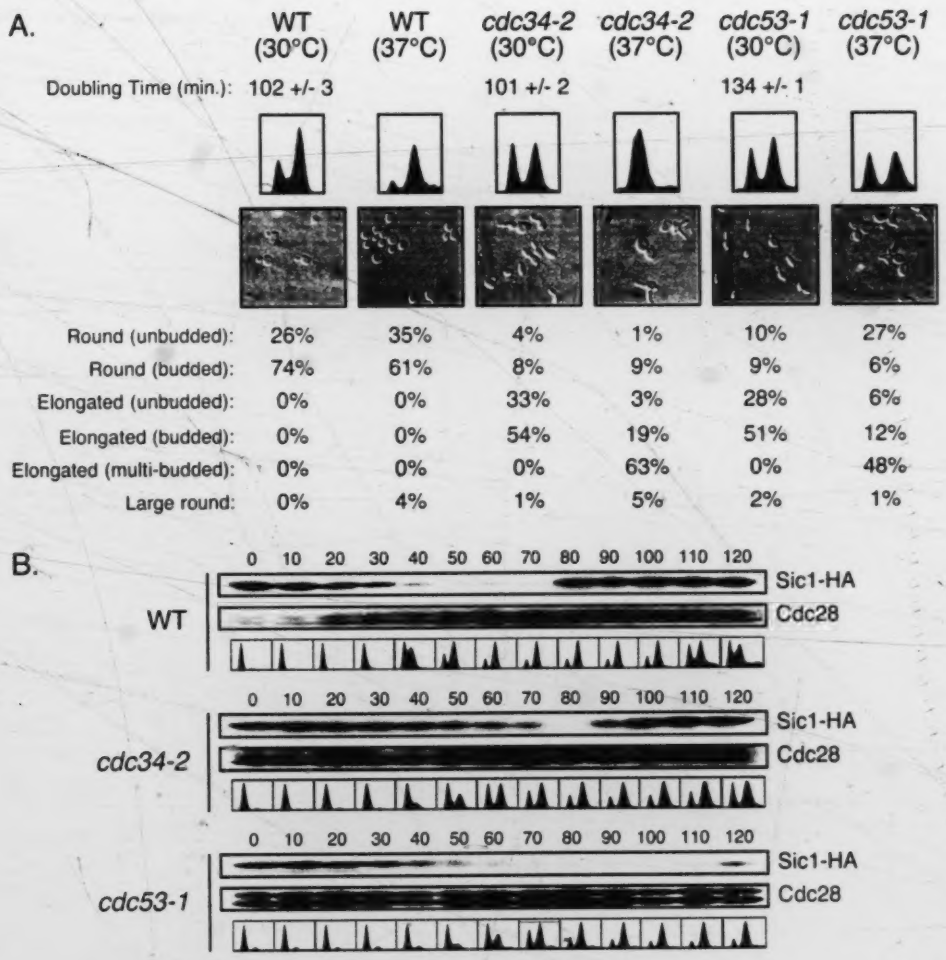
A.
WT (30°C)
WT (37°C)
cdc34-2 (30°C)
cdc34-2 (37°C)
cdc53-1 (30°C)
cdc53-1 (37°C)
Doubling Time (min.): 102 +/- 3
101 +/- 2
134 +/- 1
Round (unbudded): 26% 35% 4% 1% 10% 27%
Round (budded): 74% 61% 8% 9% 9% 6%
Elongated (unbudded): 0% 0% 33% 3% 28% 6%
Elongated (budded): 0% 0% 54% 19% 51% 12%
Elongated (multi-budded): 0% 0% 0% 63% 0% 48%
Large round: 0% 4% 1% 5% 2% 1%
B.
WT
cdc34-2
cdc53-1
0 10 20 30 40 50 60 70 80 90 100 110 120
Sic1-HA
Cdc28

Figure 3.3 ***cdc53-1*** **mutants display uncharacterized defects.**

(A) Morphology and DNA content. Wild-type (*WT*), *cdc34-2*, and *cdc53-1* cells were grown in YPD at 30°C to mid-log phase and shifted to 37°C for 6 hours. Samples from both temperatures were analyzed by DIC microscopy and flow cytometry. Images displaying the morphologies of the cells, as well as the DNA content from each sample are shown. The cells' morphologies were grouped as round (unbudded), round (budded), elongated (unbudded), elongated (budded), elongated (multi-budded) and large round, and the population percentages within each sample are displayed under the respective images. **(B)** Sic1 turnover in wild-type (*WT*), *cdc34-2* and *cdc53-1* cells at their permissive temperature. *WT*, *cdc34-2* and *cdc53-1* cells expressing *SIC1-HA* under its own promoter were arrested in the G1 phase of the cell cycle with α-factor and then synchronously released for growth into YPD medium at 30°C. Samples were taken at 10-minute time intervals and analyzed by immunoblotting for Sic1 protein levels or by flow cytometry for DNA content. Protein loads were determined to be consistent from sample to sample by immunoblotting for Cdc28 protein levels.

2N population of cells was found to persist even when the culture was incubated overnight at 37°C. *cdc53-1* cells also showed mixed morphologies at the non-permissive temperature. While a majority of the cells arrested with single or multiple elongated buds, a significant proportion (27%) arrested as round unbudded cells (Figure 3.3A). This comparison indicated that in addition to a Sic1 turnover defect leading to an arrest at the G1/S transition and an elongated morphology, the *cdc53-1* strain was also defective in some other function(s) causing the round unbudded morphology and arrest with 2N DNA content that is consistent with a G2/M defect in the cell cycle.

Additional differences between the *cdc34-2* and *cdc53-1* strains were observed when comparing their growth characteristics at the permissive temperature of 30°C. For instance, it was observed that the doubling time of the *cdc53-1* strain was approximately 30 minutes longer then that of the *WT* and *cdc34-2* strains (Figure 3.3A). We tested whether or not this delay could be attributed to a defect in Sic1 turnover at the permissive temperature. To this end, the levels of HA-epitope tagged Sic1 were followed in each strain using synchronized cells released from α-factor arrest at 30°C. Furthermore, analysis by flow-cytometry was employed to follow the DNA content of the cultures at each time-point used to measure Sic1 levels (Figure 3.3B).

In the *WT* strain, Sic1 abundance dramatically decreased by 40 minutes after release from α-factor arrest. Loss of Sic1 was coincident with the onset of DNA replication indicated by the presence of a 2N DNA peak. Re-accumulation of Sic1 occurred between 70-80 minutes after α-factor release, and the cells began re-entry into G1 phase of the cell cycle between 100-110 minutes after release. By comparison to the *WT* strain, Sic1 turnover appeared to be delayed and less efficient in the *cdc34-2* mutant. This was coincident with delay in the accumulation of cells with a 2N DNA content until 80 minutes after α-factor release by comparison to 50 minutes for the *WT* strain. Furthermore, DNA replication appeared to proceed even without complete degradation of Sic1, albeit less efficiently. These observations are consistent with a defect in Sic1 degradation at 30°C in the *cdc34-2* strain, although we cannot rule out the possibility that this delay stems from a defect in α-factor release. Unlike the *cdc34-2* strain, Sic1 turnover in the *cdc53-1* strain was as efficient as in the *WT* control. Surprisingly, the accumulation of *cdc53-1* cells with a 2N DNA content was delayed in spite of efficient

Sic1 turnover. In addition, Sic1 re-accumulation was delayed, and by 120 minutes after release from α-factor these cells had not re-entered G1 phase. Thus, at 30°C the *cdc53-1* strain shows a delay in S-phase entry, and a delay in G2/M, which occur independently of Cdc53's role in Sic1 degradation.

These studies show that the *cdc34-2* and *cdc53-1* strains exhibit distinctly different defects under conditions permissive for growth and division. The *cdc34-2* mutation appears to primarily cause defects associated with Sic1 degradation and causes weak cell integrity defects. In contrast, the *cdc53-1* mutation causes a number of defects not directly attributable to Sic1 turnover including cell cycle defects and more severe cell integrity related defects at both the permissive and non-permissive temperatures.

3.2.3 Cdc34/SCF mutants are defective in the induction of Slt2 phosphorylation in response to heat stress and caffeine.

A potential cause for the distinct phenotypes associated with the *cdc34-2* and *cdc53-1* strains was that these mutations affect the yeast cell integrity MAPK pathway to different degrees. In particular, we wished to determine the extent to which the cell integrity pathway was stimulated in the *cdc34-2* and *cdc53-1* backgrounds.

The cell integrity pathway consists of a phosphorylation cascade that is stimulated under stress conditions, leading to the phosphorylation of the MAPK Slt2 (3, 20, 26). As such, monitoring the induction of Slt2 phosphorylation may be used to measure the response of the cell integrity pathway to stress conditions. Based on western analysis using an antibody specific for phospho-Slt2, *WT* cells showed a strong induction of Slt2 phosphorylation in response to both heat shock and caffeine treatment (Figure 3.4) consistent with previous reports (26). The *cdc34-2* mutant also showed an induction of Slt2 phosphorylation under both conditions, but to a lesser extent than that seen for the *WT* strain. This indicated that the *cdc34-2* mutant showed a partial defect in phospho-Slt2 induction in response to heat stress and caffeine (Figure 3.4, left panels). By comparison, the *cdc53-1* mutant showed a profoundly reduced induction of Slt2 phosphorylation in response to heat stress and caffeine (Figure 3.4, right panels). These observations suggest that the cell integrity phenotypes observed in the *cdc34-2* and *cdc53-1* mutants stem from a defect in MAPK signaling. The extent to which these phenotypes are exhibited is also

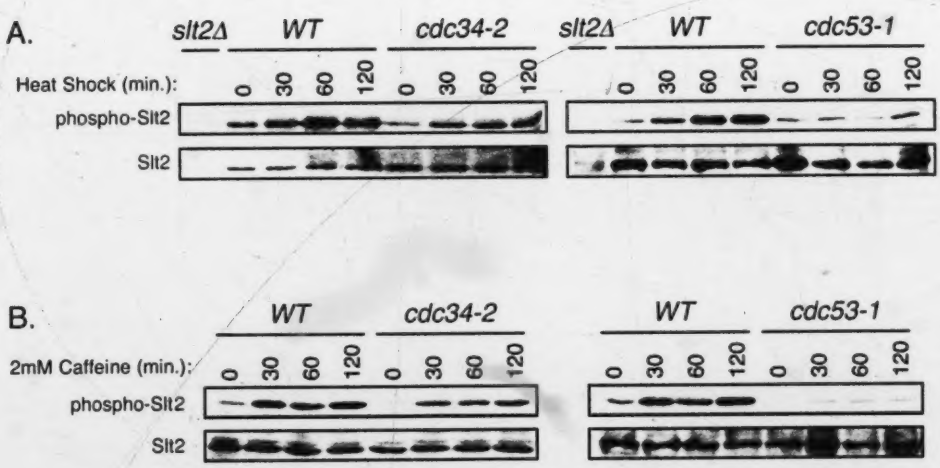

Figure 3.4 Slt2 phosphorylation is defective in *cdc53-1* and *cdc34-2* cells in response to heat or caffeine stress. Wild-type (*WT*), *cdc34-2* and *cdc53-1* cells were grown in YPD medium to mid-log phase at 30°C, and then were either **(A)** shifted to 37°C or **(B)** transferred to YPD containing 2 mM caffeine at 30°C (bottom panels). Cell samples were taken before (0 min.) or at the indicated time points (30, 60 and 120 min.) following the treatment. As a negative control, a sample from a *slt2Δ* strain after 120 minutes of growth at 37°C or in the presence of 2 mM caffeine was examined. The samples were analyzed for dually phosphorylated Slt2 and total Slt2 protein levels by immunoblotting. Comparisons of the Slt2 phosphorylation levels between the *WT* cells and the *cdc34-2* cells (on the left) and the *WT* and the *cdc53-1* cells (on the right) are shown.

reflected in the degree to which Slt2 is phosphorylated in each strain. This also raises the possibility that the defects associated with *cdc53-1* at 30°C may stem, at least in part, from a defect in Slt2 phosphorylation given that Slt2 also functions to regulate cell cycle progression (14, 23, 49). Overall these results indicate that the Cdc34/SCF complex functions to regulate the induction Slt2 phosphorylation in response to stress.

3.2.4 *cdc34-2 slt2Δ* and *cdc53-1 slt2Δ* strains show strong lysis defects.

To further probe the relationship between Slt2 and Cdc34/SCF mutants, *SLT2* was deleted in the *cdc34-2* and *cdc53-1* backgrounds and the affect of these synthetic mutations on the cell integrity phenotypes was tested. The *slt2Δ* strain was temperature sensitive at 37°C when grown on YPD. This temperature sensitive defect was not exacerbated by the addition of 0.005% SDS to the medium, and was suppressed in the presence of 1M sorbitol (Figure 3.5A). Microscopic inspection of the *slt2Δ* cells at 37°C showed that they lyse, and that this lysis defect is osmotically suppressed by 1M sorbitol (Figure 3.5B). When *slt2Δ* was combined with either the *cdc34-2* or the *cdc53-1* mutations a strong synthetic defect was observed. The *cdc34-2 slt2Δ* and *cdc53-1 slt2Δ* defects are similar to that observed for *slt2Δ* in that the presence of SDS does not exacerbate their growth defects, and the presence of 1M sorbitol in the growth medium suppresses the defect up to 35°C, and partially suppresses it at 37°C (Figure 3.5A). Microscopic inspection of *cdc53-1 slt2Δ* cells shows that they also possess a lysis defect at both 30°C and 37°C (Figure 3.5B). Furthermore, while the lysis defects associated with *cdc53-1 slt2Δ* cells can be suppressed in 1M sorbitol, these cells still exhibited an elongated bud morphology at both temperatures. The strong synthetic lysis defects observed for these strains are so strong that the presence of SDS cannot exacerbate them, indicate that Slt2 and the Cdc34/SCF complex function in parallel pathways to regulate cell wall integrity and biosynthesis in yeast.

We also tested the effect of deleting *SLT2* on caffeine sensitivity (Figure 3.5A). The *slt2Δ* strain was found to be sensitive to the presence of 2 mM caffeine in the growth medium. When made in combination with the *cdc34-2* and *cdc53-1* mutations, deletion of *SLT2* was synthetically lethal under this condition. These defects indicate that Slt2 and

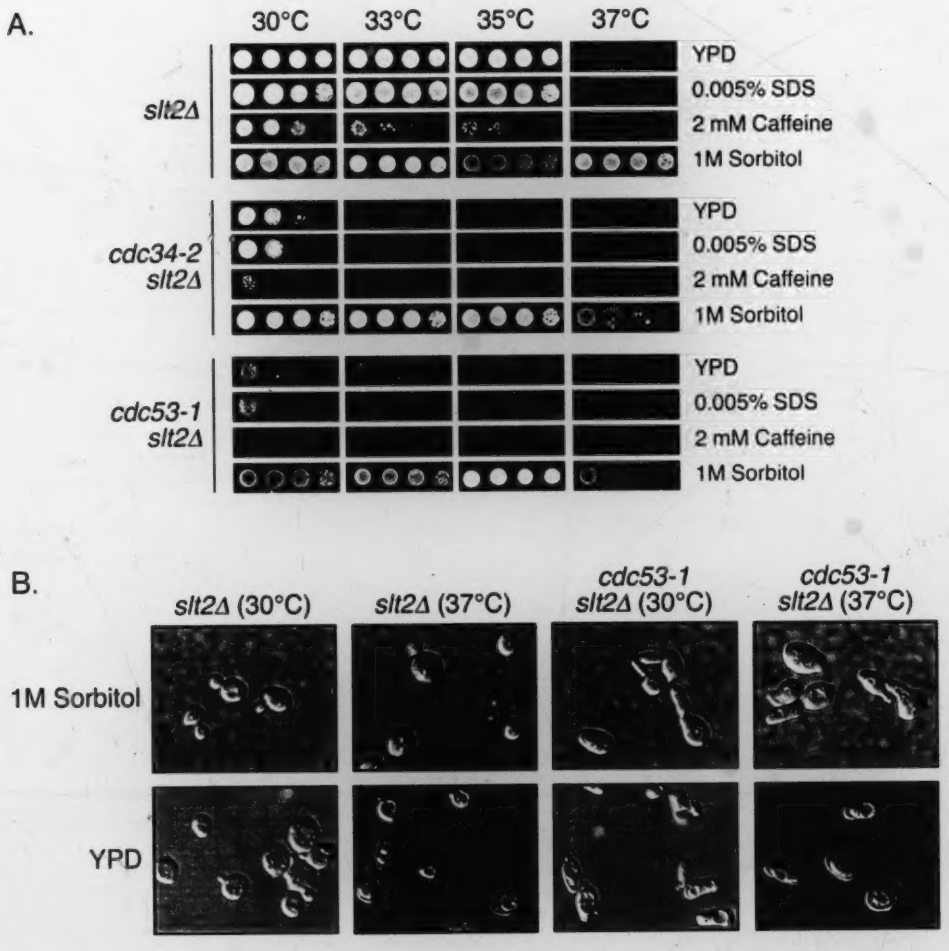

Figure 3.5 Deletion of *SLT2* in *cdc53-1* and *cdc34-2* mutants causes enhances lysis defects.
(A) *slt2Δ* plating experiments. *slt2Δ*, *cdc34-2 slt2Δ* and *cdc53-1 slt2Δ* cells were grown in liquid YPD containing 1M sorbitol at 30°C to mid-log phase. Serial dilutions of the cells were prepared and 10^5, 10^4, 10^3 and 10^2 cells were spotted onto plates with YPD, YPD containing 1M sorbitol, YPD containing 0.0050% SDS and YPD containing 2 mM caffeine media. The cells were then grown at 30°C, 33°C, 35°C and 37°C for 3 days. **(B)** Morphology of *slt2Δ* mutants. *slt2Δ* and *cdc53-1 slt2Δ* cells were grown in YPD containing 1M sorbitol at 30°C to mid-log phase, and were then shifted to 37°C, or into YPD medium without sorbitol at 30°C or 37°C for 6 hours. Samples of each were analyzed by DIC microscopy. Images displaying the morphologies of the cells are shown.

the Cdc34/SCF complex also function in parallel pathways to mitigate caffeine sensitivity in yeast.

3.2.5 Effect of *LRG1*, *SAC7* and *KNR4* deletions on phospho-Slt2 levels.

Stress induction of phospho-Slt2 is dependent upon the cell integrity MAPK pathway (3, 20, 26). Upstream regulators of this pathway stimulate the formation of a Rho1•GTP complex, which binds to, and activates, the Pkc1 kinase (17, 29), thereby initiating a MAPK cascade that ultimately leads to the phosphorylation and activation of Slt2 (Figure 3.6A) (10). Several regulators of this pathway have been shown to affect the phosphorylation state of Slt2. These include the Rho1-GAPs Lrg1 and Sac7, which negatively regulate Rho1 mediated signaling by stimulating its GTPase activity (Figure 3.6A). Deletion of the *LRG1* or *SAC7* genes has been shown to cause constitutive Slt2 phosphorylation (3, 21, 26). Another protein known to regulate Slt2 activity is Knr4, which acts at the level of Slt2 in the pathway by interacting with, and directing Slt2's downstream functions (27). Deletion of *KNR4* has also been shown to cause constitutive Slt2 phosphorylation (27).

Since the *cdc34-2* and *cdc53-1* strains showed a defect in phospho-Slt2 induction (Figure 3.4) and Lrg1 overexpression resulted in lethality (Figure 3.1), we wanted to determine if these effects were related. We addressed this by examining the effect of deleting *LRG1* in the Cdc34/SCF mutant backgrounds on the phosphorylation state of Slt2. We included in this analysis deletion strains of *SAC7*, as it also functions as a Rho1-GAP, and deletion strains of *KNR4*, as it functions at point in the cell integrity MAPK pathway downstream of both Sac7 and Lrg1. As expected from previous studies (3, 21, 26, 27), the *lrg1Δ*, *sac7Δ* and *knr4Δ* strains all showed constitutive Slt2 phosphorylation at 30°C, which did not allow for further induction of Slt2 phosphorylation under conditions of heat stress (i.e. at 37°C) (Figure 3.6B). These effects were mimicked upon deletion of these genes in the *cdc34-2* strain. However, we found that the while the *cdc53-1 lrg1Δ* and the *cdc53-1 sac7Δ* strains showed constitutive Slt2 phosphorylation, the *cdc53-1 knr4Δ* strain did not (Figure 3.6B). These results suggest that the Cdc34/SCF complex may function to regulate the induction of the cell integrity MAPK pathway upstream of, or at the level of Slt2.

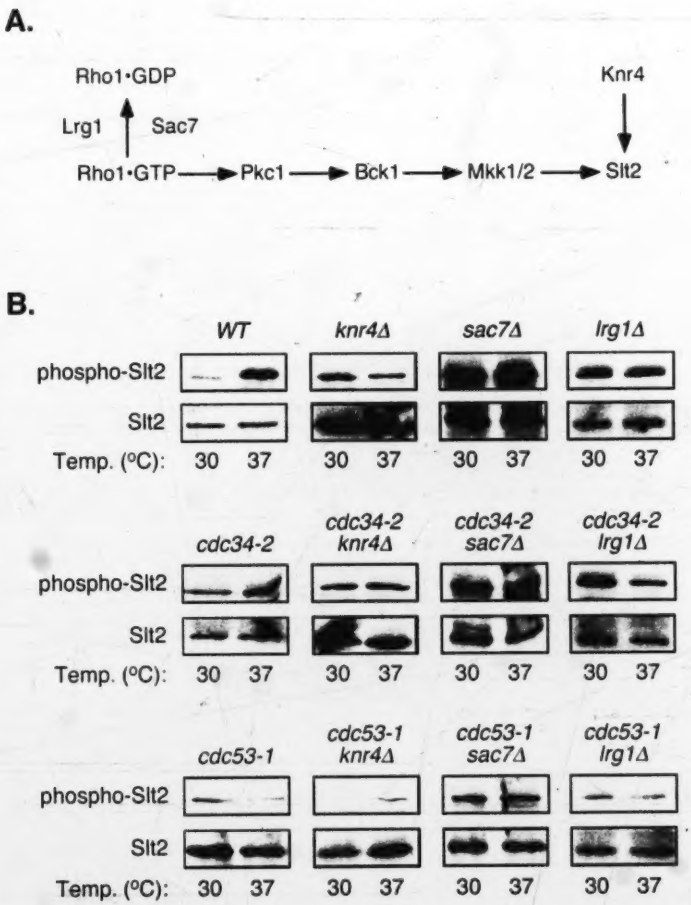

Figure 3.6 Effect of *LRG1*, *SAC7* and *KNR4* deletions on phospho-Slt2 levels.

(A) The proposed model of cell integrity signal transduction. Several signals promote the binding of Rho1 to GTP, thereby activating it, and allowing it to perform one of its many functions. For cell integrity signaling it is thought that Rho1 activates Pkc1, which subsequently begins a MAPK signal transduction cascade consisting of the MAPKKK Bck1, the redundant MAPKKs Mkk1 and Mkk2, and the MAPK Slt2. **(B)** Slt2 phosphorylation in *lrg1Δ*, *sac7Δ*, and *knr4Δ* mutants. Wild-type (top), *cdc34-2* (middle) and *cdc53-1* cells (bottom) with or without *KNR4* deleted, *SAC7* deleted, or *LRG1* deleted were grown in YPD medium to mid-log phase at 30°C, and were then shifted to 37°C for 120 minutes. Samples from each temperature were analyzed for phosphorylated Slt2 and total Slt2 protein levels by immunoblotting.

3.2.6 Deletion of *KNR4* enhances the cell integrity defects in *cdc34-2* and *cdc53-1* mutants.

Deletion of *KNR4* has previously been shown to affect the activity of Slt2, resulting in several phenotypes associated with cell integrity defects (27). We therefore examined these phenotypes in more detail in the *cdc53-1 knr4Δ* and *cdc34-2 knr4Δ* strains. The *knr4Δ* strain showed mild temperature sensitivity that was suppressed by 1M sorbitol. This strain also showed sensitivity to 0.005% SDS and 2 mM caffeine (Figure 3.7A) indicative of its role in regulating Slt2's function in response to stress. Deletion of *KNR4* significantly increased the SDS and caffeine sensitivity of the *cdc53-1* and *cdc34-2* cells (compare Figure 3.2A and Figure 3.7A). In addition, deletion of *KNR4* virtually eliminated the elongated morphology characteristic of Cdc34/SCF mutants at both the permissive and non-permissive temperatures, resulting in a pronounced accumulation of round unbudded cells (Figure 3.7B). Furthermore, analysis of the DNA content of *cdc34-2 knr4Δ* and *cdc53-1 knr4Δ* strains showed a broad peak at the 1N position, suggesting that these cells arrest with either unreplicated or partially replicated DNA (Figure 3.7B). This latter observation may stem from the proposed misregulation of SBF function as a consequence of deleting *KNR4* (27). These results suggest that the function of the Cdc34/SCF complex and Knr4 in mediating cell integrity act in parallel. Given that Knr4 interacts with Slt2 and Cdc34/SCF plays a role in phospho-Slt2 induction, these functions likely converge at the level of Slt2.

3.2.7 Deletion of *SAC7* enhances the defects in *cdc34-2* and *cdc53-1* mutants.

Unlike *knr4Δ* cells, *sac7Δ* cells showed no temperature sensitivity, no additional sensitivity to caffeine, and partial sensitivity to 0.005% SDS by comparison to *WT* (Figure 3.8A). However, combined with the *cdc34-2* and *cdc53-1* mutations, the deletion of *SAC7* caused a mild synthetic growth defect and a strong synthetic SDS defect, but no additional sensitivity to caffeine (compare Figure 3.2A and Figure 3.8A). As such, the effect of caffeine does not appear to relate to the function of Sac7 in the cell integrity pathway. Deletion of *SAC7* in *cdc53-1* and *cdc34*-cells also leads to an unpolarized growth phenotype at 37°C, resulting in a round unbudded morphology. This morphology is consistent with a novel defect in Cdc34/SCF mutants that is independent of Sic1

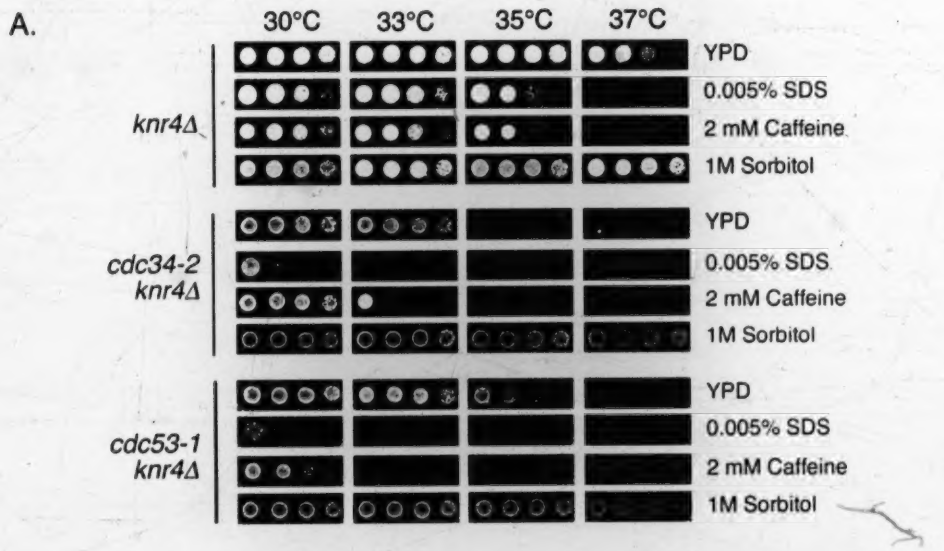

B.

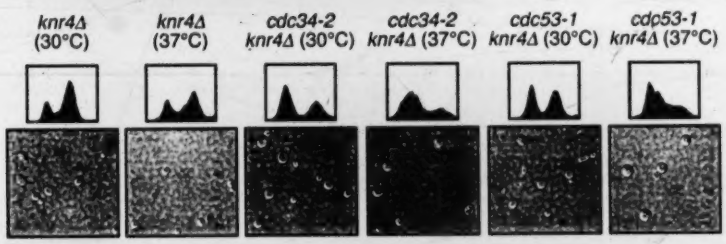

	knr4Δ (30°C)	knr4Δ (37°C)	cdc34-2 knr4Δ (30°C)	cdc34-2 knr4Δ (37°C)	cdc53-1 knr4Δ (30°C)	cdc53-1 knr4Δ (37°C)
Round (unbudded):	47%	60%	64%	77%	44%	49%
Round (budded):	53%	40%	36%	23%	28%	34%
Elongated (unbudded):	0%	0%	0%	0%	8%	5%
Elongated (budded):	0%	0%	0%	0%	15%	12%
Elongated (multi-budded):	0%	0%	0%	0%	0%	0%
Large round:	0%	0%	0%	0%	5%	0%

Figure 3.7 Deletion of *KNR4* enhances the cell integrity defects in Cdc34/SCF mutants.
(A) *knr4Δ* plating experiments. *knr4Δ*, *cdc34-2 knr4Δ* and *cdc53-1 knr4Δ* cells were grown in liquid YPD at 30°C to mid-log phase. Serial dilutions of the cells were prepared and 10^5, 10^4, 10^3 and 10^2 cells were spotted onto plates with YPD, YPD containing 1M sorbitol, YPD containing 0.005% SDS and YPD containing 2mM caffeine media. The cells were then grown at 30°C, 33°C, 35°C and 37°C for 3 days. **(B)** Morphology and DNA content of *knr4Δ* cells. *knr4Δ*, *cdc34-2 knr4Δ*, and *cdc53-1 knr4Δ* cells were grown in YPD at 30°C to mid-log phase and shifted to 37°C for 6 hours. Samples from both temperatures were analyzed by DIC microscopy and flow cytometry. Images displaying the morphologies of the cells as well as the DNA content from each sample are shown. The cells' morphologies were grouped as in Figure 3.3A and the population percentages within each sample are displayed under the images.

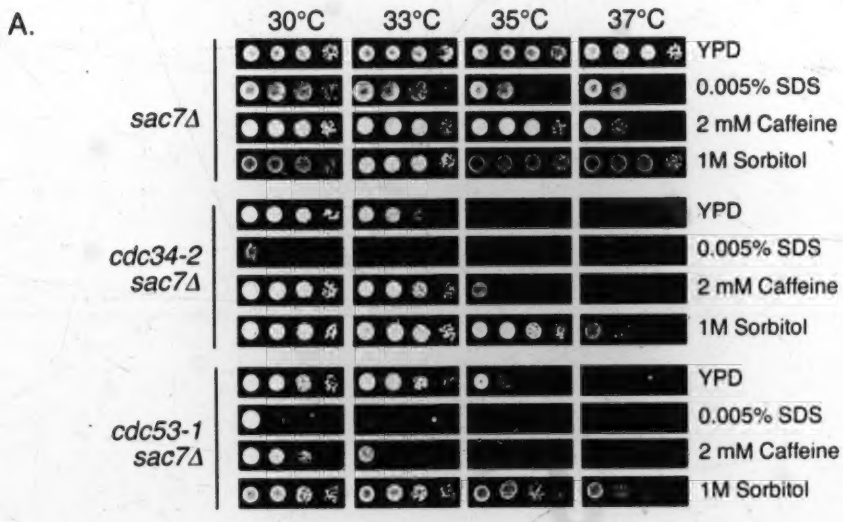

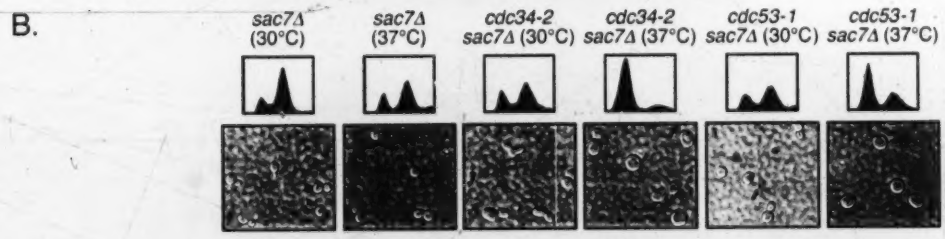

	sac7Δ (30°C)	sac7Δ (37°C)	cdc34-2 sac7Δ (30°C)	cdc34-2 sac7Δ (37°C)	cdc53-1 sac7Δ (30°C)	cdc53-1 sac7Δ (37°C)
Round (unbudded):	35%	46%	16%	46%	45%	57%
Round (budded):	65%	54%	12%	15%	43%	23%
Elongated (unbudded):	0%	0%	30%	9%	1%	1%
Elongated (budded):	0%	0%	39%	4%	8%	2%
Elongated (multi-budded):	0%	0%	3%	26%	0%	17%
Large round:	0%	0%	0%	0%	3%	0%

Figure 3.8 Deletion of *SAC7* enhances the defects in Cdc34/SCF mutants.
(A) *sac7Δ* plating experiments. *sac7Δ*, *cdc34-2 sac7Δ* and *cdc53-1 sac7Δ* cells were grown in liquid YPD at 30°C to mid-log phase. Serial dilutions of the cells were prepared and 10^5, 10^4, 10^3 and 10^2 cells were spotted onto plates with YPD, YPD containing 1M sorbitol, YPD containing 0.005% SDS and YPD containing 2mM caffeine media. The cells were then grown at 30°C, 33°C, 35°C and 37°C for 3 days. **(B)** Morphology and DNA content of *sac7Δ* cells. *sac7Δ*, *cdc34-2 sac7Δ*, and *cdc53-1 sac7Δ* cells were grown in YPD at 30°C to mid-log phase and shifted to 37°C for 6 hours. Samples from both temperatures were analyzed by DIC microscopy and flow cytometry. Images displaying the morphologies of the cells as well as the DNA content from each sample are shown. The cells' morphologies were grouped as in Figure 3.3A and the population percentages within each sample are displayed under the images.

stabilization. These observations suggest that the constitutive phosphorylation of Slt2 observed in the *cdc34-2 sac7Δ* and *cdc53-1 sac7Δ* strains (Figure 3.6B) does not alleviate, but rather may increase *cdc34-2* and *cdc53-1* SDS sensitivity. Alternatively, these results suggest that the defects might be due to direct cell wall defects and that proper regulation of the cell integrity pathway is required for the maintenance of cell integrity and cell growth.

3.2.8 Deletion of *LRG1* suppresses the *cdc34-2* and *cdc53-1* growth and cell integrity defects.

As Lrg1 and Sac7 are both Rho1-GAPs, and deletion of their genes cause constitutive Slt2 phosphorylation, it was possible that the *lrg1Δ* and *sac7Δ* strains would exhibit similar phenotypes. However, overexpression of *LRG1* in the Cdc34/SCF mutant strains caused a synthetic lethal effect (Figure 3.1A) that was not apparent from the overexpression of *SAC7*, suggesting that Lrg1 might have a distinct relationship to the Cdc34/SCF complex. Furthermore, Lrg1 has been shown to play a negative function in relation to the maintenance of cell integrity that is distinct from Sac7 (21, 44). We therefore tested the effects of deleting *LRG1* in *cdc34-2* and *cdc53-1* mutants. The *lrg1Δ* strain showed no obvious defects by comparison to *WT*, while deletion of *LRG*1 in both the *cdc34-2* and *cdc53-1* backgrounds suppressed the temperature sensitivity, as well as the SDS and caffeine sensitivity of these strains (Figure 3.9A). At 37°C the *cdc34-2 lrg1Δ* and cells exhibited an elongated cell morphology and an accumulation of 1N DNA content (Figure 3.9B). Despite this, the ability of the *cdc34-2 lrg1Δ* cells to grow at 37°C indicates that deletion of *LRG1* suppresses defects associated with these cells, allowing them to progress through the cell cycle. Furthermore, the elongated morphology and DNA content of these cells indicates that while the cell integrity defects may be alleviated by the deletion of *LRG1*, this does not fully suppress defects associated with the stabilization of Sic1 in these cells. Similar observations were made for the *cdc53-1 lrg1Δ* strain, except that deletion of *LRG1* had a stronger suppressive effect on *cdc53-1* by comparison to *cdc34-2*. Analysis of the DNA content of *cdc53-1 lrg1Δ* cells also shows a mixed population of 1N and 2N DNA contents.

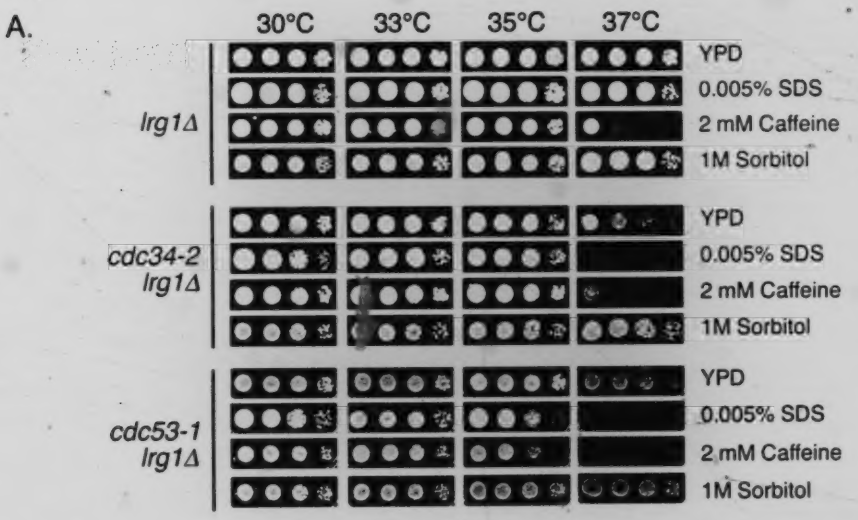

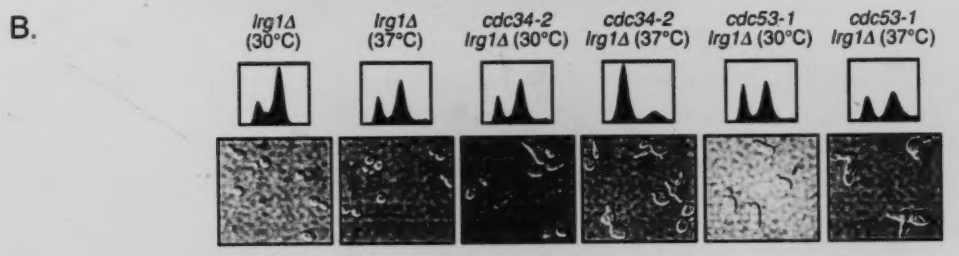

Round (unbudded):	31%	28%	13%	7%	6%	3%
Round (budded):	69%	72%	26%	14%	6%	3%
Elongated (unbudded):	0%	0%	18%	2%	33%	21%
Elongated (budded):	0%	0%	43%	1%	54%	12%
Elongated (multi-budded):	0%	0%	1%	76%	1%	61%
Large round:	0%	0%	0%	0%	0%	0%

Figure 3.9 Deletion of *LRG1* suppresses the growth defects associated with Cdc34/SCF mutants.
(A) *lrg1Δ* plating experiments. *lrg1Δ*, *cdc34-2 lrg1Δ* and *cdc53-1 lrg1Δ* cells were grown in liquid YPD at 30°C to mid-log phase. Serial dilutions of the cells were prepared and 10^5, 10^4, 10^3 and 10^2 cells were spotted onto plates with YPD, YPD containing 1M sorbitol, YPD containing 0.005% SDS and YPD containing 2mM caffeine media. The cells were then grown at 30°C, 33°C, 35°C and 37°C for 3 days. **(B)** Morphology and DNA content of *lrg1Δ* cells. *lrg1Δ*, *cdc34-2 lrg1Δ*, and *cdc53-1 lrg1Δ* cells were grown in YPD at 30°C to mid-log phase and shifted to 37°C for 6 hours. Samples from both temperatures were analyzed by DIC microscopy and flow cytometry. Images displaying the morphologies of the cells as well as the DNA content from each sample are shown. The cells' morphologies were grouped as in Figure 3.3A and the population percentages within each sample are displayed under the images.

The suppressive effect of deleting *LRG1* does not appear to result from the constitutive Slt2 phosphorylation, which was also seen with the *sac7Δ* strains, but instead display strong defects in combination with *cdc34-2* and *cdc53-1* (Figure 3.8A). This suggests that deletion of *LRG1* is not suppressing the defects in these cells by overcoming the Slt2 phosphorylation defects, but rather may be suppressing other defects. Since Lrg1 has been characterized as having a negative function on mediating 1,3-β-glucan synthesis, it is possible that deletion of *LRG1* directly alleviates defects that may be associated with the *cdc34-2* and *cdc53-1* mutations by promoting cell wall biosynthesis, similar to that seen with other cell integrity mutants (21, 44).

3.3 Discussion

We have identified a novel function for the Cdc34/SCF ubiquitination complex in the yeast cell integrity pathway. This conclusion is based on a number of observations including: 1) *cdc34-2* and *cdc53-1* strains exhibit cell integrity phenotypes, 2) *cdc34-2* and *cdc53-1* strains display defects in the induction of Slt2 phosphorylation, 3) *cdc34-2 slt2Δ* and *cdc53-1 slt2Δ* strains show a severe synthetic lysis defect, and 4) the identification of genetic interactions between the Cdc34/SCF complex and regulators of the cell integrity pathway. Together, this study indicates that the Cdc34/SCF complex regulates cell integrity through the mediation of Slt2 phosphorylation and likely cell wall synthesis. Both of these Cdc34/SCF cell integrity functions appear to be necessary to ensure proper cell wall integrity/synthesis during cell growth and in response to stress (Figure 3.10A).

A role for the Cdc34/SCF complex in the regulation of the cell integrity pathway is inferred from the observation that the induction of Slt2 phosphorylation is defective in both the *cdc34-2* and *cdc53-1* strains in response to elevated temperature and caffeine (Figure 3.4). Synthetic cell integrity defects observed for the *cdc34-2 knr4Δ* and *cdc53-1 knr4Δ* strains also indicate that the role of the Cdc34/SCF complex converges with that of Knr4 (27) (Figure 3.7). Knr4 plays a role in the induction of Slt2 phosphorylation, given that the *knr4Δ* strain shows constitutive Slt2 phosphorylation (27). This function of Knr4

is dependent upon the Cdc34/SCF complex, given that a *cdc53-1 knr4Δ* strain does not exhibit any constitutive Slt2 phosphorylation (Figure 3.6).

A synthetic relationship between Sac7 and the Cdc34/SCF complex in the regulation of cell integrity is inferred from the observation that *sac7Δ* cells show only slight SDS sensitivity, while *cdc34-2 sac7Δ* and *cdc53-1 sac7Δ* cells show a severe synthetic defect under identical conditions (Figure 3.8A). Previous studies have suggested that constitutive Slt2 phosphorylation causes defects in growth and stress response (22, 45, 46, 48). Therefore, it is likely that the SDS sensitivity in *SAC7* deletion strains at least partially stems from the constitutive phosphorylation of Slt2 (Figure 3.6), which may either desensitize or over-stimulate the pathway. This is supported by the fact that hyperactive alleles of Rho1 and Mkk1 are very toxic to *cdc53-1* and *cdc34-2* mutants. However, since the phosphorylation of Slt2 does not match the degree of the defects associated with *SAC7* deletion in the *cdc34-2* and *cdc53-1* strains, it is likely that additional defects in Cdc34/SCF mutants are exacerbated when cell integrity signaling is misregulated. Curiously, the *sac7Δ* strains did not show additional caffeine sensitivity (Figure 3.8A), suggesting that SDS sensitivity may stem from the loss of some other Sac7 function not directly related to Slt2 phosphorylation. Alternatively, it is possible that the response of the cell integrity MAPK pathway to caffeine is not affected by constitutive Slt2 phosphorylation by the deletion of *SAC7*.

Interestingly, a novel relationship with the cell cycle is evident for the function of the Cdc34/SCF complex in the regulation of cell integrity. This is suggested by an accumulated round cell morphology in Cdc34/SCF mutants, which is distinct from the elongated multibudded morphology associated with the stabilization of Sic1. A correlation between this phenotype and the cell integrity defects is evident from the examination of c*dc53-1* and *cdc34-2* mutants (compare Figures 3.2A and 3.3A). Further support for this relationship is apparent from an increase in both the cell integrity defects and the round cell morphology in *cdc34-2* and *cdc53-1* strains having either *SAC7* or *KNR4* deleted (Figures 3.7 and 3.8). A similar synthetic effect has also been reported for a *cdc34-2 wsc1Δ* strain (15). These observations indicate that perturbing the cell integrity function of the Cdc34/SCF complex leads to a novel cell cycle defect, distinct from that of Sic1 turnover.

The Cdc34/SCF complex appears to regulate cell wall synthesis in a manner that may be distinct from its role in Slt2 phosphorylation (Figure 3.10A). Deletion of *SLT2* in the *cdc34-2* and *cdc53-1* backgrounds causes a severe lysis defect that is suppressed in the presence 1M sorbitol (Figure 3.5). These observations suggest that Slt2 and Cdc34/SCF function in parallel to ensure proper cell wall synthesis under normal growth conditions. We also propose that the regulation of Slt2 phosphorylation and cell wall synthesis functions of the Cdc34/SCF complex are required to ensure cell wall integrity during conditions of cellular stress, and possibly during vegetative growth.

The interplay between these cell integrity functions provides a theoretical basis for the different degree to which the *cdc34-2* and *cdc53-1* strains exhibit cell integrity phenotypes. Both strains exhibit cell wall defects as revealed by the enhanced lysis defects that are caused by *SLT2* deletion, and the ability to osmotically suppress these defects. However, these strains differ in the degree to which Slt2 phosphorylation is induced in response to stress. The mild *cdc34-2* induction defect still allows for sufficient Slt2 phosphorylation that compensates for the *cdc34-2* cell wall synthesis defect. As such, the *cdc34-2* strain only shows cell integrity defects under harsher conditions, such as a higher SDS concentration (Figure 1B). In the case of *cdc53-1*, its cell wall defects would not be compensated for in a similar fashion given the inability of this strain to induce Slt2 phosphorylation. These differences may also provide a basis for the distinct cell cycle phenotypes observed for the *cdc53-1* strain at both its permissive and non-permissive temperatures (Figure 2), although confirmation of this requires further experimentation.

The effect that Lrg1 has on both *cdc34-2* and *cdc53-1* may also be understood in relation to these Cdc34/SCF cell integrity functions. In addition to its role in cell integrity signaling (Figure 3.6) (21), Lrg1 negatively regulates 1,3-β-glucan synthase activity by stimulating Rho1's GTPase activity (44). Overexpression of Lrg1 may therefore function to downregulate both Slt2 phosphorylation and 1,3-β-glucan synthase activity, thus, leading to lethality in the *cdc34-2* and *cdc53-1* strains (Figure 3.1). In contrast, deletion of *LRG1* increases 1,3-β-glucan synthase activity that may function to suppress the lysis defect associated with the *cdc34-2* and *cdc53-1* mutations. Deletion of *LRG1* also causes constitutive Slt2 phosphorylation, which may account for the minor cell integrity

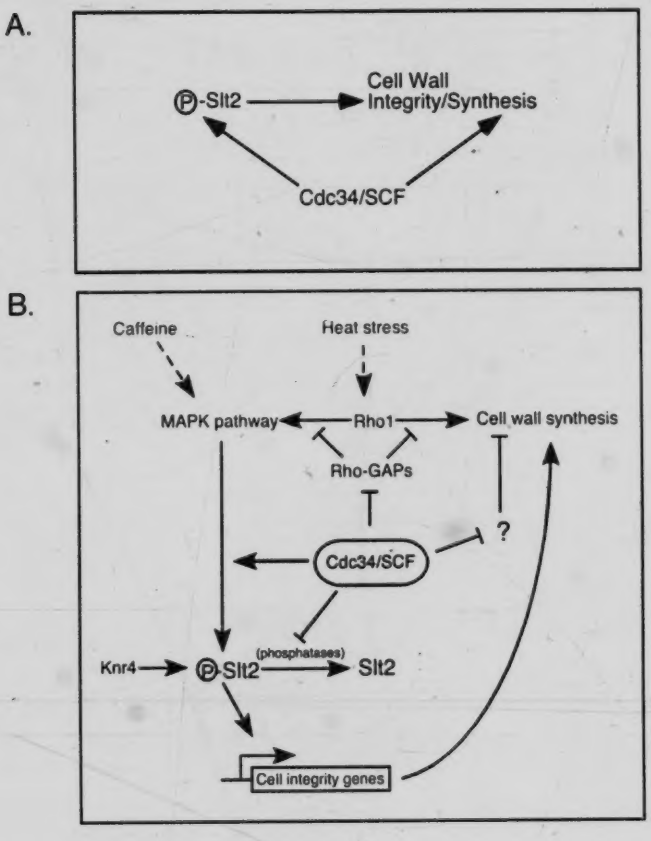

Figure 3.10 Proposed functions of the Cdc34/SCF complex in the regulation of cell integrity.
(A) The Cdc34/SCF complex mediates both the phosphorylation of Slt2 and cell wall integrity/synthesis by targeting an unknown substrate for ubiquitination. **(B)** The Cdc34/SCF complex may function at many different levels to mediate cell integrity related functions. Attractive targets for Cdc34/SCF ubiquitination are the Rho1-GAPs, which function to mediate both Slt2 phosphorylation and cell wall synthesis. However, several other possible targets also exist.

phenotypes still apparent in the *cdc34-2 lrg1Δ* and *cdc53-1 lrg1Δ* strains (Figure 3.9A). Thus, deletion of *LRG1* partially suppresses the cell integrity *cdc34-2* and *cdc53-1* defects, allowing the cells to progress through the cell cycle even at 37°C, but does not appear to completely alleviate the Sic1 turnover defect, given that the *cdc34-2 lrg1Δ* and *cdc53-1 lrg1Δ* strains still show an elongated multibudded morphology (Figure 3.9B).

Since the Cdc34/SCF complex functions to ubiquitinate target proteins, its cell integrity role most likely reflect this activity. While we have not at this time identified such targets, likely candidates include negatively regulators of Slt2 phosphorylation and of cell wall synthesis (Figure 3.10B). An appealing possibility is the direct regulation of the Rho-GAPs, such as Lrg1, by ubiquitination. Regulation of these effectors has the potential to mediate both Slt2 phosphorylation and cell wall synthesis, and can account for all the observed cell integrity defects in Cdc34/SCF mutants. Another possibility is that Cdc34/SCF mediated ubiquitination may function to stimulate cell integrity signaling, rather than to inhibit a negative regulator, similar to that observed with other ubiquitination complexes (4). The identification of these cell integrity targets will ultimately provide a basis for the cell integrity function of the Cdc34/SCF complex in the regulation of Slt2 phosphorylation and cell wall synthesis.

3.4 Materials and methods

3.4.1 Yeast Strains.

All yeast strains used were isogenic to K699 (the strains are listed in Table 3.1). The *BAR1* gene was knocked out using the pJGsst1 plasmid (provided to us by David Stuart, University of Alberta), which contains an *URA3*-marked *BAR1/SST1* deletion. The *URA3* gene on this plasmid is flanked by redundant *Escherichia coli HisG* sequences allowing for the loss of the *URA3* gene by recombination as previously described (7, 33).

Strains expressing *SIC1* with a single carboxyl-terminal HA epitope (*SIC1-HA*), were constructed in two steps. First, the pSic1::URA3 plasmid, which replaces the entire *SIC1* ORF with the *URA3* gene, was used to knockout *SIC1* in each strain. Second, the YIplac128-SIC1-HA plasmid that contains the *SIC1-HA* coding region under control of

Table 3.1 Yeast strains used in Chapter 3

Yeast Srains	Genotype	Source/Reference
W303	MATa *ade2-101 his3-11,15 leu2-3,112 trp1-1 ura3-1 can1-100*	M. Tyers
MTY740	W303 MATa *cdc53-1*	M. Tyers
MTY670	W303 MATa *cdc34-2*	M. Tyers
BVY011	W303 MATa *bar1Δ*	This Study
BVY012	W303 MATa *cdc34-2 bar1Δ*	This Study
BVY013	W303 MATa *cdc53-1 bar1Δ*	This Study
BVY029	W303 MATa *bar1Δ sic1::URA3 LEU2::SIC1-HA*	This Study
BVY030	W303 MATa *cdc34-2 bar1Δ sic1::URA3 LEU2::SIC1-HA*	This Study
BVY031	W303 MATa *cdc53-1 bar1Δ sic1::URA3 LEU2::SIC1-HA*	This Study
BVY036	W303 MATa *bar1Δ lrg1::kan^r*	This Study
BVY037	W303 MATa *cdc34-2 bar1Δ lrg1::kan^r*	This Study
BVY038	W303 MATa *cdc53-1 bar1Δ lrg1::kan^r*	This Study
BVY039	W303 MATa *bar1Δ slt2::kan^r*	This Study
BVY040	W303 MATa *cdc34-2 bar1Δ slt2::kan^r*	This Study
BVY041	W303 MATa *cdc53-1 bar1Δ slt2::kan^r*	This Study
BVY045	W303 MATa *bar1Δ knr4::kan^r*	This Study
BVY046	W303 MATa *cdc34-2 bar1Δ knr4::kan^r*	This Study
BVY047	W303 MATa *cdc53-1 bar1Δ knr4::kan^r*	This Study
BVY086	W303 MATa *sic1::kan^r*	This Study
BVY087	W303 MATa *cdc34-2 sic1::kan^r*	This Study
BVY088	W303 MATa *cdc53-1 sic1::kan^r*	This Study
BVY121	W303 MATa *sac7::kan^r*	This Study
BVY122	W303 MATa *cdc34-2 sac7::kan^r*	This Study
BVY123	W303 MATa *cdc53-1 sac7::kan^r*	This Study

the *SIC1* promoter and terminator was used to integrate this gene into the *leu2* locus of each *sic1Δ::URA3* strain.

Strains harboring *sic1Δ::kan*^{r}, *slt2Δ::kan*^{r}, *knr4Δ::kan*^{r}, *sac7Δ::kan*^{r}, or *lrg1Δ::kan*^{r} deletions were generated by homologous recombination using PCR products. Each PCR product was synthesized from genomic DNA derived from the appropriate *kan*^{r} deletion strain (Open Biosystems) and included the *kan*^{r} gene flanked by ~100-500 bp of DNA sequence from the upstream and downstream flanking regions of the target gene. Each strain was subsequently transformed with the appropriate PCR product and plated onto YPD medium containing 200 μg/ml G418 to select for integrants. For *slt2Δ::kan*^{r} strains selection was carried out on medium containing both G418 and 1M sorbitol. The resulting knockout strains were then confirmed by PCR and functional analysis.

3.4.2 Growth media.

Yeast strains were cultured in rich liquid medium (1% yeast extract, 2% bacto-peptone) containing 2% dextrose (YPD). Exceptions included the *slt2Δ* strains, which were grown in YPD medium supplemented with 1M sorbitol and strains transformed with either the YCP111.GAL (YCP) or YCp111.GAL-Lrg1 (YCP.Lrg1) plasmids (Figure 3.1), which were cultured in liquid SD medium (0.67% yeast nitrogen base lacing amino acids, the appropriate amino acids) containing either 2% dextrose (SD-D), 2% galactose (SD-G) or 2% raffinose (SD-R). Solid YPD, SD-D and SD-G media were prepared as above except that 2% bacto-agar was added to each. For the cell integrity plating experiments, YPD solid medium was supplemented with 2mM caffeine, 1M sorbitol, 0.5M NaCl or sodium dodecyl sulphate (SDS) to a final concentration of either 0.005% or 0.0075%.

3.4.3 Plating experiments.

For all plating experiments a single colony for each strain examined was used to inoculate YPD liquid medium. The *slt2Δ* strains (Figure 3.4) were initially grown in YPD medium supplemented with 1M sorbitol. Each culture was incubated at 30°C and grown

to mid log phase (OD_{600} of ~ 0.5-1.0) prior to plating. A dilution series of each culture was subsequently prepared, and 10^5, 10^4, 10^3 and 10^2 cells were spotted onto four separate plates of the appropriate solid culture medium. The plates were then incubated at 30°C, 33°C, 35°C and 37°C for 3 days prior to documentation. All plating experiments were carried out in duplicate using two separate colonies and were confirmed by at least one repetition of the experiment.

For *LRG1* overexpression (Figure 3.1) the *WT*, *cdc34-2* and *cdc53-1* strains were transformed with either an empty control plasmid (YCP111.GAL/YCP) or with the same plasmid carrying the *LRG1* coding region under control of the *GAL1* promoter (YCP111.GAL-Lrg1/YCP.Lrg1). Plating experiments using each transformed strain followed the same procedure as described above except that single colonies were initially used to inoculate SD-R liquid medium. A dilution series of each culture was subsequently prepared and the appropriate volume of each spotted onto SD-D or SD-G solid medium lacking leucine (for plasmid selection). Plates were then incubated at 30°C for 3 days prior to documentation.

YCp111.GAL was constructed using a fragment of the pESC(Trp) plasmid (Invitrogen) that contains a multiple cloning sequence, a transcriptional terminator and the *GAL1* and *GAL10* promoters. This fragment was generated by PCR using oligonucleotides that introduced a 5' PstI and a 3' MfeI restriction site. These sites were used to ligate this fragment into the PstI and EcoRI restriction sites of the YCplac111 plasmid (*CEN/ARS, LEU2* plasmid). The *LRG1* coding region was PCR amplified from genomic DNA and inserted into the EcoR1 and SstI sites of YCp111.GAL multiple cloning sequence to generated YCp111.GAL-Lrg1.

3.4.4 Sic1 Turnover Experiments.

A single colony of BVY029, BVY030 or BVY031 (see Table 3.1) was used to inoculate 50 ml of YPD liquid medium. Cultures were incubated at 30°C and grown to an OD_{600} of ~0.5. Cells were then collected by centrifugation and resuspended in YPD medium containing 100 nM α-factor and incubated at 30°C until >80% of the cells displayed mating factor polarizations. To release from α-factor arrest, the cells were collected by centrifugation, then resuspended in YPD. This wash was repeated twice to

ensure complete removal of α-factor. After the final wash cells were resuspended in YPD to a final OD_{600} of ~1.0 then incubated at 30°C for an additional 2 hr. Aliquots were taken from each culture after the final resuspension and every ten minutes thereafter to determine the OD_{600}, Sic1-HA protein levels and cell cycle state (see flow cytometry below) of each culture at each time-point.

The level of Sic1-HA present at each time-point was determined by western blotting analysis. To this end a 1.5 ml aliquot was taken at each time-point, the cells collected by centrifugation and the cell pellet immediately frozen in liquid nitrogen. Cells were subsequently lysed by resuspending the pellet in 2x SDS load buffer [500 mM Tris-HCl pH 6.8, 20% glycerol, 10% SDS, 0.1% bromophenol blue, 100 mM DTT] followed by boiling for 5 minutes. The volume of 2x SDS load buffer used for each aliquot was normalized based on the OD_{600} of each culture at each time point. Cells lysates were then clarified by centrifugation and subsequently loaded onto and ran over a 12% SDS-polyacrylamide gel followed by transfer to a polyvinylidene fluoride (PVDF) membrane. To visualize Sic1-HA each membrane was initially blocked overnight at 4°C using TBS-T buffer [50mM Tris-HCl pH 7, 150 mM NaCl, 0.1% Tween-20] with 2% w/v skim milk powder. The membrane was then probed at room temperature for 2-hours using a monoclonal, horseradish peroxidase (HRP) conjugated anti-HA antibody (3F10; Roche) diluted 1:1000 in TBS-T. Three 10-minute washes in TBS-T were then performed on the membrane, and Sic-HA was then visualized using ECL (Amersham Biosciences). As a loading control, the membranes were stripped and re-probed for Cdc28 using the monoclonal anti-PSTAIR (Sigma) at a 1:4000 dilution and the secondary HRP conjugated anti-mouse IgG antibody (Promega) at a 1:2500 dilution.

3.4.5 Slt2 phosphorylation assays.

Cultures of BVY011, BVY012 or BVY013 were grown in YPD liquid medium at 30°C to an OD_{600} of ~0.5 after which they were either shifted to 37°C, or the cells collected by centrifugation and resuspended in YPD liquid medium supplemented with 2 mM caffeine and reincubated at 30°C. Aliquots of each culture were taken prior to (0 minute), 30, 60, and 120 minutes after the temperature or medium shift for analysis.

Cell lysis and subsequent western blot analysis for Slt2 or phosphorylated Slt2 followed the same basic procedure as that outlined for Sic1-HA with the following exceptions. Cell lysates were loaded onto a 10% polyacrylamide gel. To detect dually phosphorylated Slt2, the membranes were probed with an anti-phospho-p44/42 MAPK (Thr^{202}/Tyr^{204}) primary antibody (Cell Signaling Technology, New England Biolabs) diluted 1:1000 in TBS-T with 2% w/v skim milk powder overnight at 4°C. Membranes were then washed and probed with a HRP conjugated anti-rabbit (Cell Signaling Technology, New England Biolabs) secondary antibody at 1:1000 dilution in TBS-T for 2 hours at room temperature. Total Slt2 was detected by stripping and reprobing the membranes with an anti-Mpk1 primary antibody (Santa Cruz Biotechnology) at 1:100 dilution in TBS-T/M followed by a HRP conjugated anti-mouse antibody (Santa Cruz Biotechnology) at a dilution of 1:1000 in TBS-T using the same conditions as described for detection of phosphorylated Slt2.

3.4.6 Microscopy.

To examine cellular morphologies, cells from an exponentially growing culture were initially fixed by the addition of formaldehyde to a final concentration of 4% v/v and subsequent incubation at temperature for 10 min. Cells were then collected by centrifugation, and resuspended in phosphate buffered saline (PBS) containing 4% formaldehyde, and incubated at room temperature for 1 hour. The samples were subsequently washed two times with PBS, and briefly sonicated at the lowest setting to disperse cell clumps and spotted onto a microscope slide for analysis. Cells were visualized by DIC microscopy using a Zeiss Axioskop 2 microscope, and documented using a Spot digital camera and Spot software 3.0.4 (Diagnostic Instruments). Percentages for each morphological category considered were determined from visual inspection of at least 200 cells from each culture.

3.4.7 Flow Cytometry.

To assess the DNA content of cells, an aliquot of each culture was taken, and the cells collected by centrifugation. Cells were then fixed by resuspending them in 70% ethanol followed by overnight incubation at 4°C. Fixed cells were subsequently stained

with propidium iodide and analyzed by flow cytometry using a FACScan instrument (Becton Dickinson), as described previously (8).

3.5 References

1. Blondel, M., J. M. Galan, Y. Chi, C. Lafourcade, C. Longaretti, R. J. Deshaies, and M. Peter. 2000. Nuclear-specific degradation of Far1 is controlled by the localization of the F-box protein Cdc4. Embo J 19:6085-97.
2. Cardozo, T., and M. Pagano. 2004. The SCF ubiquitin ligase: insights into a molecular machine. Nat Rev Mol Cell Biol 5:739-51.
3. de Nobel, H., C. Ruiz, H. Martin, W. Morris, S. Brul, M. Molina, and F. M. Klis. 2000. Cell wall perturbation in yeast results in dual phosphorylation of the Slt2/Mpk1 MAP kinase and in an Slt2-mediated increase in FKS2-lacZ expression, glucanase resistance and thermotolerance. Microbiology 146 (Pt 9):2121-32.
4. Deng, L., C. Wang, E. Spencer, L. Yang, A. Braun, J. You, C. Slaughter, C. Pickart, and Z. J. Chen. 2000. Activation of the IkappaB kinase complex by TRAF6 requires a dimeric ubiquitin-conjugating enzyme complex and a unique polyubiquitin chain. Cell 103:351-61.
5. Deshaies, R. J. 1999. SCF and Cullin/Ring H2-based ubiquitin ligases. Annu Rev Cell Dev Biol 15:435-67.
6. Drury, L. S., G. Perkins, and J. F. Diffley. 1997. The Cdc4/34/53 pathway targets Cdc6p for proteolysis in budding yeast. Embo J 16:5966-76.
7. Elion, E. A., B. Satterberg, and J. E. Kranz. 1993. FUS3 phosphorylates multiple components of the mating signal transduction cascade: evidence for STE12 and FAR1. Mol Biol Cell 4:495-510.
8. Epstein, C. B., and F. R. Cross. 1992. CLB5: a novel B cyclin from budding yeast with a role in S phase. Genes Dev 6:1695-706.
9. Feldman, R. M., C. C. Correll, K. B. Kaplan, and R. J. Deshaies. 1997. A complex of Cdc4p, Skp1p, and Cdc53p/cullin catalyzes ubiquitination of the phosphorylated CDK inhibitor Sic1p. Cell 91:221-30.
10. Gustin, M. C., J. Albertyn, M. Alexander, and K. Davenport. 1998. MAP kinase pathways in the yeast Saccharomyces cerevisiae. Microbiol Mol Biol Rev 62:1264-300.
11. Harrison, J. C., E. S. Bardes, Y. Ohya, and D. J. Lew. 2001. A role for the Pkc1p/Mpk1p kinase cascade in the morphogenesis checkpoint. Nat Cell Biol 3:417-20.
12. Heinisch, J. J., A. Lorberg, H. P. Schmitz, and J. J. Jacoby. 1999. The protein kinase C-mediated MAP kinase pathway involved in the maintenance of cellular integrity in Saccharomyces cerevisiae. Mol Microbiol 32:671-80.
13. Henchoz, S., Y. Chi, B. Catarin, I. Herskowitz, R. J. Deshaies, and M. Peter. 1997. Phosphorylation- and ubiquitin-dependent degradation of the cyclin-dependent kinase inhibitor Far1p in budding yeast. Genes Dev 11:3046-60.
14. Igual, J. C., A. L. Johnson, and L. H. Johnston. 1996. Coordinated regulation of gene expression by the cell cycle transcription factor Swi4 and the protein kinase C MAP kinase pathway for yeast cell integrity. Embo J 15:5001-13.
15. Ivanovska, I., and M. D. Rose. 2000. SLG1 plays a role during G1 in the decision to enter or exit the cell cycle. Mol Gen Genet 262:1147-56.

16. Jung, U. S., A. K. Sobering, M. J. Romeo, and D. E. Levin. 2002. Regulation of the yeast Rlm1 transcription factor by the Mpk1 cell wall integrity MAP kinase. Mol Microbiol 46:781-9.
17. Kamada, Y., H. Qadota, C. P. Python, Y. Anraku, Y. Ohya, and D. E. Levin. 1996. Activation of yeast protein kinase C by Rho1 GTPase. J Biol Chem 271:9193-6.
18. Kishi, T., and F. Yamao. 1998. An essential function of Grr1 for the degradation of Cln2 is to act as a binding core that links Cln2 to Skp1. J Cell Sci 111 (Pt 24):3655-61.
19. Levin, D. E., and E. Bartlett-Heubusch. 1992. Mutants in the S. cerevisiae PKC1 gene display a cell cycle-specific osmotic stability defect. J Cell Biol 116:1221-9.
20. Levin, D. E., B. Bowers, C. Y. Chen, Y. Kamada, and M. Watanabe. 1994. Dissecting the protein kinase C/MAP kinase signalling pathway of Saccharomyces cerevisiae. Cell Mol Biol Res 40:229-39.
21. Lorberg, A., H. P. Schmitz, J. J. Jacoby, and J. J. Heinisch. 2001. Lrg1p functions as a putative GTPase-activating protein in the Pkc1p-mediated cell integrity pathway in Saccharomyces cerevisiae. Mol Genet Genomics 266:514-26.
22. Madaule, P., R. Axel, and A. M. Myers. 1987. Characterization of two members of the rho gene family from the yeast Saccharomyces cerevisiae. Proc Natl Acad Sci U S A 84:779-83.
23. Madden, K., Y. J. Sheu, K. Baetz, B. Andrews, and M. Snyder. 1997. SBF cell cycle regulator as a target of the yeast PKC-MAP kinase pathway. Science 275:1781-4.
24. Marini, N. J., E. Meldrum, B. Buehrer, A. V. Hubberstey, D. E. Stone, A. Traynor-Kaplan, and S. I. Reed. 1996. A pathway in the yeast cell division cycle linking protein kinase C (Pkc1) to activation of Cdc28 at START. Embo J 15:3040-52.
25. Martin, H., M. C. Castellanos, R. Cenamor, M. Sanchez, M. Molina, and C. Nombela. 1996. Molecular and functional characterization of a mutant allele of the mitogen-activated protein-kinase gene SLT2(MPK1) rescued from yeast autolytic mutants. Curr Genet 29:516-22.
26. Martin, H., J. M. Rodriguez-Pachon, C. Ruiz, C. Nombela, and M. Molina. 2000. Regulatory mechanisms for modulation of signaling through the cell integrity Slt2-mediated pathway in Saccharomyces cerevisiae. J Biol Chem 275:1511-9.
27. Martin-Yken, H., A. Dagkessamanskaia, F. Basmaji, A. Lagorce, and J. Francois. 2003. The interaction of Slt2 MAP kinase with Knr4 is necessary for signalling through the cell wall integrity pathway in Saccharomyces cerevisiae. Mol Microbiol 49:23-35.
28. Mathias, N., S. L. Johnson, M. Winey, A. E. Adams, L. Goetsch, J. R. Pringle, B. Byers, and M. G. Goebl. 1996. Cdc53p acts in concert with Cdc4p and Cdc34p to control the G1-to-S-phase transition and identifies a conserved family of proteins. Mol Cell Biol 16:6634-43.
29. Nonaka, H., K. Tanaka, H. Hirano, T. Fujiwara, H. Kohno, M. Umikawa, A. Mino, and Y. Takai. 1995. A downstream target of RHO1 small GTP-binding protein is PKC1, a homolog of protein kinase C, which leads to activation of the MAP kinase cascade in Saccharomyces cerevisiae. Embo J 14:5931-8.

30. Paravicini, G., M. Cooper, L. Friedli, D. J. Smith, J. L. Carpentier, L. S. Klig, and M. A. Payton. 1992. The osmotic integrity of the yeast cell requires a functional PKC1 gene product. Mol Cell Biol 12:4896-905.
31. Perkins, G., L. S. Drury, and J. F. Diffley. 2001. Separate SCF(CDC4) recognition elements target Cdc6 for proteolysis in S phase and mitosis. Embo J 20:4836-45.
32. Philip, B., and D. E. Levin. 2001. Wsc1 and Mid2 are cell surface sensors for cell wall integrity signaling that act through Rom2, a guanine nucleotide exchange factor for Rho1. Mol Cell Biol 21:271-80.
33. Reneke, J. E., K. J. Blumer, W. E. Courchesne, and J. Thorner. 1988. The carboxy-terminal segment of the yeast alpha-factor receptor is a regulatory domain. Cell 55:221-34.
34. Schmidt, A., T. Schmelzle, and M. N. Hall. 2002. The RHO1-GAPs SAC7, BEM2 and BAG7 control distinct RHO1 functions in Saccharomyces cerevisiae. Mol Microbiol 45:1433-41.
35. Schneider, B. L., E. E. Patton, S. Lanker, M. D. Mendenhall, C. Wittenberg, B. Futcher, and M. Tyers. 1998. Yeast G1 cyclins are unstable in G1 phase. Nature 395:86-9.
36. Schwob, E., T. Bohm, M. D. Mendenhall, and K. Nasmyth. 1994. The B-type cyclin kinase inhibitor p40SIC1 controls the G1 to S transition in S. cerevisiae. Cell 79:233-44.
37. Seol, J. H., R. M. Feldman, W. Zachariae, A. Shevchenko, C. C. Correll, S. Lyapina, Y. Chi, M. Galova, J. Claypool, S. Sandmeyer, K. Nasmyth, and R. J. Deshaies. 1999. Cdc53/cullin and the essential Hrt1 RING-H2 subunit of SCF define a ubiquitin ligase module that activates the E2 enzyme Cdc34. Genes Dev 13:1614-26.
38. Skowyra, D., K. L. Craig, M. Tyers, S. J. Elledge, and J. W. Harper. 1997. F-box proteins are receptors that recruit phosphorylated substrates to the SCF ubiquitin-ligase complex. Cell 91:209-19.
39. Skowyra, D., D. M. Koepp, T. Kamura, M. N. Conrad, R. C. Conaway, J. W. Conaway, S. J. Elledge, and J. W. Harper. 1999. Reconstitution of G1 cyclin ubiquitination with complexes containing SCFGrr1 and Rbx1. Science 284:662-5.
40. Varelas, X., D. Stuart, M. Ellison, and C. Ptak. (Submitted).
41. Verma, R., R. S. Annan, M. J. Huddleston, S. A. Carr, G. Reynard, and R. J. Deshaies. 1997. Phosphorylation of Sic1p by G1 Cdk required for its degradation and entry into S phase. Science 278:455-60.
42. Verma, R., R. M. Feldman, and R. J. Deshaies. 1997. SIC1 is ubiquitinated in vitro by a pathway that requires CDC4, CDC34, and cyclin/CDK activities. Mol Biol Cell 8:1427-37.
43. Verna, J., A. Lodder, K. Lee, A. Vagts, and R. Ballester. 1997. A family of genes required for maintenance of cell wall integrity and for the stress response in Saccharomyces cerevisiae. Proc Natl Acad Sci U S A 94:13804-9.
44. Watanabe, D., M. Abe, and Y. Ohya. 2001. Yeast Lrg1p acts as a specialized RhoGAP regulating 1,3-beta-glucan synthesis. Yeast 18:943-51.

45. Watanabe, Y., K. Irie, and K. Matsumoto. 1995. Yeast RLM1 encodes a serum response factor-like protein that may function downstream of the Mpk1 (Slt2) mitogen-activated protein kinase pathway. Mol Cell Biol 15:5740-9.
46. Watanabe, Y., G. Takaesu, M. Hagiwara, K. Irie, and K. Matsumoto. 1997. Characterization of a serum response factor-like protein in Saccharomyces cerevisiae, Rlm1, which has transcriptional activity regulated by the Mpk1 (Slt2) mitogen-activated protein kinase pathway. Mol Cell Biol 17:2615-23.
47. Willems, A. R., S. Lanker, E. E. Patton, K. L. Craig, T. F. Nason, N. Mathias, R. Kobayashi, C. Wittenberg, and M. Tyers. 1996. Cdc53 targets phosphorylated G1 cyclins for degradation by the ubiquitin proteolytic pathway. Cell 86:453-63.
48. Yashar, B., K. Irie, J. A. Printen, B. J. Stevenson, G. F. Sprague, Jr., K. Matsumoto, and B. Errede. 1995. Yeast MEK-dependent signal transduction: response thresholds and parameters affecting fidelity. Mol Cell Biol 15:6545-55.
49. Zarzov, P., C. Mazzoni, and C. Mann. 1996. The SLT2(MPK1) MAP kinase is activated during periods of polarized cell growth in yeast. Embo J 15:83-91.

CHAPTER 4 – Characterization of the relationship between the Cdc34/SCF ubiquitination complex and transcription.

4.1 Introduction

Several signaling networks in eukaryotic cells mediate the highly complex series of events related to cellular growth. In the yeast *Saccharomyces cerevisiae*, a major driving force of the cell cycle is the coordinated regulation of these signals to the expression of distinct sets of genes (39, 60). In this way, yeast cells have developed an intricate method of responding to varying conditions. A significant mode of transcriptional regulation is ubiquitination, which involves the attachment of ubiquitin (Ub) onto protein substrates through an enzymatic cascade consisting of an Ub-activating enzyme, an Ub-conjugating enzyme, and an Ub-ligase. Ub or the assembly of multi-Ub chains onto a protein destines it for a variety of effects, commonly targeting that protein for proteasomal degradation. The relationship between Ub and transcription can be observed at many different levels, such as in the regulation of plasma membrane sensors, the activity of signal transduction effectors, and the function of distinct transcription factors (48).

The Cdc34 Ub-conjugating enzyme together with the SCF (Skp1-Cdc53-Hrt1/Rbx-F.box) Ub-ligase functions as a vital regulator of several transcriptional events. The most direct link between the Cdc34/SCF complex and transcription is its role in mediating the activity of the transcription factors Gcn4 and Met4 (29, 33, 37). Gcn4 is a transcriptional activator that functions to regulate genes responsible for the biosynthesis of amino acids and purines in response to amino acid starvation (7, 49). Under favorable growth conditions, the Cdc34/SCF complex ubiquitinates Gcn4, targeting it for proteasomal degradation (45). In this manner, Gcn4 protein levels are kept low, thereby sustaining minor expression of its target genes. However, under conditions of amino acid starvation Gcn4 protein levels are stabilized largely as a result of decreased ubiquitination (24, 29), thereby adapting gene expression to cellular conditions.

Met4 also serves as a target for Cdc34/SCF mediated ubiquitination. Met4 has been observed to have several cellular roles, including a function in cell cycle regulation

(50). However, the best-defined role for Met4 is in the activation of genes responsible for the synthesis of sulfur containing amino acids (such as methionine and cysteine) under conditions in which methionine levels are low (62). In the presence of sufficient amounts of methionine, the Cdc34/SCF complex assembles a multi-Ub chain onto Met4 (14), which leads to the reduction of its activity in both a proteolytic and non-proteolytic manner (37). This provides a tightly regulated mode of Met4 activation, thus ensuring the controlled expression of its target genes.

Several indirect connections also exist between the Cdc34/SCF complex and transcription. At least two signal transduction cascades, the mating pathway and the cell integrity pathway, are influenced by the activity of the Cdc34/SCF complex. Both these pathways consist of a series of mitogen activated protein kinase (MAPK) phosphorylation events that mediate a specific program of gene expression (20). In the case of the mating pathway, the Cdc34/SCF complex is thought to target the MAPK kinase (MAPKK) Ste7 for ubiquitination in response to prolonged exposure to mating pheromone (66). The assembly of multi-Ub chains onto Ste7 destines it for proteasomal degradation, ultimately leading to an attenuation of the MAPK signaling cascade. In this manner, Ste7 kinase activity and downstream transcriptional regulation are tightly controlled.

The role for the Cdc34/SCF complex in the regulation of the cell integrity pathway is less clear, but it appears to have an influence on cell growth (see Chapter 3). This pathway primarily functions to coordinate the dynamic integrity of the cell wall with cell cycle progression. In response to varying signals, usually originating from plasma-membrane/cell wall localized sensors, this pathway is activated through the initiation of a MAPK cascade, resulting in the phosphorylation and activation of the MAPK Slt2 (41). Activated Slt2 subsequently induces the action of downstream transcription factors thereby promoting gene expression (2, 31). The studies described in Chapter 3 have indicated that defects present within Cdc34/SCF mutants are consistent with the misregulation of this pathway. Notably, these cells display a diminished response to pathway activating conditions, resulting in decreased Slt2 phosphorylation and cell growth defects.

The primary transcription factors targeted by the cell integrity pathway are thought to be Rlm1, and the SBF complex, which is composed of Swi4 and Swi6. Both Rlm1 and SBF mediate the expression of genes involved in cell wall biogenesis (32, 40). Signaling to Rlm1 is dependent entirely on Slt2, which regulates the expression of at least 25 genes (31, 32) (see Table 1.3). These genes respond primarily to environmental stresses that activate the pathway, such as heat shock. Their primary function is to adapt the cell wall to such stressing conditions (31). Alternatively, cell integrity mediated regulation of the SBF transcription factor is directly integrated with progression of the cell cycle (27, 40). The SBF, together with the MBF transcription factor (made up of Mbp1 and Swi6), are also responsible for the large transcriptional burst that occurs at the G1-S phase transition of the cell cycle, which includes the expression of the G1 and S phase cyclins (26, 47). These two factors direct the expression of genes required for the early stages of the cell cycle, such as DNA replication, SPB duplication and bud growth. Misregulation of cell integrity signaling to the SBF transcription factor results in cell cycle defects, including the improper coordination of cell wall synthesis with cell growth (27, 40).

The interrelationships between the Cdc34/SCF complex and cell integrity signaling led me to investigate the affect that Cdc34/SCF mutations have on cell integrity mediated transcription. This analysis revealed an increase in the activity of the Rlm1, SBF and MBF transcription factors. This transcriptional induction was largely dependent on Slt2 signaling, as deletion of *SLT2* eliminated it. The widespread importance of the Cdc34/SCF complex in the regulation of varying transcriptional events, such as the regulation of the Gcn4 and Met4 transcriptional activators, also prompted me to examine its transcriptional related roles on a global nature. I used DNA microarrays to examine the transcriptional variance in Cdc34/SCF mutants, revealing the induced expression of several distinct sets of genes, including genes required for amino acid biosynthesis, sulfur metabolism, cell wall biosynthesis and cellular signaling, among others. This chapter highlights the importance of the Cdc34/SCF complex in transcriptional regulation, and provides us with the first view of the extent of its roles.

4.2 Results

4.2.1 The activities of the SBF, MBF and Rlm1 transcription factors are induced in the *cdc34-2* and *cdc53-1* strains.

I have previously shown (in Chapter 3) that inducible phosphorylation of the cell integrity MAPK Slt2 in response to heat stress is impaired to different degrees in the *cdc53-1* and *cdc34-2* strains. Downstream targets of Slt2 include the transcriptional activators SBF and Rlm1, which regulate the expression of several cell integrity and cell cycle related genes (32, 40). As such, I wanted to determine whether the *cdc53-1* and *cdc34-2* Slt2 phosphorylation defects correlated with the regulation of these transcriptional activators.

To examine this, I utilized plasmids carrying a *LacZ* reporter gene under the control of a minimal *CYC1* promoter, lacking any upstream activating sequences (UASs) (*CYC1::LacZ*), and driven by multiple SBF specific UASs (4x SCB elements – *SCB::LacZ*) (1), or Rlm1 specific UASs (2x [CTA(T/A)$_4$TAG] – *RLM1::LacZ*) (32). I also examined the effect on MBF specific transcription, which plays a somewhat redundant function with SBF during cell cycle progression. To this end, I used a similar reporter plasmid that is driven by multiple MBF specific UASs (4x MCB elements – *MCB::LacZ*) (64). These plasmids were individually transformed into a wild-type (*WT*), a *cdc53-1*, and a *cdc34-2* strain for analysis. The strains were grown at their permissive temperature (30°C) to mid-log phase, and were then shifted to their non-permissive temperature (37°C) for four hours. Samples of each strain were taken at both temperatures, and the β-galactosidase activity was measured *in vitro*. β-galactosidase activity for each culture was then expressed in terms of fold change relative to the activity observed in the *WT* strain at 30°C.

It was expected that any transcriptional effects that might occur within the *cdc53-1* and *cdc34-2* strains would be apparent after the shift to their non-permissive temperature. Furthermore, it was expected that such transcriptional effects would reflect these strains impaired induction of Slt2 phosphorylation. Thus, it was surprising to find that at 30°C β-galactosidase activity in the *cdc53-1* and *cdc34-2* strains was dramatically higher for both the SBF (~4-5 fold) and MBF (~5-fold) reporters by comparison to *WT*

strain (Figure 4.1A). At 37°C SBF and MBF activities were reduced in the *WT* strain, consistent with previous observations that the activity of these transcription factors is reduced in response to heat shock (56). A similar decrease in SBF and MBF activity was observed in the *cdc53-1* and *cd34-2* strains. However, the fold increase of SBF and MBF activities at 37°C *cdc53-1* and *cdc34-2* strains showed a similar fold increase to that observed at 30°C when compared to the *WT* strain. Thus, while basal SBF and MBF activities are higher in the *cdc53-1* and *cdc34-2* strains, these transcriptional activators remain responsive to stimuli, such as heat stress. Furthermore, the similar increase in SBF and MBF activity in *cdc53-1* and *cdc34-2* strains does not correlate with the differences observed in their Slt2 phosphorylation defects (see Figure 3.4), suggesting that this effect is not related to Slt2 signaling.

Unlike SBF and MBF activity, Rlm1 activity in the *WT* strain increased at 37°C when compared to 30°C, consistent with previous observations (32). An increase in Rlm1 activity was observed in both the *cdc53-1* and *cdc34-2* mutant strains when compared to the *WT* strain at 30°C. However, Rlm1 activity at this temperature in the *cdc53-1* mutant was significantly higher than that seen for the *cdc34-2* mutant (~3-fold compared to ~1.5-fold, respectively). The *cdc53-1* and *cdc34-2* stains also showed an increase in Rlm1 activity at 37°C when compared to the *WT* strain. Differences in Rlm1 activity between the mutants are consistent with the stronger cell integrity defects associated with *cdc53-1* cells. However, the high basal levels observed in Rlm1 activity inversely correlates to the defects in Slt2 phosphorylation observed for these strains (see Figure 3.4), suggesting that either the Rlm1 dependent transcriptional effects are not related to Slt2 activity, or that the differences between the *cdc53-1* and *cdc34-2* strains may be as a result of the misregulated direction of Slt2 activity.

To better understand the relationship between Slt2 activity and the effects observed for SBF, MBF and Rlm1 transcription in *cdc53-1* and *cdc34-2* mutants, the reporter assays were carried out with *SLT2* deletion strains 30°C. To prevent lysis of these strains were grown in liquid medium containing 1M sorbitol. The cells were subsequently transferred to liquid medium lacking sorbitol for a short growth period and β-galactosidase assays were then conducted. SBF and Rlm1 basal activities were completely abolished when *SLT2* was deleted, whereas MBF activity was substantially

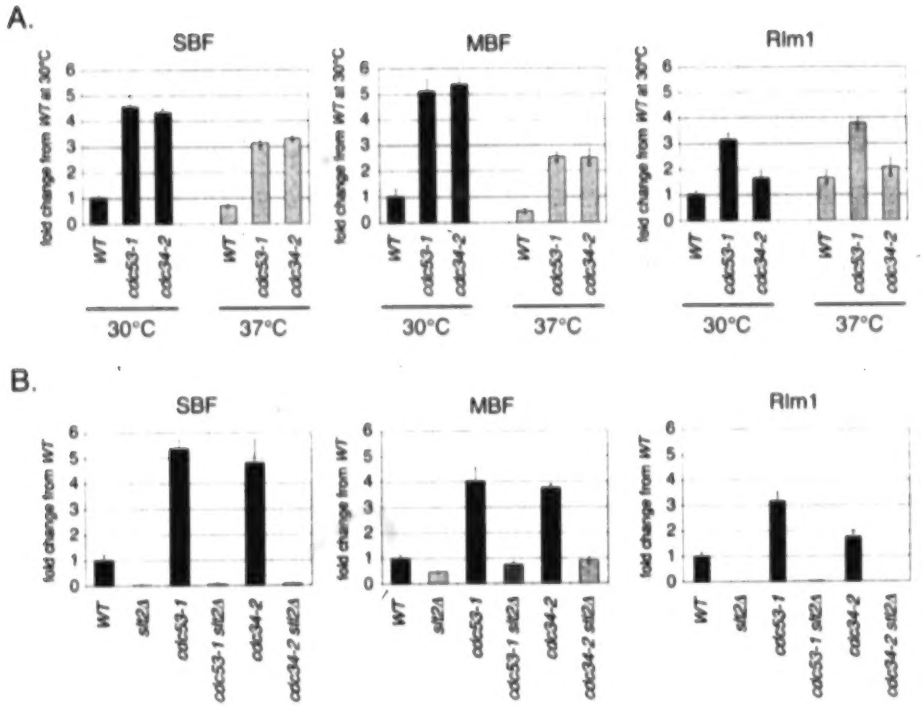

Figure 4.1 The SBF, MBF and Rlm1 transcription factors show increased activity in *cdc53-1* and *cdc34-2* mutants. **(A)** SBF, MBF and Rlm1 reporter assays. Wild-type (*WT*), *cdc53-1* and *cdc34-2* cells were transformed with the *SCB::LacZ* (SBF), *MCB::LacZ* (MBF), or *Rlm1::LacZ* (Rlm1) plasmid. The strains were grown to mid-log phase at 30°C and were then shifted to 37°C for 4 hours. Samples from each temperature were taken, lysates were prepared, and the β-galactosidase activity was measured. The transcriptional activity of each mutant strain is represented as a fold change compared to the WT cells at 30°C. **(B)** *SLT2* is required for SBF, MBF and Rlm1 transcription. *WT*, *cdc53-1* and *cdc34-2* cells with (in dark grey) and without (in light grey) *SLT2* deleted were transformed with the *SCB::LacZ* (SBF), *MCB::LacZ* (MBF) or the *Rlm1::LacZ* plasmid (Rlm1). The strains were grown to mid-log phase at 30°C in medium containing 1M sorbitol, and were then shifted to medium without sorbitol for 4 hours. Samples for each were taken, lysates were prepared, and the β-galactosidase activity was measured.

reduced but was still detectable (Figure 4.1B). Furthermore, the transcriptional differences observed between the *WT*, *cdc53-1* and *cdc34-2* strains disappeared when *SLT2* was deleted, indicating that the transcriptional induction that was observed in *cdc53-1* and *cdc34-2* cells is dependent on signaling through the cell integrity pathway. The reduction in transcriptional activity in the *slt2Δ* strains was not a result of cell lysis, as this effect was observed in the *WT* strain (which does not lyse at this temperature), and was also observed in samples from cells growing in 1M sorbitol. These results confirm the importance of Slt2 dependent signaling in the regulation of Rlm1 and SBF transcription, and suggest that a key role exists for this pathway in the regulation of MBF transcription.

To confirm that the transcriptional misregulation in these strains is indicative of a novel defect associated with Cdc34/SCF ubiquitination I further analyzed SBF dependent transcription in these strains. I chose to investigate SBF transcriptional activity due to its role in both cell wall integrity and cell cycle progression (40). I initially looked to see if the transcriptional activation was specific to the mutations used. For this, I co-transformed a plasmid carrying either *CDC53* or *CDC34* under the control of galactose inducible promoters with the *SCB::LacZ* reporter plasmid into the *cdc53-1* and *cdc34-2* cells, respectively. I also transformed an empty plasmid into *WT*, *cdc53-1* and *cdc34-2* cells as a control, and subsequently measured SBF transcriptional activities of these strains growing at their permissive temperature (30°C) in either glucose or galactose media. In the presence of glucose medium, wherein expression of either *CDC53* or *CDC34* is low, only a minimal reduction in SBF activity was observed (Figure 4.2A, glucose). However, when *CDC53* and *CDC34* expression were respectively induced in the presence of galactose medium, a significant drop in SBF activity to near that of the *WT* control occurred (Figure 4.2A, galactose). This indicated that the transcriptional effects observed are attributable to the respective mutations.

The SBF is composed of a heterodimer consisting of the Swi6 activator, also found in the MBF, and the DNA binding protein Swi4 that specifically recognizes the SCB element. Therefore, to ensure that the observed transcriptional activation of the *SCB::LacZ* reporter plasmid in *cdc53-1* and *cdc34-2* strains was specific to the misregulation of the SBF transcriptional factor I measured the β-galactosidase activity in

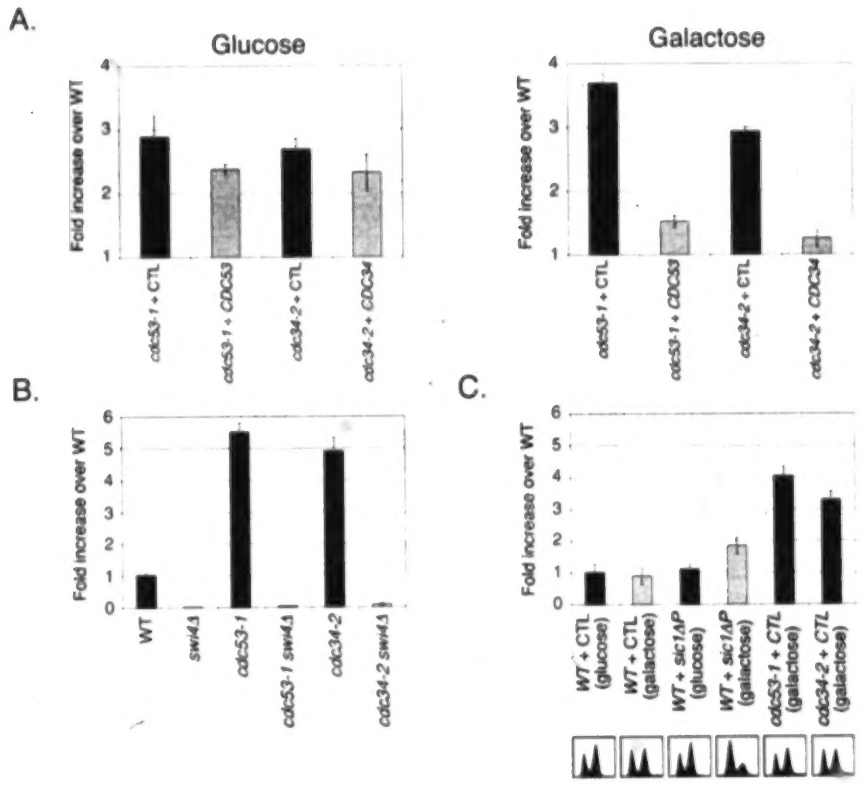

Figure 4.2 Cdc34/SCF mediated transcriptional effects are specific and novel.
(A) Cdc34 and Cdc53 complement *cdc34-2* and *cdc53-1* transcriptional defects respectively. *WT*, *cdc53-1* and *cdc34-2* cells were transformed with *SCB::LacZ* together with an empty plasmid (CTL). The *cdc53-1* and *cdc34-2* cells were also transformed with *SCB::LacZ* together with a plasmid containing *CDC53* or *CDC34* under the control of a galactose promoter, respectively. The strains were grown to mid-log phase at 30°C in SD-raffinose medium and were then shifted into either SD-glucose (left panel) or SD-galactose medium (right panel)for 4 hours. Samples of each were taken, lysates were prepared, and the β-galactosidase activity was measured. **(B)** *SWI4* is required for the induction of SBF transcription in Cdc34/SCF mutants. *WT*, *cdc53-1* and *cdc34-2* cells with (in dark grey) and without (in white) *SLT2* deleted were transformed with the *SCB::LacZ*. The strains were grown to mid-log phase at 30°C. Samples for each were taken, lysates were prepared, and the β-galactosidase activity was measured. **(C)** Transcriptional effect of Sic1 stabilization. *WT*, *cdc53-1* and *cdc34-2* cells were transformed with *SCB::LacZ* together with an empty plasmid (CTL). The WT cells were also transformed with *SCB::LacZ* together with a plasmid carrying a derivative of sic1 that is not targeted for ubiquitin-mediated degradation (*sic1ΔP*) under the control of a galactose inducible promoter. The strains were grown to mid-log phase at 30°C in SD-raffinose medium and were then shifted into either SD-glucose or SD-galactose medium for 4 hours. Samples of each were taken, lysates were prepared, and the β-galactosidase activity was measured.

SWI4 deleted strains. SBF dependent transcription was completely eliminated when *SWI4* was deleted in all the strains, indicating that the induced transcriptional activity required the DNA binding component of the SBF (Figure 4.2B). Thus, increased transcription from the SBF reporter stems from an effect of the *cdc53-1* and *cdc34-2* mutations on SBF activity rather then the result of some general transcriptional defect.

The Cdc34/SCF complex functions to target for ubiquitination a number of cell cycle regulators during the late G1 phase of the cell cycle, the point in the cell cycle that SBF transcriptional activity is known to peak. This raised the possibility that the *cdc53-1* and *cdc34-2* mutations effected cell cycle progression through the G1/S transition to the extent that active SBF may accumulate. If true, such an accumulation could account for the increased activity observed for the SBF reporter assay. To test this possibility, a late G1 phase arrest was induced in a *WT* strain by expressing a non-degradable derivative of the cyclin-CDK inhibitor *SIC1* (*sic1ΔP*) (63). *WT* cells were co-transformed with the *SCB::LacZ* reporter plasmid and a plasmid expressing *sic1ΔP* under the control of a galactose inducible promoter. These cells were then grown to mid-log phase in raffinose containing medium, and shifted into either galactose or glucose containing medium. As a control, *WT*, *cdc53-1*, and *cdc34-2* cells carrying the *SCB::LacZ* reporter plasmid and an empty plasmid were treated in a similar manner. Samples from each strain were taken, and the DNA content and β-galactosidase activity were measured. The majority of the cells expressing *sic1ΔP* arrested in the G1 phase of the cell cycle, resulting in a slight increase in SBF transcriptional activity (Figure 4.2C). However, the extent of transcriptional induction was much less than in the *cdc53-1* and *cdc34-2* cells at their permissive temperature, which are not largely arrested in the G1 phase of the cell cycle (Figure 4.2C). This result suggests that the transcriptional induction of SBF activity cannot solely be explained by a late G1 phase cell cycle arrest.

4.2.2 The transcriptional profile of *cdc53-1* and *cdc34-2* strains.

The Cdc34/SCF complex clearly plays an important role in the transcriptional regulation of several events. This includes the well-characterized role in the direct regulation of the Gcn4 and Met4 transcriptional activators, as well as the observed role in the regulation of cell integrity mediated transcription. In order to gain a better

understanding of the global extent of Cdc34/SCF mediated transcriptional regulation, and to determine possible expression patterns related to cell integrity, I pursued a DNA microarray analysis of *cdc53-1* and *cdc34-2* cells. To this end, I measured the transcript levels from three independent cultures of *cdc53-1* and *cdc34-2* cells and compared them to *WT* cells, all growing at mid-log phase at the permissive temperature of 30°C. I reasoned that at this temperature these cells would grow efficiently without any major cell cycle defects, yet still exhibit selected transcriptional defects, such as those observed with the LacZ reporter plasmids.

The analysis revealed that 211 genes (approximately 3.35% of the genome) in *cdc53-1* cells, and 180 genes (approximately 2.85% of the genome) in *cdc34-2* cells had an average expression change of 2-fold or greater compared to the *WT* cells (see Appendix 4.1). The effect on expression was almost entirely due to gene induction, as 174 genes in the *cdc53-1* mutant and 143 genes in the *cdc34-2* mutant were induced 2 fold or greater, suggesting that the Cdc34/SCF complex primarily functions as a negative regulator of transcription. Only 17 genes in the *cdc53-1* mutant and 16 genes in the *cdc34-2* mutant were repressed by 2 fold or greater. A relatively high correlation between the overall expression patterns of the *cdc53-1* and *cdc34-2* cells is observed (r^2=0.533, Figure 4.3). The two mutants share 95 genes that were significantly expressed (45% of the *cdc53-1*, and 53% of the *cdc34-2* expressed genes), and 7 genes that were significantly repressed in both mutants (41% of the *cdc53-1* and *cdc34-2* repressed genes). The high similarity in expression patterns indicates that Cdc53 (and most likely the SCF) functions with Cdc34 to regulate transcriptional responses.

Functional analysis of the significantly induced genes shared between both mutants reveals an enrichment for several groups of genes. Based on Gene Ontology annotations there is an enrichment of genes involved in sulfur utilization and assimilation (31.0-fold enrichment: 3.1% of the genes in the dataset versus 0.1% genes in the genome), vitamin metabolism (9.3-fold enrichment), amino acid metabolism (5.0-fold enrichment), cell wall organization and biogenesis (3.5 fold enrichment), responses to mating pheromone (3.4-fold enrichment), responses to external stimulus (3.0-fold enrichment), and ion transport (2.8-fold enrichment). A large portion of the induced genes have unclassified functions (approximately 40%). Interestingly, very few cell cycle

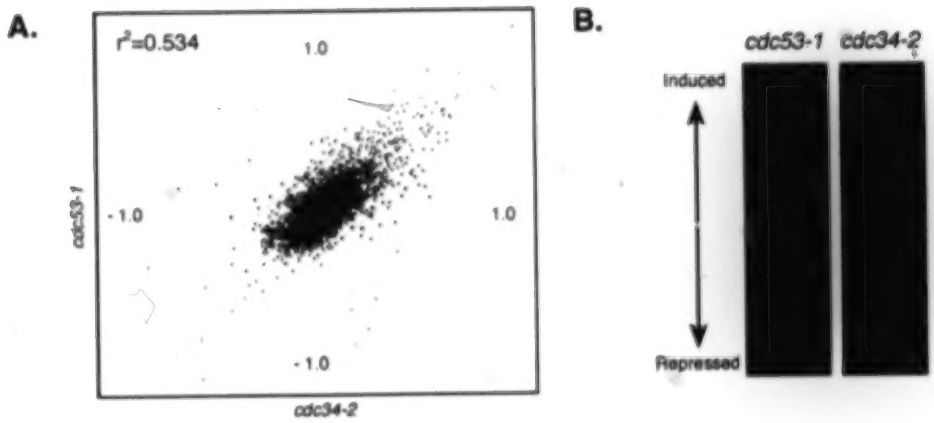

Figure 4.3 A strong correlation exists between the transcriptional profiles of *cdc53-1* and *cdc34-2* mutants. **(A)** Log_{10} ratio scatter plot comparing the expression profiles of *cdc53-1* and *cdc34-2* cells. A scatter plot comparing the expression profiles of the *cdc53-1* and *cdc34-2* microarray experiments performed at 30°C is shown. A linear trendline was generated from this comparison (middle line) and the genes whose expression varied by 2-fold or greater from that of the trendline are shown outside the upper and lower lines. Genes that are induced for expression are shown in red, and genes repressed in their expression are shown in green (the greater the fold change, the brighter the color). **(B)** A side-by-side comparison of the transcriptional profiles of *cdc53-1* and *cdc34-2* mutants. The expression profile of *cdc53-1* mutants at 30°C is shown (on the left) in descending order from the most highly induced genes (in red) to the most repressed genes (in green). The same genes are depicted from the expression profile of the *cdc34-2* mutant at 30°C (on the right).

regulated genes had a variance in their expression, suggesting that the observed transcriptional effects are most likely linked to a direct function of the Cdc34/SCF complex rather than with defects associated with cell cycle progression.

The few genes that are significantly repressed in both the *cdc53-1* and *cdc34-2* cells do not group into distinct processes, as most of them have unknown functions (Table 4.1). However, insight into these repressed genes may be observed from the three genes that have been characterized: *DIP5*, which encodes an amino acid permease, *CHA1*, which is involved in the catabolism of hydroxy amino acids, and *DSE4*, which expresses a cell wall glucanase.

Differences between the expression profiles of *cdc53-1* and *cdc34-2* cells do exist. A significant induction of 166 distinct genes was observed within the *cdc53-1* cells, and conversely, 85 distinct genes were induced in the *cdc34-2* cells. A substantial proportion of these genes grouped into similar processes as those shared between the two strains, such as genes involved in amino acid metabolism and sulfur metabolism. However, distinct processes within each strain were also apparent. The *cdc34-2* mutant expressed genes involved in purine base metabolism (22-fold enrichment), and in carbohydrate metabolism (9.1-fold enrichment). Alternatively, *cdc53-1* cells exhibited an increase in genes involved in sporulation and spore wall assembly (5-fold enrichment), and signal transduction (2.4-fold enrichment). Interestingly, genes encoding the Ub-conjugating enzymes Cdc34 and Ubc5 were also induced within the *cdc53-1* cells, suggesting that Cdc34 and possibly Ubc5 function with the SCF to relieve the defects associated with the *cdc53-1* mutant.

Differences between the *cdc53-1* and *cdc34-2* cells are also evident in the repression of genes (Table 4.1). Consistent with previous studies, the *cdc53-1* cells exhibit a reduced expression of two glucose transporters (*HTX1*, and *HTX4*), both of which are regulated by the SCF^{Grr1} complex. Of the genes characterized, the largest grouping of repressed genes is observed in the *cdc34-2* cells. Three sets are evident, which include three ammonium transporter genes (*MEP1*, *MEP2* and *MEP3*), two genes involved in nitrogen catabolism (*GAT1* and *DAL3*), and three genes encoding amino-acid permeases (*CAN1*, *GAP1* and *PUT4*). In fact, one of these genes (*PUT4*), which is considerably repressed in the *cdc34-2* cells, is significantly induced in the *cdc53-1* cells.

Table 4.1 Genes repressed in *cdc53-1* and *cdc34-2* cells.

ORF	Name	Description	Fold repression	
			cdc53-1	*cdc34-2*
YAR066W		Uncharacterized	-4.35	
YAR068W		Uncharacterized	-5.88	
YCL064C	Cha1	Catabolism of hydroxy amino acids	-12.50	-4.00
YDL037C	Bsc1	Similarity to glucan 1,4-alpha-glucosidase		-2.56
YDL038C		Uncharacterized	-4.35	-2.78
YDL039C	Prm7	Pheromone-regulated protein	-3.57	-2.38
YEL063C	Can1	Arginine permease		-2.78
YFL021W	Gat1	Involved in nitrogen catabolite repression		-2.08
YGR121C	Mep1	Ammonia permease		-2.00
YHR092C	Hxt4	High-affinity glucose transporter	-2.13	
YHR094C	Hxt1	Low-affinity glucose transporter	-2.00	
YIR032C	Dal3	Ureidoglycolate hydrolase		-3.33
YJL213W		Uncharacterized	-2.38	-2.33
YJR003C		Uncharacterized	-2.00	
YKR039W	Gap1	General amino acid permease		-33.33
YMR006C	Plb2	Lysophospholipase/phospholipase B	-3.23	
YNL024C		Putative S-adenosylmethionine-dependent methyltransferase	-2.04	
YNL034W		Uncharacterized		-2.22
YNL083W		Uncharacterized	-2.17	
YNL119W	Ncs2	Plays a role in invasive growth	-2.38	
YNL142W	Mep2	Ammonia permease		-5.26
YNR067C	Dse4	Glucanase	-2.94	-2.27
YOL014W		Uncharacterized	-2.22	-7.69
YOR032C	Hms1	Overexpression confers hyperfilamentous growth	-2.13	
YOR348C	Put4	Proline-specific permease, also capable of transporting Ala and Gly	+2.35	-2.22
YPL265W	Dip5	Dicarboxylic amino acid permease, also a transporter for Gln, Asn, Ser, Ala, and Gly	-3.03	-3.85
YPR138C	Mep3	Ammonia permease		-2.08

Taken together, these observations are suggestive that although Cdc34 and Cdc53 function primarily together, the *cdc53-1* and *cdc34-2* mutations display several differential defects.

The variance in expression levels of all of these genes does not clearly implicate the misregulation of only one transcription factor, and suggest that multiple defects occur that may either directly cause or indirectly signal for these transcriptional effects. Analysis of the promoter regions strengthens this idea, as potential promoter elements for several transcription factors are evident (see Appendix 4.2). Interestingly, many of these genes have potential binding sites for multiple transcription factors, suggesting the possibility of the misregulation of several transcription factors that may act on the same gene to cause the observed effects in the *cdc53-1* and *cdc34-2* mutants.

4.2.3 Variation in cell wall related transcripts in *cdc53-1* and *cdc34-2* mutants.

A considerable fraction of the induced genes (32 genes) in both the *cdc53-1* and *cdc34-2* cells function either directly or indirectly with the yeast cell wall (listed in Table 4.2). The expression patterns of several of these genes parallel that of cell wall damage and misregulation of the cell integrity pathway (5, 17). From this overall grouping, 6 different sets of related genes can be highlighted. The first subgroup comprises 9 genes (*ECM8, ECM13, FMP45, FKS2, FKS3, ECM17, PIR3, KTR2, ECM40,* and *PKH2*) that are involved in cell wall organization and biogenesis. Compromised cell wall integrity results in the transcriptional induction of at least three of these genes (*FKS2, PIR3* and *KTR2*). Two of these genes, *FKS2* (a catalytic component of the 1,3-β-glucan synthase) and *PIR3* (a protein linked directly to 1,3-β-glucan), have also been shown to be directly regulated by the cell integrity pathway (12, 17, 31, 68). A further link to the cell wall integrity is evident by the induction of *PKH2*. This gene encodes a yeast homologue of mammalian 3'phosphoinositide kinase 1 (PDK1), which has been shown to phosphorylate and activate Pkc1, thereby activating the MAPK cascade of the cell integrity pathway (28).

A comparison between the transcriptional profiles of mutants that activate the cell integrity pathway (such as hyperactive alleles of Rho1 and Pkc1) and the Cdc34/SCF mutants reveals that they parallel each other relatively well. In fact, there is a 3-fold

Table 4.2 Cell integrity related genes induced in *cdc53-1* and *cdc34-2* cells.

ORF	Name	Description	Fold changes		Putative Promoter elements						
			cdc53-1	*cdc34-2*	SCB	MCB	Rlm1	Met4	Gcn4	STRE	HSTF
Cell wall organization/biogenesis*											
YBR076W	Ecm8	Cell wall organization and biogenesis	2.5	2.4	2	0	2	0	2	0	0
YBL043W	Ecm13	Cell wall organization and biogenesis	4.5	3.3	0	0	0	0	3	0	2
YDL222C	Fmp45	Cell cortex protein	3.5	4.5	0	0	0	0	3	1	1
YGR032W[2]	Fks2	Catalytic component of 1,3-β-glucan synthase	3.4	2.3	2	0	2	1	0	0	0
YJR137C	Ecm17	Sulfite reductase β-subunit		2.2	0	0	1	0	4	0	2
YKL163W	Pir3	Cell wall organization and biogenesis	2.9		0	0	1	1	0	1	1
YKR061W	Ktr2	N-linked glycosylation of cell wall mannoproteins	2.0		0	0	0	0	1	0	2
YMR062C	Ecm40	Mitochondrial ornithine acetyltransferase	4.1	2.2	0	0	0	0	4	0	0
YMR306W[2]	Fks3	1,3-β-glucan synthase	2.3		3	3	0	0	0	0	2
YOL100W	Pkh2	Ser/Thr protein kinase, cell wall biogenes	2.1		0	0	0	2	1	1	1
Polysaccharide biosynthesis*											
YER096W[3]	Shc1	Activator of Chs3p (chitin synthase III)	2.3		0	1	0	0	3	1	1
YLR273C	Pig1	phosphatase regulatory subunit		2.1	2	2	0	0	3	0	2
GPI-anchored cell wall proteins[1]											
YAL063C	Flo9	Thought to be involved in flocculation		2.3	0	0	0	0	1	0	0
YER011W	Tir1	Protein of the Srp1p/Tip1p family of Ser-Ala-rich proteins		2.5	0	0	0	0	2	0	0
YIR019C	Muc1	Regulated via Ste12, Tec1 and Flo8		3.2	0	0	0	0	1	0	2
YLR042C		Uncharacterized protein	4.9	3.5	2	0	2	0	1	1	0
YLR343W		Uncharacterized protein		2.0	0	0	1	0	1	0	0
YOL132W	Gas4	Uncharacterized protein	2.3	2.0	0	0	0	0	1	0	0
YOL155C		Similarity to glucan 1,4-α-glucosidase	4.7	4.1	0	0	0	0	4	1	2
YOR382W	Fit2	Involved in the retention of siderophore-iron in the cell wall	3.1		1	0	1	0	0	1	1
Spore wall assembly & sporulation*											
YDR104C	Spo71	Required for spore wall formation	2.1		0	0	2	0	1	0	1
YDR523C	Sps1	Ser/Thr Kinase required for spore wall formation	2.2		1	1	1	0	2	0	0
YIL099W	Sga1	Glucan 1,4-alpha-glucosidase activity	4.1	2.7	1	0	0	0	3	5	0
YNL202W	Sps19	Functions during spore wall formation	3.3	3.9	0	0	0	0	1	1	0
YOL091W	Spo21	Component of the meiotic outer plaque	3.5		0	0	0	0	0	0	2
YOR177C	Mpc54	Component of the meiotic outer plaque	2.1		0	0	2	0	2	0	0

continued on next page

* based on Gene Ontology annotations. [1] based on ref (11). [2] also included in polysaccharide biosynthesis group. [3] also included in spore wall assembly & sporulation group

Table 4.2 continued. Cell integrity related genes induced in *cdc53-1* and *cdc34-2* cells.

ORF	Name	Description	Fold changes		Putative Promoter elements						
			cdc53-1	*cdc34-2*	SCB	MCB	Rlm1	Met4	Gcn4	STRE	HSTF
Cell surface receptor linked signal transduction*											
YCR073C	Ssk22	Protein kinase, activation of MAPKK during osmolarity sensing	2.1		1	1	1	0	1	1	0
YDR085C[4]	Afr1	regulation of α-factor signalling, induction of morphogenesis	2.3		0	0	2	0	0	1	1
YDR461W[4]	Mfa1	a-factor mating pheromone precursor	2.7		0	0	0	0	1	0	0
YKL178C[4]	Ste3	Cell surface a-factor receptor, pheromone response	2.0	2.1	0	0	2	0	2	1	1
Response to external stimulus*											
YBR093C	Pho5	Glycoprotein at cell surface, acid phosphatase	2.1		0	0	1	0	3	0	0
YBR040W	Fig1	Integral membrane protein involved in regulation of signaling for mating		5.3	0	0	1	0	1	0	2
YDL223C	Hbt1	Involved in mating projection formation, polarized cell morphogenesis	2.5	2.1	0	1	1	0	0	2	0
YEL060C[3]	Prb1	Cell wall protein involved in vanadate resistance	2		0	0	1	0	1	1	1
YFL014W	Hsp12	Responds to dessication, heat shock and osmotic stress	2.8		0	0	2	0	0	5	0
YGL032C	Aga2	Adhesion subunit of a-agglutinin of a-cells	2.4	2.2	0	0	1	0	2	1	2
YIL121W	Qdr2	similarity to antibiotic resistance proteins	4.8	2.7	0	0	0	0	2	0	0
YMR175W	Sip18	Responds to dessication and osmostress		4.1	0	0	0	0	3	3	0
YOR031W	Crs5	Copper-binding metallothionein	2.5	2.1	0	0	1	0	2	2	0
YPL163C	Svs1	Cell wall protein involved in vanadate resistance	2.2	2.4	2	1	1	0	1	0	2
YPL223C	Gre1	Hydrophilin, induced by osmotic stress	2.7	3.2	0	0	0	0	1	0	2

[3] also included in spore wall assembly & sporulation group. [4] also included in the response to external stimulus group

enrichment of genes that are induced by activation of Rho1 and a 2-fold enrichment of genes induced by the activation of Pkc1 (see Appendix 4.3). Furthermore, analysis of the promoter regions of the induced genes reveals that a significant proportion of the genes have potential SBF (22% of the *cdc53-1*, and 29% of the *cdc34-2* genes), MBF (16% of the *cdc53-1* and 18% of the *cdc34-2* genes) and Rlm1 (49% of the *cdc53-1*, and 42% of the *cdc34-2* genes) promoter binding sites. The induction of these genes is consistent with the reporter assay results, which suggest a relationship to the cell integrity pathway.

Related to genes involved in cell wall biogenesis is the second group of induced genes, which encodes two proteins involved in polysaccharide biosynthesis (*SHC1* and *PIG1*). Shc1 has been shown to act as an activator of the chitin synthase III (CSIII) enzyme, and is expressed at alkaline pH conditions or during the sporulation process (25, 58). Pig1 encodes a glycogen-targeting subunit of the type I protein phosphatase Glc7, which is involved in regulating ion homeostasis (67).

The third subset of induced genes encodes glycosyl-phosphatidylinositol (GPI)-anchored cell wall proteins (*FLO9*, *TIR1*, *FLO11/MUC1*, *GAS4*, *FIT2*, *YLR042C*, *YLR343W*, and *YOL155C*). These mannoproteins are largely incorporated into the yeast cell wall to mediate several of the cells responses to environmental conditions. The genes induced constitute a substantial portion of the known GPI-anchored proteins, as there are approximately 60-70 that have been identified (11). The best characterized of these genes is *TIR1*, which has been implicated in the cell's adaptation to anaerobic conditions and low temperatures (11). *TIR1* has also been implicated in responses to cell wall damage and acid pH adaptation, which are mediated by a branch of the cAMP pathway (6). A role for TIR1 has also been suggested in vegetative growth, as it is induced for expression at the S-G2 phase transition of the cell cycle (10). The only other characterized gene of this group is *FLO11*, which has a role in mediating cell-cell and cell-surface adhesion, and as such, its induction results in invasive or filamentous growth (22). The induction of this gene is primarily under the control of MAPK signaling, the cAMP cascade and the Gcn4 transcription factor (8, 57).

The fourth group is made up of genes involved in the regulation of sporulation (*SPO71*, *SPO21*, *SPS1*, *SGA1*, *SPS19*, *and MPC54*). Two of these genes (*SPO71*, *and SPS1*) are key to the formation of the spore wall. *SPS1* encodes a serine/threonine kinase

that is highly similar to the Ste20 MAPK, and is required for the proper progression of transcriptional, biochemical and morphological events during sporulation (15). The induction of these genes suggests that *cdc34-2* and *cdc53-1* mutants possess defects related to either signaling and/or transcription in the sporulation pathway.

The final two groups are made up of genes encoding proteins that mediate signal transduction from cell surface receptors, and proteins that are involved in responses to external stimulus (*SSK22, STE3, AFR1, MFA1, PHO5, FIG1, HBT1, PRB1, HSP12, AGA2, QDR2, SIP18, CRS5, SVS1,* and *GRE1*). Several of these genes (*STE3, AFR1, MFA1, FIG1, HBT1,* and *AGA2*) are involved in the mating signaling pathway. Curiously, the majority of these genes are normally expressed in MATα cells. For example, *AGA2* encodes the adhesion subunit of the a-agglutinin protein found in MATα cells, which functions to mediate cell-cell association during mating (9), and *STE3* encodes the cell surface a-factor receptor found normally only in MATα cells, which mediates a MAPK signaling cascade in response to pheromone (21, 61). Signaling from Ste3 in response to mating pheromone results in the induction of a MAPK cascade that leads to the induced expression of many genes, including *AFR1, MFA1*. Interestingly, ubiquitination of a PEST-like sequence within Ste3 has been implicated in its endocytosis, and thereby in the regulation its signaling properties (54, 55). Since my analysis was of MATa cells, these observations indicate the occurrence of mating related signaling and/or transcriptional defects in *cdc53-1* and *cdc34-2* mutants.

Within this subset of genes there are also four genes (*SSK22, HSP12, SIP18,* and *GRE1*) that are induced in response to osmotic and temperature stress. Expression of these genes is largely dependent on Hog1 MAPK and cAMP signaling, as well as the Msn2-Msn4 transcription factors (16, 43, 46, 51). Interestingly, analysis of the promoter regions of the induced genes in the *cdc53-1* and *cdc34-2* mutants reveals that a large percentage of these genes possess either STRE promoter elements (49% of the *cdc53-1*, and 47% of the *cdc34-2* genes), which are recognized by the stress related transcription factors Msn2 and Msn4, or HSTF promoter elements (62% of the *cdc53-1*, and 65% of the *cdc34-2* genes), which are recognized by the heat shock transcription factor.

4.2.4 Gcn4 regulated transcripts are induced in *cdc53-1* and *cdc34-2* mutants.

A well-defined target of Cdc34/SCF ubiquitination is the transcription factor Gcn4. The primary function of Gcn4 is to activate the expression of genes required for amino acid biosynthesis in response to amino acid deprivation. However, global expression profiling of *gcn4* mutants has revealed that Gcn4 functions in numerous other processes, which include purine base biosynthesis, vitamin biosynthesis, glycogen metabolism, and amino acid transport (49). Under normal growth conditions Gnc4 is targeted for ubiquitination by the Cdc34/SCF^{Cdc4} complex and is subsequently degraded by the 26S proteasome (45). Therefore, increased levels of Gcn4 would alter the transcription of its targets and may affect the growth of cells, which is evident from observations that over-expression of Gcn4 results in toxicity to cells (45).

Analysis of the altered gene expression resulting from the *cdc53-1* and *cdc34-2* mutants suggests that stabilization of Gcn4 protein levels significantly contributes to the overall expression patterns observed. A comparison between the genes induced by two-fold or greater in the *cdc53-1* or *cdc34-2* mutants with that of the genes induced two-fold or greater from a previous study on the global gene expression mediated by Gnc4, reveals an approximately 3.5-fold enrichment for Gcn4 target genes in the *cdc53-1* and *cdc34-2* mutants (Figure 4.4). This enrichment includes 44% of the up-regulated genes in *cdc53-1* (85 genes) and *cdc34-2* (71 genes), which had similar expression patterns as that of the Gcn4 experiment (see Appendix 4.3).

Several of the induced genes are also characterized transcriptional targets of Gcn4. These genes include *HIS3*, *HIS4*, *ARG1*, *ADE1*, *ADE2*, *MET16*, *ARO3*, *CPA2*, *CPA1*, *GDH3*, *PHO5*, and *PCL5*, and the majority of these genes are involved in the regulation of amino acid biosynthesis. The only characterized target gene within this group that is not directly involved in this process is *PCL5*, which encodes a cyclin for the Pho85 cyclin dependent kinase (CDK) (44). *PCL5* expression is induced when Gcn4 protein levels are high, and Pcl5-Pho85 functions in a negative feed back loop to phosphorylate Gcn4, which targets it for ubiquitination and subsequent degradation (59). The induction of *PCL5* within the *cdc53-1* and *cdc34-2* mutants further indicates that Gcn4 protein levels are high, and its expression might function to regulate Gcn4 protein levels sufficiently for cell viability.

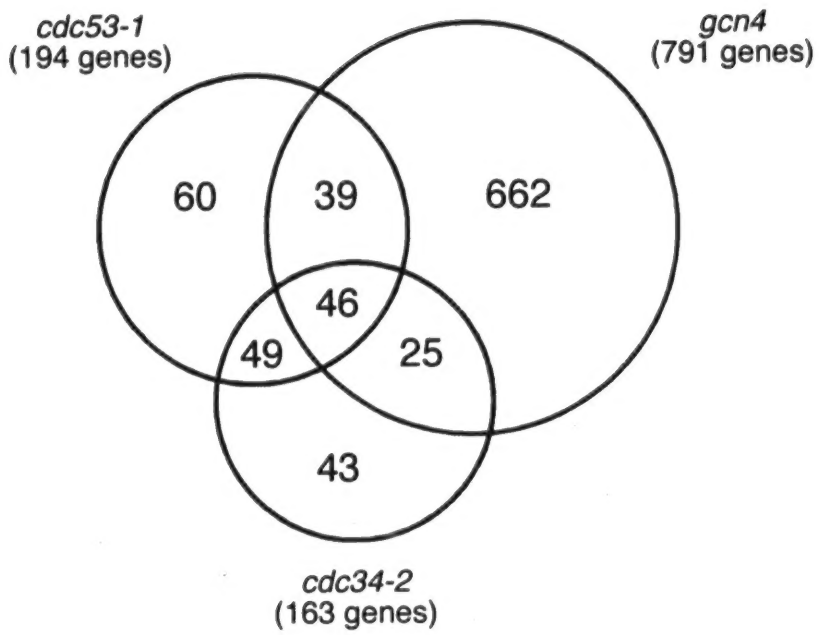

Figure 4.4 Overlap between the significantly induced genes in *cdc53-1* and *cdc34-2* mutants and those suggested to be Gcn4 targets. A Venn diagram is shown illustrating the overlap of genes that are significantly induced for expression by 2-fold or greater from the expression profiles of *cdc53-1* and *cdc34-2* mutants, and from an experiment examining the effects of the Gcn4 transcription factor by comparing a wild-type strain to a *gcn4Δ* strain that have been treated with 100mM 3AT (ref. 49).

Promoter analysis of the induced genes (see Appendix 4.2) reveals that approximately 80% of the genes induced in the *cdc53-1* and *cdc34-2* mutants possess potential Gcn4 binding elements, which supports the idea that Gcn4 is a major contributor to the observed gene induction. However, Gcn4 does not appear to be the sole source of the observed defects, as many of the induced genes either contain no Gcn4 promoter elements, or their expression patterns vary tremendously from Gcn4 regulated expression.

4.2.5 Met4 specific transcripts are induced in *cdc53-1* and *cdc34-2* mutants.

Another transcription factor that is directly regulated by Cdc34/SCF is Met4. It functions primarily as a transcriptional activator of genes required for methionine biosynthesis, and its activity is negatively regulated by the Cdc34/SCF^{Met30} complex ubiquitination. Therefore, under conditions that would compromise Cdc34/SCF function, Met4 transcriptional activity would be expected to be higher. This hypothesis is confirmed from my analysis of gene expression in *cdc53-1* and *cdc34-2* mutants. I observe that a number of characterized targets of Met4 are induced for expression (Table 4.3), which include *MET10*, *MET16*, *MET14*, and *MET3*. Furthermore, *MET32*, which encodes a Met4 cofactor, and two other methionine metabolism genes (*MET1* and *MET2*) are also induced for expression. Met4 promoter elements were found in approximately 12% of the genes induced in both the *cdc53-1* and *cdc34-2* mutants (Appendix 4.2). Together these observations suggest that a portion of the genes induced in these mutants result from the improper regulation of Met4 activity.

4.2.6 A role for the Cdc34/SCF complex in maintaining genomic integrity.

A close inspection of the induced genes in the *cdc53-1* and *cdc34-2* mutants reveals additional transcriptional patterns that suggest a role for the Cdc34/SCF complex in maintaining genomic integrity. This role is evident from the significant induction of several genes that are involved in mediating DNA damage repair (*RNR3*, *MIG3*, *HUG1*, *RAD55*, *RAD59*, *MSH6*, *PES4*, and *REC102*). While a number of these genes are known targets of the SBF and MBF transcription factors and are cell cycle regulated, they appear to group into a similar functional group. For example, a significant induction of *RNR3* occurs, which encodes a large subunit of ribonucleotide reductase (13). *RNR3* is thought

Table 4.3 Sulfur metabolism and Met4 related genes induced in *cdc53-1* and *cdc34-2* cells.

ORF	Name	Description	Fold changes		Putative Promoter elements		
			cdc53-1	*cdc34-2*	Met31/Met32[1] [AAACTGTG(G)]	[TGGCAAATG][2]	Met4/Cbf1[3] [TCACGTG]
Characterized Met4 target genes							
YFR030W	Met10	Subunit alpha of assimilatory sulfite reductase	3.5	3.7	0	0	0
YKL001C	Met14	Adenylylsulfate kinase		3.4	0	0	1
YJR010W	Met3	Catalyzes the primary step of intracellular sulfate activation	3.1	4.9	0	0	2
YPR167C	Met16	Phosphoadenylylsulfate reductase	2.6	2.7	0	0	1
Sulfur metabolism genes							
YBR294W	Sul1	High affinity sulfate permease	3.2	2.7	0	0	0
YDR253C	Met32	Transcriptional regulator of sulfur amino acid metabolism		2.0	0	0	0
YKR069W	Met1	Siroheme synthase S-adenosyl-L-methionine uroporphyrinogen III transmethylase		2.2	1	0	0
YLR092W	Sul2	High affinity sulfate permease	2.1	3.5	0	0	2
YNL277W	Met2	L-homoserine-O-acetyltransferase		3.5	0	0	1
Other genes containing Met4 promoter elements							
YAL067C	Seo1	Putative permease	3.7	4.0	1	0	0
YCL026C-A	Frm2	Involved in the integration of lipid signaling pathways with cellular homeostatis	3.0		0	1	0
YDL059C	Rad59	Repair of double-strand breaks in DNA		2.9	0	0	1
YDL182W	Lys20	Homocitrate synthase	2.8		0	1	0
YDL198C	Ggc1	Mitochondrial GTP/GDP transporter	2.0		0	1	0
YDR076W	Rad55	Recombinational repair of double-strand breaks	2.0		0	0	1
YDR088C	Slu7	Involved in splicing	2.2		0	1	0
YFR023W	Pes4	Poly(A) binding protein	4.9	4.7	1	0	0
YER081W	Ser3	3-phosphoglycerate dehydrogenase	3.7	2.4	1	0	0
YGL081W		Uncharacterized	2.9	3.2	1	0	0
YGL121C	Gpg1	Involved in regulation of pseudohyphal growth	2.0		0	1	0
YGR032W	Fks2	Catalytic component of 1,3-β-glucan synthase	3.4	2.4	1	0	0
YJL038C		Uncharacterized	17.7	11.1	1	0	0
YJL045W	Sdh1b	similar to succinate dehydrogenase flavoprotein (sdh1)		3.3	0	1	0
YJR130C	Str2	Cystathionine gamma-synthase activity	2.9		0	1	0
YKL163W	Pir3	Cell wall organization and biogenesis	2.9		1	0	0
YLR280C		Uncharacterized		2.1	1	0	0
YMR169C	Ald3	Aldehyde Dehydrogenase (NAD(P)+)	2.1		1	1	0
YMR107W	Spg4	Required for survival at high temperature	4.9	3.0	1	0	0
YMR118C		Uncharacterized	3.3		0	1	0
YNL333W	Snz2	Stationary phase-induced gene family		2.2	0	1	0
YNR050C	Lys9	Lysine biosynthesis	2.4	2.0	1	0	0
YOL100W	Pkh2	MAPKKK cascade during cell wall biogenes	2.1		1	0	1
YPL081W	Rps9A	Ribosomal protein		2.1	0	1	0
YPL171C	Oye3	NAD(P)H dehydrogenase	4.6	5.1	0	0	1

[1] ref.(4), [2] ref.(34), [3] ref.(36)

to respond to the accumulation of DNA lesions, and has been shown to be induced for expression (sometimes more than 100-fold) during DNA damage (13, 30). Furthermore, *RAD55* and *RAD59* encode proteins that mediate a response to repair double stranded DNA breaks through recombinational repair mechanisms.

Another interesting relationship to the maintenance of genomic integrity is the induction of *MTW1* and *NSL1*, which are essential components of the MIND complex (made up of Mtw1-Nnf1-Nsl1-Dsn1). This complex is involved in joining kinetochore subunits that contact DNA to those that contact microtubules, and is required for accurate chromosome segregation. As such, this observation suggests a role for the Cdc34/SCF complex in the regulation of the MIND complex.

It therefore appears that the overall effects observed within *cdc53-1* and *cdc34-2* mutants reveal a variety of roles for the Cdc34/SCF complex in the mediation of transcription, suggesting that numerous uncharacterized targets of ubiquitination exist.

4.3 Discussion

We have previously shown that the Cdc34/SCF complex functions to mediate cell integrity. Mutations within this complex result in several cell integrity related phenotypes, including caffeine sensitivity, and temperature sensitive lysis defects that can be osmotically suppressed (Chapter 3). Defects in the induction of Slt2 phosphorylation were also observed in Cdc34/SCF mutants, so it was therefore expected that there would also be defects in the activation of its downstream functions, such as the induction of Rlm1 and SBF transcription (32, 40). Therefore, it was somewhat surprising to find that Rlm1 and SBF transcriptional activity was significantly induced in *cdc53-1* and *cdc34-2* mutants. (Figure 4.1A). These mutants displayed transcriptional effects even at their permissive temperatures, indicating that defects are present in these cells under favorable growth conditions. The transcriptional effects of these defects were dependent on signaling from Slt2, as deletion of *SLT2* eliminated the reporter activity from these transcription factors (Figure 4.1B). Interestingly, MBF transcriptional activity was also increased in a Slt2 dependent manner, suggesting an uncharacterized role for the cell integrity pathway in the regulation of this transcription factor, which might relate to the

role of Slt2 in the regulation of the Swi6 activator (40). The differences observed between SBF and MBF regulation may be accounted for from the observation that Slt2 regulates the SBF in a Swi6 dependent and independent fashion (2), suggesting that separate signals mediate different responses. Further analysis of the increase in SBF transcriptional activity confirmed that this effect was caused by defects associated with a novel function for the Cdc34/SCF complex in the regulation of this pathway (Figure 4.2).

The cell integrity related transcriptional effects observed in *cdc53-1* and *cdc34-2* mutants can be rationalized in terms of a simple model for Cdc34/SCF function (Figure 4.5). This model places the function of the Cdc34/SCF complex either at the level of the signaling pathway, resulting in the regulation of transcription, or at the level of the transcription factors themselves. Evidence supporting both potential roles has been observed for the Cdc34/SCF complex in the mediation of several transcriptional effects. Support for a role in signaling is most apparent from its role in the regulation of the MAPKK Ste7 of the mating pathway. Ste7 is targeted for ubiquitination by the Cdc34/SCF complex and subsequent degradation in response to prolonged mating pheromone, thereby affecting downstream transcription (65). My observations suggest that a similar mode of regulation might occur for Slt2 phosphorylation, particularly in response to pathway inducing stress conditions. Such an effect would very likely result in transcriptional variation. However, from what is known about Slt2 activity, it is predicted that the downstream transcriptional activity would be reduced rather than induced when Slt2 is not phosphorylated properly. Since this does not appear to be the case in the *cdc53-1* and cdc*34-2* mutants, another explanation should exist. Slt2 activation may not correlate with its phosphorylation state. In fact, such an idea has been suggested from studies on the Slt2 effector protein Krn4, which reveal that deletion of *KNR4* results in an increase in Slt2 phosphorylation, but a decrease in Rlm1 transcription (42). It could therefore be possible that the Cdc34/SCF complex mediates the interaction between Slt2 and such effectors, thereby resulting in the regulation of downstream transcription. However, the Cdc34/SCF complex may function directly on the Rlm1, SBF and MBF transcription factors in a similar manner to that observed for other transcription factors, such as Met4 or Gcn4 (37, 45).

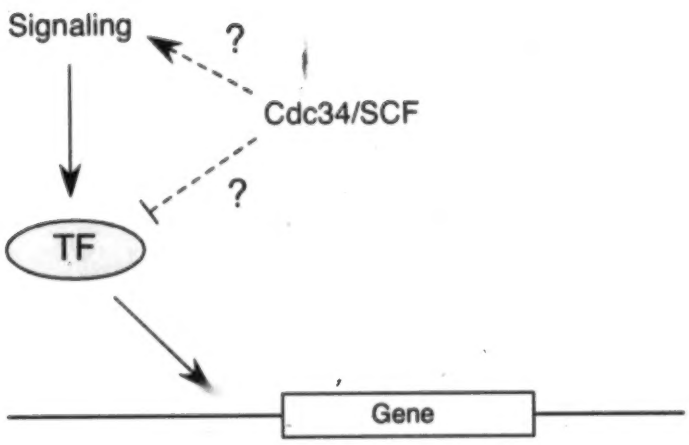

Figure 4.5 A simplified model illustrating the known modes of Cdc34/SCF mediated regulation of transcription. The Cdc34/SCF complex has been shown to regulate transcription either directly by affecting the function of the transcription factor (as in case of the Gcn4 and Met4 transcription factors), or at the level of signaling to the transcription factor (as in the case of the Ste7 MAPKK).

Comparison of global gene expression patterns of *cdc53-1* and *cdc34-2* mutants to those of wild-type cells growing at the permissive temperature of 30°C reveals that the Cdc34 and the SCF complex function together to regulate diverse transcriptional effects in the cell. This function is primarily geared to negatively regulate transcription, as over 90% of the genes that had a 2-fold or greater variance in transcription were induced. Analysis of these Cdc34/SCF mutants at their permissive temperature proved to be ideal, as these cells had relatively normal growth characteristics with no cell cycle arrests, and we did not have to deal with transcriptional variance that would most likely occur from elevated temperatures (18). Examination of this sort for other temperature sensitive alleles of essential genes could also prove to be very informative.

The most apparent function for the Cdc34/SCF complex in transcription is in the regulation of the Gcn4 and Met4 transcription factors, which function to primarily mediate amino acid biosynthesis. Both of these proteins are targeted for ubiquitination by the Cdc34/SCF complex, resulting in the inhibition of their activity (37, 45). The regulation of several of other transcription factors is also suggested by this analysis, including the SBF, MBF, Rlm1, Msn2-Msn4, and the Hsf1. However, it is not apparent at what level this regulation occurs. For example, Cdc34/SCF may function directly on the transcription factor, as with Gcn4 or Met4, or it may function as a regulator of a signaling pathway, as with the MAPKK Ste7 or the MAPK Slt2 (Figure 4.5).

The transcriptional regulation of several proteins related to signal transduction is affected by the *cdc53-1* and *cdc34-2* mutations, including proteins related to the cell integrity pathway, the sporulation pathway, the mating pathway, the HOG pathway, and the cAMP pathway. These signaling pathways are all linked to either the regulation of factors at the cell wall, or to factors that respond to signals from the cell wall (Table 2.1). It is therefore possible that the cell integrity defects we observed in the Cdc34/SCF mutants may be a result of a combined misregulation of all these pathways. At least two of these pathways appear to be directly regulated by the Cdc34/SCF complex: 1) the cell integrity pathway, as we have observed a role in Slt2 phosphorylation (see Chapter 3), and 2) the mating pathway, since the MAPKK Ste7 is a known ubiquitination target (66). A more thorough study of the Cdc34/SCF complex in the regulation of signaling pathways may reveal more direct relationships with several of these pathways.

Interesting relationships that are not normally associated with Cdc34/SCF function are also evident from the microarray analysis. Since the analysis was of MATa cells, there was a curious expression of several MATα specific mating genes, which was observed in the Cdc34/SCF mutants examined. The cause for these effects is not clear, but it may relate mating signaling defects. Alternatively, it is possible that the Cdc34/SCF complex may play a role in genomic silencing, particularly at the MAT locus, as Cdc34 has been implicated in the regulation of chromatin assembly (23). Another interesting observation was the induction of several genes that respond to DNA damage, suggesting that the Cdc34/SCF complex functions to mediate genomic integrity. Several other responses may also be included in the transcriptional programs of the *cdc53-1* and *cdc34-2* mutants, which might not be as obvious.

The observations made in this chapter highlight the functions of the Cdc34/SCF complex in the regulation of transcription. While these roles appear to be complex, it is evident that this ubiquitination complex impacts on selected events. It primarily does so in a negative manner either by targeting transcription factors directly, or by targeting other factors (many of which appear to be unknown). It remains to be seen how interconnected these transcriptional effects are, and further study on their specifics will surely shed some light on these roles.

4.2 Materials and methods

4.4.1 Plasmids and yeast strains.

The YCP111.GAL plasmid was constructed by inserting the GAL1/10 promoter and terminator regions of the pESC(Trp) plasmid (Stratagene) into YPClac111. This region was amplified by PCR using oligonucleotides possessing the PstI and MfeI restriction sites, and inserted into the PstI and EcoRI restriction sites of YCPlac111. The *CDC53* gene was cut from pESC200 (see Section 2.4.1). and inserted into YCP111.GAL using the BamHI and XhoI restriction sites to generate YCP111.GAL-Cdc53. The *CDC34* gene was amplified by PCR and inserted 3' of the FLAG epitope tag in the YCP111.GAL plasmid using the Xho1 and Kpn1 restriction sites to generate YCP111.GAL-Cdc34. For the YCP111.GAL-sic1ΔP plasmid, the GAL promoter region

followed by a gene encoding a nondegradable version of Sic1 (*sic1ΔP*) (63) was removed from YIP.GAL-Sic1ΔP (provided to us by David Stuart, University of Alberta) and inserted into YCPlac111 using the EcoRI and HindIII restriction sites.

All the yeast used were isogenic to the K699 (W303) strain (*ade2-101 his3-11,15 leu2-3,112 trp1-1 ura3-1 can1-100*). The *slt2Δ* and *swi4Δ* strains were constructed by homologous recombination. The G418 gene flanked 3' and 5' by a region extending from approximately 100 to 500 base pairs (bp) upstream and downstream of the gene to be knocked out was generated by PCR from genomic DNA isolated from the BY4741 yeast deletion collection. This resulting DNA product was transformed into the target strain and selected for by growth on G418. The resulting knockout strain was confirmed by PCR and functional analysis.

4.4.2 β-Galactosidase reporter assays.

Cells carrying a plasmid with the *LacZ* gene under the control of the minimal *CYC1* promoter region, lacking upstream activating sequences (*CTL::LacZ*, pLGΔSS (19)), or under the control of 4x*SCB* promoter elements (*SCB::*LacZ, pBA251 (1)), 4x*MCB* promoter elements (*MCB::LacZ*, pBA487 (64)) or 2x*Rlm1* promoter elements (*Rml1::LacZ*, p1434 (32)) were grown in SD medium (0.67% yeast nitrogen base and the appropriate amino acids) lacking uracil (-Ura) to an optical density at 600 nm (OD_{600}) of 0.5 - 0.8. Cell samples were collected by centrifugation and a liquid β-Galactosidase assay using O-nitrophenol β-D-galactopyranoside (ONPG) as a substrate was performed according to the procedure outlined by CLONETECH Laboratories, Inc. Briefly, cells were lysed by rapid freeze thaw in Z buffer [60 mM Na_2HPO_4, 40 mM NaH_2PO_4, 10 mM KCl, 1 mM $MgSO_4$, pH 7.0] and incubated in the presence of β-mercaptoethanol and ONPG [0.67 mg/ml final] at 30°C until a yellow color developed. Reactions were stopped by the addition of Na_2CO_3 [300 mM final]. The β-galactosidase units were then determined (1 unit β-galactosidase is defined by the amount that hydrolyzes 1μmol of ONPG to o-nitrophenol and D-galactose per minute per cell (3). All samples were assayed in triplicate, and an average of the β-galactosidase units with standard deviation is shown in the results. The pLGΔSS, pBA251 and pBA487 plasmids were provided to use by Brenda Andrews (University of Toronto), and the p1434 plasmid was provided to

use by David Levin (Johns Hopkins University).

4.4.3 Microarray cultures and RNA Isolation.

Triplicate cultures of isogenic W303 wild-type (*WT*), *cdc53-1* and *cdc34-2* cells were grown at 30°C in YPD (1% yeast extract, 2% bactopeptone and 2% dextrose) to an OD_{600} of 0.8. Cells were collected by centrifugation, washed twice with ice-cold water and total RNA was immediately extracted from the cells by the hot acid phenol method (35). Messenger RNA (mRNA) was then isolated using the Easy-mRNA kit (Qiagen), and cDNA was synthesized from the mRNA by reverse transcription, and biotin-labeled cRNA was constructed and purified using the procedures described by Affymetrix. UV spectroscopy was used to quantitate the RNA.

4.4.4 Microarray Analysis.

Biotin-labeled cRNA was hybridized to Affymetrix yeast S98 whole-genome oligonucleotide microarray chips according to the manufacturers procedures. The chips were processed using the Affymetrix Fluidics Station 400 and the arrays were imaged using the Affymetrix GeneArray Scanner (570 nm, 3 μm pixel resolution). Each array was scanned twice and the images were averaged. The acquired images were then analyzed using the default parameters in Affymetrix's MicroArray Suite 5.0 (MAS 5.0). Subsequently the data was analyzed using Micro DB, Data Mining Tool 3.0 (DMT 3.0) and GeneSpring 6.2.

Statistical analysis (according to MAS 5.0) revealed that 84% and 85% of the genome in the *cdc53-1* and *cdc34-2* cells, respectively, produced a statistically relevant signal. Approximately 14% of the genes were absent in all the samples analyzed. The relevant genes from the triplicate *cdc53-1* and *cdc34-2* samples were compared in every various combination to those from the triplicate WT samples (for example, nine different fold changes were calculated for the *cdc53-1* strain by comparing the three *cdc53-1* samples to the three different *WT* samples), and from this an average fold gene expression was generated.

4.4.5 Promoter analysis.

Promoter regions ranging from -600 bp to the ATG codon were analyzed for potential regulatory elements using the promoter database from *Saccharomyces cerevisiae* (SCPD; http://cgsigma.cshl.org/jian). A search for Rlm1 regulatory elements ($CTA(T/A)_4TAG$; with one mismatch) was performed manually using the same promoter regions.

Appendix 4.1 Genes induced by 2 fold or greater in *cdc53-1* and *cdc34-2* mutants

ORF	Yeast name	*cdc53-1* fold-change	*cdc34-2* fold-change	Description
YAL034W-A	Mtw1	2.32		Essential component of the MIND kinetochore complex
YAL061W		2.41	2.37	Similarity to alcoholsorbitol dehydrogenase
YAL062W	Gdh3	2.35	2.03	NADP-linked glutamate dehydrogenase, NADP(+)-dependent glutamate dehydrogenase
YAL063C	Flo9		2.33	Lectin-like protein with similarity to Flo1p, thought to be expressed and involved in flocculation
YAL067C	Seo1	3.65	4	Putative permease, member of the allantoate transporter subfamily
YAR015W	Ade1		2.42	Required for 'de novo' purine nucleotide biosynthesis
YAR069C		2.16		Potential membrane protein
YBL043W	Ecm13	4.46	3.32	ExtraCellular Mutant cell wall organization and biogenesis
YBL065W		2.08	2.13	Questionable ORF
YBR040W	Fig1		5.32	Integral membrane protein required for efficient mating
YBR043C	Qdr3	2.05		Similarity to benomylmethotrexate resistance protein
YBR047W	Fmp23	3.25	2.02	The authentic, non-tagged protein was localized to the mitochondria
YBR076W	Ecm8	2.5	2.44	ExtraCellular Mutant
YBR093C	Pho5	2.08		One of 3 repressible acid phosphatases, transported to the cell surface
YBR096W		2.35		Hypothetical protein
YBR116C		2.28		Questionable ORF
YBR117C	Tkl2	2.16		Transketolase, homologous to tkl1
YBR145W	Adh5	2.99	2.13	Alcohol dehydrogenase isoenzyme V
YBR147W		9.19	3.94	Strong similarity to hypothetical protein YOL092W
YBR256C	Rib5	2.19		Riboflavin synthase alpha-chain
YBR285W		3.79	4.13	Hypothetical protein
YBR294W	Sul1	3.22	2.68	Sulfate uptake is mediated by specific sulfate transporters SUL1 and SUL2
YBR295W	Pca1	2.23		Putative P-type Cu(2+)-transporting ATPase, coupled to transmembrane movement of ions
YBR296C	Pho89	3.79		Na+Pi cotransporter, active in early growth phase
YCL024W	Kcc4		2.35	SerThr kinase of the bud neck involved in the septin checkpoint, negatively regulates Swe1
YCL026C	Frm2	3.01		Protein involved in the integration of lipid signaling pathways with cellular homeostatis
YCL030C	His4	3.7	3.62	Histidinol dehydrogenase
YCR073C	Ssk22	2.14		Protein kinase, activation of MAPKK during osmolarity sensing
YCR098C	Git1	2.24		Permease involved in the uptake of glycerophosphoinositol (GroPIns)
YDL021W	Gpm2		2.85	Converts 3-phosphoglycerate to 2-phosphoglycerate in glycolysis
YDL059C	Rad59		2.85	Protein involved in the repair of double-strand breaks in DNA
YDL170W	Uga3	2.23		Zinc-finger transcription factor of the Zn(2)-Cys(6) binuclear cluster domain type
YDL181W	Inh1	2.06	2.46	Protein that inhibits ATP hydrolysis by the F1F0-ATP synthase
YDL182W	Lys20	2.76		Homocitrate synthase, highly homologous to YDL131W

Appendix 4.1 Genes induced by 2 fold or greater in *cdc53-1* and *cdc34-2* mutants

ORF	Yeast name	*cdc53-1* fold-change	*cdc34-2* fold-change	Description
YDL198C	Ggc1	2		Mitochondrial GTPGDP transporter, essential for mitochondrial genome maintenance
YDL218W		3.13	2.92	Weak similarity to hypothetical protein YNR061c
YDL222C	Fmp45	3.46	4.46	Localized to the mitochondria; cell cortex protein
YDL223C	Hbt1	2.54	2.08	Substrate of the Hub1p ubiquitin-like protein that localizes to the shmoo tip (mating projection)
YDR010C		2.06	2.02	Hypothetical protein
YDR034W-B		3.13		Identified by SAGE expression analysis
YDR035W	Aro3	3.15		DAHP synthase; a.k.a. phospho-2-dehydro-3-deoxyheptonate aldolase
YDR038C	Ena5	2.62		Protein with similarity to P-type ATPase sodium pumps
YDR039C	Ena2	3.13		Plasma membrane; P-type ATPase sodium pump, involved in Na+ efflux to allow salt tolerance
YDR041W	Rsm10	2.05		Mitochondrial ribosomal protein of the small subunit
YDR042C		3.32	2.89	Hypothetical protein
YDR046C	Bap3	2.05		Valine transporter, branched-chain amino acid permease
YDR048C		2.76	2.03	Questionable ORF
YDR054C	Cdc34	2.96		Ubiquitin-conjugating enzyme, E2
YDR056C		2.19		Hypothetical protein
YDR058C	Tgl2	2.62		TriGlyceride Lipase
YDR059C	Ubc5	3.27		Ubiquitin-conjugating enzyme
YDR061W		2.41		Mitochondrial protein, member of the ATP-binding cassette (ABC) transporter family
YDR068W	Dos2	2.06		Unknown function
YDR070C	Fmp16	3.46	2.5	The authentic, non-tagged protein was localized to the mitochondria
YDR073W	Snf11	2.06		component of SWISNF global transcription activator complex
YDR076W	Rad55	2.03		Involved in the recombinational repair of double-strand breaks in DNA
YDR085C	Afr1	2.3		Coordinates regulation of alpha-factor receptor signalling and induction of morphogenesis during conjugation
YDR088C	Slu7	2.16		Involved in 3' splice site choices and acts in concert with Prp18 during the 2nd step of splicing
YDR089W		2		Weak similarity to Streptococcus transposase, membrane organization and biogenesis
YDR097C	Msh6	2.52		Protein required for mismatch repair in mitosis and meiosis
YDR104C	Spo71	2.06		Required for spore wall formation during sporulation; dispensible for nuclear divisions during meiosis
YDR105C	Tms1	2.24		Putative membrane protein, conserved in mammals
YDR215C		10.24		Hypothetical protein
YDR216W	Adr1	4.42	2.46	Controls expression of ADH2, peroxisomal genes, & genes required for EtOH, glycerol, & fatty acid use
YDR242W	Amd2	3.22		Putative amidase
YDR253C	Met32		2.02	Zinc finger DNA binding factor, transcriptional regulator of sulfur amino acid metabolism
YDR304C	Cpr5	2.96	2.48	Peptidyl-prolyl cis-trans isomerase (cyclophilin) of the endoplasmic reticulum
YDR374C		2.42	2.19	Similarity to hypothetical A. thaliana protein BAC F21M12

Appendix 4.1 Genes induced by 2 fold or greater in *cdc53-1* and *cdc34-2* mutants

ORF	Yeast name	*cdc53-1* fold-change	*cdc34-2* fold-change	Description
YDR380W	Aro10	3.08	2.58	Phenylpyruvate decarboxylase, catalyzes decarboxylation of phenylpyruvate to phenylacetaldehyde
YDR406W	Pdr15	2.06		Probable multidrug resistance transporter, ATP-binding cassette (ABC) transporter activity
YDR461W	Mfa1	2.68		a-factor mating pheromone precursor
YDR523C	Sps1	2.16		Serinethreonine kinase homologous to Ste20p, required for spore wall formation
YEL008W		4.78		Hypothetical protein
YEL059W		2.7		Hypothetical protein
YEL060C	Prb1	2		Vacuolar protease B, needed for protein degradation during sporulation, & proper spore morphology
YEL065W	Sit1	2.06		Ferrioxamine B transporter, transcription is induced during iron deprivation and diauxic shift
YER011W	Tir1		2.46	Encodes a stress-response cell wall mannoprotein, regulated by acidic pH & cold-shock
YER028C	Mig3		4.46	Probable transcriptional repressor involved in response to toxic agents such as hydroxyurea
YER029C	Smb1		2.18	Associated with U1 snRNP
YER073W	Ald5	2.21		Aldehyde dehydrogenase (NAD+), activated by K+
YER081W	Ser3	3.73	2.44	3-phosphoglycerate dehydrogenase, catalyzes the first step in serine and glycine biosynthesis
YER096W	Shc1		2.32	Sporulation-specific activator of Chs3p,transcriptionally induced at alkaline pH
YER121W		2.56		Hypothetical protein
YER175C	Tmt1	3.56	2.05	Trans-aconitate Methyltransferase 1
YER187W			2.13	Similarity to killer toxin KHS precursor
YFL014W	Hsp12	2.79	2.08	Induced by heat shock, entry into stationary phase, depletion of glucose, and addition of lipids
YFL017C	Gna1		2.02	Involved in UDP-N-acetylglucosamine biosynthesis
YFL017W-A	Smx2	2.3	2.02	snRNP G protein, nuclear mRNA splicing, via spliceosome
YFL030W	Agx1	2.02		Alanine : glyoxylate aminotransferase, catalyzes the synthesis of glycine from glyoxylate
YFR018C		2.23		Similarity to human glutaminyl-peptide cyclotransferase
YFR023W	Pes4	4.89	4.67	Poly(A) binding proteinSuppressor of DNA polymerase epsilon mutation
YFR030W	Met10	3.48	3.73	Subunit alpha of assimilatory sulfite reductase
YGL032C	Aga2	2.44	2.21	Adhesion subunit of a-agglutinin of a-cells
YGL063W	Pus2		2.24	Pseudouridine synthase 2
YGL081W		2.89	3.17	Hypothetical protein
YGL117W		6.7	2.64	Hypothetical protein
YGL121C	Gpg1	2.02		Involved in regulation of pseudohyphal growth; requires Gpb1p or Gpb2p to interact with Gpa2p
YGL184C	Str3		2.62	Sulfur Transfer
YGL230C		4.49		Hypothetical protein
YGR032W	Fks2	3.38	2.35	Catalytic component of 1,3-beta-D-glucan synthase
YGR049W	Scm4		2.26	Protein that suppresses ts allele of *CDC4* when overexpressed
YGR053C		2.18	2.21	Hypothetical protein

Appendix 4.1 Genes induced by 2 fold or greater in *cdc53-1* and *cdc34-2* mutants

ORF	Yeast name	*cdc53-1* fold-change	*cdc34-2* fold-change	Description
YGR065C	Vht1	2.08		Similarity to P.putida phthalate transporter, vitamin H transporter
YGR131W			2.08	Strong similarity to Nce2p
YGR236C	Spg1	2.21		Protein required for survival at high temperature during stationary phase
YGR243W	Fmp43	2.76	2.81	The authentic, non-tagged protein was localized to mitochondria
YGR278W	Cwc1	2.48	2.05	Essential protein, component of a complex containing Cef1p, putative spliceosomal component
YHL035C	Vmr1	3.17		Protein of unknown function, member of the ATP-binding cassette (ABC) family, integral to membrane
YHR018C	Arg4	5.36	2.56	Argininosuccinate lyase
YHR022C		3.2		RAS-related protein
YHR029C		2.39		Thymidylate synthase
YHR033W		5.53	4.39	Unknown function
YHR054C			2.06	Weak similarity to YOR262w
YHR071W	Pcl5	6.02	3.68	Cyclin, interacts with Pho85
YHR137W	Aro9	2.62		Aromatic aminotransferase, catalyzes the first step of Trp, Phe, and Tyr catabolism
YHR176W	Fmo1		2.08	Flavin-containing monooxygenase
YIL024C		2.02		Hypothetical protein
YIL059C		2.37	3.05	Hypothetical protein
YIL063C	Yrb2	2.14	2.44	Nuclear protein, involved in nuclear export
YIL066C	Rnr3		2.66	Ribonucleotide-diphosphate reductase (RNR), large subunit
YIL099W	Sga1	2.68	4.13	Intracellular sporulation-specific glucoamylase, glucan 1,4-alpha-glucosidase activity
YIL121W	Qdr2	4.78	2.72	Similarity to antibiotic resistance proteins
YIL136W	OM45		2.02	Major constituent of the mitochondrial outer membrane
YIL152W		2.33	2	Hypothetical protein
YIL155C	Gut2	2.06		Mitochondrial glycerol-3-phosphate dehydrogenase; expression is repressed by glucose and cAMP
YIL160C	Pot1	2.19		Peroxisomal 3-oxoacyl CoA thiolase
YIL164C	Nit1	2.5		Nitrilase, member of the nitrilase superfamily
YIL165C		2.85		Putative pseudogene
YIR010W		2.16		Hypothetical protein
YIR019C	Muc1Flo11		3.22	GPI-anchored cell surface glycoprotein required for pseudohyphal formation and invasive growth
YIR028W	Dal4	3.73		Allantoin permease; expression sensitive to nitrogen catabolite repression and induced by allophanate
YIR034C	Lys1	2.24		Saccharopine dehydrogenase, lysine biosynthesis, aminoadipic pathway
YIR043C		2.05	2.72	Putative pseudogene
YJL037W		3.08	2.19	Strong similarity to hypothetical protein YJL038c
YJL038C		17.68	11.14	Strong similarity to hypothetical protein YJL037w
YJL045W	SDH1b		3.25	Strong similarity to succinate dehydrogenase flavoprotein (sdh1)

Appendix 4.1 Genes induced by 2 fold or greater in *cdc53-1* and *cdc34-2* mutants

ORF	Yeast name	*cdc53-1* fold-change	*cdc34-2* fold-change	Description
YJL079C	Pry1	3.01	2.66	Protein of unknown function
YJL088W	Arg3		2.74	Ornithine carbamoyltransferase (carbamoylphosphate:L-ornithine carbamoyltransferase)
YJL089W	Sip4	2.46	2.35	Shows homology to DNA binding domain of Gal4p, has a leucine zipper motif and acidic region
YJR010W	Met3	3.08	4.92	ATP sulfurylase, catalyzes the primary step of intracellular sulfate activation
YJR025C	Bna1	2.99	2.72	3-hydroxyanthranilic acid dioxygenase, required for biosynthesis of nicotinic acid
YJR072C	Npa3	2.26	2.85	Protein required for cell viability
YJR078W	Bna2	4.56	4.78	Required for biosynthesis of nicotinic acid from tryptophan via kynurenine pathway
YJR079W		5	4.78	Questionable ORF
YJR109C	Cpa2	3.56		Catalyzes a step in the synthesis of citrulline, an arginine precursor
YJR112W	Nnf1		2.37	Essential component of the MIND kinetochore complex
YJR130C	Str2	2.89		Cystathionine gamma-synthase activity
YJR137C	Ecm17		2.23	Sulfite reductase beta subunit, involved in amino acid biosynthesis.
YJR154W			2.44	Hypothetical protein
YJR155W	Aad10		2.05	Putative aryl-alcohol dehydrogenase
YJR156C	Thi11	2.32	2.66	Proposed biosynthetic enzyme involved in pyrimidine biosynth. Pathway
YKL001C	Met14		3.35	Required for sulfate assimilation and involved in methionine metabolism
YKL023W		2.21		Weak similarity to human cyclin II
YKL050C			2.05	Similarity to YMR031c
YKL093W	Mbr1		2.08	MBR1 protein precursor
YKL162C-A		3.51		Similar to PIR1, PIR2 and PIR3 proteins
YKL163W	Pir3	2.92		Cell wall organization and biogenesis
YKL178C	Ste3	2	2.05	Cell surface a factor receptor, transcribed in alpha cells and required for mating by alpha cells
YKL188C	Pxa2		2.44	Peroxisomal ABC transporter 2
YKL199C	Ykt9	2.14		Protein of unknown function
YKL218C		3.51	2.52	Threonine dehydratase
YKR053C	Ysr3	2.02		Dihydrosphingosine 1-phosphate phosphatase, membrane protein involved in sphingolipid metabolism
YKR061W	Ktr2	2.03		Putative mannosyltransferase, involved in N-linked glycosylation of cell wall mannoproteins
YKR069W	Met1		2.23	Involved in sulfate assimilation, methionine metabolism, and siroheme biosynthesis
YKR080W	Mtd1		3.79	NAD-dependent 5,10-methylenetetrahydrafolate dehydrogenase
YLL012W		2.05		Similarity to triacylglycerol lipases
YLL055W			2.23	Similarity to Dal5p
YLL057C	Jlp1		3.68	Similar to Fe(II)-dependent sulfonatealpha-ketoglutarate dioxygenase
YLL067C			2.33	Strong similarity to subtelomeric encoded proteins
YLR042C		3.48	4.92	Hypothetical protein

Appendix 4.1 Genes induced by 2 fold or greater in *cdc53-1* and *cdc34-2* mutants

ORF	Yeast name	*cdc53-1* fold-change	*cdc34-2* fold-change	Description
YLR053C			2.08	Hypothetical protein
YLR092W	Sul2	2.09	3.51	High affinity sulfate permease, sulfate uptake is mediated by SUL1 and SUL2
YLR099C	Ict1		2.54	Protein of unknown function, null mutation leads to an increase in sensitivity to Calcofluor white
YLR100W	Erg27	2.18	2.62	3-keto sterol reductase
YLR152C		2.35		Similarity to YOR3165w and YNL095c
YLR231C	Bna5	2.09	2.89	Kynureninase, required for biosynthesis of nicotinic acid from tryptophan
YLR237W	Thi7	2.99	4.49	Thiamine transporter
YLR273C	Pig1		2.13	Putative type 1 phosphatase regulatory subunit
YLR280C			2.13	Questionable ORF
YLR329W	rec102		2.26	mRNA is induced early in sporulation, required for wild-type level of chromosome pairing
YLR343W			2.03	Strong similarity to Gas1p and C.albicans pH responsive protein
YLR364W			2.37	Hypothetical protein
YLR377C	Fbp1		2.03	Fructose-1,6-bisphosphatase, required for glucose metabolism
YML058W	Hug1	2.72		Involved in the Mec1p-mediated checkpoint pathway, responds to DNA damage or replication arrest
YML070W	Dak1		2.05	Putative dihydroxyacetone kinase response to stress
YML109W	Zds2	2.92	2.33	Protein that interacts with silencing proteins at the telomere, involved in transcriptional silencing
YML133C			2.21	Hypothetical protein Y .2
YMR062C	Ecm40	4.09	2.16	Catalyzes the fifth step in arginine biosynthesis
YMR070W	Mot3		2.11	DNA-binding protein implicated in heme-dependent repression
YMR095C	Sno1	5.2	3.85	Stationary phase induced gene
YMR096W	Snz1	4.06	2.62	Involved in cellular response to nutrient limitation and growth arrest
YMR101C	Srt1	2.46	2.52	Cis-prenyltransferase involved in dolichol synthesis
YMR107W	Spg4	4.89	2.96	Protein required for survival at high temperature during stationary phase
YMR118C		3.3		Strong similarity to succinate dehydrogenase
YMR120C	Ade17		4	Enzyme of 'de novo' purine biosynthesis
YMR169C	Ald3	2.14		Aldehyde Dehydrogenase (NAD(P)+), induced in response to heat shock, and osmotic stress
YMR175W	Sip18		4.06	Responds to dessication and osmostress
YMR263W	Sap30		2.52	Subunit of the histone deacetylase B complex
YMR279C		2.11		Strong similarity to aminotriazole resistance protein
YMR303C	Adh2	3.1		Alcohol dehydrogenase II
YMR306W	Fks3	2.23		Has similarity to 1,3-beta-D-glucan synthase catalytic subunits Fks1p and Fks2p
YMR322C	Sno4	3.88	2.32	Possible chaperone and cysteine protease
YNL046W		2.16	2.08	Hypothetical protein
YNL202W	Sps19	3.3	3.85	Late sporulation specific gene which may function during spore wall formation

Appendix 4.1 Genes induced by 2 fold or greater in *cdc53-1* and *cdc34-2* mutants

ORF	Yeast name	*cdc53-1* fold-change	*cdc34-2* fold-change	Description
YNL228W		11.85		Questionable ORF
YNL270C	Alp1	3.1	2.23	Basic amino acid transporter, involved in uptake of cationic amino acids
YNL277W	Met2		3.51	Catalyzes the first step of the methionine biosynthetic pathway
YNL289W	Pcl1	2.37	2.81	G1 cyclin that associates with PHO85
YNL333W	Snz2		2.21	Stationary phase-induced gene family
YNR050C	Lys9	2.35	2.02	Lysine biosynthesis, aminoadipic pathway, saccharopine dehydrogenase
YNR064C		3.15	2.79	Similarity to R.capsulatus 1-chloroalkane halidohydrolase
YNR065C	Ysn1	3.15	2.66	Sortilin homolog, interacts with proteins of the endocytic machinery
YNR073C		2.32	2.39	Strong similarity to E.coli D-mannonate oxidoreductase
YOL010W	Rcl1		2.18	RNA terminal phosphate cyclase-like protein involved in rRNA processing at sites A0, A1, and A2
YOL024W		7.02	8.57	Hypothetical protein
YOL037C		4.81		Questionable ORF
YOL058W	Arg1	4.56	3.7	Arginosuccinate synthetase
YOL091W	Spo21	3.48		Component of the meiotic outer plaque of the spindle pole body, required prior to prospore membrane formation
YOL100W	Pkh2	2.08		SerThr protein kinase, Pkb-activating Kinase Homologue, MAPKKK during cell wall biogenes
YOL104C	Ndj1		2.35	Meiosis-specific telomere protein
YOL132W	Gas4	2.33	2	Similarity to glycophospholipid-anchored surface glycoprotein Gas1p, localizes to the cell wall
YOL155C		4.74	4.13	Similarity to glucan 1,4-alpha-glucosidase Sta1p and YAR066w
YOL160W		6.2	5.7	Hypothetical protein
YOL161C			2.74	Strong similarity to members of the Srp1pTip1p family
YOR011W	Aus1		2.56	Transporter of the ATP-binding cassette family, involved in uptake of sterols and anaerobic growth
YOR028C	Cin5		2.74	Basic leucine zipper transcriptional factor, mediates drug resistance and salt tolerance
YOR031W	Crs5	2.52	2.06	Copper-binding metallothionein, required for wild-type copper resistance
YOR100C	Crc1	3.46	2.32	Similarity to mitochondrial carrier proteins
YOR114W			2.08	Hypothetical protein
YOR128C	Ade2		2.68	Phosphoribosylamino-imidazole-carboxylase
YOR177C	Mpc54	2.11		Component of the meiotic outer plaque, a membrane-organizing center
YOR185C	Gsp2		2.39	Involved in the maintenance of nuclear organization, RNA processing and transport
YOR192C			2.08	Strong similarity to Thi10p
YOR202W	His3	3.05	2.46	Imidazoleglycerol-phosphate dehydratase, catalyzes the sixth step in histidine biosynthesis
YOR203W		2.96	2.56	Protein required for cell viability
YOR226C	Isu2		2.08	NifU-like protein A
YOR253W	Nat5	2.09		Peptide alpha-N-acetyltransferase activity
YOR302W		2.7		CPA1 leader peptide

Appendix 4.1 Genes induced by 2 fold or greater in *cdc53-1* and *cdc34-2* mutants

ORF	Yeast name	*cdc53-1* fold-change	*cdc34-2* fold-change	Description
YOR303W	Cpa1	2.64		Catalyzes a step in the synthesis of citrulline, an arginine precursor
YOR348C	Put4	2.35		Proline-specific permease (also capable of transporting alanine and glycine)
YOR382W	Fit2	3.08		GPI-achored cell wall mannoprotein, involved in the retention of siderophore-iron in the cell wall
YPL017C		2.32		Putative S-adenosylmethionine-dependent methyltransferase of the seven beta-strand family
YPL033C			5.08	Weak similarity to YLR426w
YPL058C	Pdr12	2.16		Plasma membrane, weak-acid-inducible ATP-binding cassette (ABC) transporter
YPL081W	Rps9A		2.08	Ribosomal protein S9A (S13) (rp21) (YS11)
YPL092W	Ssu1	4.67	3.48	Sensitive to sulfiteputative sulfite pumpplasma membrane
YPL135W	Isu1	2.33		NifU-like protein A, Iron-sulfur cluster nifU-like protein
YPL163C	Svs1	2.23	2.41	Serine and threonine rich protein, involved in vanadate resistance, Cell wall.
YPL171C	Oye3	4.56	5.12	NAD(P)H dehydrogenase
YPL223C	Gre1	2.66	3.25	Stress induced (osmotic, ionic, oxidative, heat shock & heavy metals); regulated by the HOG pathway
YPL258C	Thi21	2.79	2	Transcribed in the presence of low level of thiamine and repressed in high level of thiamine
YPL264C		3.51	2.16	Strong similarity to YMR253c
YPR006C	Icl2		2.18	Functions in the methylcitrate cycle to catalyze the conversion of 2-methylisocitrate to succinate and pyruvate
YPR027C			2.23	Similarity to YNL019c and YNL033w
YPR077C		2.35		Questionable ORF
YPR078C		2.85		Hypothetical protein
YPR143W		2	2.33	Hypothetical protein
YPR167C	Met16	2.64	2.72	3 phosphoadenylylsulfate reductase
YPR193C	Hpa2	2.44		Tetrameric histone acetyltransferase, similarity to Gcn5p, Hat1p, Elp3p, and Hpa3p
YPR194C	Opt2	2.66		Oligopeptide transporter
YPR195C		2.3		Hypothetical protein
YPR204W			2.09	Strong similarity to subtelomeric encoded proteins

Appendix 4.2 Promoter analysis of the induced genes in *cdc53-1* and *cdc34-2* mutants

ORF	Yeast name	SCB elements	MCB elements	GCN4(1 mismatch)	GCN4 promoter	Rim1 (1 mismatch)	Rim1 promoter	STRE elements	HSTF elements	met31/32 promoter	Cbf1 promoter	Met4 promoter
YAL034W-A	Mtw1	1	0	2	0	0	0	0	1	0	0	0
YAL061W		0	0	1	0	1	0	3	3	0	0	0
YAL062W	Gdh3	0	0	3	0	2	0	0	0	0	0	0
YAL063C	Flo9	0	0	1	0	0	0	0	0	0	0	0
YAL067C	Seo1	0	0	1	0	0	0	1	2	1	0	0
YAR015W	Ade1	0	0	3	2	0	0	1	1	0	0	0
YAR069C		0	0	0	0	0	0	0	1	0	0	0
YBL043W	Ecm13	0	0	3	2	0	0	0	2	0	0	0
YBL065W		0	0	3	1	0	0	0	0	0	0	0
YBR040W	Fig1	0	0	1	0	1	0	0	2	0	0	0
YBR043C	Qdr3	0	0	4	1	1	0	0	1	0	0	0
YBR047W	Fmp23	0	0	0	1	0	0	2	1	0	0	0
YBR076W	Ecm8	2	0	2	2	2	0	0	0	0	0	0
YBR093C	Pho5	0	0	3	0	1	0	0	0	0	0	0
YBR096W		0	0	2	0	0	0	0	0	0	0	0
YBR116C		0	0	2	1	0	0	0	3	0	0	0
YBR117C	Tki2	0	0	1	0	0	0	1	1	0	0	0
YBR145W	Adh5	2	0	4	1	0	0	1	3	0	0	0
YBR147W		0	0	3	2	0	0	1	0	0	0	0
YBR256C	Rib5	0	1	3	0	1	0	0	0	0	0	0
YBR285W		0	0	2	0	1	0	2	3	0	0	0
YBR294W	Sul1	0	0	4	1	1	0	0	1	0	0	0
YBR295W	Pca1	1	0	1	0	3	0	0	0	0	0	0
YBR296C	Pho89	0	0	3	1	1	0	0	1	0	0	0
YCL024W	Kcc4	1	2	2	0	0	0	1	1	0	0	0
YCL026C	Frm2	0	0	2	0	0	0	0	1	0	0	1
YCL030C	His4	0	1	6	3	0	0	1	0	0	0	0
YCR073C	Ssk22	1	1	1	0	1	0	1	0	0	0	0
YCR098C	Git1	1	0	3	0	0	0	2	2	0	0	0
YDL021W	Gpm2	2	0	1	0	1	0	1	2	0	0	0
YDL059C	Rad59	0	1	0	0	2	0	0	1	0	1	0
YDL170W	Uga3	0	0	4	1	0	0	1	0	0	0	0
YDL181W	Inh1	0	0	2	1	1	0	2	2	0	0	0
YDL182W	Lys20	0	0	1	0	0	0	0	1	0	0	1
YDL198C	Ggc1	1	0	6	2	0	0	0	0	0	0	1
YDL218W		0	0	2	0	0	0	1	0	0	0	0
YDL222C	Fmp45	0	0	3	1	0	0	1	1	0	0	0
YDL223C	Hbt1	0	1	0	0	1	0	2	0	0	0	0
YDR010C		0	0	2	0	0	0	1	0	0	0	0
YDR034W-B		0	0	0	0	1	0	3	1	0	0	0
YDR035W	Aro3	0	0	1	0	1	0	1	0	0	0	0
YDR038C	Ena5	0	1	0	0	2	0	0	1	0	0	0

Appendix 4.2 Promoter analysis of the induced genes in *cdc53-1* and *cdc34-2* mutants

ORF	Yeast name	SCB elements	MCB elements	GCN4(1 mismatch)	GCN4 promoter	Rim1 (1 mismatch)	Rim1 promoter	STRE elements	HSTF elements	met31/32 promoter	Cbf1 promoter	Met4 promoter
YDR039C	Ena2	0	1	0	0	2	0	0	1	0	0	0
YDR041W	Rsm10	0	0	4	1	0	0	1	1	0	0	0
YDR042C		2	2	2	0	0	0	0	1	0	0	0
YDR046C	Bap3	1	0	2	0	0	0	1	0	0	0	0
YDR048C		0	0	2	0	0	0	1	1	0	0	0
YDR054C	Cdc34	0	0	1	0	0	0	0	1	0	0	0
YDR056C		0	0	4	0	3	0	1	1	0	0	0
YDR058C	Tgl2	0	3	3	0	0	0	0	0	0	0	0
YDR059C	Ubc5	0	1	2	0	0	0	0	1	0	0	0
YDR061W		0	0	2	1	1	0	0	1	0	0	0
YDR068W	Dos2	0	0	2	1	0	0	1	0	0	0	0
YDR070C	Fmp16	0	0	0	0	1	0	1	1	0	0	0
YDR073W	Snf11	1	1	0	0	2	1	0	1	0	0	0
YDR076W	Rad55	0	1	2	0	0	0	1	0	0	1	0
YDR085C	Afr1	0	0	0	0	2	1	1	0	0	0	0
YDR088C	Slu7	0	0	1	0	0	0	0	2	0	0	1
YDR089W		0	0	2	1	2	0	1	0	0	0	0
YDR097C	Msh6	1	2	0	0	1	0	2	2	0	0	0
YDR104C	Spo71	0	0	1	0	2	0	0	1	0	0	0
YDR105C	Tms1	0	0	1	0	0	0	0	1	0	0	0
YDR215C		0	0	1	0	1	0	0	1	0	0	0
YDR216W	Adr1	0	0	0	0	1	0	0	1	0	0	0
YDR242W	Amd2	0	0	2	0	5	0	0	0	0	0	0
YDR253C	Met32	0	0	2	0	1	0	0	2	0	0	0
YDR304C	Cpr5	0	0	5	1	0	0	1	2	0	0	0
YDR374C		1	0	3	0	0	0	0	0	0	0	0
YDR380W	Aro10	0	1	0	0	1	0	0	1	0	0	0
YDR406W	Pdr15	0	0	0	0	0	0	3	0	0	0	0
YDR461W	Mfa1	0	0	1	0	0	0	0	0	0	0	0
YDR523C	Sps1	1	1	2	1	1	0	0	0	0	0	0
YEL008W		0	0	0	0	1	0	1	0	0	0	0
YEL059W		0	0	3	1	1	0	1	1	0	0	0
YEL060C	Prb1	0	0	1	0	1	0	1	1	0	0	0
YEL065W	Sit1	0	0	1	0	0	0	0	0	0	0	0
YER011W	Tir1	0	0	2	0	0	0	0	0	0	0	0
YER028C	Mig3	0	2	1	0	0	0	1	1	0	0	0
YER029C	Smb1	0	0	4	0	0	0	1	1	0	0	0
YER073W	Ald5	0	0	3	1	0	0	1	1	0	0	0
YER081W	Ser3	0	0	1	0	0	0	1	2	1	0	0
YER096W	Shc1	0	1	3	1	0	0	1	1	0	0	0
YER121W		0	0	3	0			2	2	0	0	0
YER175C	Tmt1	0	0	6	1	1	0	0	0	0	0	0

Appendix 4.2 Promoter analysis of the induced genes in *cdc53-1* and *cdc34-2* mutants

ORF	Yeast name	SCB elements	MCB elements	GCN4(1 mismatch)	GCN4 promoter	Rlm1 (1 mismatch)	Rlm1 promoter	STRE elements	HSTF elements	met31/32 promoter	Cbf1 promoter	Met4 promoter
YER187W		0	0	2	0	0	0	0	0	0	0	0
YFL014W	Hsp12	0	0	0	0	2	0	5	0	0	0	0
YFL017C	Gna1	0	0	1	0	0	0	0	2	0	0	0
YFL017W-A	Smx2	0	0	4	0	2	0	2	0	0	0	0
YFL030W	Agx1	0	0	1	0	2	0	1	1	0	0	0
YFR018C		1	1	2	1	1	0	1	0	0	0	0
YFR023W	Pes4	1	0	2	0	1	0	0	0	1	0	0
YFR030W	Met10	1	1	5	0	1	0	1	2	0	0	0
YGL032C	Aga2	0	0	2	0	1	0	1	2	0	0	0
YGL063W	Pus2	0	0	1	0	1	0	1	1	0	0	0
YGL081W		0	0	0	0	0	0	0	2	1	0	0
YGL117W		0	0	2	1	1	0	0	0	0	0	0
YGL121C	Gpg1	0	0	0	0	1	0	0	2	0	0	1
YGL184C	Str3	1	0	5	2	0	0	0	2	0	0	0
YGL230C		0	0	2	0	1	0	0	2	0	0	0
YGR032W	Fks2	2	0	0	0	2	0	0	0	1	0	0
YGR049W	Scm4	1	0	2	0	0	0	0	0	0	0	0
YGR053C		0	0	1	0	0	0	1	1	0	0	0
YGR065C	Vht1	1	0	3	1	1	0	0	0	0	0	0
YGR131W		1	0	0	0	0	0	0	1	0	0	0
YGR236C	Spg1	0	1	1	0	0	0	0	1	0	0	0
YGR243W	Fmp43	0	0	0	0	0	0	1	1	0	0	0
YGR278W	Cwc1	0	0	2	0	2	0	0	3	0	0	0
YHL035C	Vmr1	0	0	0	0	1	0	2	0	0	0	0
YHR018C	Arg4	1	0	3	1	0	0	1	1	0	0	0
YHR022C		0	0	0	0	0	0	0	3	0	0	0
YHR029C		0	0	3	0	1	0	0	0	0	0	0
YHR033W		0	0	0	0	1	0	1	1	0	0	0
YHR054C		0	0	2	0	0	0	1	1	0	0	0
YHR071W	Pcl5	0	0	1	0	0	0	1	1	0	0	0
YHR137W	Aro9	0	0	2	1	0	0	0	0	0	0	0
YHR176W	Fmo1	1	0	0	0	0	0	1	1	0	0	0
YIL024C		0	0	3	0	0	0	0	1	0	0	0
YIL059C		0	0	4	0	3	0	1	0	0	0	0
YIL063C	Yrb2	1	1	6	1	0	0	1	1	0	0	0
YIL066C	Rnr3	3	2	1	0	1	0	0	1	0	0	0
YIL099W	Sga1	1	0	3	0	0	0	5	0	0	0	0
YIL121W	Qdr2	0	0	2	0	0	0	0	0	0	0	0
YIL136W	OM45	0	0	2	1	0	0	2	3	0	0	0
YIL152W		0	0	1	0	0	0	1	1	0	0	0
YIL155C	Gut2	0	0	2	0	0	0	1	1	0	0	0
YIL160C	Pot1	0	1	0	0	1	0	0	2	0	0	0

Appendix 4.2 Promoter analysis of the induced genes in *cdc53-1* and *cdc34-2* mutants

ORF	Yeast name	SCB elements	MCB elements	GCN4(1 mismatch)	GCN4 promoter	Rim1 (1 mismatch)	Rim1 promoter	STRE elements	HSTF elements	met31/32 promoter	Cbf1 promoter	Met4 promoter
YIL164C	Nit1	2	0	3	1	0	0	1	1	0	0	0
YIL165C		0	0	1	0	1	0	1	2	0	0	0
YIR010W		1	0	2	0	2	0	1	0	0	0	0
YIR019C	Muc1Flo11	0	0	1	0	0	0	0	2	0	0	0
YIR028W	Dal4	0	0	0	0	0	0	0	1	0	0	0
YIR034C	Lys1	0	0	5	3	0	0	1	0	0	0	0
YIR043C		0	0	1	0	1	0	0	1	0	0	0
YJL037W		0	0	2	0	1	1	1	0	0	0	0
YJL038C		0	0	1	0	0	0	1	0	1	0	0
YJL045W	SDH1b	0	1	1	0	1	0	0	0	0	0	1
YJL079C	Pry1	1	0	2	2	0	0	1	1	0	0	0
YJL088W	Arg3	2	1	6	2	0	0	0	2	0	0	0
YJL089W	Sip4	0	0	2	1	0	0	0	1	0	0	0
YJR010W	Met3	0	0	1	0	0	0	1	0	0	2	0
YJR025C	Bna1	0	0	2	1	0	0	0	1	0	0	0
YJR072C	Npa3	1	1	2	1	0	0	1	1	0	0	0
YJR078W	Bna2	1	0	3	2	1	0	0	1	0	0	0
YJR079W		0	1	0	0	0	0	0	1	0	0	0
YJR109C	Cpa2	0	0	3	2	3	0	1	2	0	0	0
YJR112W	Nnf1	0	0	4	0	0	0	0	1	0	0	0
YJR130C	Str2	0	0	2	0	0	0	0	2	0	0	1
YJR137C	Ecm17	0	0	4	1	1	0	0	2	0	0	0
YJR154W		1	2	6	1	1	0	0	1	0	0	0
YJR155W	Aad10	0	0	3	0	0	0	0	1	0	0	0
YJR156C	Thi11	1	0	1	0	0	0	0	1	0	0	0
YKL001C	Met14	1	1	3	0	0	0	0	4	0	1	0
YKL023W		0	0	2	0	0	0	1	2	0	0	0
YKL050C		2	1	2	0	1	0	2	3	0	0	0
YKL093W	Mbr1	0	0	1	0	0	0	1	0	0	0	0
YKL162C-A		0	0	3	0	0	0	1	0	0	0	0
YKL163W	Pir3	0	0	0	0	1	1	1	1	1	0	0
YKL178C	Ste3	0	0	2	0	2	0	1	1	0	0	0
YKL188C	Pxa2	0	0	3	0	0	0	0	0	0	0	0
YKL199C	Ykt9	0	1	1	0	0	0	0	0	0	0	0
YKL218C		0	0	5	1	0	0	0	0	0	0	0
YKR053C	Ysr3	0	1	1	0	1	0	0	1	0	0	0
YKR061W	Ktr2	0	0	1	0	2	1	0	1	0	0	0
YKR069W	Met1	0	0	7	0	1	0	0	2	1	0	0
YKR080W	Mtd1	0	0	4	2	1	0	0	0	0	0	0
YLL012W		0	1	0	0	4	0	0	1	0	0	0
YLL055W		0	0	4	0	0	0	2	1	0	0	0
YLL057C	Jlp1	0	0	4	1	0	0	1	2	0	0	0

Appendix 4.2 Promoter analysis of the induced genes in *cdc53-1* and *cdc34-2* mutants

ORF	Yeast name	SCB elements	MCB elements	GCN4(1 mismatch)	GCN4 promoter	Rlm1 (1 mismatch)	Rlm1 promoter	STRE elements	HSTF elements	met31/32 promoter	Cbf1 promoter	Met4 promoter
YLL067C		1	0	2	0	1	0	0	1	0	0	0
YLR042C		2	0	1	0	2	0	1	0	0	0	0
YLR053C		1	2	2	1	0	0	1	0	0	0	0
YLR092W	Sul2	0	0	2	0	0	0	0	1	0	2	0
YLR099C	Ict1	1	0	2	0	0	0	1	1	0	0	0
YLR100W	Erg27	0	0	0	0	0	0	1	1	0	0	0
YLR152C		0	0	2	1	0	0	1	1	0	0	0
YLR231C	Bna5	1	0	1	0	0	0	0	1	0	0	0
YLR237W	Thi7	1	0	6	1	1	0	0	3	0	0	0
YLR273C	Pig1	2	2	3	0	0	0	0	2	0	0	0
YLR280C		0	0	0	0	0	0	1	3	1	0	0
YLR329W	rec102	0	0	2	0	1	0	1	0	0	0	0
YLR343W		0	0	1	0	1	0	0	0	0	0	0
YLR364W		1	0	0	0	1	0	0	0	0	0	0
YLR377C	Fbp1	1	0	0	0	1	0	0	3	0	0	0
YML058W	Hug1	0	0	1	0	0	0	0	0	0	0	0
YML070W	Dak1	0	1	1	0	1	0	0	0	0	0	0
YML109W	Zds2	0	1	0	0	1	0	0	0	0	0	0
YML133C		1	0	0	0	0	0	0	1	0	0	0
YMR062C	Ecm40	0	0	4	1	0	0	0	0	0	0	0
YMR070W	Mot3	0	0	1	1	1	0	0	0	0	0	0
YMR095C	Sno1	0	0	6	3	1	0	0	0	0	0	0
YMR096W	Snz1	0	0	5	3	1	0	0	0	0	0	0
YMR101C	Srt1	0	0	0	0	1	0	0	1	0	0	0
YMR107W	Spg4	1	0	6	0	2	0	0	1	1	0	0
YMR118C		0	0	1	0	1	0	0	1	0	0	1
YMR120C	Ade17	0	0	5	2	0	0	1	1	0	0	0
YMR169C	Ald3	0	0	2	1	0	0	2	1	1	0	1
YMR175W	Sip18	0	0	3	0	0	0	3	0	0	0	0
YMR263W	Sap30	0	0	0	0	0	0	0	2	0	0	0
YMR279C		1	1	0	0	0	0	1	2	0	0	0
YMR303C	Adh2	1	0	0	0	2	0	2	0	0	0	0
YMR306W	Fks3	3	3	0	0	0	0	0	2	0	0	0
YMR322C	Sno4	0	0	2	0	0	0	2	5	0	0	0
YNL046W		0	0	2	0	1	0	1	0	0	0	0
YNL202W	Sps19	0	0	1	0	0	0	1	0	0	0	0
YNL228W		0	0	3	0	1	0	0	0	0	0	0
YNL270C	Alp1	0	0	2	0	0	0	0	1	0	0	0
YNL277W	Met2	0	0	4	0	1	0	0	1	0	1	0
YNL289W	Pcl1	4	1	0	0	0	0	0	1	0	0	0
YNL333W	Snz2	0	0	1	0	0	0	0	3	0	0	1
YNR050C	Lys9	0	0	2	0	0	0	1	3	1	0	0

Appendix 4.2 Promoter analysis of the induced genes in *cdc53-1* and *cdc34-2* mutants

ORF	Yeast name	SCB elements	MCB elements	GCN4(1 mismatch)	GCN4 promoter	Rlm1 (1 mismatch)	Rlm1 promoter	STRE elements	HSTF elements	met31/32 promoter	Cbf1 promoter	Met4 promoter
YNR064C		0	0	6	0	0	0	0	0	0	0	0
YNR065C	Ysn1	0	0	2	0	1	0	0	1	0	0	0
YNR073C		2	0	6	0	2	0	0	0	0	0	0
YOL010W	Rcl1	1	0	1	0	1	1	1	1	0	0	0
YOL024W		0	0	3	0	2	0	0	0	0	0	0
YOL037C		1	0	2	1	2	0	1	0	0	0	0
YOL058W	Arg1	0	0	6	2	1	0	0	0	0	0	0
YOL091W	Spo21	0	0	0	0	0	0	0	2	0	0	0
YOL100W	Pkh2	0	0	1	0	0	0	1	1	1	1	0
YOL104C	Ndj1	0	0	0	0	2	0	0	0	0	0	0
YOL132W	Gas4	0	0	1	1	0	0	0	0	0	0	0
YOL155C		0	0	4	0	0	0	1	2	0	0	0
YOL160W		0	0	0	0	0	0	1	1	0	0	0
YOL161C		1	1	1	0	1	0	1	1	0	0	0
YOR011W	Aus1	0	0	0	0	0	0	0	2	0	0	0
YOR028C	Cin5	0	0	0	0	0	0	1	1	0	0	0
YOR031W	Crs5	0	0	2	0	1	0	2	0	0	0	0
YOR100C	Crc1	0	0	3	1	0	0	1	1	0	0	0
YOR114W		2	1	2	0	0	0	1	1	0	0	0
YOR128C	Ade2	1	0	5	2	0	0	0	2	0	0	0
YOR177C	Mpc54	0	0	2	0	2	0	0	0	0	0	0
YOR185C	Gsp2	0	0	4	1	1	0	2	1	0	0	0
YOR192C		0	0	1	0	0	0	0	0	0	0	0
YOR202W	His3	0	0	5	2	0	0	0	3	0	0	0
YOR203W		0	0	2	0	0	0	2	2	0	0	0
YOR226C	Isu2	0	0	4	2	1	0	1	0	0	0	0
YOR253W	Nat5	0	0	0	0	1	0	0	2	0	0	0
YOR302W		0	0	3	2	0	0	3	0	0	0	0
YOR303W	Cpa1	0	0	3	2	1	0	2	0	0	0	0
YOR348C	Put4	0	1	1	0	2	0	3	3	0	0	0
YOR382W	Fit2	1	0	0	0	1	0	1	1	0	0	0
YPL017C		1	1	2	0	0	0	2	1	0	0	0
YPL033C		0	0	3	1	2	0	0	1	0	0	0
YPL058C	Pdr12	0	0	0	0	0	0	0	1	0	0	0
YPL081W	Rps9A	1	2	1	0	0	0	2	0	0	0	1
YPL092W	Ssu1	0	0	4	0	0	0	2	0	0	0	0
YPL135W	Isu1	0	0	3	1	1	0	2	2	0	0	0
YPL163C	Svs1	2	1	1	0	1	0	0	2	0	0	0
YPL171C	Oye3	1	0	1	0	2	0	0	1	0	1	0
YPL223C	Gre1	0	0	1	0	0	0	0	2	0	0	0
YPL258C	Thi21	0	3	0	0	1	0	1	2	0	0	0
YPL264C		1	0	5	1	1	0	1	2	0	0	0

Appendix 4.2 Promoter analysis of the induced genes in *cdc53-1* and *cdc34-2* mutants

ORF	Yeast name	SCB elements	MCB elements	GCN4(1 mismatch)	GCN4 promoter	Rlm1 (1 mismatch)	Rlm1 promoter	STRE elements	HSTF elements	met31/32 promoter	Cbf1 promoter	Met4 promoter
YPR006C	Icl2	0	0	0	0	0	0	0	1	0	0	0
YPR027C		0	0	1	0	0	0	0	0	0	0	0
YPR077C		0	0	0	0	0	0	0	0	0	0	0
YPR078C		1	0	1	0	1	0	0	0	0	0	0
YPR143W		0	0	4	0	0	0	0	1	0	0	0
YPR167C	Met16	0	0	4	1	0	0	0	1	0	1	0
YPR193C	Hpa2	0	0	3	0	1	1	1	1	0	0	0
YPR194C	Opt2	0	0	3	0	1	0	1	2	0	0	0
YPR195C		0	0	4	1	2	0	0	1	0	0	0
YPR204W		1	1	2	0	0	0	0	0	0	0	0

Appendix 4.3 Comparison between the transcriptional profiles of *cdc53-1* and *cdc34-2* mutants with published datasets (ref. 2, 5, 17, 18, 38, 52, 53)

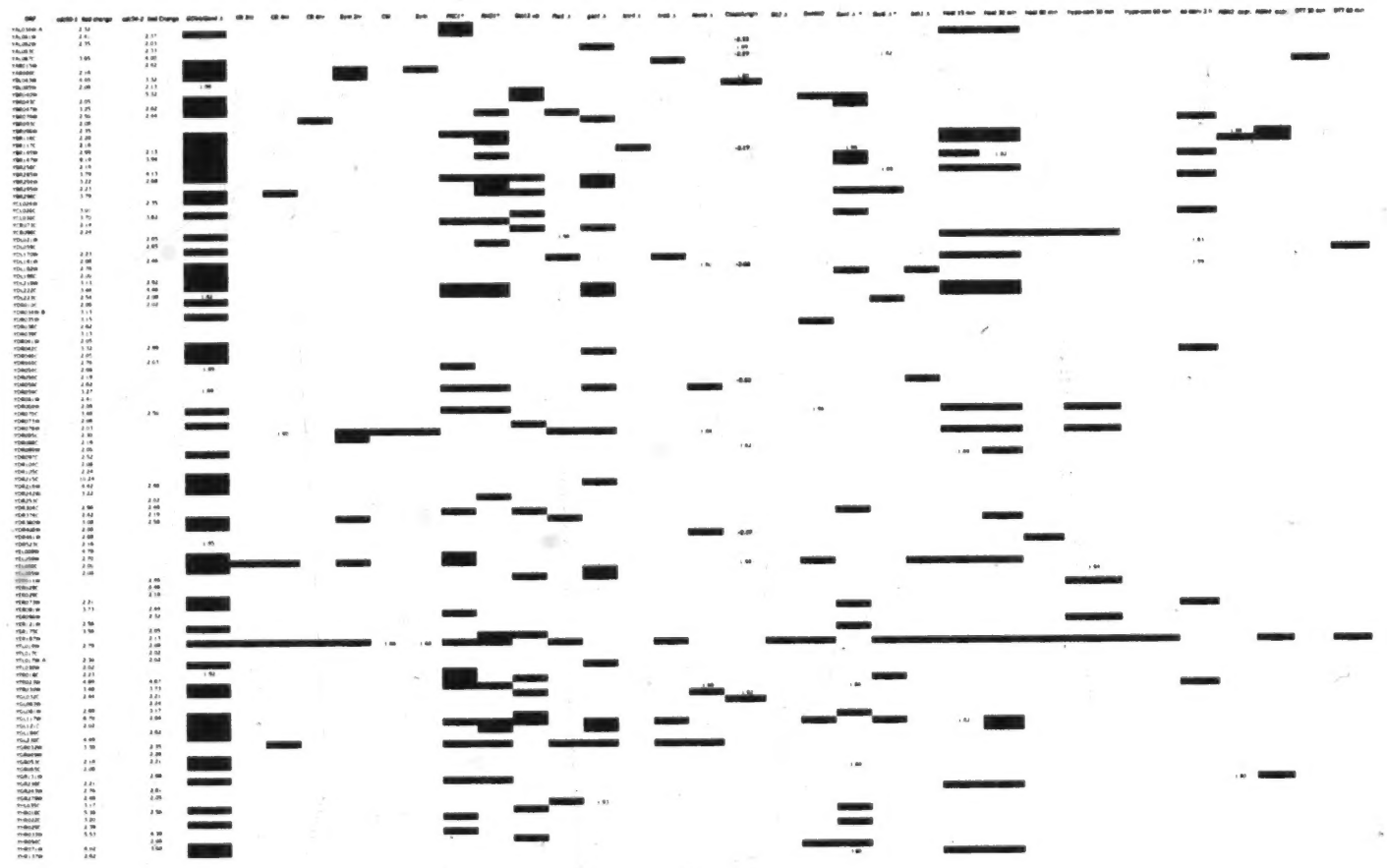

Appendix 4.3 Comparison between the transcriptional profiles of *cdc53-1* and *cdc34-2* mutants with published datasets (ref. 2, 5, 17, 18, 38, 52, 53)

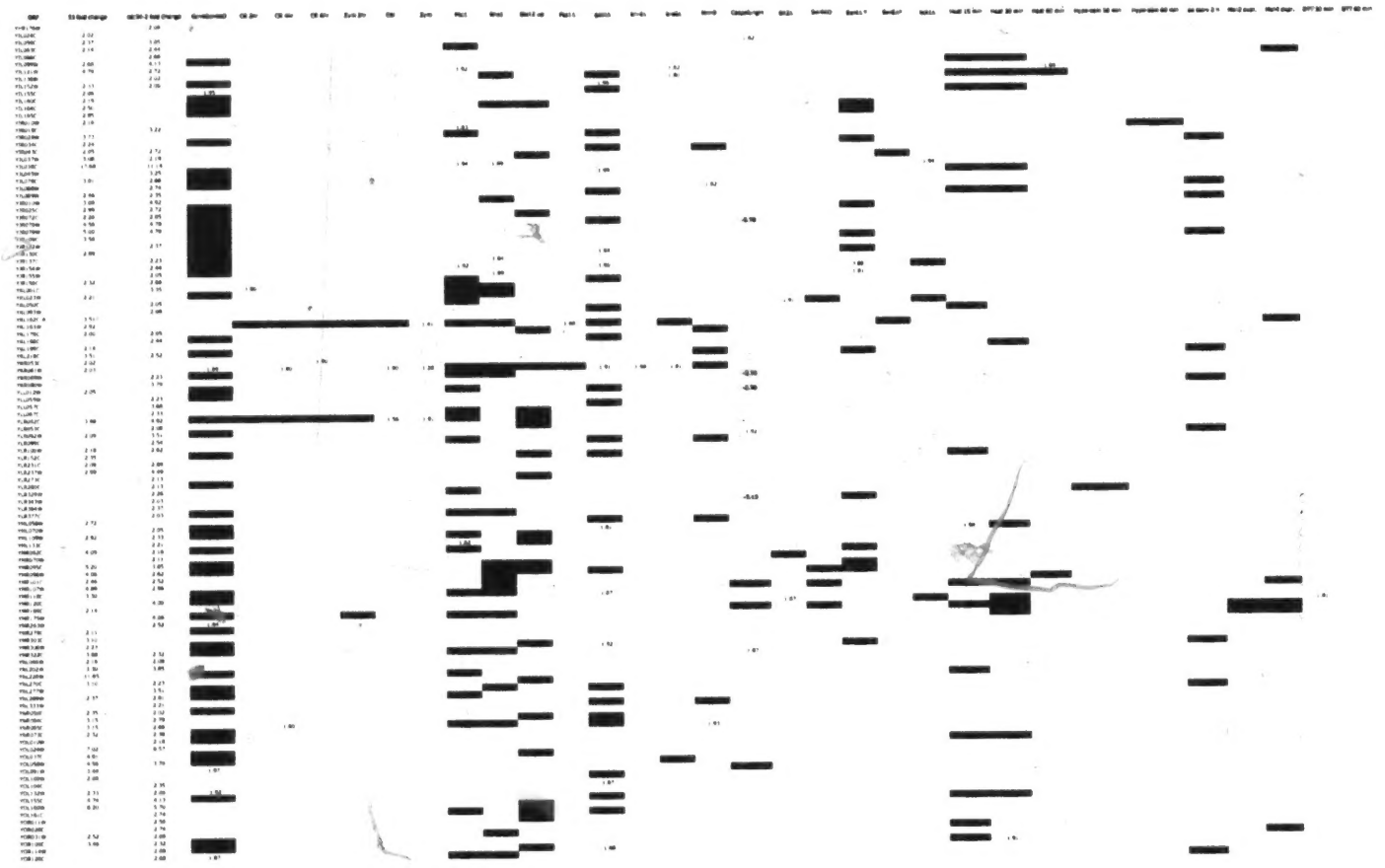

Appendix 4.3 Comparison between the transcriptional profiles of *cdc53-1* and *cdc34-2* mutants with published datasets (ref. 2, 5, 17, 18, 38, 52, 53)

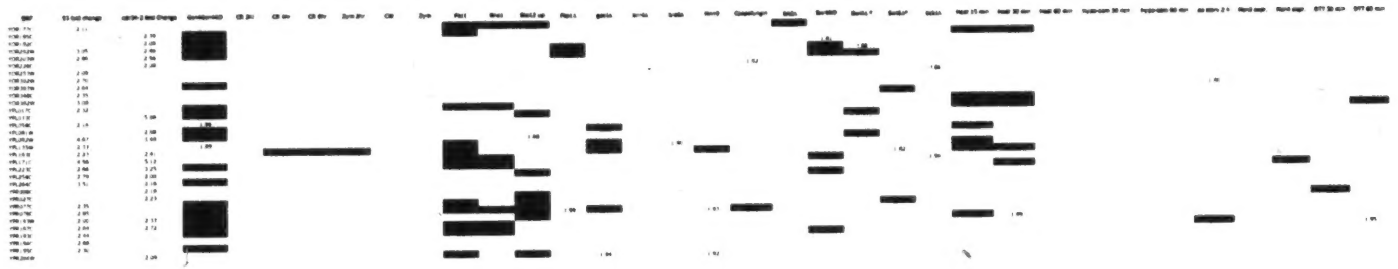

4.5 References

1. Andrews, B. J., and I. Herskowitz. 1989. Identification of a DNA binding factor involved in cell-cycle control of the yeast HO gene. Cell 57:21-9.
2. Baetz, K., J. Moffat, J. Haynes, M. Chang, and B. Andrews. 2001. Transcriptional coregulation by the cell integrity mitogen-activated protein kinase Slt2 and the cell cycle regulator Swi4. Mol Cell Biol 21:6515-28.
3. Bartel, P. L., and S. Fields. 1995. Analyzing protein-protein interactions using two-hybrid system. Methods Enzymol 254:241-63.
4. Blaiseau, P. L., and D. Thomas. 1998. Multiple transcriptional activation complexes tether the yeast activator Met4 to DNA. Embo J 17:6327-36.
5. Boorsma, A., H. de Nobel, B. ter Riet, B. Bargmann, S. Brul, K. J. Hellingwerf, and F. M. Klis. 2004. Characterization of the transcriptional response to cell wall stress in Saccharomyces cerevisiae. Yeast 21:413-27.
6. Bourdineaud, J. P. 2000. At acidic pH, the diminished hypoxic expression of the SRP1/TIR1 yeast gene depends on the GPA2-cAMP and HOG pathways. Res Microbiol 151:43-52.
7. Braus, G. H. 1991. Aromatic amino acid biosynthesis in the yeast Saccharomyces cerevisiae: a model system for the regulation of a eukaryotic biosynthetic pathway. Microbiol Rev 55:349-70.
8. Braus, G. H., O. Grundmann, S. Bruckner, and H. U. Mosch. 2003. Amino acid starvation and Gcn4p regulate adhesive growth and FLO11 gene expression in Saccharomyces cerevisiae. Mol Biol Cell 14:4272-84.
9. Cappellaro, C., C. Baldermann, R. Rachel, and W. Tanner. 1994. Mating type-specific cell-cell recognition of Saccharomyces cerevisiae: cell wall attachment and active sites of a- and alpha-agglutinin. Embo J 13:4737-44.
10. Caro, L. H., G. J. Smits, P. van Egmond, J. W. Chapman, and F. M. Klis. 1998. Transcription of multiple cell wall protein-encoding genes in Saccharomyces cerevisiae is differentially regulated during the cell cycle. FEMS Microbiol Lett 161:345-9.
11. Caro, L. H., H. Tettelin, J. H. Vossen, A. F. Ram, H. van den Ende, and F. M. Klis. 1997. In silicio identification of glycosyl-phosphatidylinositol-anchored plasma-membrane and cell wall proteins of Saccharomyces cerevisiae. Yeast 13:1477-89.
12. de Nobel, H., C. Ruiz, H. Martin, W. Morris, S. Brul, M. Molina, and F. M. Klis. 2000. Cell wall perturbation in yeast results in dual phosphorylation of the Slt2/Mpk1 MAP kinase and in an Slt2-mediated increase in FKS2-lacZ expression, glucanase resistance and thermotolerance. Microbiology 146 (Pt 9):2121-32.
13. Elledge, S. J., and R. W. Davis. 1990. Two genes differentially regulated in the cell cycle and by DNA-damaging agents encode alternative regulatory subunits of ribonucleotide reductase. Genes Dev 4:740-51.
14. Flick, K., I. Ouni, J. A. Wohlschlegel, C. Capati, W. H. McDonald, J. R. Yates, and P. Kaiser. 2004. Proteolysis-independent regulation of the transcription factor Met4 by a single Lys 48-linked ubiquitin chain. Nat Cell Biol 6:634-41.

15. Friesen, H., R. Lunz, S. Doyle, and J. Segall. 1994. Mutation of the SPS1-encoded protein kinase of Saccharomyces cerevisiae leads to defects in transcription and morphology during spore formation. Genes Dev 8:2162-75.
16. Garay-Arroyo, A., and A. A. Covarrubias. 1999. Three genes whose expression is induced by stress in Saccharomyces cerevisiae. Yeast 15:879-92.
17. Garcia, R., C. Bermejo, C. Grau, R. Perez, J. M. Rodriguez-Pena, J. Francois, C. Nombela, and J. Arroyo. 2004. The global transcriptional response to transient cell wall damage in Saccharomyces cerevisiae and its regulation by the cell integrity signaling pathway. J Biol Chem 279:15183-95.
18. Gasch, A. P., P. T. Spellman, C. M. Kao, O. Carmel-Harel, M. B. Eisen, G. Storz, D. Botstein, and P. O. Brown. 2000. Genomic expression programs in the response of yeast cells to environmental changes. Mol Biol Cell 11:4241-57.
19. Guarente, L. 1983. Yeast promoters and lacZ fusions designed to study expression of cloned genes in yeast. Methods Enzymol 101:181-91.
20. Gustin, M. C., J. Albertyn, M. Alexander, and K. Davenport. 1998. MAP kinase pathways in the yeast Saccharomyces cerevisiae. Microbiol Mol Biol Rev 62:1264-300.
21. Hagen, D. C., and G. F. Sprague, Jr. 1984. Induction of the yeast alpha-specific STE3 gene by the peptide pheromone a-factor. J Mol Biol 178:835-52.
22. Halmé, A., S. Bumgarner, C. Styles, and G. R. Fink. 2004. Genetic and epigenetic regulation of the FLO gene family generates cell-surface variation in yeast. Cell 116:405-15.
23. Harkness, T. A., G. F. Davies, V. Ramaswamy, and T. G. Arnason. 2002. The ubiquitin-dependent targeting pathway in Saccharomyces cerevisiae plays a critical role in multiple chromatin assembly regulatory steps. Genetics 162:615-32.
24. Hinnebusch, A. G. 1997. Translational regulation of yeast GCN4. A window on factors that control initiator-trna binding to the ribosome. J Biol Chem 272:21661-4.
25. Hong, S. K., S. B. Han, M. Snyder, and E. Y. Choi. 1999. SHC1, a high pH inducible gene required for growth at alkaline pH in Saccharomyces cerevisiae. Biochem Biophys Res Commun 255:116-22.
26. Horak, C. E., N. M. Luscombe, J. Qian, P. Bertone, S. Piccirrillo, M. Gerstein, and M. Snyder. 2002. Complex transcriptional circuitry at the G1/S transition in Saccharomyces cerevisiae. Genes Dev 16:3017-33.
27. Igual, J. C., A. L. Johnson, and L. H. Johnston. 1996. Coordinated regulation of gene expression by the cell cycle transcription factor Swi4 and the protein kinase C MAP kinase pathway for yeast cell integrity. Embo J 15:5001-13.
28. Inagaki, M., T. Schmelzle, K. Yamaguchi, K. Irie, M. N. Hall, and K. Matsumoto. 1999. PDK1 homologs activate the Pkc1-mitogen-activated protein kinase pathway in yeast. Mol Cell Biol 19:8344-52.
29. Irniger, S., and G. H. Braus. 2003. Controlling transcription by destruction: the regulation of yeast Gcn4p stability. Curr Genet 44:8-18.
30. Jia, X., and W. Xiao. 2003. Compromised DNA repair enhances sensitivity of the yeast RNR3-lacZ genotoxicity testing system. Toxicol Sci 75:82-8.

31. Jung, U. S., and D. E. Levin. 1999. Genome-wide analysis of gene expression regulated by the yeast cell wall integrity signalling pathway. Mol Microbiol 34:1049-57.
32. Jung, U. S., A. K. Sobering, M. J. Romeo, and D. E. Levin. 2002. Regulation of the yeast Rlm1 transcription factor by the Mpk1 cell wall integrity MAP kinase. Mol Microbiol 46:781-9.
33. Kaiser, P., K. Flick, C. Wittenberg, and S. I. Reed. 2000. Regulation of transcription by ubiquitination without proteolysis: Cdc34/SCF(Met30)-mediated inactivation of the transcription factor Met4. Cell 102:303-14.
34. Kellis, M., N. Patterson, M. Endrizzi, B. Birren, and E. S. Lander. 2003. Sequencing and comparison of yeast species to identify genes and regulatory elements. Nature 423:241-54.
35. Kohrer, K., and H. Domdey. 1991. Preparation of high molecular weight RNA. Methods Enzymol 194:398-405.
36. Kuras, L., R. Barbey, and D. Thomas. 1997. Assembly of a bZIP-bHLH transcription activation complex: formation of the yeast Cbf1-Met4-Met28 complex is regulated through Met28 stimulation of Cbf1 DNA binding. Embo J 16:2441-51.
37. Kuras, L., A. Rouillon, T. Lee, R. Barbey, M. Tyers, and D. Thomas. 2002. Dual regulation of the met4 transcription factor by ubiquitin-dependent degradation and inhibition of promoter recruitment. Mol Cell 10:69-80.
38. Lagorce, A., N. C. Hauser, D. Labourdette, C. Rodriguez, H. Martin-Yken, J. Arroyo, J. D. Hoheisel, and J. Francois. 2003. Genome-wide analysis of the response to cell wall mutations in the yeast Saccharomyces cerevisiae. J Biol Chem 278:20345-57.
39. Lee, T. I., N. J. Rinaldi, F. Robert, D. T. Odom, Z. Bar-Joseph, G. K. Gerber, N. M. Hannett, C. T. Harbison, C. M. Thompson, I. Simon, J. Zeitlinger, E. G. Jennings, H. L. Murray, D. B. Gordon, B. Ren, J. J. Wyrick, J. B. Tagne, T. L. Volkert, E. Fraenkel, D. K. Gifford, and R. A. Young. 2002. Transcriptional regulatory networks in Saccharomyces cerevisiae. Science 298:799-804.
40. Madden, K., Y. J. Sheu, K. Baetz, B. Andrews, and M. Snyder. 1997. SBF cell cycle regulator as a target of the yeast PKC-MAP kinase pathway. Science 275:1781-4.
41. Martin, H., J. M. Rodriguez-Pachon, C. Ruiz, C. Nombela, and M. Molina. 2000. Regulatory mechanisms for modulation of signaling through the cell integrity Slt2-mediated pathway in Saccharomyces cerevisiae. J Biol Chem 275:1511-9.
42. Martin-Yken, H., A. Dagkessamanskaia, F. Basmaji, A. Lagorce, and J. Francois. 2003. The interaction of Slt2 MAP kinase with Knr4 is necessary for signalling through the cell wall integrity pathway in Saccharomyces cerevisiae. Mol Microbiol 49:23-35.
43. Martinez-Pastor, M. T., G. Marchler, C. Schuller, A. Marchler-Bauer, H. Ruis, and F. Estruch. 1996. The Saccharomyces cerevisiae zinc finger proteins Msn2p and Msn4p are required for transcriptional induction through the stress response element (STRE). Embo J 15:2227-35.

44. Measday, V., L. Moore, R. Retnakaran, J. Lee, M. Donoviel, A. M. Neiman, and B. Andrews. 1997. A family of cyclin-like proteins that interact with the Pho85 cyclin-dependent kinase. Mol Cell Biol 17:1212-23.
45. Meimoun, A., T. Holtzman, Z. Weissman, H. J. McBride, D. J. Stillman, G. R. Fink, and D. Kornitzer. 2000. Degradation of the transcription factor Gcn4 requires the kinase Pho85 and the SCF(CDC4) ubiquitin-ligase complex. Mol Biol Cell 11:915-27.
46. Miralles, V. J., and R. Serrano. 1995. A genomic locus in Saccharomyces cerevisiae with four genes up-regulated by osmotic stress. Mol Microbiol 17:653-62.
47. Moll, T., E. Schwob, C. Koch, A. Moore, H. Auer, and K. Nasmyth. 1993. Transcription factors important for starting the cell cycle in yeast. Philos Trans R Soc Lond B Biol Sci 340:351-60.
48. Muratani, M., and W. P. Tansey. 2003. How the ubiquitin-proteasome system controls transcription. Nat Rev Mol Cell Biol 4:192-201.
49. Natarajan, K., M. R. Meyer, B. M. Jackson, D. Slade, C. Roberts, A. G. Hinnebusch, and M. J. Marton. 2001. Transcriptional profiling shows that Gcn4p is a master regulator of gene expression during amino acid starvation in yeast. Mol Cell Biol 21:4347-68.
50. Patton, E. E., C. Peyraud, A. Rouillon, Y. Surdin-Kerjan, M. Tyers, and D. Thomas. 2000. SCF(Met30)-mediated control of the transcriptional activator Met4 is required for the G(1)-S transition. Embo J 19:1613-24.
51. Posas, F., and H. Saito. 1998. Activation of the yeast SSK2 MAP kinase kinase by the SSK1 two-component response regulator. Embo J 17:1385-94.
52. Reinoso-Martin, C., C. Schuller, M. Schuetzer-Muehlbauer, and K. Kuchler. 2003. The yeast protein kinase C cell integrity pathway mediates tolerance to the antifungal drug caspofungin through activation of Slt2p mitogen-activated protein kinase signaling. Eukaryot Cell 2:1200-10.
53. Roberts, C. J., B. Nelson, M. J. Marton, R. Stoughton, M. R. Meyer, H. A. Bennett, Y. D. He, H. Dai, W. L. Walker, T. R. Hughes, M. Tyers, C. Boone, and S. H. Friend. 2000. Signaling and circuitry of multiple MAPK pathways revealed by a matrix of global gene expression profiles. Science 287:873-80.
54. Roth, A. F., and N. G. Davis. 2000. Ubiquitination of the PEST-like endocytosis signal of the yeast a-factor receptor. J Biol Chem 275:8143-53.
55. Roth, A. F., D. M. Sullivan, and N. G. Davis. 1998. A large PEST-like sequence directs the ubiquitination, endocytosis, and vacuolar degradation of the yeast a-factor receptor. J Cell Biol 142:949-61.
56. Rowley, A., G. C. Johnston, B. Butler, M. Werner-Washburne, and R. A. Singer. 1993. Heat shock-mediated cell cycle blockage and G1 cyclin expression in the yeast Saccharomyces cerevisiae. Mol Cell Biol 13:1034-41.
57. Rupp, S., E. Summers, H. J. Lo, H. Madhani, and G. Fink. 1999. MAP kinase and cAMP filamentation signaling pathways converge on the unusually large promoter of the yeast FLO11 gene. Embo J 18:1257-69.
58. Sanz, M., J. A. Trilla, A. Duran, and C. Roncero. 2002. Control of chitin synthesis through Shc1p, a functional homologue of Chs4p specifically induced during sporulation. Mol Microbiol 43:1183-95.

59. Shemer, R., A. Meimoun, T. Holtzman, and D. Kornitzer. 2002. Regulation of the transcription factor Gcn4 by Pho85 cyclin PCL5. Mol Cell Biol 22:5395-404.
60. Simon, I., J. Barnett, N. Hannett, C. T. Harbison, N. J. Rinaldi, T. L. Volkert, J. J. Wyrick, J. Zeitlinger, D. K. Gifford, T. S. Jaakkola, and R. A. Young. 2001. Serial regulation of transcriptional regulators in the yeast cell cycle. Cell 106:697-708.
61. Sprague, G. F., Jr., R. Jensen, and I. Herskowitz. 1983. Control of yeast cell type by the mating type locus: positive regulation of the alpha-specific STE3 gene by the MAT alpha 1 product. Cell 32:409-15.
62. Thomas, D., and Y. Surdin-Kerjan. 1997. Metabolism of sulfur amino acids in Saccharomyces cerevisiae. Microbiol Mol Biol Rev 61:503-32.
63. Verma, R., R. S. Annan, M. J. Huddleston, S. A. Carr, G. Reynard, and R. J. Deshaies. 1997. Phosphorylation of Sic1p by G1 Cdk required for its degradation and entry into S phase. Science 278:455-60.
64. Verma, R., J. Smiley, B. Andrews, and J. L. Campbell. 1992. Regulation of the yeast DNA replication genes through the Mlu I cell cycle box is dependent on SWI6. Proc Natl Acad Sci U S A 89:9479-83.
65. Wang, Y., and H. G. Dohlman. 2002. Pheromone-dependent ubiquitination of the mitogen-activated protein kinase kinase Ste7. J Biol Chem 277:15766-72.
66. Wang, Y., Q. Ge, D. Houston, J. Thorner, B. Errede, and H. G. Dohlman. 2003. Regulation of Ste7 ubiquitination by Ste11 phosphorylation and the Skp1-Cullin-F-box complex. J Biol Chem 278:22284-9.
67. Williams-Hart, T., X. Wu, and K. Tatchell. 2002. Protein phosphatase type 1 regulates ion homeostasis in Saccharomyces cerevisiae. Genetics 160:1423-37.
68. Zhao, C., U. S. Jung, P. Garrett-Engele, T. Roe, M. S. Cyert, and D. E. Levin. 1998. Temperature-induced expression of yeast FKS2 is under the dual control of protein kinase C and calcineurin. Mol Cell Biol 18:1013-22.

CHAPTER 5 – Summary and future directions.

5.1 Thesis summary

The Cdc34/SCF complex is one of the central regulators of the budding yeast cell cycle (19). Many of its functions are highly conserved in higher eukaryotes, including several roles in the regulation of the human cell cycle. The overall objective of this thesis was to provide insight into the function of the Cdc34/SCF complex from both a mechanistic and cellular perspective. The principal arguments in this thesis have been separated into three chapters (Chapters 2, 3 and 4), and together significantly contribute to the knowledge of Cdc34 and the SCF complex, and provide a novel framework for their future study.

5.1.1 Summary of Chapter 2

Chapter 2 was aimed at providing insight into catalytic mechanism of function of the Cdc34 Ub-conjugating enzyme. It had previously been hypothesized that E2 enzymes, including Cdc34, self-associate to facilitate the assembly of poly-Ub chains (18, 22). However, such an interaction had only been shown to occur in the presence of a cross-linker *in vitro* (18). All other analysis of Cdc34 described it as a monomeric species that was capable of building poly-Ub chains onto protein substrates (18). I chose to test whether Cdc34 self-associates in a more direct manner. The approach I used was aimed at determining if Cdc34 self-associates in yeast cells, which would reduce the occurrence of any possible artifactual interactions.

Using a co-immunoprecipitation strategy from whole cell extracts, I showed that Cdc34 does in fact self-associate. I extended my analysis in an attempt to determine its properties and potential role(s) of this interaction. Several key residues that facilitated the self-association of Cdc34 paralleled residues that had previously been described to be important for its function *in vivo* (1, 6). Interestingly, these residues were predicted to group around and include the catalytic cysteine residue required for Ub thiolester formation, suggesting that Ub thiolester was involved in facilitating the interaction. This was shown to be the case *in vitro*, as purified Cdc34~Ub thiolester interacted as dimeric

species. However, the formation of Cdc34~Ub thiolester was not the only determinant in Cdc34 self-association, since one of the derivatives (S97D - which lies very near the active site cysteine) that was observed to be defective in the interaction was still capable of forming Ub thiolester. Therefore, it appears that Cdc34 self-association is a complex interaction, which requires the formation and most likely the proper positioning of Ub thiolester at its catalytic site.

Analysis of the autoubiquitination properties of the Cdc34 derivatives defective in self-association showed that they were also defective in the formation of poly-Ub chains. Furthermore, *in vitro* analysis showed that purified Cdc34~Ub thiolester dimer efficiently assembled di-Ub conjugates, but was defective in the formation of higher order chains in the absence of a continuous source of Ub thiolester. These results suggest that a dimeric species of Cdc34~Ub thiolester facilitates the formation of poly-Ub chains. Although many questions still remain unanswered, these observations provide us with a better understanding of the mechanism of Cdc34 function, and may represent a general view of E2 function.

5.1.2 Summary of Chapter 3

Chapter 3 deals with the central issue of the biological function(s) of the Cdc34/SCF complex. Analysis of temperature sensitive *cdc53-1* (R488C-*cdc53*) and *cdc34-2* (G58R-*cdc34*) *S. cerevisiae* mutants revealed that in addition to their characterized phenotypes, such as the accumulation of Sic1 (21), these cells also displayed novel defects that appear to be separate from the known functions of the Cdc34/SCF complex. These defects include a cell cycle arrest, resulting in an unbudded round morphology and diminished cell wall integrity. The growth characteristics of these cells under stress conditions were consistent with a role for the Cdc34/SCF complex in mediating the cell integrity signal transduction pathway. I addressed this possibility by analyzing the signal through this pathway at the level of Slt2 phosphorylation (the MAPK of the cell integrity pathway). I observed that Slt2 phosphorylation in *cdc53-1* and *cdc34-2* mutants was defective under conditions that normally activate the pathway, such as heat stress or the presence of caffeine, suggesting a role for the Cdc34/SCF complex in mediating this signal. Furthermore, genetic interactions with several components of the

cell integrity pathway were observed, one of which displayed synthetic suppression of the temperature sensitive growth defects associated with both *cdc53-1* and *cdc34-2* mutants. Despite not identifying potential ubiquitination targets that may account for these defects, Chapter 3 highlights the importance of this novel function, and suggests that it is one of the principal roles for the Cdc34/SCF complex in mediating cell growth.

5.1.3 Summary of Chapter 4

The final issue addressed in this thesis (in Chapter 4) is the role of the Cdc34/SCF complex in the regulation of cellular transcription. This analysis was prompted by the observation that downstream transcriptional targets of the cell integrity signal transduction pathway (Rlm1 and the SBF complex) were induced in their activity in *cdc53-1* and *cdc34-2* mutants. The induction was dependent on signaling through this pathway, as deletion of *SLT2* in these strains abrogated the activity of these transcription factors. Furthermore, the induced activity was not a result of Sic1 accumulation in these cells, suggesting that these observations are due to a novel function for the Cdc34/SCF complex. These observations, together with the known functions of the Cdc34/SCF complex in the regulation of the Gcn4 and Met4 transcription factors, as well as its role in the regulation of other signaling pathways, indicated that the Cdc34/SCF complex was an important regulator of several distinct transcriptional programs (4, 5, 12, 27). As such, I performed a global microarray analysis of the *cdc53-1* and *cdc34-2* mutants to examine any possible influence the Cdc34/SCF complex may have on transcription.

The microarray analysis of these cells provided many interesting observations: 1) The *cdc53-1* and *cdc34-2* cells displayed a highly similar overall gene expression pattern, with slight differences in their significantly induced or repressed genes; 2) A considerable proportion of gene expression was most likely due to the increased activity of the Gcn4 transcription factor, as a significant number of these genes possessed potential Gcn4 promoter binding sites and their expression resembled the expression patterns of previous microarray studies performed with a *gcn4Δ* mutant; 3) The transcriptional activator Met4 contributed to the overall expression patterns, as many genes possessed Met4 promoter elements and several known target genes were upregulated; 4) Several signal transduction pathways seemed to be misregulated in these cells, resulting in the induction of a variety

of genes. The most obvious appeared to relate to signaling through the mating pathway and the cell integrity pathway; 5) Very few G1-S phase regulated genes were induced for expression, suggesting that these mutants, under the conditions that we examined, possess growth defects unrelated to their known roles in cell cycle progression; 6) Finally, the transcriptional defects in these mutants appeared to be quite specific (only approximately 3% of the genome was significantly affected), and were not a result of global transcriptional misregulation. Overall this analysis provides us with a view of the global effects of the Cdc34/SCF complex on transcription. At the present time many of the defects observed are not well understood, but these results will provide a solid framework for future studies.

5.2 Future directions

Several potential projects could stem from the studies in this thesis, many of which would address important new issues regarding the Cdc34/SCF complex. This final section discusses the possible direction of future studies, and introduces some initial observations that may provide some insight into these potential investigations.

5.2.1 Cdc34 self-association and the assembly of poly-Ub chains.

The most obvious study missing in the analysis of Cdc34 self-association is the examination of this interaction in the ubiquitination of a distinct target protein (such as Sic1). It remains to be seen what specific effect Cdc34 self-association has on target ubiquitination. Such a study would be relatively easy to perform, as the *in vitro* ubiquitination of several target proteins for Cdc34 has been previously described (23, 24, 28). Purified Cdc34, Cdc34~Ub thiolester, or Cdc34 derivatives defective in self-association could be used in these reactions to determine the effects of these E2 derivatives on target ubiquitination. Additionally, recent studies have described a potential role for Cdc34~Ub thiolester, and possibly Cdc34 self-association, in the dissociation of Cdc34 from the SCF complex (2). As such, examining the role of Cdc34 self-association in the dissociation from the SCF complex would provide important insight into the mechanism of Cdc34 function.

Despite not having information on the ubiquitination of a Cdc34/SCF target protein, we did gain insight into the role of Cdc34 self-association in the assembly of poly-Ub chains by the analysis of Cdc34 autoubiquitination, as described in Chapter 2. Although the biological role for Cdc34 autoubiquitination is unclear (and should be addressed with more studies), *in vitro* analysis of this function for Cdc34 does have its advantages over the examination of other target proteins. Unlike other *in vitro* systems, the autoubiquitination of Cdc34 depends solely upon Cdc34, Ub and E1, without the requirement for an E3 and a target protein. Thus, examination of this process in detail may provide mechanistic insight into the catalysis of poly-Ub chain assembly and the function of E1 in this process, which might otherwise be difficult to examine.

One observation that I made while examining the ability of purified Cdc34~Ub thiolester to assemble autoubiquitin chains was that Ub is transferred primarily to a Cdc34 within a dimer, and in order for higher order chains to be assembled, an active E1 is required to recharge the existing Cdc34-Ub conjugates (see Figure 2.10). I examined this observation in a little more detail to better understand the role of E1 in this process. Purified Cdc34~Ub thiolester was incubated with ^{35}S labeled Ub (^{35}S-Ub), and with or without E1 in the presence or absence of ATP cocktail. As described in section 2.3.8, E1 was required for the formation of higher order poly-Ub chains, and the catalytic activity of E1 was necessary for this function, as the active site cysteine was required (see Figure 2.10). However, under these *in vitro* conditions E1 could perform this function in an ATP independent manner (Figure 5.1), suggesting that Ub is capable of back-transferring from Cdc34~Ub thiolester to the active site of E1. The active E1~Ub thiolester most likely can then recharge Cdc34-Ub conjugates leading to the formation of higher order poly-Ub chains. Such a back-transferring mechanism has not been reported for the Ub pathway and raises the possibility that such a mechanism might occur in the cell. This process could potentially be used to scavenge unused E2~Ub thiolester in the cell, and could be a general function for E1.

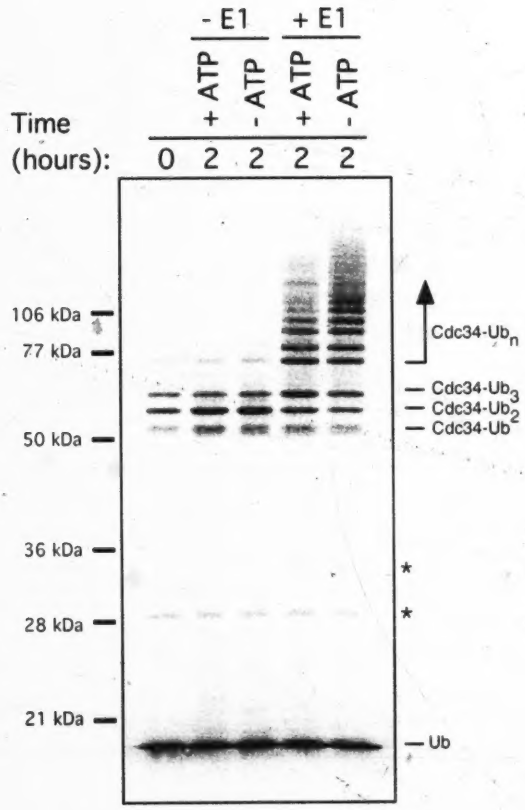

Figure 5.1 ATP independent function for E1 in Cdc34~Ub thiolester mediated autoubiquitination of Cdc34.

Purified Cdc34~^{35}S-Ub [100nM] was incubated at 30°C with or without Uba1 (E1) [10nM] in the presence or absence of ATP cocktail. DTT was added to all the samples to terminate the reactions, and products from each reaction were subsequently separated by 12% SDS-PAGE and visualized by autoradiography. The positions of Cdc34-Ub$_n$ conjugates are indicated by the arrow, as is the position of free Ub. The asterisk (*) indicates a contamination band that purifies with ^{35}S-Ub.

5.2.2 The role of S73 and S97 phosphorylation with respect to thiolester formation, Cdc34 self-association, and poly-Ub chain assembly.

Cdc34 catalytic function appears to depend on several residues in its catalytic core domain. I have identified a role for some of these residues in Cdc34 self-association, notably Ser73 and Ser97. These residues function in co-operation with the unique 12 amino acid insert near the catalytic active site of Cdc34. Our collaborator (Mark Goebl, Indiana University) has shown that Ser73 and Ser97 are phosphorylated. Since these residues play an important role in Cdc34 self-association, Ub thiolester utilization, and autoubiquitination, it is logical that phosphorylation of these residues might play a role in these processes. I performed an initial experiment to investigate this possibility by examining the ability of phosphorylated Cdc34 to catalyze autoubiquitin chain formation.

The kinase responsible for the phosphorylation of these residues is not known, so the phosphorylation of Cdc34 could not be performed *in vitro*. I therefore utilized an antibody specific for the Ser97 phosphorylated form of Cdc34 (anti-phospho-Ser97, given to us by Mark Goebl, Indiana University) to isolate Cdc34 by immunoprecipitation from yeast whole cell extracts. Cdc34 amino-terminally tagged with a Flag epitope tag (Flag-Cdc34) under the control of a galactose-inducible promoter was overexpressed in yeast cells by growth in galactose-containing medium. The cells were lysed and subjected to immunoprecipitation using either an anti-Flag antibody to pull down the major cellular constituent of Cdc34, or the anti-phospho-Ser97 antibody to pull down phosphorylated Cdc34. The immunoprecipitates were then incubated together with ^{35}S-Ub, and with or without E1 and ATP cocktail, and subsequently analyzed by immunoblotting to determine the amount of Cdc34 pulled down, and autoradiography to examine the extent of autoubiquitin chain formation. Cdc34 pulled down with the anti-Flag antibody efficiently assembled autoubiquitin chains in the presence of E1, whereas the phospo-Ser97 form of Cdc34 did not, suggesting that the phosphorylation of S97 on Cdc34 results in the inhibition of its catalytic activity (Figure 5.2). However, problems exist in this experiment that need to be addressed before any conclusions can be made, including the method of phospho-Ser97 Cdc34 purification, which involved the binding of an antibody to the phospho-Ser97 residue. Since Ser97 lies adjacent to the catalytic cysteine residue, it is very possible that the binding of the antibody to this site occludes the

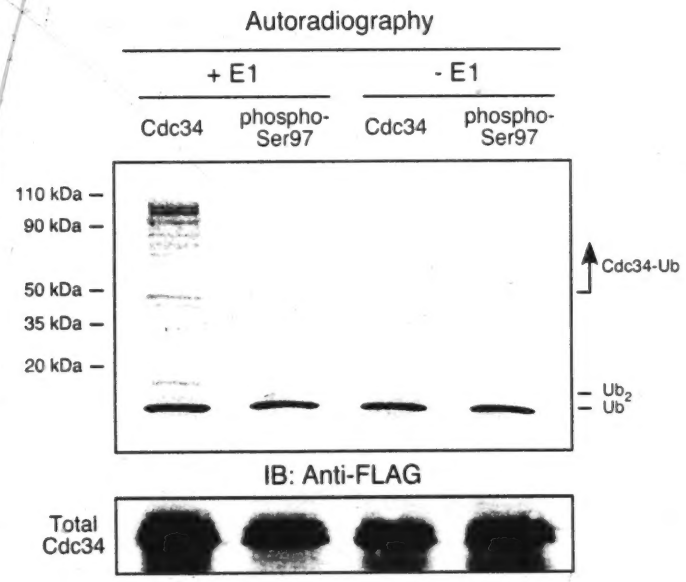

Figure 5.2 Autoubiquitination of phopho-S97 Cdc34.

Flag-Cdc34 was expressed in YPH499 yeast cells. Cdc34 and Cdc34 phosphorylated on Ser97 (phospho-Ser97) were immunoprecipitated with anti-Flag and anti-phospho-Ser97 antibodies, respectively. Protein levels were measured and 100 nM Cdc34 was incubated with 200 nM ^{35}S-Ub and with (+E1) or without (- E1) 10 nM Uba1 and ATP cocktail for 2 hours. Samples were subsequently analyzed by 12% SDS-PAGE, followed by immunoblotting (IB) with anti-FLAG antibody to detect the total Cdc34 in the reaction, and by autoradiography to determine the extent of poly-Ub chain assembly. Ub, di-Ub and Cdc34-Ub conjugates are indicated.

formation of Ub thiolester, thereby preventing Cdc34 activity. Despite this problem however, the result would still suggest that modification of this area within Cdc34 disrupts its function, inciting the need for further analysis of Cdc34 phosphorylation.

Identifying the kinase(s) responsible for Cdc34 phosphorylation (of both Ser73 and Ser97, as well as other potential residues) would help clarify the function of this modification. Several approaches can be used to identify such a kinase, which could range from genetic approaches to high-throughput biochemical analysis. Identification of this kinase would allow us to phosphorylate Cdc34 *in vitro*, and apply the methods described in Chapter 2 to analyze the role of this modification in more detail. Analysis *in vivo* could also provide some information into its function. For example, simple experiments such as examining the phosphorylation state of Cdc34 under varying cell cycle or environmental stress conditions could be done, or the localization of Cdc34 phospho-forms could be followed. It remains to be seen what the role for Cdc34 phosphorylation is, but based on my observations it appears that this modification will be important in regulating Cdc34 function.

5.2.3 Structural analysis of Cdc34 and Cdc34~Ub thiolester.

Very little is known about Cdc34 from a structural perspective. Cdc34 is predicted to have a typical E2 structure consisting of a core Ub-conjugating domain (UBC) domain within which lies the catalytic cysteine. Cdc34 is also known to possess a number of distinct features, including amino- and carboxyl-terminal extensions and a 12 amino acid residue catalytic domain insert (see figure 2.13). However, the structural role that these regions play in Cdc34 function is not established. The carboxyl-terminal extension has been shown to contribute to Cdc34's ability to interact with the SCF complex, but this extension is not predicted to lie near the conserved patch of residues that has been shown to mediate the interaction with RING finger domain E3s (2, 8, 17, 18). The results in Chapter 2 indicate that this extension is not required for Cdc34 self-association, but other studies have indicated a contributing role for it in this process (18). Furthermore, NMR analysis of Ubc1, which also possesses a carboxyl-terminal extension, suggests that this region interacts with its catalytic active site region to possibly mediate Ub thiolester formation (13). In collaboration with Sean McKenna (a

graduate student in our lab at the time), an initial structural analysis of Cdc34 was attempted using an NMR approach. Our initial analysis revealed that at least the 51 carboxyl-terminal residues of Cdc34 did not contribute much to the typical secondary structure, as determined by comparison of the 2D ^{1}H-^{15}N HSQC spectra of Cdc34 and Cdc34Δ244 (residues 244-295 deleted) (9). Additional comparisons between Cdc34 and Cdc34Δ244 revealed that the 51 carboxyl-terminal residues of Cdc34 did not affect the formation or utilization of Cdc34~Ub thiolester (9).

The importance for Ub thiolester in Cdc34 function is obvious from my studies. However, little is known about it from a structural perspective. NMR chemical shift perturbation methodologies using Ub that was selectively ^{15}N-labeled have been previously employed to successfully map the surface of Ub that interacts with E2 enzymes (3, 11). Therefore, a similar NMR approach was undertaken in an attempt to gain insights into the Cdc34~Ub thiolester bond. The most significant interactions upon thiolester formation were determined, and mapped to a solvent-exposed face on Ub stretching from the carboxyl-terminal Gly76 towards the centrally positioned Lys48 (Figure 5.3). A similar face on Ub appeared to be used in other E2~Ub thiolester interactions, with a few notable differences observed (3, 10).

Potentially the most interesting observation made by our NMR analysis was that Ub non-covalently interacted with Cdc34 in the absence of E1 and ATP/Mg^{2+}. We observed changes in the ^{1}H-^{15}N-HSQC NMR spectrum of ^{15}N-Ub for several residues involved in this interaction: Ile13, Asp24, Gln40, Leu43, Gly47, Arg48, Gln49, His68, Leu69, Val70, and Leu71. When mapped onto the surface structure of Ub, these residues cluster to a face centrally located on one side of the Ub molecule (Figure 5.4). This interaction does not appear to involve the same residues as thiolester formation, although the general surface region is similar, and could be a result of an interaction with the thiolester site. A non-covalent interaction has the potential to: (i) Mediate Cdc34 self-association, as this interaction is dependent on Ub thiolester; (ii) Allow for the positioning of Ub in such a way as to mediate poly-Ub chain assembly. This has been observed for the complex of Ubc13 and the Ub-conjugating-like protein Mms2, in which Mms2 non-covalently interacts with Ub to position a specific lysine (Lys63) on Ub near the active site of Ubc13. A curious observation is that Lys48 within Ub is one of the

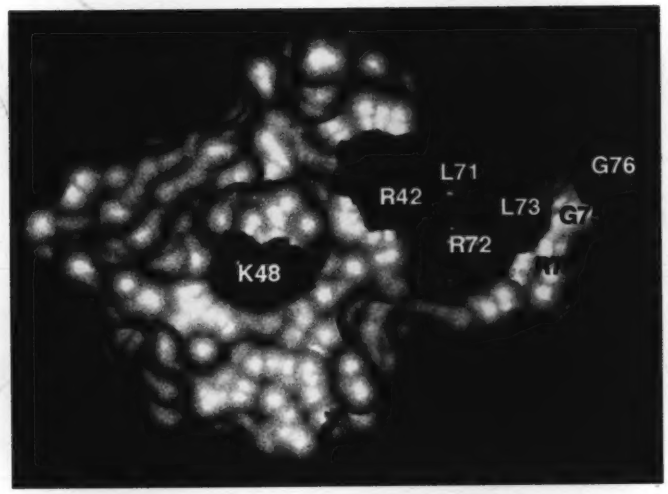

Figure 5.3 Distinct surface regions on Ub responsible for mediating the thiolester interaction with Cdc34. Surface residues of Ub that undergo significant 1H-15N HSQC NMR chemical shift changes upon the formation Cdc34~Ub thiolester are shown in red. Residues important for thiolester formation that are common to the E2's studied are labeled in white, as well as Arg74 and Gly75 which are known to participate in the interface. The work in this figure was done by Sean McKenna.

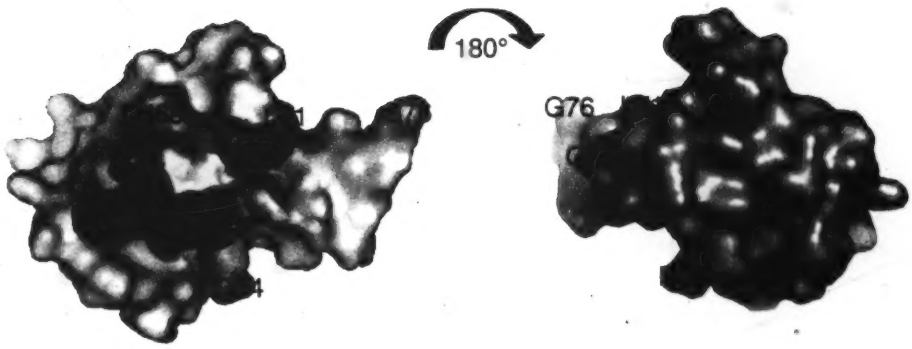

Figure 5.4 A non-covalent interaction between Ub and Cdc34.
The surface residues within Ub that underwent significant changes in chemical shift upon a non-covalent interaction with Cdc34 are shown in red, as determined by NMR analysis. Gly76 is also indicated as a point of reference. This experiment was done by Sean McKenna.

residues involved in the non-covalent interaction. This does not necessarily negate the positioning of Ub for Lys48 linked poly-chain formation, as the interaction may shift Lys48 in a favorable position for conjugation; (iii) Be involved in Cdc34's interaction with the E1. Structural studies have revealed an Ub resembling domain within E1 that has been implicated in E2 binding. The observed non-covalent interaction between Ub and Cdc34 might resemble the interaction between Cdc34 and the Ub-like domain in E1. I would like to caution that these results are preliminary and the role of this non-covalent interaction in Cdc34 function is unclear, and requires further investigation. However, this interaction does appear to be relevant, as it is supported by genetic observations *in vivo* (16).

Taken together, my observations suggest that the interactions between Cdc34 and Ub are central in mediating Cdc34's catalytic function. Therefore further investigation into these interactions is necessary for understanding Cdc34's mechanism of action.

5.2.4 Identification of Cdc34/SCF target protein(s) that relate to cell integrity.

Examination of the temperature sensitive *cdc53-1* and *cdc34-2* mutants provided us with a novel relationship between the Cdc34/SCF complex and the regulation of cellular integrity. As such, an extensive search for ubiquitination target(s) that are involved in mediating these affects is a required future study.

Several potential targets may mediate signaling through the cell integrity pathway. Candidate targets include the RhoGAP proteins, which include Sac7 and Lrg1. Many of these proteins, including Sac7 and Lrg1, contain several PEST sequences, which have been shown to target proteins for phosphorylation and subsequent interaction with the SCF complex (20). Sac7 has been shown to be a target of cyclin-CDK phosphorylation further suggesting this possibility (26). The observation that the deletion of *LRG1* rescues the temperature sensitivity of the *cdc53-1* and *cdc34-2* mutants supports the idea that Lrg1 could be a critical target (Figure 3.9). This is further supported by the toxicity of *LRG1* over-expression in Cdc34/SCF mutants (Figure 3.1). Misregulation of Rho1 activity in such a manner could explain both the cell wall biosynthesis and cell integrity signaling defects associated with these mutants. I have performed some initial experiments to address these possibilities, but my results were not conclusive, and were

not pursued due to time limitations. Another potential ubiquitination target in the cell integrity pathway is the Slt2 MAPK. This protein has been identified as being ubiquitinated in a high-throughput examination of ubiquitinated proteins (15). Furthermore, the Ub pathway has been observed to regulate several other MAPKs, suggesting this as a strong possibility. Since I have not examined this possibility, it remains open for future studies.

Due to the nature of ubiquitination, it is not easy to identify target proteins, and only a small group has been identified for the Cdc34/SCF complex (see Table 1.2). Examination of individual proteins within the pathway is not the best approach at identifying such a target. Rather, it would be better to perform genetic screens on Cdc34/SCF mutants under cell integrity specific conditions. A potentially easy screen could be an over-expression analysis of the genome in Cdc34/SCF mutants grown on either 1M sorbitol (at 37°C) or 0.005% SDS (at 30°C). The overexpression of a target protein under both these conditions should cause lethality. Another potential screen could utilize the LacZ reporter plasmids described in Chapter 4. Synthetic suppression of the high transcriptional activity could be examined in a genetic screen by mating the yeast genomic deletion set with the *cdc53-1* and *cdc34-2* mutants, and determining which genes when deleted could suppress this effect. Regrettably, I again did not have the time to pursue such studies.

5.2.5 Identifying the F.box component(s) of the SCF complex that mediate cell integrity.

One issue that was not directly addressed in my studies, regarding the role of the Cdc34/SCF complex in mediating cell integrity, relates to the F.box protein component of the SCF involved in this process. Initial analysis of the *cdc4-1* mutant suggests that Cdc4 does not significantly contribute to this function. Unlike the *cdc53-1* cells, the *cdc4-1* mutant displayed only slight defects related to cell integrity. This included negligible osmotic suppression of its growth defects in the presence of 1M sorbitol, and a minor sensitivity to lysis in the presence of 0.005% SDS (Figure 5.5). However, these slight defects do suggest that Cdc4 does contribute to a certain extent in this process, supporting the idea that proper G1-S progression contributes to cellular integrity, and may relate to

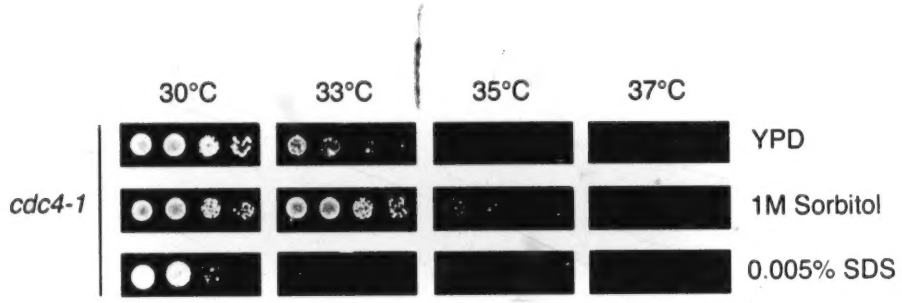

Figure 5.5 Cell integrity defects associated with *cdc4-1* cells.
cdc4-1 budding yeast cells were grown in liquid YPD at 30°C to mid-log phase. Serial dilutions of the cells were prepared and 10^5, 10^4, 10^3 and 10^2 cells were spotted onto plates with YPD, YPD containing 1 M sorbitol, and YPD containing 0.005% SDS. The cells were then grown at 30°C, 33°C, 35°C, and 37°C for 3 days.

the function of Cdc4 in targeting Sic1 for Ub-mediated degradation. Analysis of other F.box mutants was not conducted, and it remains unclear what the targeting subunit(s) may be. Identifying this component of the SCF complex may aid our search for an ubiquitination target related to this function.

5.2.6 Investigating the cell cycle relationship between the Cdc34/SCF complex and cell integrity.

There is an apparent cell cycle relationship between the Cdc34/SCF complex and the cell integrity pathway. Mutations within the Cdc34/SCF complex have been known for years to arrest in the G1 phase of the cell cycle, primarily due to the accumulation of Sic1 (21). Deletion of *SIC1* in these cells allows them to replicate their DNA, but a defect remains in these cells that causes them to arrest following DNA replication, and prior to mitosis (21). The cause of this arrest is not known. One exception to the typical Cdc34/SCF mutant phenotype is the *cdc53-1* mutation, which has been suggested to have a "leaky" cell cycle defect, as it does not primarily arrest in the G1 phase of the cell cycle, but rather displays a mixed population of cells with replicated and unreplicated DNA (Figure 3.1 and (7)). However, this mutant displays severe growth defects, and my data indicates that the *cdc53-1* mutant is deficient in cell integrity signaling and displays strong cell integrity related defects. Additionally, this mutant displays cell cycle progression defects that appear to be unrelated to Sic1 degradation at both the G1 and G2/M phases of the cell cycle (Figure 3.1). As such, it is possible that the cell cycle phenotypes associated with *cdc53-1*, which may also exist in other Cdc34/SCF mutants, may in part be mediated by cell integrity defects.

Several checkpoints could potentially mediate the observed cell cycle delays in the *cdc53-1* mutant. One is the morphogenesis checkpoint, which inhibits the mitotic activation of Cdc28 by increasing Swe1 and decreasing Mih1 function in response to the depolarization of the cell. An activation of this checkpoint in a *cdc53-1* mutant could occur for numerous reasons. First, we have observed a regulatory function for the Cdc34/SCF complex in cell integrity signaling, which is required for the checkpoint. Second, we have observed depolarization of the actin cytoskeleton and chitin distribution in these cells. Third, the stability of Swe1 is dependent on Cdc34/SCF ubiquitination.

Taken together with the observed phenotypes associated with the *cdc53-1* strain, a strong circumstantial argument can be made for the activation of the morphogenesis checkpoint in these cells, and should therefore be pursued.

An additional checkpoint, which is known as the cell integrity checkpoint, has recently been observed to respond to defects in cell wall biosynthesis. This checkpoint regulates the transcription factor Fkh2 through a relatively unknown pathway, resulting in the reduced expression of Clb2 and a G2/M cell cycle delay (25). Since Cdc34/SCF mutants exhibit cell integrity related defects the cell cycle delays we observe in *cdc53-1* cell may possibly be attributed to this checkpoint. As such, it would be of interest to investigate this potential relationship in more detail.

Activation of checkpoints that relate to cell wall biosynthesis and polarization in Cdc34/SCF mutants can possibly account for the G2/M delays observed in these cells when Sic1 is deleted. However, these mutants (especially the *cdc53-1* mutant) also possess G1 related cell cycle defects that cannot be attributed to the misregulation of Sic1. These defects are much more pronounced when combined with deletions of regulatory components of the cell integrity pathway, such as *SAC7* or *KNR4*. A temperature sensitive synthetically lethal growth phenotype is observed in these cells, which primarily results in a G1 arrest that is uncharacteristic of a Sic1 mediated arrest (Figure 3.5). It is therefore possible that a checkpoint in this stage of the cell cycle monitors some aspect of cell integrity, such as bud formation or cell polarization. Although this is speculation at the moment, my observations are consistent with such an idea.

5.2.7 Further examination of the roles of the Cdc34/SCF complex in cell integrity pathway mediated transcription.

While I have characterized an increased transcriptional response in Cdc34/SCF mutants in relation to the misregulation of the cell integrity pathway, I have not examined this effect thoroughly. The observation that cell integrity related transcription was induced in *cdc53-1* and *cdc34-2* cells suggests two possibilities: 1) The increase in transcription contributes to the defects; 2) The increase in transcription mediates the suppression of the defects. As an initial test for this, I overexpressed the Swi4 component

of the SBF transcription factor in *cdc53-1* and *cdc34-2* mutants to see how this would affect these cells. Overexpression of *SWI4* was much more toxic to *cdc53-1* and *cdc34-2* cells than it was to wild type cells, suggesting that general induction of this transcription factor did not have any suppressive effects, and provides evidence to support the idea that misregulation of this transcription factor might contribute to the defects in these mutants. The microarray analysis of *cdc53-1* and *cdc34-2* mutants did not answer whether induction of these genes contributes to the defects, but it did reveal that only specific genes were induced, and suggested that this effect was not due to a general up-regulation of the cell integrity related transcription factors. Rather, the microarray analysis suggested that a specific part of the cell integrity pathway is misregulated. Overall, it appears that the transcriptional connection with the cell integrity pathway is an important one, and further studies will undoubtedly reveal interesting results.

5.2.8 Cdc34/SCF regulation of Gcn4 and Met4, and their connection to cell growth.

An interesting observation that was made from the microarray analysis of the *cdc53-1* and *cdc34-2* mutants was their induction of Gnc4 and Met4 target genes. Misregulation of the activity of these transcription factors can result in growth defects; over-expression of Gcn4 leads to slower growth of wild-type cells (12), and stabilization of Met4 (as a result of inactivation of Met30) results in G1-S cell cycle defects (14). The specific effects of misregulation of either of these transcription factors has not been characterized, and would be worth pursuing due to their effects on cellular growth. It would be of interest to see if increased protein levels of Gcn4 or Met4 contribute to the growth defects observed in Cdc34/SCF mutants. Simple analysis of such effects in wild-type cells over-expressing *GCN4* or *MET4* would provide some initial clues into such a relationship. For example, it would be interesting to see if cells that have higher levels of Gcn4 or Met4 result in cell integrity defects similar to that observed in Cdc34/SCF mutants.

One final point worth mentioning is that stabilization of these transcription factors appears to result in a specific up-regulation of their transcriptional activity. For this reason, it can be conceived that increasing the levels of any transcription factor may

result in the expression of their respective target genes. A central issue in studying gene transcription is the identification of distinct transcriptional targets. Therefore, based on these results one can predict that overexpression of a transcription factor would provide a means to uncover its target genes. Further analysis of this hypothesis could prove to be very valuable in the study of numerous transcription factors.

5.3 Conclusions

The Cdc34 Ub-conjugating enzyme, together with the SCF Ub-ligase, makes up one of the central regulators of the budding yeast cell cycle. This complex functions to mediate the activity of a variety of processes through the targeted ubiquitination of several proteins. This thesis provides a careful examination of the mechanism of Cdc34 function, revealing that its catalytic function is dependent on its ability to self-associate. The importance of Ub thiolester formation in Cdc34 self-association is described, providing a strong model of this E2's mode of action. This thesis also examines a novel function for Cdc34 and the SCF complex in mediating cell growth through the maintenance of cellular integrity. My analysis reveals that Cdc34/SCF complex performs this function via the regulation of the cell integrity signal transduction pathway. Furthermore, a role for the Cdc34/SCF complex in directing cellular transcription is examined, indicating a complex network of regulation that includes its role in mediating signal transduction and specific transcriptional factor activity. Overall this thesis significantly contributes to the understanding of this ubiquitination complex.

5.4 Materials and Methods

5.4.1 Autoubiquitination of phospho-Ser97 Cdc34.

Flag-Cdc34 under the control of a galactose inducible promoter (pESC1, see Table 2.1) was expressed in exponentially growing YPH499 yeast cells by growing the cells in the presence of SSG medium (0.67% yeast nitrogen base, 2% galactose, and the appropriate amino acids). The cells were harvested, washed with water and lysed in ice-cold lysis buffer [50mM HEPES (pH 7.5), 100mM NaCl, 1 mM EDTA, protease

inhibitor cocktail (Sigma)] using glass beads. Lysates were then centrifuged at 10 000 g for 15 minutes at 4°C to remove debris. The supernatants were precleared with 25 µl of protein G-agarose (Roche) for 1 hour with gentle rotation at 4°C. This was followed by incubation of the lysates with 5 µl of anti-Flag antibody [0.4 mg/ml] (M2, Sigma) or with the equivalent concentration of anti-phospho-Ser97 antibody (provided to us by Mark Goebl, Indiana University) for 2 hours at 4°C, and then by incubation with 20 µl of protein G-agarose for 2 hours with gentle rotation at 4°C. The immunoprecipitate-bead complexes were gently washed 2 times ice-cold lysis buffer and 1 time with ATP cocktail [30 mM HEPES (pH 7.5), 5mM $MgCl_2$, 5 mM ATP, 0.6 units/ml inorganic phosphatase], and then resuspended in 50 µl of ATP cocktail. Cdc34 protein concentrations were estimated by coomassie blue staining of a SDS-PAGE analysis of a portion of the immunoprecipitates, as compared to a BSA standard curve.

100 nM of Flag-Cdc34 or phospho-Ser97-Flag-Cdc34 was incubated with 200nM of purified ^{35}S-Ub (see section 2.5.4 for purification) and with (+E1) or without (-E1) 10 nM purified yeast Uba1 (see section 2.5.4 for purification) for 2 hours. The reactions were then boiled in SDS load buffer + 10mM DTT for 5 minutes, and subjected to 12% SDS-PAGE, transferred to polyvinylidene fluoride membrane, and analyzed by immunoblotting with anti-Flag Horseradish Peroxidase (HRP) conjugated antibody (M2, Sigma) to confirm the amount of Cdc34 present within each reaction. The membrane was also analyzed by autoradiography to determine the extent of poly-^{35}S-Ub chain formation.

5.4.2 ATP independent Cdc34~Ub thiolester autoubiquitination reactions.

Autoubiquitination reactions were performed by incubating 100 nM of purified Cdc34~^{35}S-Ub thiolester (see section 2.5.5 for purification) in the presence or absence of 10 nM yeast Uba1 (E1, see section 2.5.4 for purification), and in the presence or absence of ATP cocktail at 30°C for 2 hours. All reactions were terminated by the addition of 10 mM DTT, immediately followed by precipitation with 10 % trichloroacetic acid. Samples were then resuspended and boiled for 5 minutes in SDS load buffer, followed by separation by 12% SDS-PAGE and analysis by autoradiography.

5.4.3 NMR spectroscopy.

NMR analysis was done by Sean McKenna (a graduate student in our lab) and is described elsewhere (9).

5.4.4 Cell integrity related examination of the *cdc4-1* mutant.

The *cdc4-1* mutant was isogenic to the K699 (W303) strain (*ade2-101 his3-11,15 leu2-3,112 trp1-1 ura3-1 can1-100)*. The cells were grown in liquid YPD medium at 30°C to mid-log phase (OD_{600} of approximately 0.5). Serial dilutions of the cells were prepared and 10^5, 10^4, 10^3 and 10^2 cells were spotted onto plates with YPD, YPD containing 1 M sorbitol, and YPD containing 0.005% SDS. The cells were then grown at 30°C, 33°C, 35°C, and 37°C for 3 days.

5.5 References

1. Banerjee, A., R. J. Deshaies, and V. Chau. 1995. Characterization of a dominant negative mutant of the cell cycle ubiquitin-conjugating enzyme Cdc34. J Biol Chem 270:26209-15.
2. Deffenbaugh, A. E., K. M. Scaglione, L. Zhang, J. M. Moore, T. Buranda, L. A. Sklar, and D. Skowyra. 2003. Release of ubiquitin-charged Cdc34-S - Ub from the RING domain is essential for ubiquitination of the SCF(Cdc4)-bound substrate Sic1. Cell 114:611-22.
3. Hamilton, K. S., M. J. Ellison, K. R. Barber, R. S. Williams, J. T. Huzil, S. McKenna, C. Ptak, M. Glover, and G. S. Shaw. 2001. Structure of a conjugating enzyme-ubiquitin thiolester intermediate reveals a novel role for the ubiquitin tail. Structure (Camb) 9:897-904.
4. Kaiser, P., K. Flick, C. Wittenberg, and S. I. Reed. 2000. Regulation of transcription by ubiquitination without proteolysis: Cdc34/SCF(Met30)-mediated inactivation of the transcription factor Met4. Cell 102:303-14.
5. Kuras, L., A. Rouillon, T. Lee, R. Barbey, M. Tyers, and D. Thomas. 2002. Dual regulation of the met4 transcription factor by ubiquitin-dependent degradation and inhibition of promoter recruitment. Mol Cell 10:69-80.
6. Liu, Y., N. Mathias, C. N. Steussy, and M. G. Goebl. 1995. Intragenic suppression among CDC34 (UBC3) mutations defines a class of ubiquitin-conjugating catalytic domains. Mol Cell Biol 15:5635-44.
7. Mathias, N., S. L. Johnson, M. Winey, A. E. Adams, L. Goetsch, J. R. Pringle, B. Byers, and M. G. Goebl. 1996. Cdc53p acts in concert with Cdc4p and Cdc34p to control the G1-to-S-phase transition and identifies a conserved family of proteins. Mol Cell Biol 16:6634-43.
8. Mathias, N., C. N. Steussy, and M. G. Goebl. 1998. An essential domain within Cdc34p is required for binding to a complex containing Cdc4p and Cdc53p in Saccharomyces cerevisiae. J Biol Chem 273:4040-5.
9. McKenna, S. 2003. Structural and Functional Investigation of the Ubiquitin Conjugation Enzymes and Their Variants: Insights Into the Mechanism of Poly-Ubiquitin Chain Formation. Thesis.
10. McKenna, S., T. Moraes, L. Pastushok, C. Ptak, W. Xiao, L. Spyracopoulos, and M. J. Ellison. 2003. An NMR-based model of the ubiquitin-bound human ubiquitin conjugation complex Mms2.Ubc13. The structural basis for lysine 63 chain catalysis. J Biol Chem 278:13151-8.
11. McKenna, S., L. Spyracopoulos, T. Moraes, L. Pastushok, C. Ptak, W. Xiao, and M. J. Ellison. 2001. Noncovalent interaction between ubiquitin and the human DNA repair protein Mms2 is required for Ubc13-mediated polyubiquitination. J Biol Chem 276:40120-6.
12. Meimoun, A., T. Holtzman, Z. Weissman, H. J. McBride, D. J. Stillman, G. R. Fink, and D. Kornitzer. 2000. Degradation of the transcription factor Gcn4 requires the kinase Pho85 and the SCF(CDC4) ubiquitin-ligase complex. Mol Biol Cell 11:915-27.
13. Merkley, N., and G. S. Shaw. 2003. Interaction of the tail with the catalytic region of a class II E2 conjugating enzyme. J Biomol NMR 26:147-55.

14. Patton, E. E., C. Peyraud, A. Rouillon, Y. Surdin-Kerjan, M. Tyers, and D. Thomas. 2000. SCF(Met30)-mediated control of the transcriptional activator Met4 is required for the G(1)-S transition. Embo J 19:1613-24.
15. Peng, J., D. Schwartz, J. E. Elias, C. C. Thoreen, D. Cheng, G. Marsischky, J. Roelofs, D. Finley, and S. P. Gygi. 2003. A proteomics approach to understanding protein ubiquitination. Nat Biotechnol 21:921-6.
16. Prendergast, J. A., C. Ptak, T. G. Arnason, and M. J. Ellison. 1995. Increased ubiquitin expression suppresses the cell cycle defect associated with the yeast ubiquitin conjugating enzyme, CDC34 (UBC3). Evidence for a noncovalent interaction between CDC34 and ubiquitin. J Biol Chem 270:9347-52.
17. Ptak, C., C. Gwozd, J. T. Huzil, T. J. Gwozd, G. Garen, and M. J. Ellison. 2001. Creation of a pluripotent ubiquitin-conjugating enzyme. Mol Cell Biol 21:6537-48.
18. Ptak, C., J. A. Prendergast, R. Hodgins, C. M. Kay, V. Chau, and M. J. Ellison. 1994. Functional and physical characterization of the cell cycle ubiquitin-conjugating enzyme CDC34 (UBC3). Identification of a functional determinant within the tail that facilitates CDC34 self-association. J Biol Chem 269:26539-45.
19. Reed, S. I. 2003. Ratchets and clocks: the cell cycle, ubiquitylation and protein turnover. Nat Rev Mol Cell Biol 4:855-64.
20. Salama, S. R., K. B. Hendricks, and J. Thorner. 1994. G1 cyclin degradation: the PEST motif of yeast Cln2 is necessary, but not sufficient, for rapid protein turnover. Mol Cell Biol 14:7953-66.
21. Schwob, E., T. Bohm, M. D. Mendenhall, and K. Nasmyth. 1994. The B-type cyclin kinase inhibitor p40SIC1 controls the G1 to S transition in S. cerevisiae. Cell 79:233-44.
22. Silver, E. T., T. J. Gwozd, C. Ptak, M. Goebl, and M. J. Ellison. 1992. A chimeric ubiquitin conjugating enzyme that combines the cell cycle properties of CDC34 (UBC3) and the DNA repair properties of RAD6 (UBC2): implications for the structure, function and evolution of the E2s. Embo J 11:3091-8.
23. Skowyra, D., K. L. Craig, M. Tyers, S. J. Elledge, and J. W. Harper. 1997. F-box proteins are receptors that recruit phosphorylated substrates to the SCF ubiquitin-ligase complex. Cell 91:209-19.
24. Skowyra, D., D. M. Koepp, T. Kamura, M. N. Conrad, R. C. Conaway, J. W. Conaway, S. J. Elledge, and J. W. Harper. 1999. Reconstitution of G1 cyclin ubiquitination with complexes containing SCFGrr1 and Rbx1. Science 284:662-5.
25. Suzuki, M., R. Igarashi, M. Sekiya, T. Utsugi, S. Morishita, M. Yukawa, and Y. Ohya. 2004. Dynactin is involved in a checkpoint to monitor cell wall synthesis in Saccharomyces cerevisiae. Nat Cell Biol 6:861-71.
26. Ubersax, J. A., E. L. Woodbury, P. N. Quang, M. Paraz, J. D. Blethrow, K. Shah, K. M. Shokat, and D. O. Morgan. 2003. Targets of the cyclin-dependent kinase Cdk1. Nature 425:859-64.
27. Wang, Y., Q. Ge, D. Houston, J. Thorner, B. Errede, and H. G. Dohlman. 2003. Regulation of Ste7 ubiquitination by Ste11 phosphorylation and the Skp1-Cullin-F-box complex. J Biol Chem 278:22284-9.
28. Winston, J. T., D. M. Koepp, C. Zhu, S. J. Elledge, and J. W. Harper. 1999. A family of mammalian F-box proteins. Curr Biol 9:1180-2.